

DISSERTATION

Submitted to the
Combined Faculty of Natural Sciences and Mathematics
Heidelberg University, Germany
for the degree of
Doctor of Natural Sciences (Dr. rer. nat.)

Presented by
Yury Kozhemyakin

Oral examination: July 13th, 2018

Synthesis and characterization of new bridged tolans

Reviewer: Prof. Dr. Uwe H. F. Bunz

Prof. Dr. Michael Mastalerz

Part of this work has been already published:

Synthesis and Properties of Functional Twisted Tolanes

Y. Kozhemyakin, A. Kretschmar, M. Krämer, F. Rominger, A. Dreuw, U. H. F. Bunz, *Chem. Eur. J.*

2017, *23*, 9908-9918. (DOI: 10.1002/chem.201701519)

Kurzzusammenfassung

Neue verbrückte Diphenylacetylderivate mit eingeschränkter Rotation der Phenylringe wurden synthetisiert und untersucht. Die optischen und elektronischen Eigenschaften des Tolans werden durch den Torsionswinkel der Phenylringe beeinflusst. Ester- und amidgebundene Linker wurden als Spannseile benutzt. Die Amidbindung hat im Vergleich zu Ester eine bessere Beständigkeit. Deswegen wurde die Möglichkeit eine Amidbrücke zu schlagen gezeigt. In der Arbeit wurden zwei verbrückte Tolane und ein doppelt verbrücktes 1,4-Bis(phenylethynyl)benzol (**I**) synthetisiert (**Abbildung I**).

Darüber hinaus wurden Zugänge zu Multi-Gramm-Mengen der funktionalisierten Tolanophane erarbeitet, die zur weiteren Derivatisierung fähig sind. TIPS-Acetylderivate besaßen nicht nur herausragende Emissions-, sondern auch interessante strukturelle Eigenschaften. Gefaltete zyklische Dimere mit innenmolekular π - π -wechselwirkenden Chromophoreinheiten wurden erhalten. Reihen zyklischer Oligomere wurden synthetisiert und untersucht.

Alle bisher bekannte verdrehte Tolanophane planarisieren sich nach der Anregung in den S_n -Zustand. Die Einführung einer zweiten Brücke in das Tolanophanmolekül (**II**) erlaubte es, die verdrillte Konformation starrer zu machen und die Emissionseigenschaften des Tolan-Chromophors besser zu verstehen. Bei dieser Verbindung **II** wird auch im angeregten Zustand eine Verdrillung beobachtet.

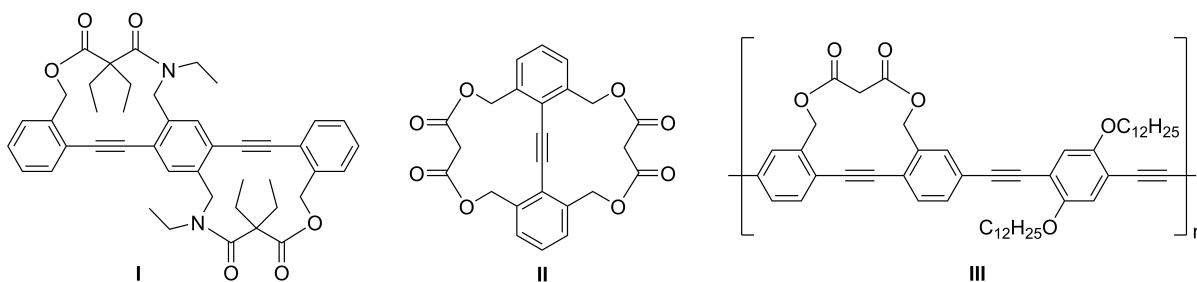


Abbildung I. Auserwählte Moleküle, die synthetisiert und untersucht wurden.

Weiterhin wurden bifunktionelle Tolanophane zur Polymerisation genutzt (**III**), und neue verbrückte Derivate von 1,4-Diphenyldiacetylen wurden untersucht, da sie Fehlstellen in Poly(*para*-phenyleneethynylenen) sind und die Eigenschaften der Polymere signifikant beeinflussen können. Diese Substanzen zeigten aber keine ausgeprägte Fluoreszenz und die Drehung der Phenylgruppen zueinander hat nur schwache Auswirkungen auf das photophysikalische Verhalten.

Abstract

Approaches to novel diphenylacetylene derivatives and related compounds with restricted rotation of the phenyl rings have been developed. Since mutual overlapping of molecular orbitals specifies the electronic communication between aromatic π -systems, regulation of the conformation within a molecule gives control over conductive and photophysical properties of tolane. Amide- and ester bound tethers have been used. The first one resists aggressive factors better, compared with ester. Introduction of amide-functionalized tethers have been demonstrated by synthesis of two bridged tolanes; a novel double-bridged 1,4-bis(phenylethynyl)benzene (**I**) was prepared (**Figure I**).

In addition, synthetic approaches leading to multi-gram amounts of bifunctional tolanophanes are shown, ready for further derivatization. TIPS-acetylene derivatives possessed not only outstanding emissive, but also interest-evoking structural properties, expressed in folded cyclic dimers with electronically interacting chromophore units by means of π - π -stacking. Considering this, series of cyclic oligomers have been synthesized and investigated.

From previous studies it was known, that in the solid state twisted tolanophanes planarize after excitation due to a special arrangement of the electronic states. Introduction of the second tether into the tolanophane molecule gives a more rigid molecule (**II**) and leads to a better understanding of the emissive properties of tolane chromophores. Compound **II** showed a twisted conformation in the excited state.

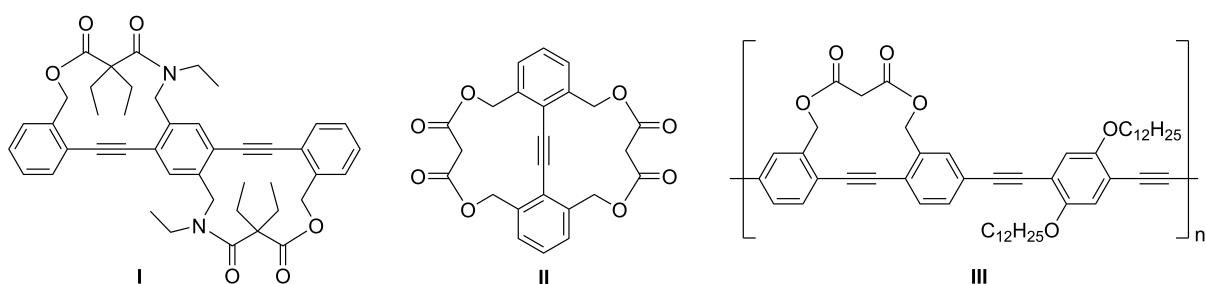


Figure I. Selected synthesized and studied molecules.

Further, bifunctional tolanophanes have been used for copolymerization (**III**). Bridged derivatives of 1,4-diphenylacetylene have been investigated, as they are usual defects in poly(*para*-phenyleneethynylene)s and can significantly affect their properties. Emissive ability of these substances appeared to be not distinct; they showed weak photophysical response on twisting.

Contents

1	Introduction	1
2	State of knowledge	3
2.1	Common information about tolane.....	3
2.2	Rotational isomerism and conformation lock.....	4
2.3	Methods of synthesis.....	8
2.3.1	Diphenylacetylene core construction	8
2.3.2	Approaches to tolanophanes.....	9
2.4	Electronic and optical properties of tolane.....	12
2.4.1	Interaction of light with materials	12
2.4.2	Interaction of light with a tolane molecule	13
2.4.3	Photophysical properties of twisted tolanes.....	15
2.5	Elongated analogues of tolane.....	16
2.5.1	1,4-Bis(phenylethynyl)benzene derivatives and PPEs.....	16
2.5.2	1,4-Diphenylbutadiyne derivatives.....	22
3	Results and Discussion	25
3.1	Aim of the work.....	25
3.2	Synthesis and Properties of Tolanophanes	25
3.2.1	Tolanophanes with diamide- and amidoester tether.....	26
3.2.2	Tolanophanes with urethane and urea functionality	32
3.2.3	Tolanophanes with increased conjugation.....	32
3.2.4	Oligomeric cyclic products.....	35
3.2.5	Doubly bridged tolane	40
3.2.6	Tethered 1,4-bis(phenylethynyl)benzole.....	42
3.2.7	Poly(<i>para</i> -phenyleneethynylene) derivative	45
3.2.8	Tethered 1,4-diphenylbutadiynes.....	49

Table of Contents

4	Summary and Outlook	53
4.1	Outlook.....	58
5	Experimental Part	62
5.1	General remarks.....	62
5.2	Instruments and Methods	62
5.3	Synthetic Procedures.....	64
6	References	96
7	Appendix	110
7.1	Optic spectroscopy.....	110
7.2	Thermogravimetric analysis and Differential scanning calorimetry.....	112
7.3	NMR spectra for selected substances.....	113

This work was written in Microsoft Word 2010. Reaction schemata were drawn in CambridgeSoft ChemDraw 17.0. Graphs and pictures were processed with Microsoft Excel 2010, OriginLab OriginPro 9.1G, Gimp 2.8 or Microsoft Paint. Bruker TopSpin 3.2 program was used for NMR spectra analysis. Evaluation of raw analytical data was accomplished with ACD/Labs Spectrus Processor 2012 or with software provided by device manufacturer.

Abbreviations

Abs	Absorption	EPA	Et ₂ O/isopentane/EtOH 5:5:2, v/v
Ac	Acetyl	eq	Equivalents
aq.	Aqueous	ESI	Electrospray Ionization
Ar	Aromatic	Et	Ethyl
BPEB	1,4-Bis(phenylethynyl)benzene	etc.	Et cetera
bs	Broad	ex	Excited
Bu	Butyl	g	Gram
ca.	Circa	GC-MS	Gas Chromatography Mass Spectrometry
cm	Centimeter	GIWAXS	Grazing-Incidence Wide-Angle X-ray Scattering
d	Doublet	h	Hour
dd	Doublet of doublets	HOMO	highest occupied molecular orbital
DEAD	Diethyl azodicarboxylate	HPLC	High-Performance Liquid Chromatography
DFT	Density Functional Theory	HRMS	High Resolution Mass Spectrometry
DHP	Dihydropyran	Hz	Hertz
DMAP	4-(dimethylamino)pyridine	IR	Infrared
DMF	Dimethylformamide	J	Coupling constant
DMSO	Dimethyl sulfoxide	LUMO	Lowest Unoccupied Molecular Orbital
DPA	Diphenylacetylene (tolane)	M	Molar
dt	Doublet of triplets	m	Multiplett
EA	Ethyl acetate	m	Meta
e.g.	Exempli gratia (for the sake of example)	m.p.	Melting point
EI	Electron Ionization		
Em	Emission		

Abbreviations

Me	Methyl	$sp/sp^2/sp^3$	$sp/sp^2/sp^3$ Hybridisation
MeOH	Methanol	t	Triplet
mg	Milligram	TEBA	Benzyltriethylammonium chloride
MHz	Megahertz	TFA	Trifluoroacetic acid
min	Minute	td	Triplet of doublets
mL	Milliliter	THF	Tetrahydrofuran
mmol	Millimole	TIPS	Triisopropylsilyl
Ms	Mesyl	TIPSA	Triisopropylsilylacetylene
MS	Mass Spectrometry	TLC	Thin layer chromatography
nm	Nanometer	TMEDA	Tetramethylethylenediamine
NMR	Nuclear Magnetic Resonance	TMS	Trimethylsilyl
o	Ortho	TMS	Trimethylsilylacetylene
OPE	Oligo(<i>para</i> -phenyleneethynylene)	Ts	Tosyl
p	Para	UPLC-MS	Ultra-Performance Liquid Chromatography Mass Spectrometry
PE	Petroleum ether	UV	Ultraviolet
Ph	Phenyl	Vis	Visible
PPE	Poly(<i>para</i> -phenyleneethynylene)	δ	Chemical shift
ppm	Parts per million	λ	Wavelength
PPTS	Pyridinium p-toluenesulfonate	ν	Wavenumber [cm^{-1}]
q	Quartet	τ	Lifetime
R_f	Retention factor	ϕ_f	Fluorescence quantum yield
RT	Room temperature		
s	Singlet		
sat.	Saturated		
SOMO	Single Occupied Molecular Orbital		

1 Introduction

Conjugated organic compounds are intensely investigated as materials for field-effect transistors,^[1] solar cells^[2] and fluorescent sensors.^[3] Impressive performance of organic light emitting diodes^[4] led to fast expansion of OLED-screens, owing to their excellent color rendering and power efficiency (**Figure 1**). The main benefits proposed by organic materials are transparency, flexibility and often lower production costs. Using of printing techniques^[5] for creating conducting circuits allows developing of fast and cost efficient production. The common property of modern organic conducting materials is the presence of the developed π -conjugated system,^[6] which promotes electron mobility and so improves charge transport.

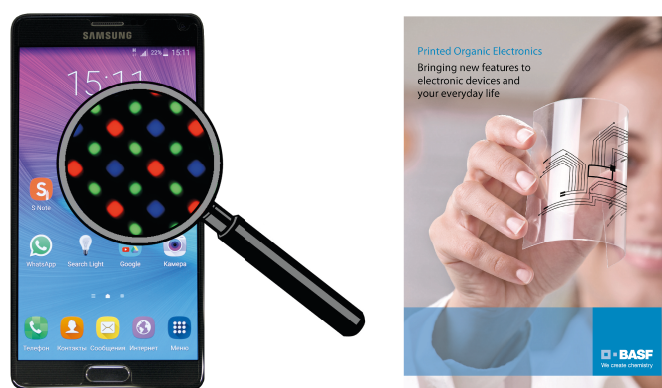


Figure 1. Left: Smartphone Samsung Galaxy Note 4 equipped with OLED-screen.^[7] Inlet: 50x-magnified matrix photo demonstrates subpixel structure. Right: Production of printed organic electronic devices. Advertisement brochure from BASF. Reproduced with permission of BASF SE.

Diverse compounds with molecular,^[8] oligomeric,^[9] or polymeric^[10,11] nature possess useful properties for organic electronics. A well-researched polymer type are poly(*para*-phenyleneethynylene)s (**1**),^[12] PPEs (**Figure 2**). PPEs consist of series of benzene rings connected together through acetylene moieties. Molecules are one-dimensional and straight, with high rigidity and have only one degree of freedom, the rotation of benzene rings around their acetylene axis.

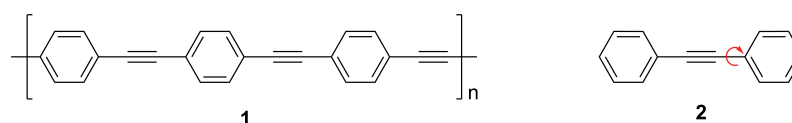


Figure 2. Structures of poly(*para*-phenyleneethynylene) (**1**) (three repetition units shown for better visual perception) and diphenyl acetylene (tolane, **2**).

The twist angle between two neighboring rings has a decisive influence on the π -conjugated system. It affects electron mobility along the chain, which is responsible for conductive and photophysical properties of the polymer. The most simple unit, which can represent the π -electron system of poly(*para*-phenyleneethynylene), is diphenylacetylene (**2**), tolane.^[13] Focused on tolane as model building block, study of the rotational isomerism and its influence on electronic properties can be transferred on PPEs and facilitate development of new beneficial materials.

2 State of knowledge

2.1 Common information about tolane

Tolane (diphenylacetylene) consists of two benzene rings connected over an acetylene spacer and is a colorless solid melting at 60-61°C.^[14] The linear rigid structure of the triple bond leaves only one degree of freedom to the molecule: the rotation of benzene rings around the C_2 symmetry axis. This influences the overlapping of molecular orbitals and, therefore, the coupling degree between both rings. Coplanar alignment provides maximum interaction between π -orbitals and allows spreading of π -conjugation system over the molecule. Orthogonally located rings are decoupled and the conjugated system is shorter. Photophysical properties of tolane have been comprehensively studied, both theoretically^[15,16-18] and experimentally.^[17,19,20,21,22] The absorption and emission of tolane is located in the ultra violet and, in contrast to PPEs, fluorescing properties of tolane are rather poor. Nevertheless, along with PPEs^[10,23,24] tolane is used as a building block in many conjugated organic compounds.^[25] Based on macrocyclic PPEs **3**,^[26] carbon nano-rings^[27] show fascinating properties and can be used as a prototype for synthetically grown carbon nanotubes.^[28] Diverse dendrimers^[29] are also objects of intense studies, especially the two-dimensional carbon allotrope γ -graphyne (**4**),^[30,31,32] which is a new conducting carbon network and is capable to make concurrence to graphene^[33] (**Figure 3**).

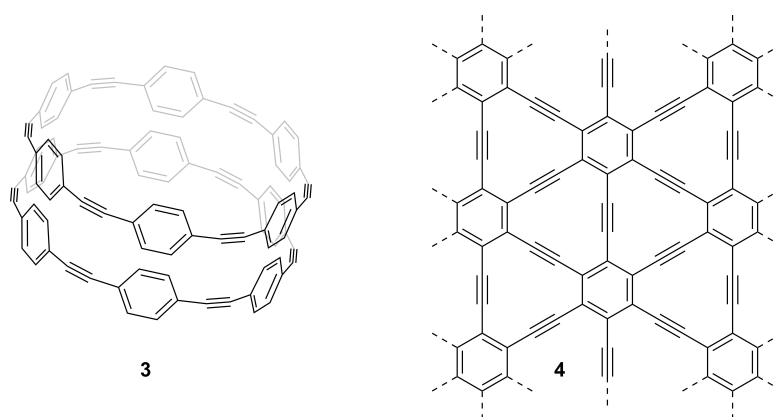


Figure 3. Structure of cyclic PPEs **3** and fragment of γ -graphyne (**4**) network.

Because of their specific electronic and photophysical properties, tolane and its derivatives find applications as useful conductive materials,^[34] switching units^[35] in molecular wires,^[36] as well as components of molecular electronic devices^[37] and even “nanocars”.^[38] Liquid crystalline^[39] properties of tolane derivatives are also under intense research due to the structural rigidity of

this structure motif. Photonics^[40] and medical^[41] applications, for example for live-cell imaging^[42] or cancer therapy,^[43] are less evident, but also fields of research.

2.2 Rotational isomerism and conformation lock

Rotation around the C_2 symmetry axis in the molecules like biphenyl (**5**) or tolane (**2**) causes significant changes in conformation-driven properties. During rotation of the benzene units, repulsive forces appear between parts of the molecule, if they come close to each other. These forces and other conformation defining factors counteract further movement and an additional energy is needed to overcome them. This energy amount, the rotational barrier, is compared with thermal energy $k_B T$, which at room temperature equals ca. 0.025 eV, or ca. 200 cm^{-1} . Lower rotational barrier values are neglected and rotation can be considered as free.

Tolane has a rigid-rod structure, whereby conformation changes by rotation of the benzene rings only.

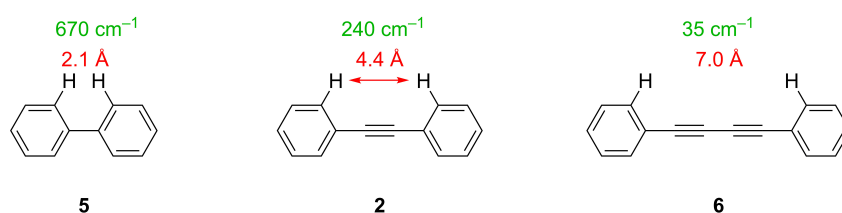


Figure 4. Rotational barriers (green) and H-H-distances (red) of chosen compounds.

The hydrogen atoms of biphenyl molecule (**5**) are located close to each other and the rotation is problematic (**Figure 4**).^[44] Increasing the distance from 2.1 \AA in **5** to 4.4 \AA in tolane (**2**) reduces the rotational barrier by two third.^[18,19,45] In 1,4-diphenylbutadiyne (**6**), where the phenyl rings are separated by two acetylene units, rotation is practically barrierless.^[46,47] For three examples from **Figure 4** favorable in-plane alignment of the phenyl rings is achieved for DPA **2** and DPB **6**. Due to strong repulsion between hydrogen atoms, biphenyl (**5**) has a 44° twisted conformation.

Substitution of the α -hydrogen atoms in tolane with sterically more demanding atoms or groups can be used to adjust the rotational barrier and the twist angle. This strategy was realized *in silico* using halogenated DPA derivatives **7a-c**, where substituent size rises from fluorine to bromine (**Figure 5**).^[48]

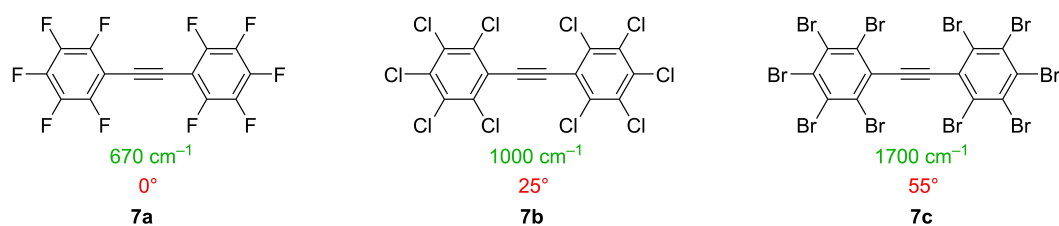


Figure 5. Calculated rotational barriers (green) and computed twist angles (red) of halogenated tolane derivatives.

Despite perfluorinated **7a** showed a rotational barrier equal to that of biphenyl (**5**, **Figure 4**), predicted planar conformation in the solid state was confirmed by X-Ray investigation.^[49] Repulsive interaction of larger α -chlorine atoms in both rings forced the molecule **7b** to take a twisted conformation, which was more noticeable by sterically more demanding bromine atoms in **7c**.

Introduction of bulky groups in the *ortho*-positions of phenyl rings also allows controlling rotamer distribution. *Para*-tolyl and mesityl substituents in α -positions of **8**^[50] and **9**^[51] respectively lead to a cumulative rise of the rotational barrier (**Figure 6**).

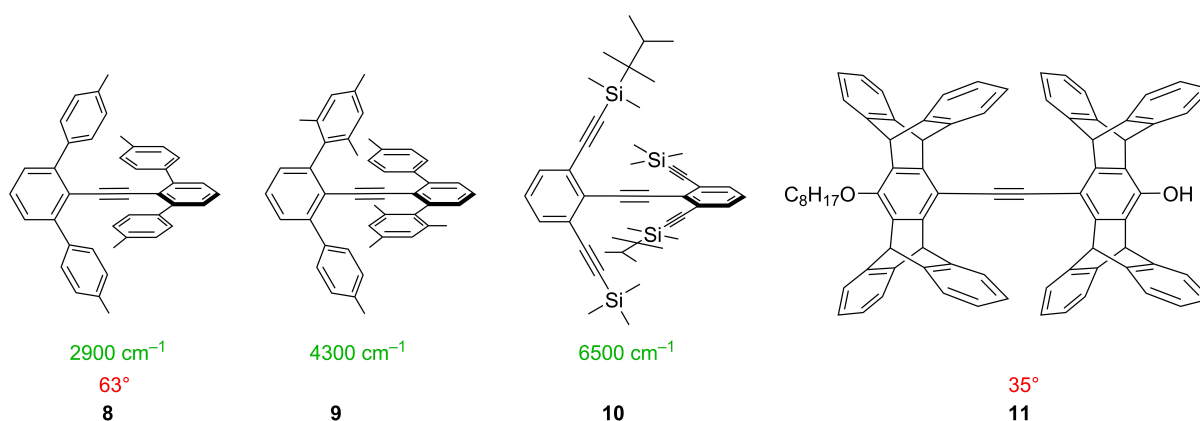


Figure 6. Twisted tolanes with restricted rotation because of bulky substituents. If known, rotational barriers shown green, twist angles shown in red.

Restricted rotation was detectable by NMR for the “exploded biphenyl” **10**.^[52] Even though planar conformation is not possible for pentiptycene substituted **11**, the twist angle in the solid state was moderate.^[53,54]

Hydrogen bond is another type of non-covalent interaction, capable restricting of the rotation in the tolane derivatives (**Figure 7**). Molecule **12** has a forced planar conformation in the solid state,^[55] whereas dicarboxylic acid **13** meets significantly less rotational hindrance, but was predicted to have a twisted structure.^[56] Complementation of the hydrogen bonding with a covalent linker led to a slightly twisted tolanophane **14**, while analog **12** was planar.^[57] Detected

by authors increased fluorescence quantum yield, accompanied by rise of the twist angle, possibly was due to the M-donating alkoxy-substituents.

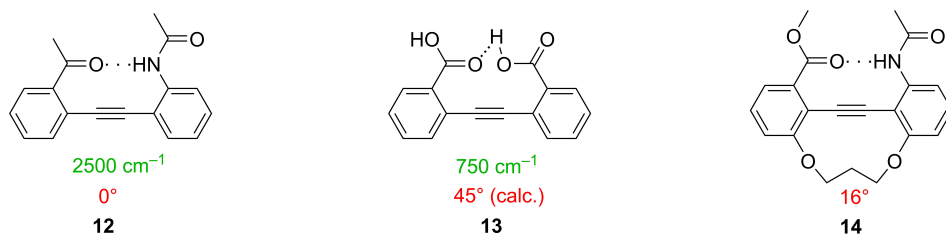


Figure 7. DPA derivatives with restricted rotation through hydrogen bonds. Rotational barriers shown green, twist angles shown red.

Fixing the position of the benzene rings is achieved by tethering them through a covalent-bound linker.^[58] Complete revolution is excluded in this case, and the (twisted) conformation of the tolane backbone is predefined by conformation of the linker. The first studied linkers with tolanes were glycols (**Figure 8**).

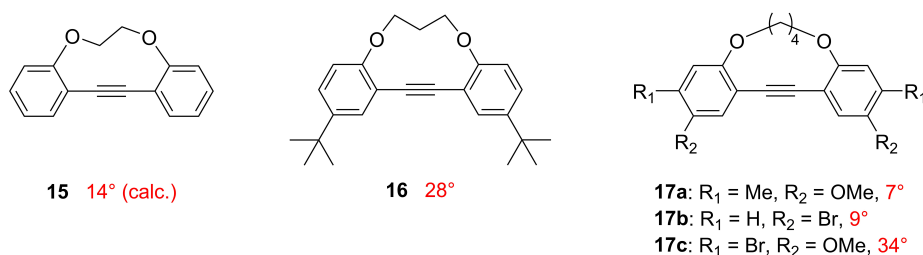


Figure 8. Tethered tolanes with diol linker. Twist angles shown in red. Theoretically predicted torsion are signed with (calc.).

Some twisting was predicted for the tolanophane **15** with the shortest tether. While having looser bounding, **16** was much more twisted in the solid state.^[59,60] The length of the tether has an important, but not the decisive influence on the torsion angle in the resulting tolanophane molecule. This tendency can be demonstrated by group of differently substituted tolanes having the same tether **17a-c**.^[61,62] In these cases, conformation in the solid state was determined by the substituents, which could not limit the rotation sterically. No correlation rule can be given, but specific packing seems the most probable explanation. In solution, where molecules are more flexible, conformational differences between **17a-c** would probably be less remarkable. Additionally, variable-temperature NMR study of the bridged tolane **15** revealed interactions between CH₂-group and the triple bond, which influenced the tether conformation.^[63]

Several dibenzylalcohols were used as a bulky tethers for tolane derivatives **18a,b** and **19** (**Figure 9**).^[64]

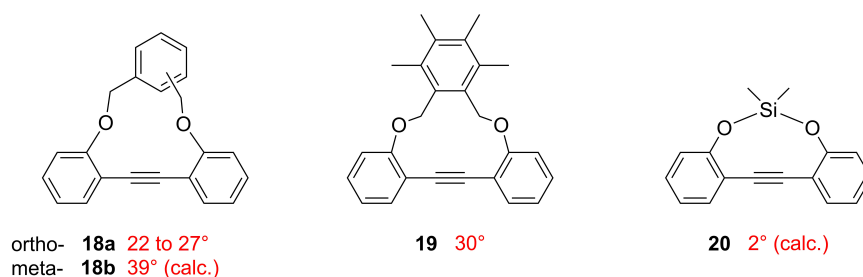


Figure 9. Structures of twisted tolanes **18a,b**, **19** and **20**. Twist angles shown in red. Theoretically predicted torsions are signed with (calc.).

X-Ray analysis of single crystals of **18a** showed presence of three moderately twisted rotamers within a crystal cell unit. Theoretical calculation of the dihedral angle in the ground state suggested a higher value (59°). Tetramethylation of the linker in **18a** led to **19** with minimal twisting increase. A planar conformation was predicted for the nine-membered tolanophane **20**, with the shortest possible linker.^[60]

Applying various ester tethers to the tolane backbone allowed screening the correlation between the nature of the linker and tolanophane conformation in **22a-h** (**Figure 10**).

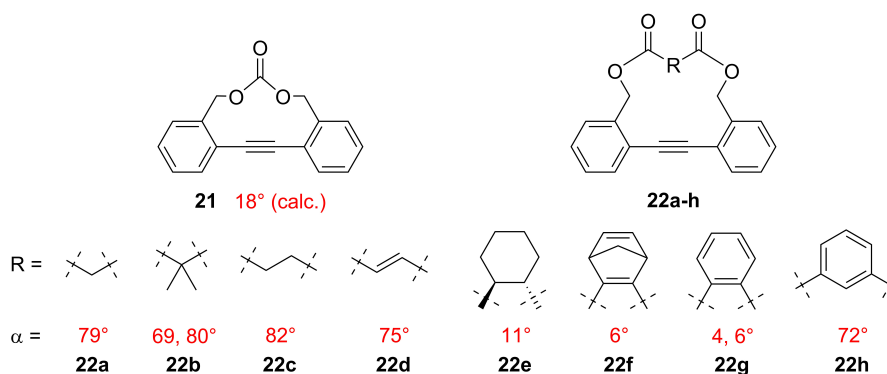


Figure 10. Twisted tolanes with ester linker. Twist angles shown in red. Theoretically predicted torsion is signed with (calc.).

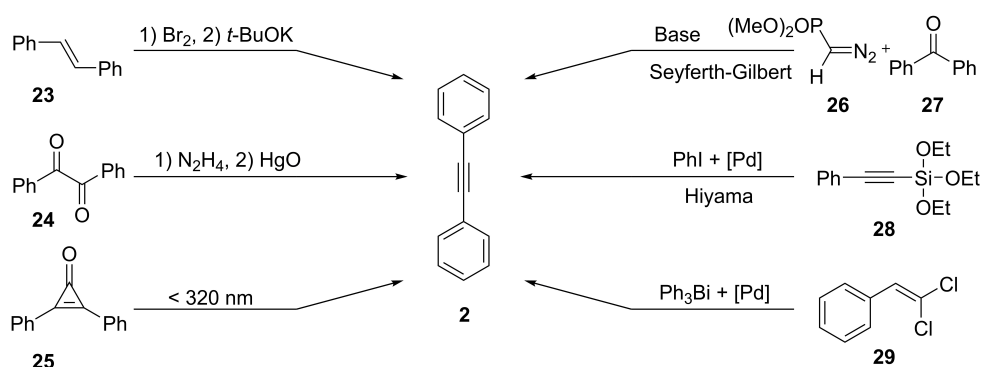
Phosgene bridged **21** was not analyzed crystallographically,^[65] but a series of diester-bridged tolane derivatives **22a-h** showed the whole spectrum of possible twist angles, starting from practically orthogonal **22a** to planar **22g**.^[66,67] Sterical parameters of the linker appear to be not as important, as its conformation. This strategy demonstrates how any specific torsion angle in tolanophane can be preserved using an appropriate tether. However, direct prediction of tolanophane conformation for a particular tether is difficult.

2.3 Methods of synthesis

This chapter deals with synthetic pathways to macrocyclic tolane-based compounds. In the first part, different approaches towards the tolane core unit are described; whereas the second part is devoted to the most important methods to build tolanophanes.

2.3.1 Diphenylacetylene core construction

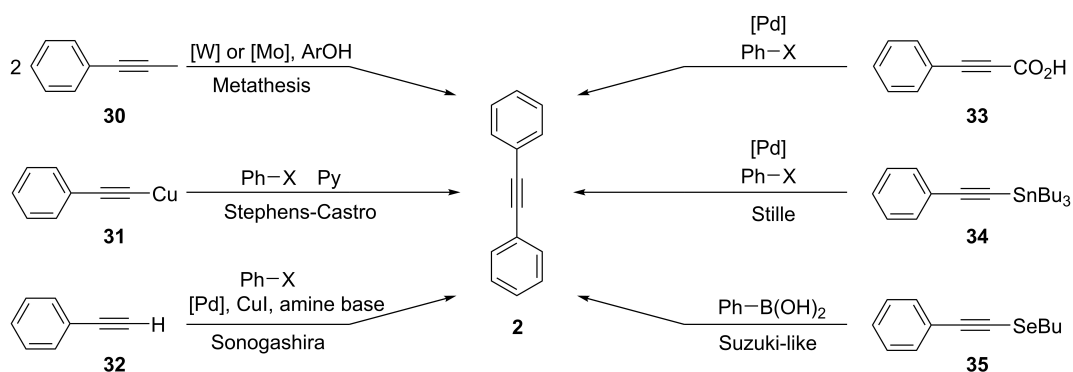
Tolane (**2**) is known for almost 150 years and many synthetic pathways have been developed to access the diphenylacetylene unit. **Scheme 1** represents some useful strategies.



Scheme 1. Different synthetic routes to tolane.

Bromination of *trans*-stilbene (**23**) followed by dehalogenation^[14] is the first published^[13] tolane synthesis and affords the desired product with a high and reproducible yield. Another long standing synthetic approach to tolane is oxidation of benzil hydrazone with mercuric oxide.^[68] Photo-induced dissociation of diphenylcyclopropenone (**25**)^[69] completes in ca. 500 fs, which makes it one of the fastest known photochemical reactions today.^[70]

Reactions shown on **Scheme 1** have mostly academic or historical impact, because of little variability or implying using rather rare reagents, like diazophosphonates **26** in Seyferth-Gilbert reaction^[71] or its later Bestmann modification.^[72] Nevertheless, palladium-catalyzed coupling of aryl-bismuth compounds^[73] and Hiyama reaction^[74] are good examples of modern approaches leading to tolanes. From a practical point of view, cross-coupling reactions^[75,76] together with alkyne metathesis^[77] are mostly used today. Some useful examples are outlined on **Scheme 2**.



Scheme 2. Cross-coupling reactions and alkyne metathesis used to obtain access to tolanes.

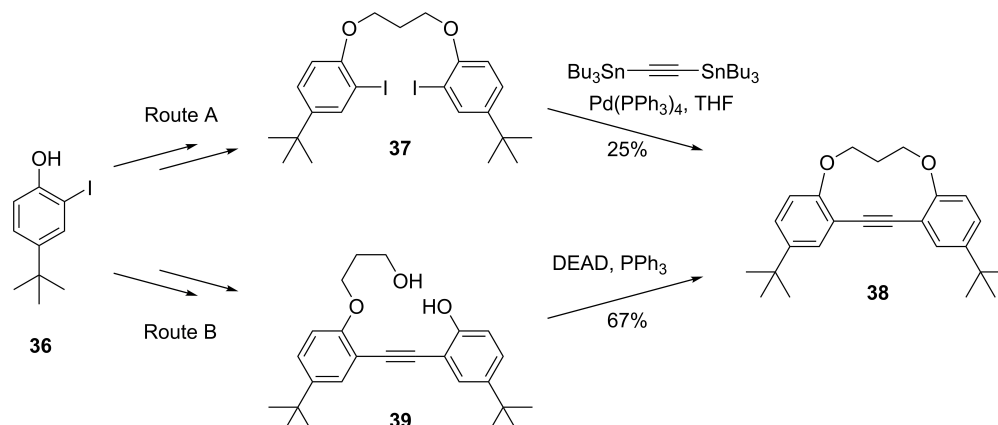
Decarboxylation-accompanied coupling^[78] and the organoselenium variation of Suzuki reaction^[79] open access to more complex tolane derivatives. Organo-tin compounds, used in Stille coupling,^[80,81] are hazardous materials. Alkyne metathesis^[82] opens accesses to tolanes, as well to poly(*para*-phenyleneethynylene)s, but can be accompanied by undesired alkyne polymerization.^[83] Emerging as further development of the Stephens-Castro reaction,^[84] the Sonogashira coupling^[85,75] is widely used for tolane synthesis. In contrast to alkyne metathesis, the Sonogashira reaction is suitable for synthesis of heteropolymeric oligomers and PPEs. Using acetylene gas, symmetric products can be synthesized in one step.^[86] Mild reaction conditions and high tolerance to functional groups stimulated development of a never-ending variety of Sonogashira reaction modifications: involving TMS-protected acetylenes,^[87,88] using immobilized recyclable catalyst^[89] or employing photo-promoted reactions.^[90]

2.3.2 Approaches to tolanophanes

A number of the cyclizing strategies leading to tolanophanes have been developed, but it is still an active field of research.^[91] Synthesis of the targeted cyclic structures always involves macrocyclization as a challenging benchmarking step because of competing intermolecular polymerization. Experimental approaches to macrocycles with DPA-subunit can be divided into two groups, depending whether the macrocyclization step includes tolane core construction or not (**Scheme 3**).

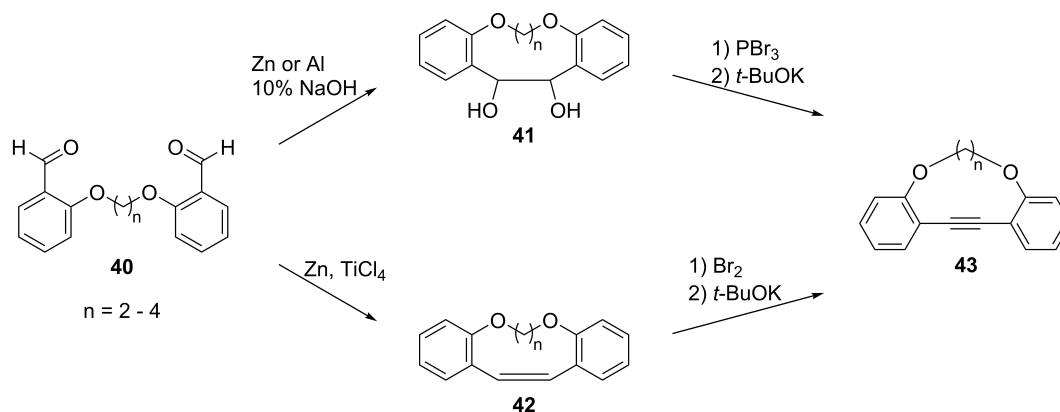
Synthesis^[60] of tolanophane **38** was achieved in two ways using Stille^[80,81] or Mitsunobu^[92] conditions in the cyclization step. Following route A, the total yield of **38** was rather low with 6% over 3 steps, compared to 43% and 7 steps for route B. Both cyclizations were carried out in high dilution conditions (0.002M and 0.009M for route A and B respectively). Higher concentrations

of 0.03M in route A lowered the yield to 18%. Route B was shown to be efficient also with a more strained ethylene glycol tether.



Scheme 3. Comparison of two possible ways to create tolanophane **38**.

Significantly better results have been obtained starting with the pre-tethered reactants under pinacol^[93] or McMurry^[94] coupling conditions, in which the cyclization step is facilitated by the formation of less strained vicinal diols and alkenes respectively (**Scheme 4**).



Scheme 4. Using aldehydes coupling reaction for tolanophanes synthesis.

The dialdehydes **40** reacted with aluminum or zinc in aqueous NaOH/ethanol solution giving the corresponding pinacols **41** in yields of 40-70%.^[95] Use of aluminum was more effective, but zinc-mediated reaction provided less by-products, although in both cases complete conversion was unachievable. Changing the solvent to polyethylene glycol (PEG-300) significantly increased the yields (92-95%).^[96] Subsequent substitution of hydroxy groups to bromine followed by elimination gave the desired tolanophanes **43** quantitatively. In presence of low-valent titanium the dialdehydes **40** coupled with a yield 75-85% to the alkenes **42** (E/Z \approx 2:1), together with 5-10% of dimer **44** (**Figure 11**).^[61,97]

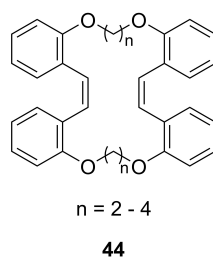
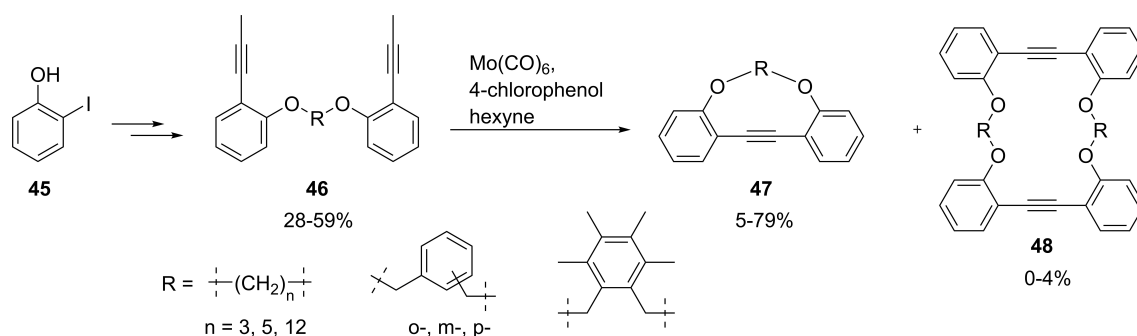


Figure 11. Dimeric byproduct in McMurry reaction.

Subsequent bromination and elimination gave the desired cyclic tolanes **43** in almost quantitative yields (90-95%). If the McMurry reaction was performed at room temperature, vicinal diols **41** could be isolated instead of alkenes **42** (yields 65-75%),^[98] which could be converted to tolanes by the described methods.

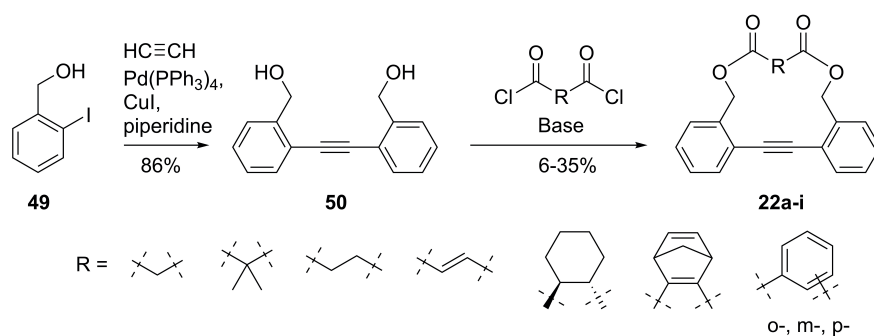
Ring closing alkyne metathesis is an alternative to access diether-linked tolanophanes. Available from *o*-iodophenol (**45**) through Sonogashira reaction with propyne, diynes **46** reacted in the presence of preactivated $\text{Mo}(\text{CO})_6$, giving cyclophanes **47** after multiple chromatographic purification (**Scheme 5**).^[99]



Scheme 5. Ring closing alkyne metathesis approach to tolanophanes.

Cyclization yield appeared to be critically dependent on aliphatic linker chain length, but dibenzyl-based tethers showed close results (18-19%).^[64] Similar to McMurry reaction, small amounts of the dimers **48** were separated in several examples.

Preliminary synthesis of the diphenylacetylene core allows testing various linkers on the same substrate. Symmetrical tolane **50**, easily accessible in a one-step Sonogashira coupling of *o*-iodobenzyl alcohol (**49**) with acetylene gas,^[100] was comprehensively exploited for studies (**Scheme 6**).^[66,67,18]



Scheme 6. Synthetic route to tolanophanes tethered with dicarboxylic acids.

Series of conformationally strained tolanophanes **22** were synthesized by cyclization of diols **50** with chlorides of diverse dicarboxylic acids^[66,67,101] as well as phosgene (for product see **21**, **Figure 10**).^[65] Yields varied from low to medium due to competitive polymerization, but the synthetic procedure was shown to be convenient and rapid.

2.4 Electronic and optical properties of tolane

2.4.1 Interaction of light with materials

Nearly all substances can absorb electromagnetic radiation in visible and ultraviolet region (light) resulting in obtaining extra energy, which is stored or dissipated. Classes of compounds, including tolane, release energy in form of light. To visualize the basic processes leading to emission of light by a substance, a Jablonski-diagram can be used (**Figure 12**).^[102]

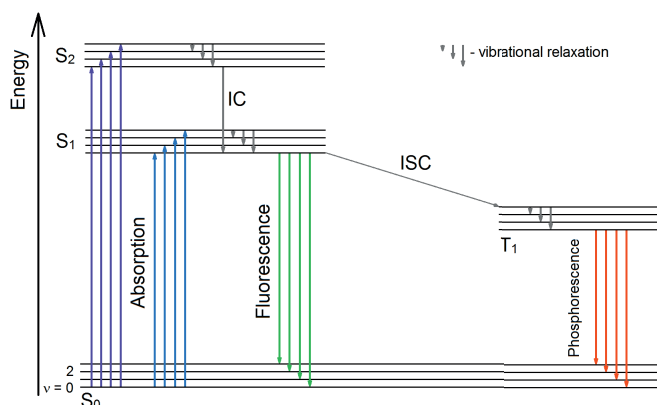


Figure 12. Typical Jablonski-diagram.

After absorption of light the molecule is excited from the ground state (S_0) into a higher energy level (singlet excited states S_1, S_2, \dots, S_n), where it is often also vibronically excited, according to the Franck-Condon principle.^[103] This process (excitation) takes only 10^{-15} s, during which the geometry of the atomic nuclei do not change (Born-Oppenheimer approximation).^[104] Parts of

the energy can be non-radiatively dissipated through rotational or vibrational movement. The process, internal conversion (IC), is a bit slower (10^{-12} s). It results in the lowest excited state (S_1 , $\nu = 0$), from which (Kasha rule)^[105] some molecules relax into the ground state by emitting a light quantum (fluorescence). Since a part of the energy was lost during internal conversion and vibronic relaxation, the emitted light has a longer wavelength (less energy) than the absorbed (red-shift). This difference is the Stokes-shift^[106] and is defined by the difference between absorption and emission maxima. One more radiationless process (intersystem crossing, ISC) is the transition from S_1 to T_1 (triplet excited state). It is spin-forbidden and occurs only at enough spin-orbital coupling. From the T_1 -state, a spin-forbidden radiation can take place, called phosphorescence. Lifetime of the S_1 -state (“fluorescence lifetime”) is about 10^{-9} s, while the timescale for phosphorescence is much longer – up to several seconds.^[107]

2.4.2 Interaction of light with a tolane molecule

In the ground state (1^1A_g) tolane molecule is in planar conformation (symmetry group D_{2h}), when π -coupling between terminal benzene rings is maximal. Charge density measurements show an ellipticity degree of the triple bond of ca. 0.25, which implies a strong conjugation level in the molecule.^[108] This is in accordance with theoretical studies, which show, that the triple bond becomes shorter by twisting the benzene rings (from 1.24 Å to 1.23 Å)^[18] and therefore closer to that in acetylene (1.20 Å),^[109] where ellipticity is zero.

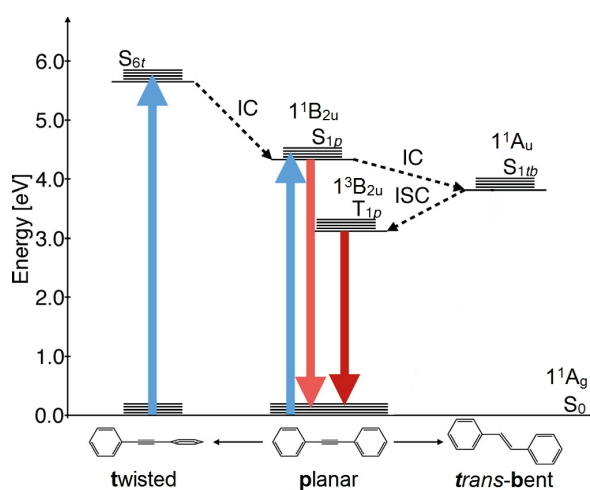


Figure 13. Simplified energy and transitions for a tolane molecule. Adapted with permission from reference.^[18] Copyright (2017) American Chemical Society.

After excitation and initial vibrational and IC relaxation the molecule reaches the excited state 1^1B_{2u} , from which according to Kasha rule radiative decay into 1^1A_g level (fluorescence)

occurs.^[105] The 1^1B_{2u} conforms to the lowest excited state (S_1) for planar and higher (S_6) for twisted (**Figure 13**).^[16,18]

In the excited state, lengths and multiplicity of triple and single bonds partly equilibrate,^[110] and the rotational barrier increases. This leads to a cumulenic-quinoidal structure,^[111] which is common for both initially planar and twisted tolane forms.^[18] This correlates with experimental fluorescence spectra, which show practically no difference for planar as well as twisted tolanes.^[66,67] An additional relaxation from the 1^1B_{2u} state is an internal conversion into a 1600 cm^{-1} lower lying other excited state (1^1A_u), called a dark state.^[112] For a long time it has been thought to be emissionless, until a weak band at 380 nm was related to it.^[22] In the dark state the tolane molecule has a *trans*-stilbene-like structure (symmetry group C_{2h}) with two electrons located on n^* -orbital similar to azobenzene (**Figure 14**).^[18]

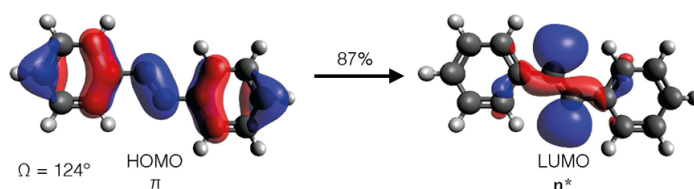


Figure 14. Hartree-Fock orbitals involved in the transition from 1^1A_g to 1^1A_u for a *trans*-stilbene-like structure. Adapted with permission from reference.^[18] Copyright (2017) American Chemical Society.

Transition from 1^1B_{2u} to 1^1A_u proceeds through an activation barrier, calculated^[18] to approximately 1400 cm^{-1} , which corresponds to ca. 900 cm^{-1} measured^[30,113,31] due to non-equilibrium energy excess after photoexcitation. The energy barrier explains the experimental decrease of the fluorescence quantum yield of tolane at elevated temperature or excitation energy. In both cases, population of the dark state is promoted and therefore non-radiative relaxation occurs.

The lowest triplet state (1^3B_{2u}), where the tolane molecule has a triple bond (D_{2h} symmetry) again,^[20,114] is populated through an intersystem crossing from the 1^1A_u state. The triplet state has a lifetime of about $1\text{ }\mu\text{s}$ and from this state phosphorescence occurs. The advantage for the molecule of the 1^1A_u to 1^3B_{2u} transition consists in the coupling of one of the π -bonds with the aromatic systems of benzene rings. The second π -bond is localized within the acetylene unit, which enhances spin-orbital coupling and therefore phosphorescence quantum yields.^[115] Experimentally, excluding some special cases,^[116] phosphorescence spectra of tolane can be observed at 77K only from species with twisted conformation in the ground state, while planar tolane shows fluorescence only.^[66] After excitation followed by planarization, twisted species

possess an energy excess, which is enough to pass the barrier between 1^1B_{2u} and 1^1A_u states.^[18] Planar tolans just relax to 1^1B_{2u} and fluoresce.

2.4.3 Photophysical properties of twisted tolans

The conjugated π -systems of the benzene rings in a tolane molecule are coupled through an acetylene moiety. The overlapping degree of the corresponding molecular orbitals defines the coupling quality and depends on the mutual position of the phenyl rings (twist angle). Adjustment of the twist angle allows to tune electronic and optical properties of tolane.^[117]

In case of near orthogonal position of the benzene units, coupling of the terminal benzene rings is lower, which results in an increased HOMO-LUMO gap.^[66] More excitation energy is needed, which is noticeable in a hypsochromic shift of the absorption maximum. In an example shown on **Figure 15**, the difference between absorption maxima of flat **22g** and twisted **22a** tolans is 27 nm.^[66]

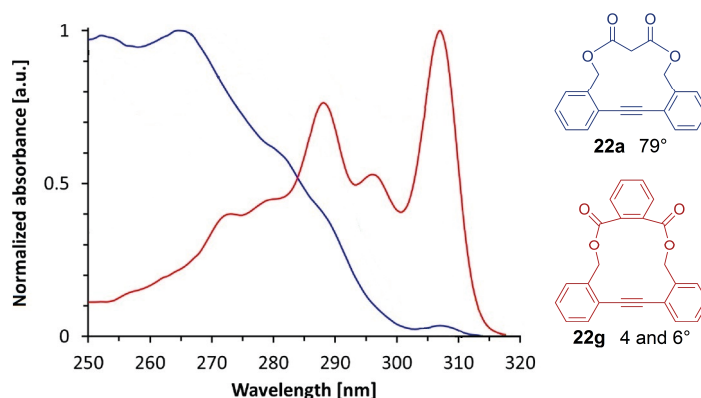


Figure 15. Absorption spectra of the ground state of planar **22g** and twisted **22a** tolans. Adapted with permission from reference.^[66] Copyright (2013) American Chemical Society.

In the solid-state, specimen with different dihedral angles can be present, while in solution molecules have a higher flexibility. Thus, absorption spectra recorded in solutions are superpositions of all possible accessible rotamers. In case of tethered tolans, the conformer composition is enriched with twisted species, as the linker is designed for preventing planarization. Otherwise, due to a low rotational barrier (ca. 200 cm^{-1}), any rotamer is present in tolane.

Since excited molecules planarize before radiative decay, the fluorescence of twisted and planar species is practically indistinguishable,^[64,66,67] and belongs exclusively to planar rotamers.^[67] For preservation of the twisted conformation tolane molecules in solution are cooled to 77K into a

solid rigid glass. In this case some tolane derivatives are unable to access planar conformation, as it was demonstrated by blue-shifted (ca. 5 nm) emission maximum of **51** (Figure 16).^[53] Additionally, at low temperature, the population of the dark state (1A_u) from excited state ($^1B_{2u}$) is reduced due to the activation barrier. This leads to a rise of fluorescence intensity and quantum yield.

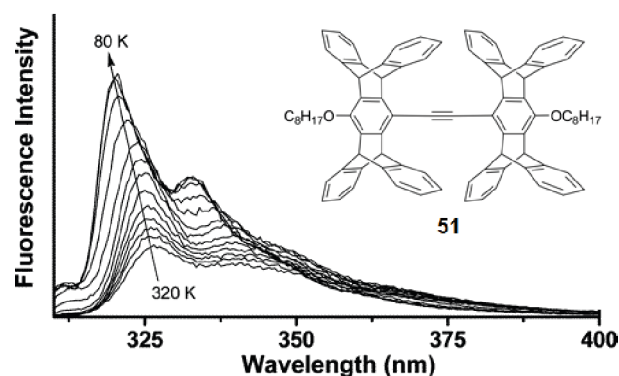


Figure 16. Blue-shifted fluorescence spectra of **51** in methyl-THF between 80 and 320 K. Adapted with permission from reference.^[53] Copyright (2006) American Chemical Society.

2.5 Elongated analogues of tolane

This part complements the main part with published data concerning extended diphenylacetylene derivatives.

2.5.1 1,4-Bis(phenylethynyl)benzene derivatives and PPEs

1,4-Bis(phenylethynyl)benzene (**52**, BPEB) is the second smallest member of the PPE family and is also intensively researched in many groups.^[118,119] Compared to tolane, BPEB is an effective fluorophore. In contrast to polymers, BPEBs possess better solubility, as well they have fixed end groups and length (like other oligomers), what leads to materials with highly reproducible properties and allows using **52** as a model compound^[120] for PPEs. Correlation between the length of the conjugated chain and photophysical properties can be visualized by comparison of the series of oligo(*para*-phenyleneethynylene)s (OPEs).^[121]

Structure of BPEB **52** resembles that of tolanes and can be defined as a rigid stick with rotation of the phenyl rings as the only degree of freedom. A greater number of phenyl rings allows to the molecule more oscillational and rotational ways for conformational changes. The twisting can be realized in two ways: twist of the end ring and in the middle (Figure 17).



Figure 17. Two possible twisted conformations of 1,4-bis(phenylethynyl)benzene (**52**).

Rotational energy barrier in both cases was estimated to be about $220\text{--}235\text{ cm}^{-1}$ in the ground state and ca. 1840 cm^{-1} in the excited state,^[122,123] which is close to respectively ca. 200 cm^{-1} and ca. 1600 cm^{-1} of tolane.^[19] The twisting angle has an essential influence on the π -conjugation between phenyl rings and, therefore, on optical and electrical properties of the molecule: planar^[124] BPEB shows several hundred times better conductivity, than twisted in single molecule devices.^[125]

Torsional distribution for PPEs in solution is usually described involving Boltzmann statistics.^[126,127] Introduction of the side substituents to OPEs and PPEs mostly does not affect directly the photo-electronic properties of the main chain,^[128] but can modify water solubility^[129] or solid-state packing.^[130,131]

Conformational control. Government over twisting conformation can be achieved through the prevention of the rings' rotation by either sterically hindrance, tether binding or other^[128,132,133] factors. Introduction of the sterically demanding groups can move the conformational energy minimum to higher twist angles (**Figure 18**).

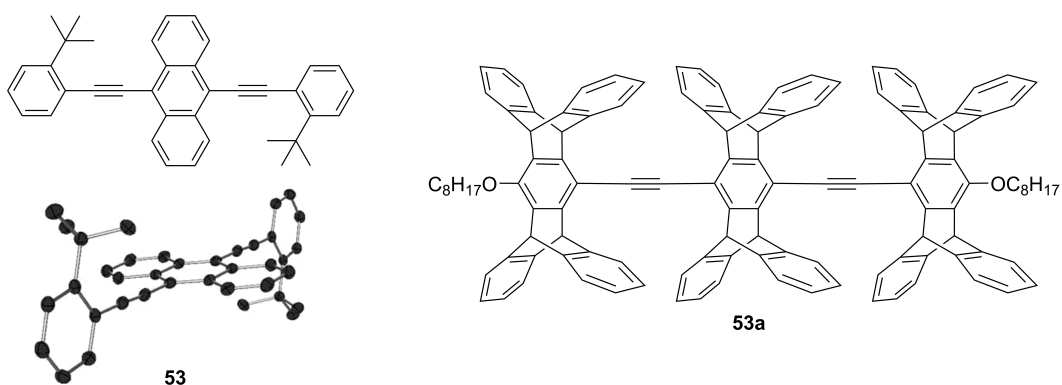


Figure 18. Sterically hindered BPEBs and derivatives. Crystal structure of **53** reproduced from reference^[134] with permission of The Royal Society of Chemistry (RSC) on behalf of the Centre National de la Recherche Scientifique (CNRS) and the RSC.

Bulky *tert*-butyl groups in the *ortho*-positions provided close to perpendicular (89°) alignment of anthranyl and phenyl moieties in the solid state of **53**.^[134] At room temperature, partial planarization was observed after excitation, but in the cryogenic glass blue-shifted absorption and emission spectra indicated, that the initial twisted conformation was preserved. For pentiptycene substituted BPEB derivative **53a**, because of large size of the substituents, a planar

conformation was less favorable both in ground and in excited state.^[53,54] Although single crystal characterization was not possible, theoretical calculations showed energy minima at 20°, 40° and 75° in the S_0 and at 20° and 75° in the S_1 states. Blue-shifted absorption and emission, longer fluorescence lifetime and higher quantum yield measured in the rigid cryogenic glass implied a twisted backbone.

Attachment of tetraphenylbenzene groups to a poly(*para*-phenyleneethynylene) core over a spacer showed a significant influence on the π -coupling system and the photophysical properties of the corresponding PPE (**54**, **Figure 19**).^[135] The effect of the bulky substituent was inversely proportional to the spacer length, providing identical optical properties in the solid state and in solution when the shortest linker (two atoms) was used.

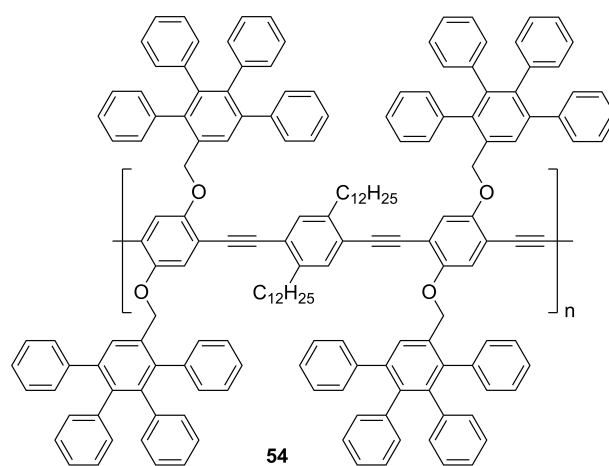


Figure 19. Sterically crowded PPE with limited rotation over the main chain.

An alternative route for fixation of the twisted conformation provides connecting of the phenyl rings with a linker. In some cases, it can bring less strain in the molecule and make synthetic attempts more fruitful. Two successful applications of this strategy are shown in **Figure 20**.^[136,101]

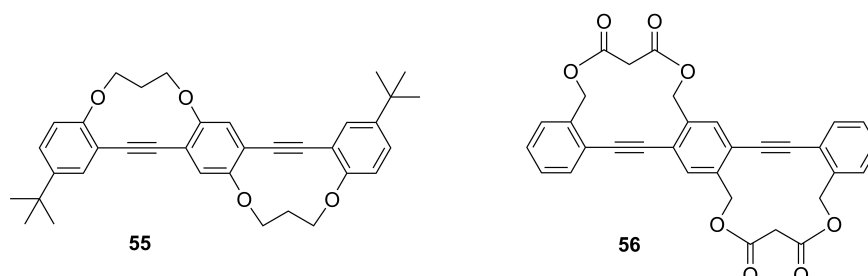


Figure 20. Tethered BPEBs.

Compared to unconstrained analogs, tethered species **55** and **56** absorbed light at shorter wavelengths. Solid-state structures and twist angles in both cases remained undetermined.

Compared to untethered ones, absorption maxima were blue shifted for 2 nm for ether **55** and ca. 40 nm for ester **56**, what implies greater dihedral angles in the case of the second. Tetraester **56** also showed a significant reduction of the fluorescence quantum yield (from 90 to 60%) compared to that of the unconstrained analog. Similar results were shown, when right-handed helical decapeptide was used as a chiral tether in compound **57b**, for which QY devaluation from 35 to 0.5% was observed (**Figure 21**).^[137]

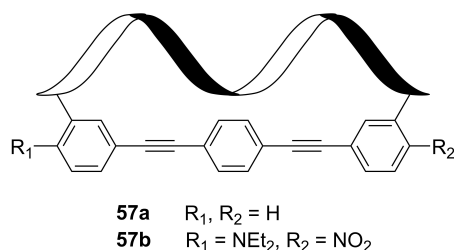
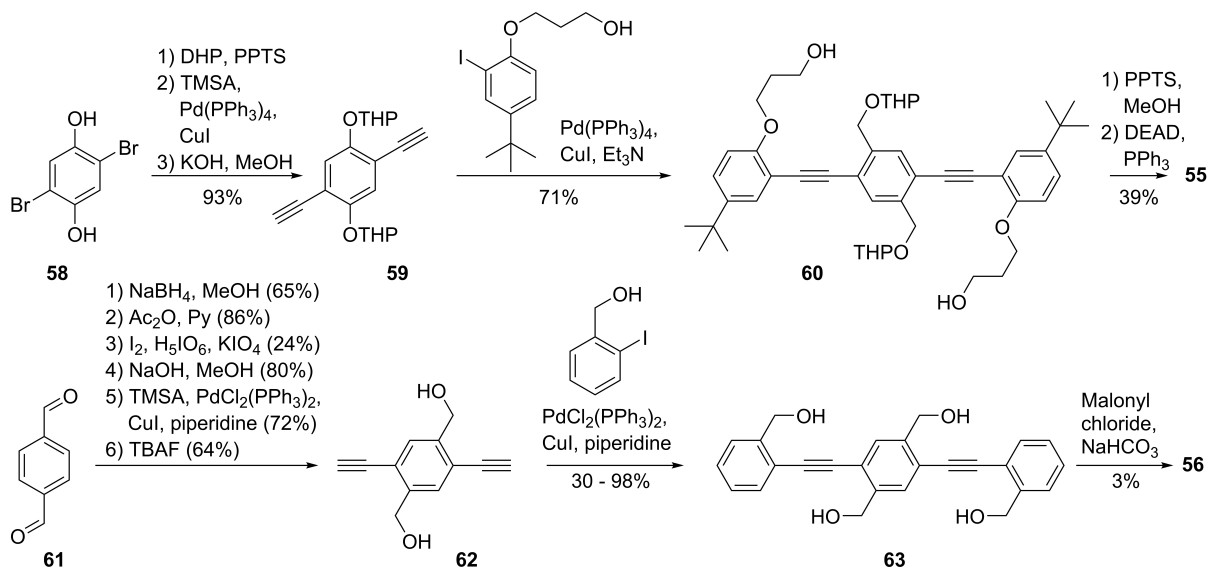


Figure 21. Chirally twisted BPEB with helical decapeptide tether.

Content of the chirally twisted conformers in **57a** was 23% at 10°C and decreasing with rise of the temperature, as it was shown by circular dichroism spectroscopy. Absorption and emission spectra of **57a** were nearly identical with that of the open-chain model compound, but significantly blue-shifted in case of the donor-acceptor modified derivative **57b**.

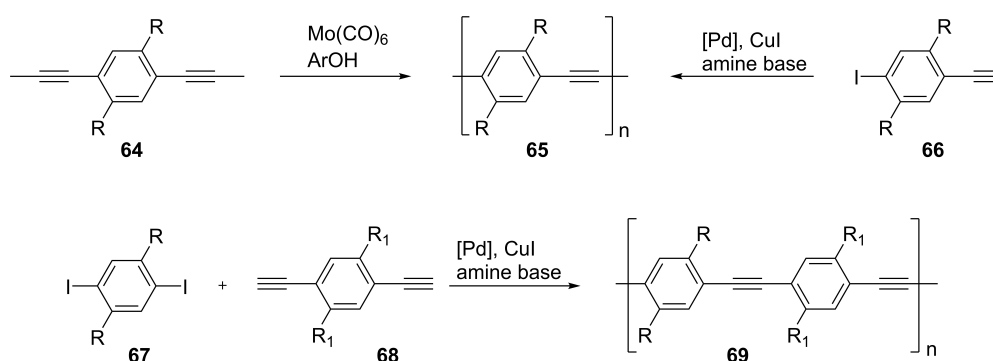
Synthesis. Synthetic approaches to oligo- and poly(*para*-phenyleneethynylene)s include construction of a functionalized π -conjugated unit, followed by introducing of substituents as well as tether. Shown in **Figure 20** molecules **55** and **56** that have been synthesized^[136,101] in similar way using Sonogashira coupling (**Scheme 7**).



Scheme 7. Total syntheses of tethered BPEBs **55** and **56** using Sonogashira reaction.

While Sonogashira couplings proceed in the most cases smoothly with intermediate to good yields, total yields of the desired products are low, due to known complications while the cyclization step (see part 2.3.2). This strategy is easily scalable to oligomers with higher molecular weight, but laboriousness increases exponentially, accompanied with proportional loss of yield.^[136]

Sonogashira coupling together with alkyne metathesis reaction are common methods in synthesis of PPEs (**Scheme 8**).^[11,24,23]



Scheme 8. Synthesis of homo- and heteropolymers (PPEs) using alkyne metathesis and Sonogashira reaction.

Alkyne metathesis gives PPEs with less dispersity, but only for homopolymers. In contrast, Sonogashira conditions open access to polymers, having two different monomeric units alternating on a regular basis. Another side of the coin is heavy controllable incorporation of the diyne fragments into the chain, which disturbs the regularity. Linked polymers have not been described in literature, but a wide spectrum of side substituents have been applied not only for solubility regulation, adjusting of rheological or packing properties, but also as sensors binding sites^[138] and conformational modifiers.^[135]

Photophysical properties. Attachment of additional phenyl rings to the π -system of the tolane elongates and enhances the conjugation within the molecule; therefore, compared to tolane, BPEB, oligo- and PPEs show a noticeable red shift in absorption and emission spectra. This tendency remains also in case of tethered twisted BPEBs, where **70** showed ca. 24 nm red shift of the absorption maximum compared to **55** (**Figure 22**).^[136]

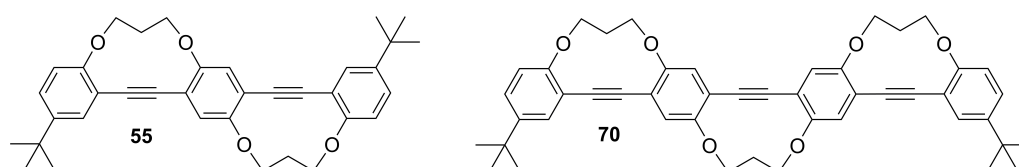


Figure 22. Tethered oligomeric phenyleneethynylenes **55** and **70** with restricted rotation.

An important aspect of the photophysical properties of BPEB and PPEs is the tendency of the molecules to aggregate because of the attraction of the π -electron systems of benzene rings (π -stacking). This effect is more noticeable when the concentration increases, reaching its maximum in the solid state. Overlapping of the π -orbitals belonging to separate molecules enhances the delocalization of electrons and impacts photophysical properties of the substance (**Figure 23**).^[139]

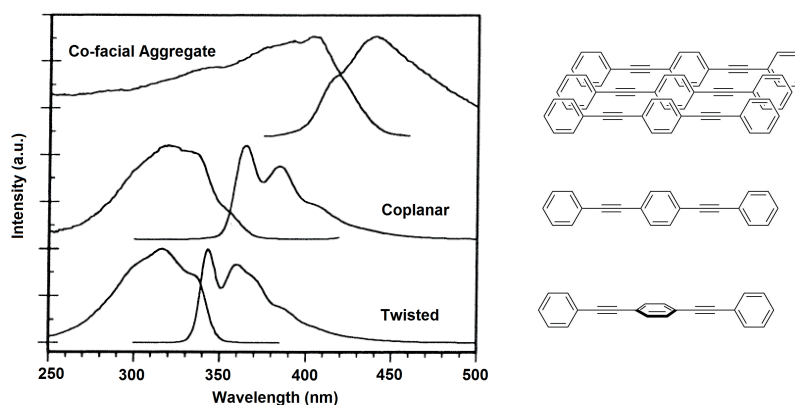


Figure 23. Excitation and emission spectra of BPEB in solution and in solid state. Adapted with permission from reference.^[139] Copyright (2001) American Chemical Society.

In case of BPEB stacked aggregates emit at 440 nm, what continues the tendency between twisted (emission maximum at 342 nm) and planar (362 nm) conformations.^[139–141] Analogous to DPA, after absorption of the light quantum BPEB moves into the first excited state (1^1B_{1u}) with chinoidal-cumulenic structure,^[111] from which molecule passes either in the ground state 1^1A_g (fluoresces)^[123] or in the dark state 1^1A_u (radiationless) (**Figure 24**).^[123]

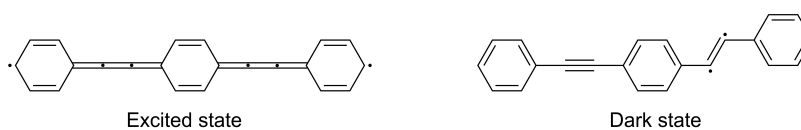


Figure 24. Schematic illustration of the excited and dark states of BPEB.

The energy barrier for transition from 1^1B_{1u} to 1^1A_u is significantly higher for BPEB (ca. 5000 cm^{-1}),¹ than for tolane (ca. 2000 cm^{-1}),¹ what makes it less favorable and promotes emissive relaxation.^[123] For this reason, the fluorescence quantum yields for BPEB are much higher (58%), than for tolane (1%), tending to 100% for PPEs.^[11,23]

¹ This value differs significantly from stated in the part 2.4.2. The reason consists in different calculation methods used by different authors. Here, both values (5000 and 2000 cm^{-1}) are taken from one source for better comparison.

2.5.2 1,4-Diphenylbutadiyne derivatives

1,4-Diphenylbutadiyne (DPB, **6**), also known in literature as diphenyldiacetylene (DPDA), is a linear molecule having two benzene rings attached to butadiyne (**Figure 25**). Despite superficial similarity of 1,4-diphenylbutadiyne to well-studied tolane, the publications amount concerning diyne systems is remarkably lower,^[142] probably due to the lack of detectable fluorescence.^[143–145]

Nevertheless, structural and electronic properties of PDB derivatives have been studied.^[146,147,148] Molecules with a butadiyne system find applications as molecular rotors,^[149] liquid crystals^[150] and fluorescent sensors.^[151] In analogy to DPA, one- and two-dimensional conducting networks,^[152] based on diphenyldiacetylene units, called graphdienes, are known, e.g., nanowires,^[153] nanotubes^[154] and nanowalls.^[155] Connected to present work, DPB attracts attention as a prolonged analog of tolane. Moreover, diphenylbutadiyne fragments are defects in PPEs.^[24] Reported improvement of the detecting properties of a PPE sensor in the presence of diyne unit,^[156] as well as possibility to suppress polymer degradation^[157] also evoke interest.

The molecule of PDB (**6**), analogous to tolane (**2**), has a stick-like structure, but in DPB the phenyl rings rotate around the acetylene bond practically without hindrance (rotational barrier in the ground state ca. 35 cm^{-1}).^[47] In solid state the benzene rings are coplanar, both in the ground and excited state the molecule has D_{2h} symmetry.^[148] The different bond length distribution and lower triple bond ellipticity (0.06) compared to tolane (0.23) are attributed to a lower conjugation degree in DPB (**6**) (**Figure 25**).^[158]

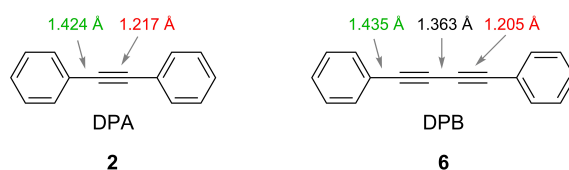
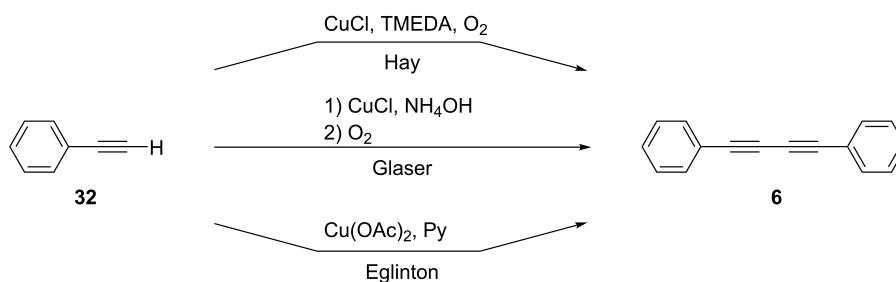


Figure 25. Comparison of the bond length values in DPA and PDB.

Synthesis. Common approach to 1,4-diphenylbutadiynes is an oxidative coupling of copper acetylenides first described by Carl Glaser.^[159] A number of modified conditions have been developed.^[160] Using coordinating diamine base by Hay^[161] and pyridine as a co-solvent by Eglinton^[162,163] allowed avoiding laborious and dangerous isolation of copper acetylenides (**Scheme 9**). Coupling under modified Sonogashira conditions^[164,165] allows involving of TMS-protected alkynes.^[87]



Scheme 9. Oxidative coupling approaches to 1,4-diphenylbutadiyne.

Photophysical properties. The absorption spectrum of unsubstituted 1,4-diphenylbutadiyne (**6**) has a vibronically resolved structure with a maximum red-shifted at ca. 30 nm, compared with that of tolane (**Figure 26**).

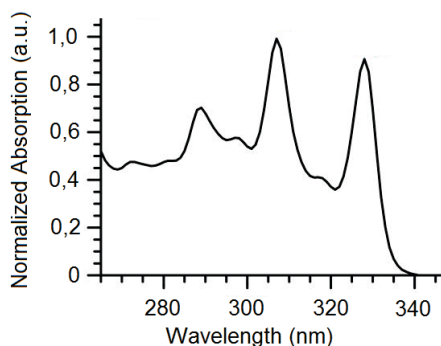


Figure 26. Absorption spectrum of DPB (**6**) in 2-methyltetrahydrofuran at room temperature. Adapted from reference^[166] with permission of The Royal Society of Chemistry (RSC) on behalf of the Centre National de la Recherche Scientifique (CNRS) and the RSC.

The longest wavelength band has been attributed to the transition between the ground (1^1A_g) and the first excited state (1^1B_{1u}),^[145] both of which have D_{2h} symmetry. The unusual thermo-induced band intensity change in the absorption spectrum supported by TDDFT-calculations showed that PDB exists as mixture of rotamers even in the cryogenic glass.^[148] In contrast to the absorption, the emission of unsubstituted PDB was reported undetectable^[143,144] or low.^[145] This was explained with a large conformational flexibility of the molecule and the close location of first excited (S_1), dark (S_2) and triplet (T_3) states, which offers non-fluorescent relaxation pathways (**Figure 27**).

Introduction of the substituents in the π -coupling system results in a broadening of the vibronic structure and a red-shift in the absorption spectrum, accompanied by a significant rise of the emission intensity.^[166,163] An aromatic ring modification in the PDB molecule allows combining of the locally excited, excimer- and exciplex-types of emission^[167,168] and design attractive fluorophores, for example single component white light emitters.^[169]

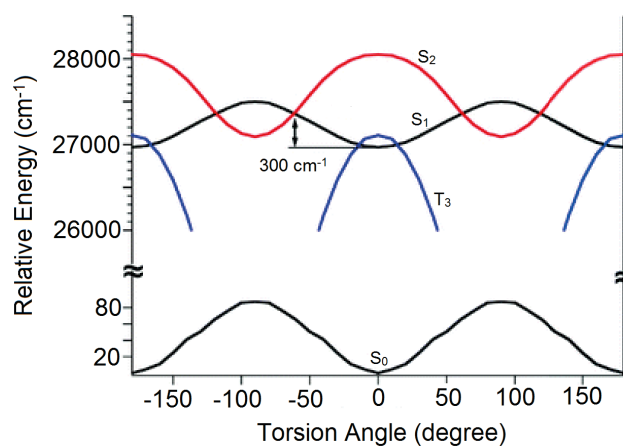


Figure 27. Torsional barriers for the ground and excited states of PDB (**6**), calculated using DFT and TDDFT B3LYP/6-311+G(d,p). Reproduced from reference^[170] with permission of the PCCP Owner Societies.

3 Results and Discussion

3.1 Aim of the work

Conjugated poly(*para*-phenyleneethynylene)s are prevalent research targets as conducting and luminescent materials. Control over electronic properties of PPEs can be provided by restricting the twist of neighboring the phenyl rings. Recently, a series of tolanophanes tethered with diester-linker have been thoroughly studied as model compounds.^[66,67,101] The present work deals with a direct restriction of the rotation in tolane molecules and a fixation of the twisted conformation. To this purpose, syntheses and photophysical characterizations of the selected bridged derivatives of diphenylacetylene, bis(phenylethynyl)benzene and other related compounds have been planned.

In detail, following objectives have been pursued. Organic conjugated compounds are known for their moderate stability. Introduction of an amide-functionalized tether instead of ester has been chosen for investigation. In this case, substances should be more robust against hydrolysis and other degradation pathways. Fitting of an additional linker has been developed to overcome possible insufficient rigidity of a single tether, which still allows planarization of tolanophanes in the excited state. Essential was the evolution from DPA to species with extended π -conjugated systems. To achieve these goals, double-functionalized π -developed tolanophane derivatives, capable of polymerization, were of interest. Parallel, double-bridged BPEB-derivative should complement transition to tethered PPEs. Bridged DPB-derivatives were also of great importance.

The described targets became of interest for thoroughly investigation. For fluorescent-active materials, ground and excited electronic states play essential roles. The ground state conformation could be investigated through X-Ray analysis of the single crystal specimens. Emission originates from the first excited state. Photophysical study of tolanophanes in solution as well in rigid cryogenic glasses was necessary for explanation of correlation between tether and its effect on opto-electronic properties of tolanes.

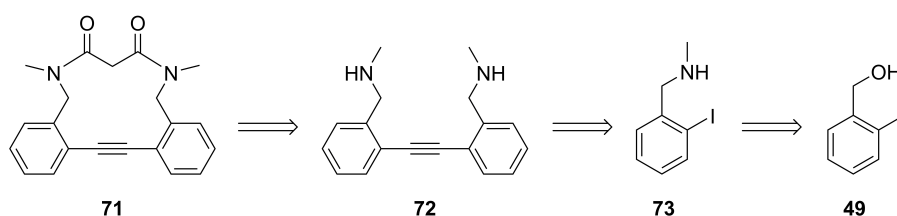
3.2 Synthesis and Properties of TolanoPhanes

In this part of the work the synthetic ways leading to the targeted molecules are described and discussed. The most important and challenging synthetic task was constructing the macrocyclic

core. Ring closing is always accompanied by polymerization.^[91,171] Commonly used reagent concentrations (0.05-0.5 M) lead to significant formation of polymers. High-diluted solution serves to prevent intermolecular interactions and suppresses competitive polymerization.

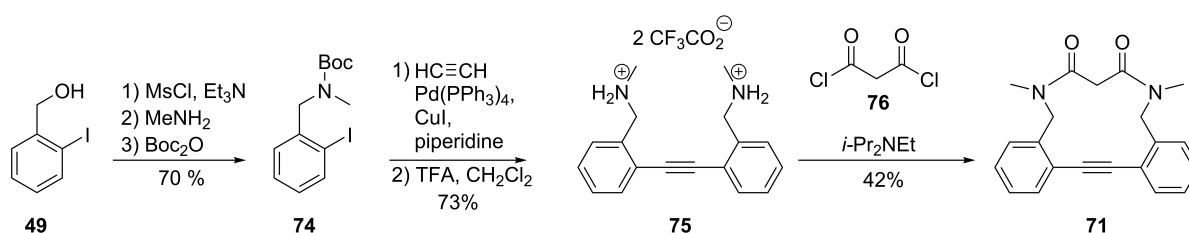
3.2.1 Tolanophanes with diamide- and amidoester tether

Construction of the macrocyclic compound **71** could be achieved in two ways: either first tether introduction, followed by ring closing (Sonogashira^[172] or metathesis),^[173] or a diphenyl acetylene core construction followed by annulation. Taking into consideration, that the straight DPA-unit is the most strained part of the tolanophane molecule, and the ring-closing step has to compete with polymerization, the second way was chosen as it is shown (**Scheme 10**).



Scheme 10. Retro synthetic route to compound **71**.

Various conditions have been tested to couple benzyl amine **73** with acetylene gas or TMS-acetylene using Sonogashira ($\text{PdCl}_2(\text{PPh}_3)_2$, $\text{Pd}(\text{PPh}_3)_4$)^[66] or Negishi ($\text{Pd}(\text{dppf})\text{Cl}_2$)^[174] procedures, without success. Chromatographic separation of the reaction mixture provided only a deep blue sticky material, unsuitable for analysis. Since amine **73** is basic and might cause adverse effects on the coupling reaction or product stability, Boc-protection was applied and the tolane **75** was isolated as bisammonium salt in a reasonable yield (**Scheme 11**).



Scheme 11. Synthetic route to diamide tolanophane **71**.

To prove the formation of the desired intermediate, a single crystal was grown. X-ray analysis showed the planar conformation of the diphenyl acetylene unit with the most distant position of the charged moieties (**Figure 28**).

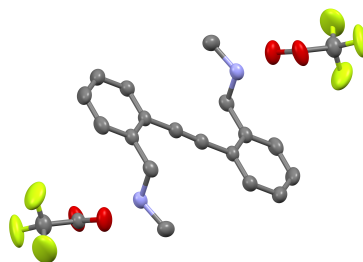


Figure 28. Ellipsoid representation of the diammonium salt **75** structure.

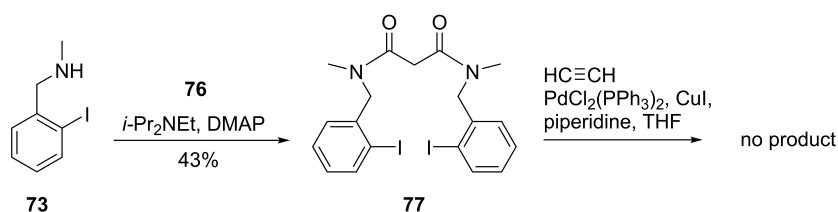
Several conditions were tested to improve the macrocyclization (**Table 1**). Methods employing CH_2Cl_2 as the only solvent did not allow the slow salt **75** addition and as a consequence showed lower product yields; the best homogeneity was achieved in acetonitrile solution, but no product was formed under this conditions (Entry 3). The best results were obtained using the high dilution procedure, *i*-Pr₂NEt as a base and mixture of CH_2Cl_2 together with acetonitrile to dissolve the trifluoroacetate **75** (Entry 4).

Table 1. Conditions for cyclization of the salt **75** to tolanophane **71**.

Entry	Solvent	Base	Conditions	Yield
1 ^a	CH_2Cl_2	Et_3N , DMAP	base added to salt, followed by malonyl chloride during 3 h	14%
2 ^b	CH_2Cl_2	Et_3N , DMAP	base added to a mixture of salt and malonyl chloride during 3 h	0%
3	acetonitrile	<i>i</i> -Pr ₂ NEt	simultaneous addition of salt and malonyl chloride to base during 4.5 h	0%
4	acetonitrile, CH_2Cl_2	<i>i</i> -Pr ₂ NEt	simultaneous addition of salt and malonyl chloride to base during 4.5 h	42%

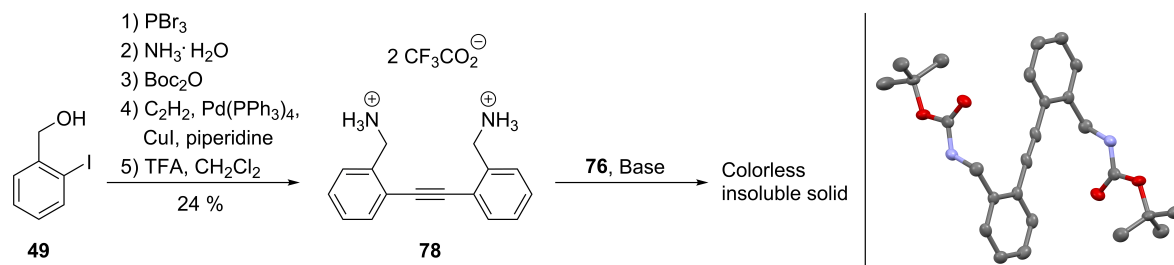
a) according to literature;^[175] b) according to literature.^[176]

To eliminate protection and deprotection steps at nitrogen atom, and shorten in this way the synthetic route, utilization of the malonic tether as acyl protective group was attempted (**Scheme 12**). Amine **73** was allowed to react with malonyl chloride to produce diamide **77** with a moderate yield, but the cyclization using Sonogashira coupling showed no product formation.



Scheme 12. Alternative route to tolanophane **71**.

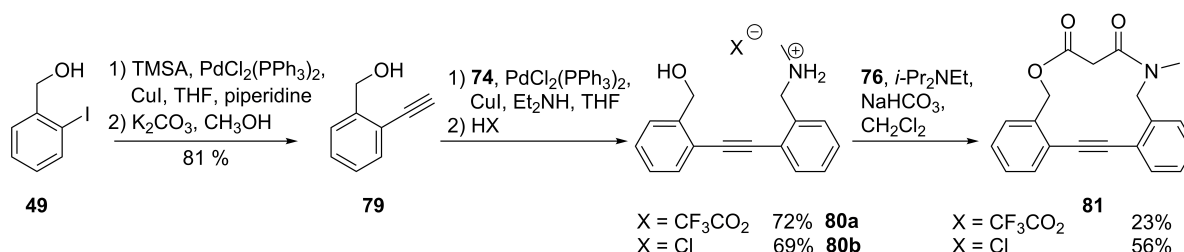
Cyclization of demethylated diammonium salt **78** was attempted according to **Scheme 13**. Absence of the methyl groups at nitrogen atoms should reduce steric hindrance and let the aromatic rings reach greater twist angles.



Scheme 13. *Left:* synthetic route to diammonium compound **78**. *Right:* crystal structure of the corresponding Boc-protected coupling product.

Diammonium compound **78** was obtained with a moderate yield without any problems, except of Sonogashira coupling reaction, where heating was needed to avoid inseparable byproduct formation. Unfortunately, several cyclization attempts led to an insoluble solid only.

Another object of interest was tolanophane **81**, having both ester and amide functions, which should be more stable, than corresponding diester made by Sebastian Menning^[66] and less strained than diamide **71**. **Scheme 14** details the synthetic path towards **81**.



Scheme 14. Synthetic route to amido ester **81**.

Addition of TMS-acetylene to 2-iodobenzyl alcohol (**49**) using Sonogashira reaction followed by deprotection gave arylacetylene **79**, which was successively coupled with Boc-protected amine **74**. Deprotection using two different acids gave salts **80a** and **80b**. The difference in yields occurred, when optimized reaction conditions were used for cyclization: chloride **80b** showed more than two times better results than trifluoroacetate **80a**. The reason might be the hydroxyl group deactivation in the salt **80a**.

For structural study, single crystal species have been prepared (**Figure 29**). Diamide **71** gave over 1 cm long high quality crystals consistent of two independent conformer with dihedral angles 43° and 58°, while the benzene rings in amidoester **81** were near orthogonal in solid state.

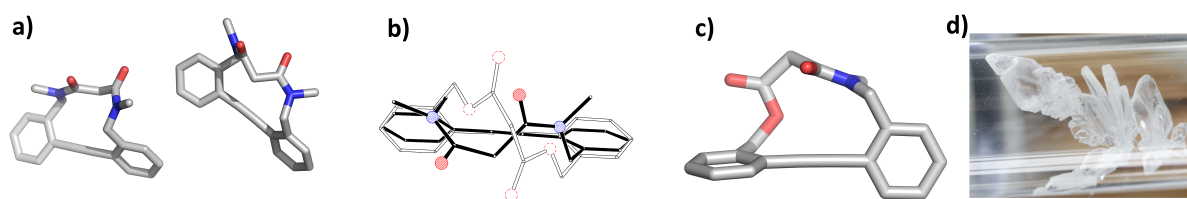
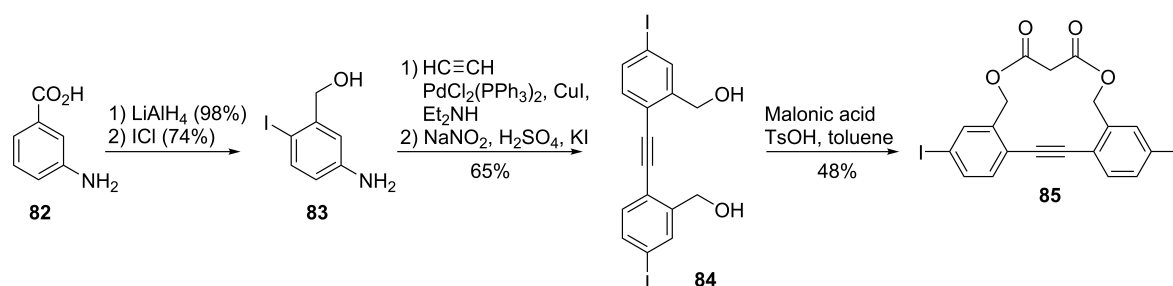


Figure 29. a) Two independent molecules of diamide **71** (twist angles 43° and 58°). b) Conformation comparison between known diester **22a** (white) and new diamide **71** (black). c) Crystal structure of amidoester **81** (twist angle 84°). d) Crystal image of **71**.

Comparison of **71** and diester **22a**^[101] revealed a conformational difference between these molecules. While benzylic CH₂-groups in ester **22a** are situated *s-cis* to carbonyls, in **71** the position is *s-trans*.

Since migrating from ester tolanophanes to amide **71** and amidoester **81** was successful, the diester was used as a model for further functionalizations. Diiodotolane **85** is a promising DPA-derivative and could serve as a starting point to many other bridged molecules with extended π -conjugation. Synthesis was realized following **Scheme 15**.



Scheme 15. Synthetic route to diiodotolane **85**.

Commercially available aminoacid **82** was reduced, and the corresponding aminoalcohol was iodinated to **83**, using ICl or I₂/NaHCO₃.^[177] Sonogashira coupling of **83** with acetylene gas followed by diazotation and Sandmeyer reaction afforded diiododiol **84**. Cyclization with malonyl chloride after several attempts gave the desired **85**, but with yield of less than 6%. Low solubility of diol **84** did not allow using the high dilution condition, and slow addition of malonyl chloride produced a complex mixture. Alternatively, acid-catalyzed Fischer esterification afforded the desired product in an acceptable yield. After numerous crystallization attempts, also involving gel-techniques,^[178] no suitable crystals for X-Ray analysis have been found.

Photophysics. The dihedral angle between two benzene rings defines coupling degree in a diphenylacetylene unit and in this way the HOMO-LUMO gap. This has an effect on optical properties.

In **Figure 30** absorption and emission spectra of **71**, **81** and **85** measured in *n*-hexane solutions at room temperature are shown. For better comparison with previous results,^[66,67] **50** (untethered) and **22a** (twist angle 79°) are also added. Photophysical properties are summarized in **Table 2**.

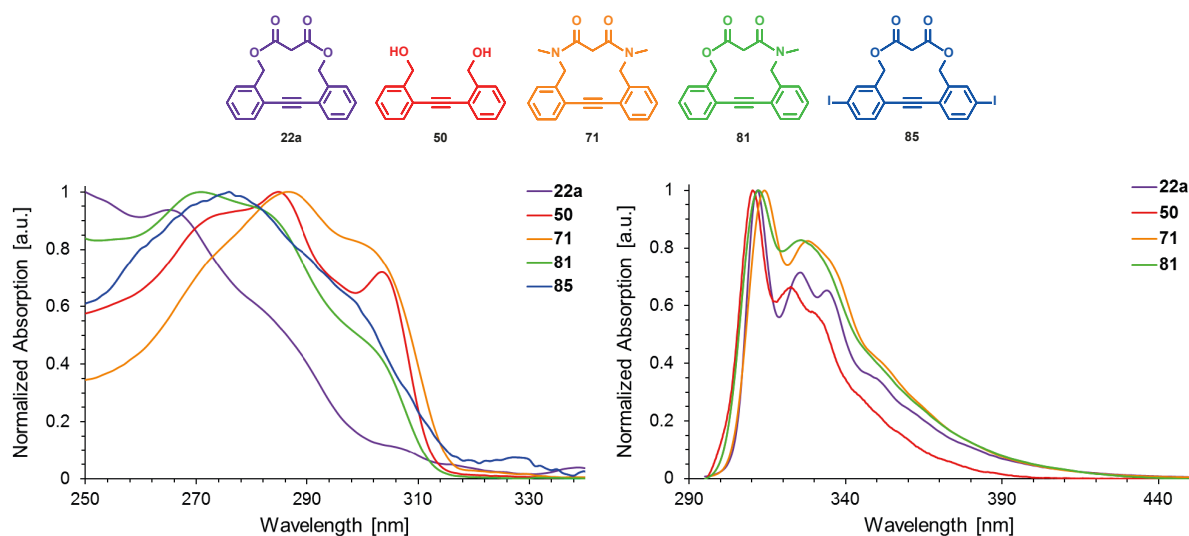


Figure 30. Left: Absorption spectra of **71**, **81** and **85**, compared to **22a** and **50**. Right: Emission spectra of **71**, **81**, **22a** and **50**. All have been recorded in *n*-hexane at room temperature. Emission spectra have been recorded with excitation at 280 nm (**22a**), 285 nm (**50**), 287 nm (**71**), 285 nm (**81**).

Table 2. Photophysical properties of **71**, **81**, **85** and **22a**.

Cpd	λ_{abs} [nm]	λ_{em} 298K (λ_{ex}) [nm]	$\lambda_{\text{em}}^{\text{c}}$ 77K (λ_{ex}) [nm]	ϵ [$10^4 \text{ L}\cdot\text{mol}^{-1}\cdot\text{cm}^{-1}$]	$\Phi_{298\text{K}}$ [%]	$\tau_{298\text{K}}^{\text{a}}$ [ns]	$\tau_{77\text{K}}^{\text{c}}$ [s]	$\lambda_{\text{abs}}^{\text{j}}$ [nm]	$\lambda_{\text{em}}^{\text{j}}$ [nm]
71	286 ^a 302 ^{a,d}	314 ^a (287)	309 ^f 448 ^g	2.36 ^b	26 ^a 12 ^b	0.4	1.3	264	314
	288 ^b 307 ^{b,d}	317 ^b (287)	(285)						
81	271 ^a 283 ^{a,d} 301 ^{a,d}	312 ^a (285)	310 ^f 461 ^g	1.33 ^b	8 ^a 10 ^b	0.3	1.0	249	310
	274 ^b 285 ^{b,d} 303 ^{b,d}	315 ^b (285)	(285)						
85	276 ^a 327 ^{a,e}	-- ^{a,b,i}	300 ^f 457 ^g	-- ^{a,b,i}	0 ^{a,b,i}	-- ^{a,i}	1.7	262	341
	272 ^b 282 ^{b,d} 302 ^{b,d}		(285)						
22a	265 ^a 284 ^{a,d} 309 ^{a,e}	312 ^a (280)	302 ^f 438 ^g	1.32 ^{b,h}	31 ^{a,h} 4 ^{b,h}	0.1 ^h	1.4 ^h	--	--
	268 ^{b,d} 290 ^{b,d}	315 ^b (280)	(264)						

a) In *n*-hexane. b) In CH_2Cl_2 . c) In EPA (diethyl ether/isopentane/ethanol 5:5:2, v/v). d) Shoulder. e) Low intensity. f) Fluorescence maximum. g) Phosphorescence maximum. h) See references.^[66,67] i) Insufficient intensity for registration (also due to low solubility). j) Calculations were performed at the time-dependent density functional theory (TDDFT) level with method cam-B3LYP and the basis set cc-pVDZ by M. Krämer and Prof. Dr. A. Dreuw. Interdisziplinäres Zentrum für Wissenschaftliches Rechnen, Ruprecht-Karls-Universität Heidelberg, Germany.

As expected, molecules with twisted solid-state conformation of benzene rings show blue-shifted absorption compared to planar ones, because of shorter π - π -coupling system. The same parameters of **50**, which is planar in the ground state, can be found in **71**, showing redshifted

absorption with a remarkable vibrational structure. Both features imply smaller twist angle in **71**, compared to **81**, what is in agreement with single crystal analysis. Diiodo **85** has a similar absorption profile as **81**, assuming a twisted conformation, while crystal structure was not determined. Except of **81**, which is non-emissive due to heavy-atom effect^[179], tolanses **71** and **81** emit at room temperature similarly. This is in agreement with previous reported **22a** and **50** (see part 2.4.2) and supposes, that emission proceeds from a planar excited state.^[180,140,118,111]

For ground state geometry fixation, substances were dissolved in EPA, which upon cooling with liquid nitrogen creates a solid transparent glass, suitable for optical measurements. Emission comparison at room and low temperature is shown in **Figure 31**.

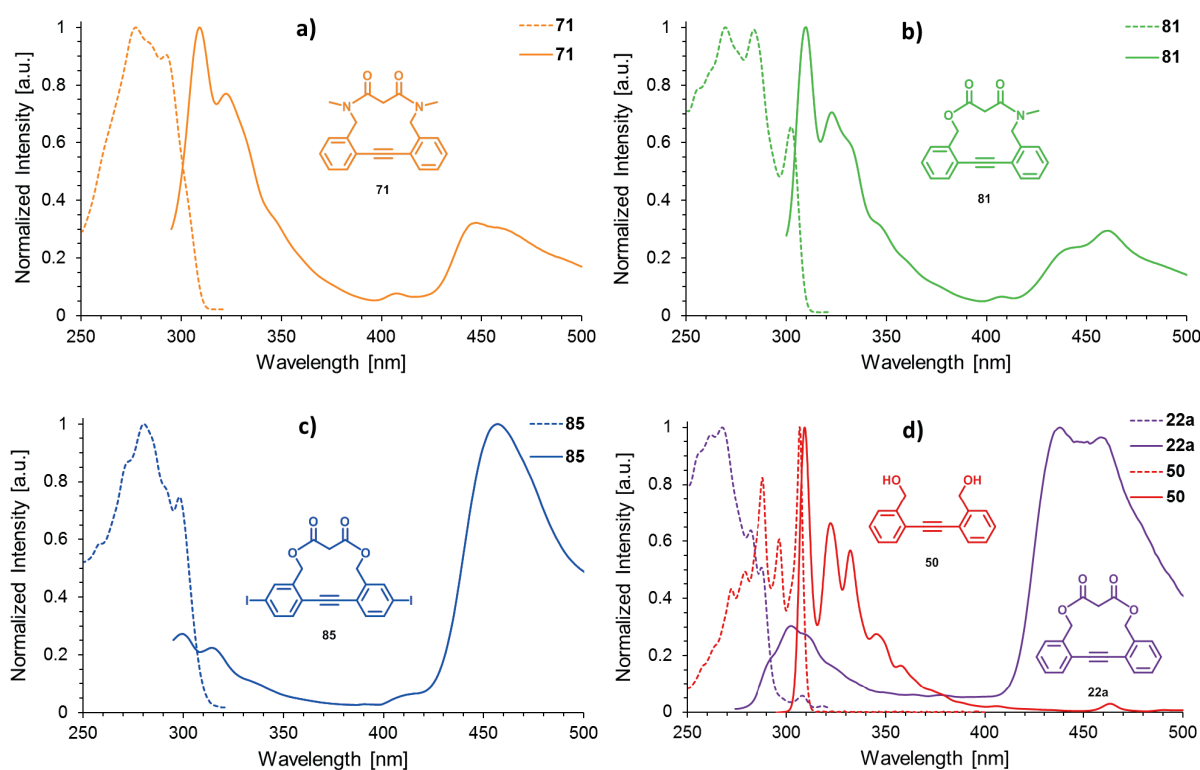


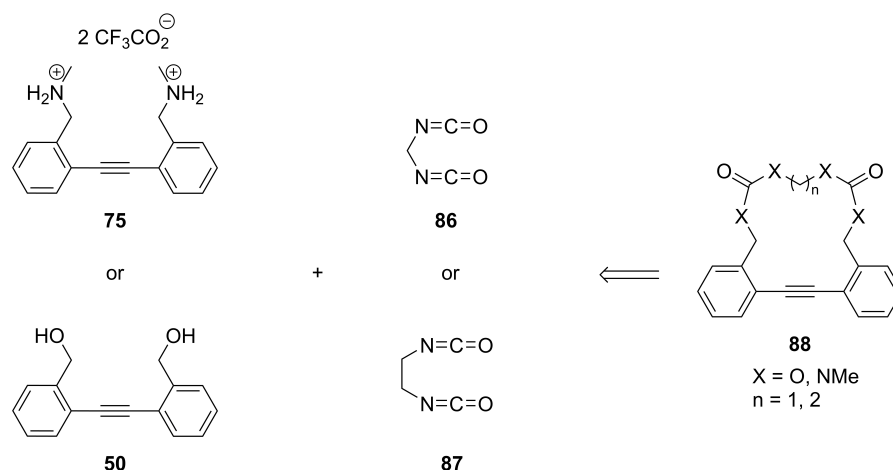
Figure 31. Absorption (dashed line) and emission (solid line) spectra in EPA at low temperature (94K for absorption, 77K for emission) for **71** (a), **81** (b), **85** (c). For comparison, spectra of **22a** and **50** (d) are shown. Emission spectra have been recorded with excitation at 264 nm (**22a**) and 285 nm (**50**, **71**, **81**, **85**).

At low temperature absorption spectra show discrete bands corresponding to vibrational energy levels. Fluorescence of **71** and **81** upon cooling did not change significantly, assuming planarization takes place as well in cryogenic glass. Additional phosphorescence bands are observed, but with lower intensity, compared to that of **22a**. On the contrary, **85** possesses strong phosphorescence, which is promoted by an increased intersystem-crossing rate due to a

heavy-atom effect.^[181] The low-temperature fluorescence maximum of **85** is blue-shifted, similar to **22a**, suggesting that **85** does not planarize in cryogenic glass unlike **71** and **81**.

3.2.2 Tolanophanes with urethane and urea functionality

Approaches to new cyclic tolanophanes can be realized using the available diol **50** and diammonium salt **75**. Carbamates and carbamides **88** were chosen for study (**Scheme 16**).



Scheme 16. Possible new class of cyclic diphenylacetylene compounds and its precursors.

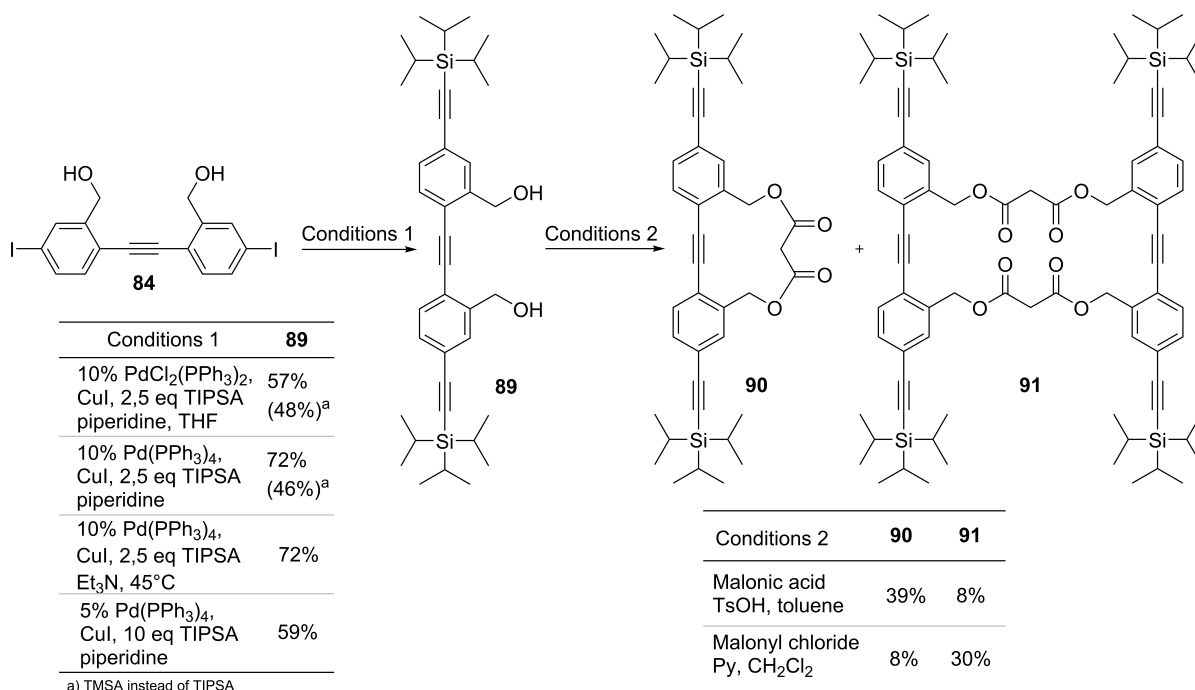
Numerous attempts have been made in synthesizing the target molecules. The most promising was using methyl- or 1,2-ethyldiisocyanate as a highly reactive electrophile.^[182] It appeared to be difficult to drive the reaction in cyclization direction, probably because the substances were too reactive. Formation of isocyanates in situ also failed.^[183] Conversion of, for example, diol **50** to its carbochloridic acid derivative could be a part of a controllable step-by-step procedure.^[184] Unfortunately, following cyclization attempts^[185] with 1,2-ethylenediamine, only inseparable mixtures were afforded. Since instrumental analysis methods like UPLC-MS did not show any desired product formation, further investigations were conducted in other directions.

3.2.3 Tolanophanes with increased conjugation

Synthetic availability of functionalized tethered tolanes allows to expand this research area on species, which are intermediates between the simplest diphenylacetylene and poly(*para*-phenyleneethynyls).

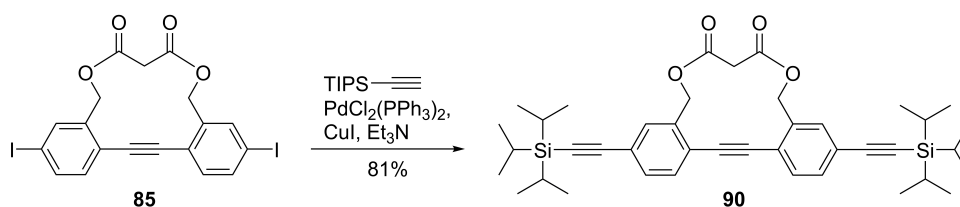
Substitution of the iodine atoms in **85** with an acetylene derivative is the easiest way to extend conjugated π -system of a tolane. Using high reactive TMS-acetylene and TIPS-acetylene helped to test the activity of the iodine substituents in coupling conditions. Difficulties on the cyclization

step did not allow involving tolanophane **85**, so diol **84** was chosen as a starting material. This afforded not only the desired monomer **90**, but additionally dimer **91** (Scheme 17).



Scheme 17. Synthetic route and conditions of **90** and **91**, starting from **84**.

Several coupling conditions have been tested to improve the yield of **89**. Reaction of the iododiol **84** with TIPS-acetylene afforded product **89** in higher yields than using less sterically demanding TMSA. The difference can be explained by more effective solubilisation, caused by TIPS-substituents. Annulation step appeared to be selective depending on the reaction conditions. In a thermodynamically controlled media, formation of monomer **90** was favored, while using malonyl chloride in presence of pyridine mainly produced dimer **91**. Nevertheless, the second product was present in both cases. Higher yields of monomer **90** without dimer formation have been achieved using tolanophane **85** in Sonogashira coupling (Scheme 18).



Scheme 18. Alternative synthesis of monomer **90**.

To investigate solid state structure, single crystal assays have been prepared for **90** and **91**, but not for diiodo **85**, which formed only microcrystalline conglomerates (Figure 32). Monomer **90** has an unremarkable angle 61° between twisted phenyl rings, whereas almost untwisted DPA-

units in dimer **91** are located in a way, that benzene rings stack nearly parallel to each other at a distance about 3.6 Å.

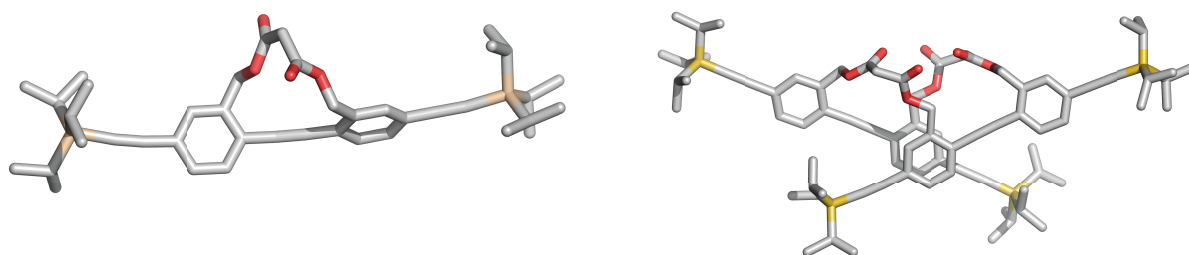


Figure 32. *Left:* crystal structure of **90**, torsion angle 61°. *Right:* crystal structure of **91**, torsion angle 7° and 9°, distance between stacked rings 3.6 Å.

Photophysics. Optical properties of tolanophanes with elongated π -system are presented in **Figure 33** and summarized in **Table 3**.

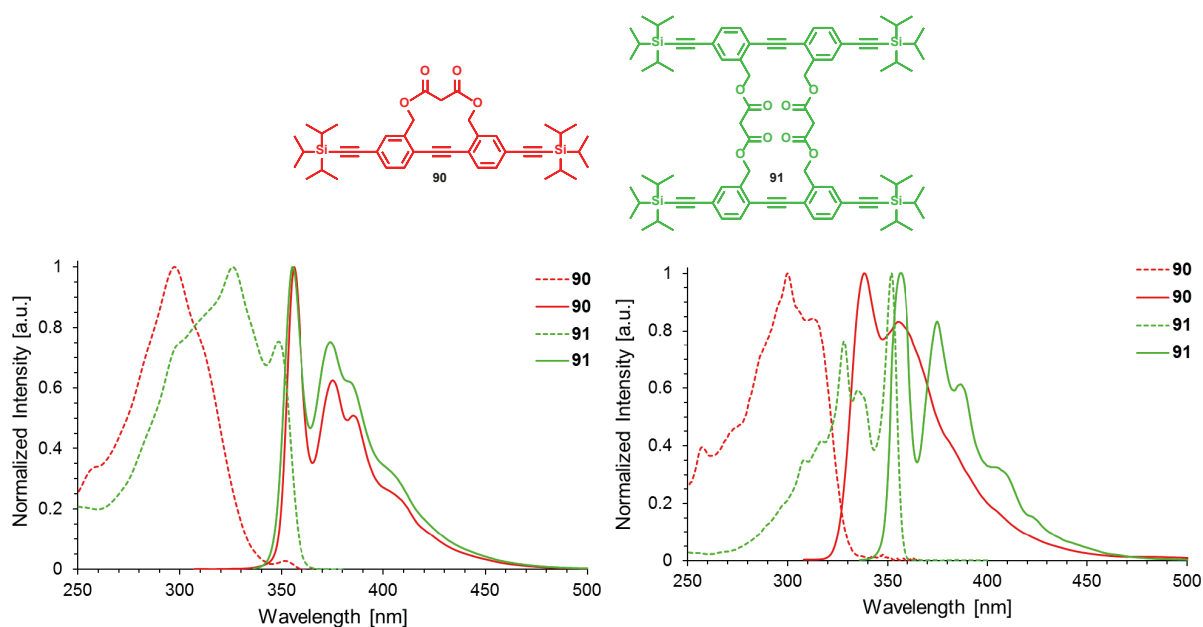


Figure 33. Absorption (dashed) and emission (solid) spectra of **90** and **91**. *Left:* in *n*-hexane at room temperature. *Right:* in EPA at 94K for absorption and 77K for emission. Emission spectra have been recorded with excitation at 297 nm (**90**), 326 nm (**91**) in *n*-hexane and at 297 nm (**90**), 325 nm (**91**) in EPA.

Dimer **91** possess the same chromophore unit as monomer **90**, therefore both **90** and **91** show identical fluorescence at room temperature in *n*-hexane solution. Fluorescence quantum yields and lifetimes are significantly improved due to extended π -system. Compared to **22a**, emission maxima are red-shifted, because **90** and **91** have chromophores with extended π -system through alkyne groups and lower twisting. Absorption maximum of **90** is strong blue-shifted as compared to **91**, supposing twisted conformation, which is in agreement with crystallographic data. It is

noteworthy, that the extinction coefficient of **91** is not twice as high as that of **90**.^[186] Together with hypsochromic shifted absorption maximum of **90** it can suggest a weak nonbonded electronic interaction between two chromophores^[187] in **91**, what is possible due to short distance between stacking benzene rings (3.6 Å).

Table 3. Photophysical properties of **90** and **91**.

Cpd	λ_{abs} [nm]	λ_{em} 298K (λ_{ex}) [nm]	$\lambda_{\text{em}}^{\text{c}}$ 77K (λ_{ex}) [nm]	ϵ [10 ⁴ L·mol ⁻¹ · cm ⁻¹]	$\Phi_{298\text{K}}$ [%]	$\tau_{298\text{K}}^{\text{a}}$ [ns]	$\tau_{77\text{K}}^{\text{c}}$ [s]	$\lambda_{\text{abs}}^{\text{j}}$ [nm]	$\lambda_{\text{em}}^{\text{j}}$ [nm]
90	297 ^a 309 ^{a,d} 351 ^{a,e}	356 ^a (297)	338 ^f -- ^g	6.76 ^b	89 ^a	0.7	-- ⁱ	275	345
	300 ^b 313 ^{b,d} 355 ^{b,e}	360 ^b (300)	(297)		88 ^b				
91	326 ^a 349 ^a	355 ^a (326)	357 ^f -- ^g	11.2 ^b	90 ^a	0.8	-- ⁱ	--	--
	328 ^b 351 ^b	359 ^b (328)	(325)		87 ^b				

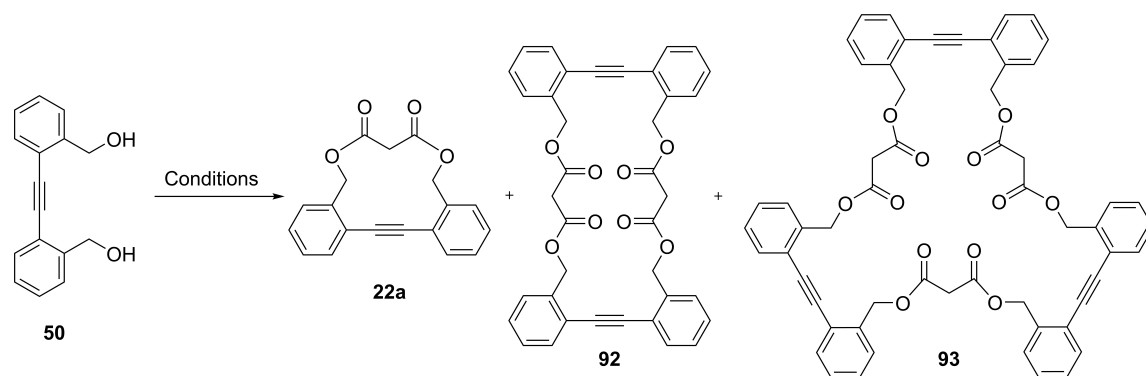
a) In *n*-hexane. b) In CH₂Cl₂. c) In EPA (diethyl ether/isopentane/ethanol 5:5:2, v/v). d) Shoulder. e) Low intensity. f) Fluorescence maximum. g) Phosphorescence maximum. h) See references.^[66,67] i) Insufficient intensity for registration (also due to low solubility). j) Calculations were performed at the time-dependent density functional theory (TDDFT) level with method cam-B3LYP and the basis set cc-pVDZ by M. Krämer and Prof. Dr. A. Dreuw. Interdisziplinäres Zentrum für Wissenschaftliches Rechnen, Ruprecht-Karls-Universität Heidelberg, Germany.

Upon cooling in cryogenic glass, absorption of **90** and **91** did not change significantly, as well as emission of **91**, which could emit only from the planar excited state. However, **90** at low temperature shows significantly blue-shifted emission, presumably occurring from twisted configuration. At the same time, **90** have no cryogenic phosphorescence, like untwisted **91**. It is not consistent with other twisted tolane species (**22a**, **81**, **85**) and can be explained, by the addition of alkyne groups, that oppresses intersystem crossing.²

3.2.4 Oligomeric cyclic products

Unusual conformational behavior of the dimeric cyclophane **91** guided the interest towards this substance class, since already known chiral tolane dimers show unusual properties.^[188] As starting material diol **50** was chosen, because synthesis and purification are optimized, and the cyclization has been thoroughly studied.^[66,67] The approach to cyclic oligomers is based on statistical distribution of malonic and diphenylacetylene moieties.^[189] During reaction optimization, products containing maximum three repetition units were separated and analyzed (**Scheme 19**). Reaction of diol **50** with malonyl chloride as well as malonic acid was tested under various conditions; some of them are listed in **Table 4**.

² Calculations, that prove the explanation, have been performed by Prof. Dr. A. Dreuw and M. Krämer in the published part of this work.



Scheme 19. Synthesis of cyclic oligomers starting from diol **50**. For reaction conditions see **Table 4**.

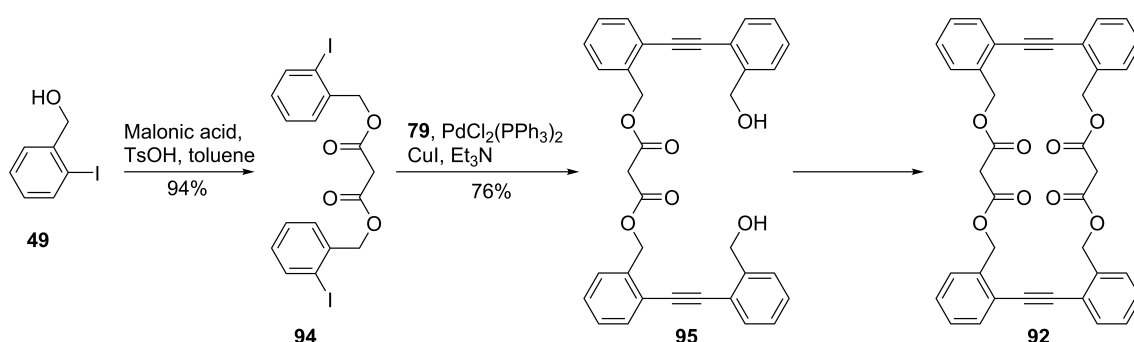
Table 4. Some reaction conditions for cyclization of diol **50**.

Entry	Solvent ^a , concentration	Base or acid	Conditions	Yield, %		
				22a	92	93
1	0.005 M	NaHCO ₃	A ^b	12	--	4
2	0.005 M	<i>i</i> -Pr ₂ NEt	A , then 4d at 40°C	4 ^c	--	--
3	0.05 M	NaHCO ₃	A	3	--	4
4	0.005 M	NaHCO ₃	A , 7 h	11	--	3 ^c
5 ^j	0.04 M	--	B ^d , KCl, TEBA, 90 min	2	--	5
6 ^j	0.04 M	NaHCO ₃	B , KCl, TEBA, 90 min	2 ^c	--	6
7 ^e	0.015 M	Py	B , 7 h	8	--	6 ^c
8 ^f	0.002 M	DMAP	B ^g , 7 h	16	--	--
9	0.08 M	NaHCO ₃	B , 5 h	1 ^c	--	6 ^c
10	0.08 M	NaHCO ₃	B , 1 h	2 ^c	--	3 ^c
11	0.04 M	--	B , 90 min	2 ^c	--	6
12	toluene, 0.04 M	--	B , 90 min	2	0.2	4
13	toluene, 0.03 M	TsOH	C ^h	34	--	--
14	CHCl ₃ , 0.01 M	TsOH	C , CuSO ₄	--	--	--
15	0.03 M	NaHCO ₃	D ⁱ	--	1	6
16	0.04 M	DMAP	D	3	--	--
17	0.03 M	<i>i</i> -Pr ₂ NEt	D	3	--	3
18 ^k	0.03 M	NaHCO ₃	D , 0°C	1	--	--
19	0.03 M	NaHCO ₃	D , 40°C	7	--	6

a) CH₂Cl₂ if no solvent given; b) condition "A" means simultaneous addition of malonyl chloride (**76**) and diol **50** solutions into base over 4.5 h according to literature;^[166] c) yield is approximate since complete purification was not achieved; d) condition "B" means addition of malonyl chloride (**76**) to mixture of diol **50** with other given components over given time at room temperature; e) according to literature;^[189] f) according to literature;^[190] g) base was added to a mixture of diol **50** and malonyl chloride (**76**); h) condition "C" means refluxing with Dean-Stark water separator; i) condition "D" means stepwise addition of malonyl chloride (**76**), see part 5.3; j) according to literature;^[191] k) according to literature.^[192]

At first, a standard high dilution method was applied (Entry 1-4). Increasing the educt concentration reduces the formation of the monomeric product **22a** and stimulated trimer **93** formation. Higher concentrated reaction mixtures required a one-pot reaction with all educt and base, because of its low solubility. This entfold a slow addition of malonyl chloride (**76**) (Entry 5-12), but even in such unfavorable conditions, formation of higher molecular weight product was promoted. Only the trimer **93** could be separated. Fischer esterification afforded solely the monomeric **22a** (Entry 13-14). Based on collected data, a combined procedure was applied to facilitate the formation of dimer **92** (Entry 15-19). At higher concentration, a half equivalent of malonyl chloride (**76**) reacted with a mixture of diol **50** and NaHCO₃. Excess of diol **50** should suppress formation of disubstituted malonic ester. Afterwards the reaction mixture was diluted and the residual equivalents of malonyl chloride (**76**) were added slowly to obtain dimer **92** for spectroscopic analysis (Entry 15).

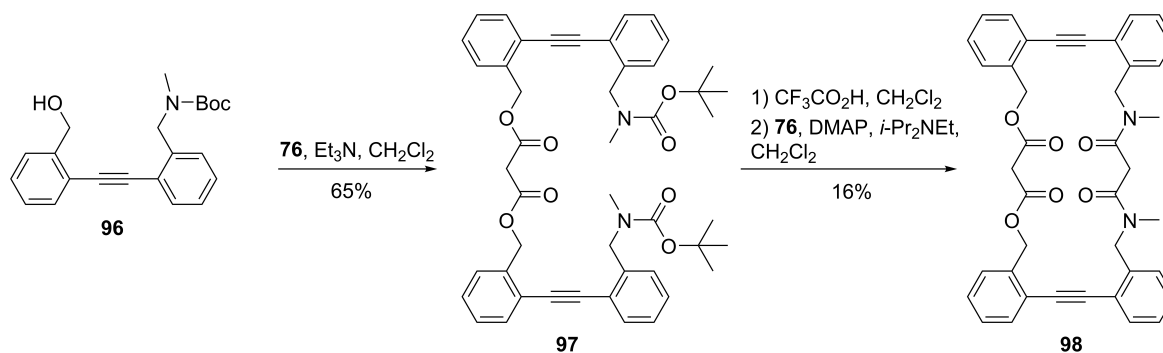
Due to the encountered difficulties in dimer synthesis another strategy has been developed (**Scheme 20**).



Scheme 20. Alternative route to dimer **92**.

Diol **95** obtained in two steps starting from 2-iodobenzyl alcohol (**49**) was subjected to numerous cyclization attempts. Using standard acylation methods involving malonyl chloride (**76**) in basic media afforded complex inseparable mixtures of products, while acid-catalyzed azeotropic esterification led to more stable monomer **22a**, as well in presence of Bu₂SnO.^[193] Other common acylation methods involving EDCI,^[194] CMPI^[195] and mixed anhydride formation^[196] also gave poor results. Comparable yield to previous experiments (about 1%) of the dimer **92** was only achieved in one example. The conditions were similar to entry 11 (**Table 4**).

The stepwise method was successfully applied in the synthesis of dimeric amido ester **98** (**Scheme 21**).



Scheme 21. Synthesis of mixed dimeric amido ester **98**.

Boc-protected diamine **97** was synthesized from available amino alcohol **96**. Deprotection followed by acylation in the presence of malonyl chloride under high diluted conditions afforded cyclic dimer **98**.

No suitable crystals were obtained for trimer **93** and dimer **98**, while after numerous attempts an untwisted and unremarkable structure of dimer **92** was revealed (**Figure 34**).

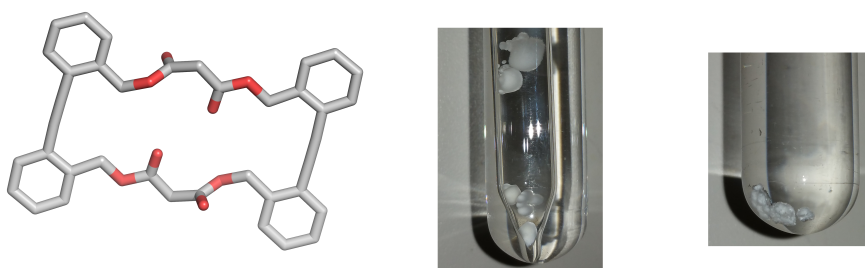


Figure 34. Left: Crystal structure of dimer **92** (torsion angle 0.4°). Middle: crystallization attempt of **98**. Right: crystallization attempt of **93**.

Photophysics. Cyclooligomeric species containing unaltered DPA-units showed similar optical properties (**Figure 35**). UV-Vis and luminescence data are summarized in **Table 5** (for **22a** see **Table 2**).

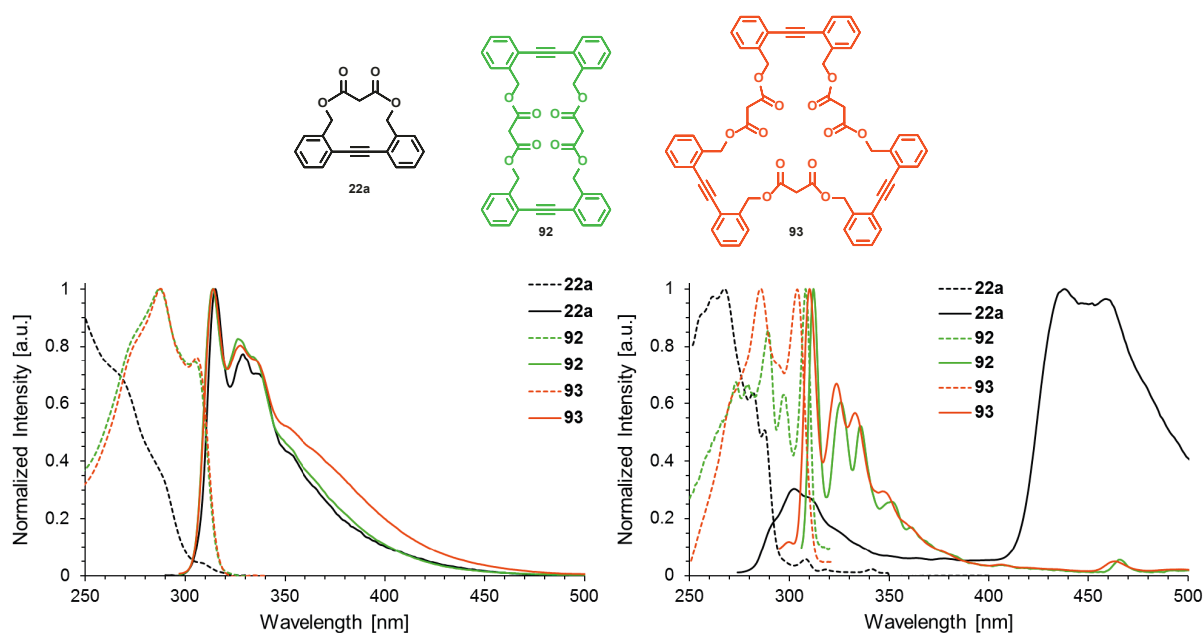


Figure 35. Absorption (dashed) and emission (solid) spectra of **92** and **93** compared to **22a**. *Left:* in CH_2Cl_2 at room temperature. *Right:* in EPA at 94K for absorption and 77K for emission. Emission spectra have been recorded with excitation at 280 nm (**22a**), 287 nm (**92**), 285 nm (**93**) in CH_2Cl_2 and at 280 nm (**22a**), 285 nm (**92**, **93**) in EPA.

Measurements at room temperature were performed in CH_2Cl_2 , because **93** was insoluble in *n*-hexane. Emission of **92** and **93** are almost identical to that of **22a**, alternatively absorption is significantly red-shifted, what conforms to planar configuration of **92** and allows assuming the same by **93**. The only emission difference at room temperature is a weak eminence between 350-450 nm for **92** and **93**, more shaped in polar solvents, like EPA. Presumably, this is caused by intramolecular excimer formation. At cryogenic temperatures **22a** shows known blue-shifted fluorescence and strong phosphorescence,^[66] whereas **92** and **93** possess photophysical properties close to that of **50** (see **Figure 31**): in cryogenic matrix the spectra display significant vibrational structure and much less or no phosphorescence.

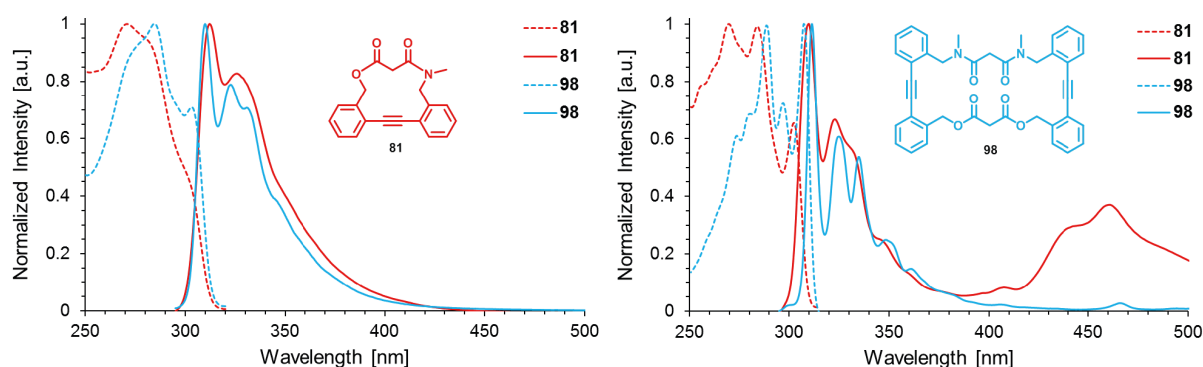


Figure 36. Absorption (dashed) and emission (solid) spectra of **98** compared to **81**. *Left:* in *n*-hexane at room temperature. *Right:* in EPA at 94K for absorption and 77K for emission. Emission spectra have been recorded with excitation at 285 nm (**81**, **98**) in *n*-hexane and in EPA.

The same results have been obtained for dimeric amidoester **98** compared to **81** (Figure 36). Red-shifted absorption maxima of **98**, both at room and at cryogenic temperatures, imply constant planar ground state configuration. Generally, **98** showed much less difference to **92** than **81** and **71**. Obviously, in line with macrocycle size growth, the effective twisting of the tether decreases, while DPA-core gets more freedom.

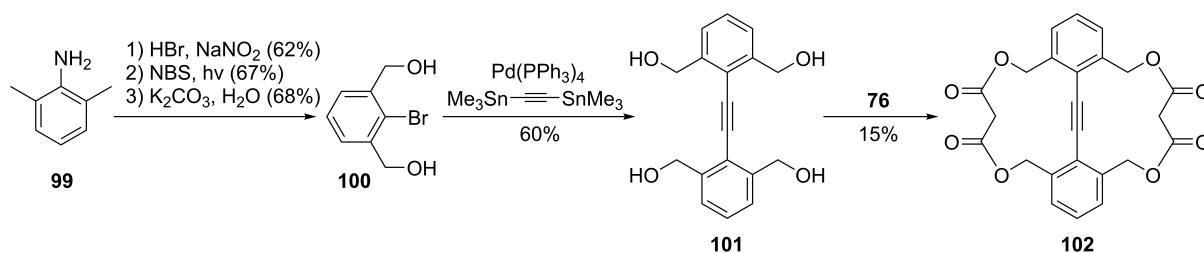
Table 5. Photophysical properties of **92**, **93** and **98**.

Cpd	λ_{abs} [nm]	λ_{em} 298K (λ_{ex}) [nm]	$\lambda_{\text{em}}^{\text{c}}$ 77K (λ_{ex}) [nm]	ϵ [$10^4 \text{ L}\cdot\text{mol}^{-1}\cdot\text{cm}^{-1}$]	$\phi_{298\text{K}}$ [%]	$\tau_{298\text{K}}^{\text{a}}$ [ns]	$\tau_{77\text{K}}^{\text{c}}$ [s]
92	273 ^a 304 ^{a,d} 287 ^b 305 ^b 309 ^{b,e}	310 ^a (273) 314 ^b (287)	312 ^f 466 ^{g,e} (285)	--	--	--	--
93	-- ^{a,h} 288 ^b 306 ^b	314 ^b (285)	310 ^f 463 ^{g,e} (285)	8.03 ^b	8 ^b	<0.1	0.8
98	285 ^a 303 ^a 287 ^b 305 ^b	310 ^a (285) 314 ^b (287)	311 ^f 466 ^{g,e} (285)	1.34 ^b	7 ^b	0.3	0.9

a) In *n*-hexane. b) In CH_2Cl_2 . c) In EPA (diethyl ether/isopentane/ethanol 5:5:2, v/v). d) Shoulder. e) Low intensity. f) Fluorescence maximum. g) Phosphorescence maximum. h) Insufficient intensity for registration (also due to low solubility).

3.2.5 Doubly bridged tolane

Changing optical properties of tolanes by restricting the rotation between two phenyl rings using either bulky substituents^[117,52] or tether^[64] is a challenging task. The excited state planarization occurs regardless of the previous position of benzene rings.^[66,67] This strategy could be extended by an introduction of two tethers on one DPA-fragment to suppress planarization. Doubly bridged tolanophane **102** is a developed version of monobridged **22a** and renders these two species comparable (Scheme 22).



Scheme 22. Synthesis of **102** starting from **99**.

Commercially available dimethylaniline **99** was converted to bromoxylene and after double radical bromination and hydrolysis, bromodiol **100** was obtained. Synthesis attempts of the

corresponding aryl iodide were unsuccessful. A number of attempts to force **100** into Sonogashira coupling with acetylene gas^[197] or TIPSA and TMSA^[198] even at microwave conditions^[199] gave either unreacted educt or a complex inseparable mixture of products. Optimized Stille coupling of bromodiol **100** afforded tetraol **101** in 60% yield. Cyclization of **101** using solely malonyl chloride (**76**) gave desired **102** as a white solid.

Single crystal species have been grown and analyzed by X-Ray. The molecular structure of **102** is shown on **Figure 37**.

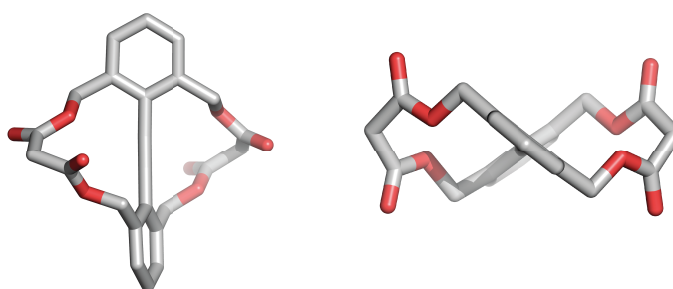


Figure 37. Crystal structure of **102** in two projections. Torsion angle is 76°.

The torsion angle between the benzene rings is 76°, the linear diphenylacetylene unit demonstrates a symmetrical double-bridged layout of the molecule. A split ArCH₂-signal in ¹H NMR³ spectrum implies a restricted conformational movement in solution and was not observed for single-bridged diester analogues.

Photophysics. Optical properties of **102** compared to that of **22a** are presented on **Figure 38** and in **Table 6**.

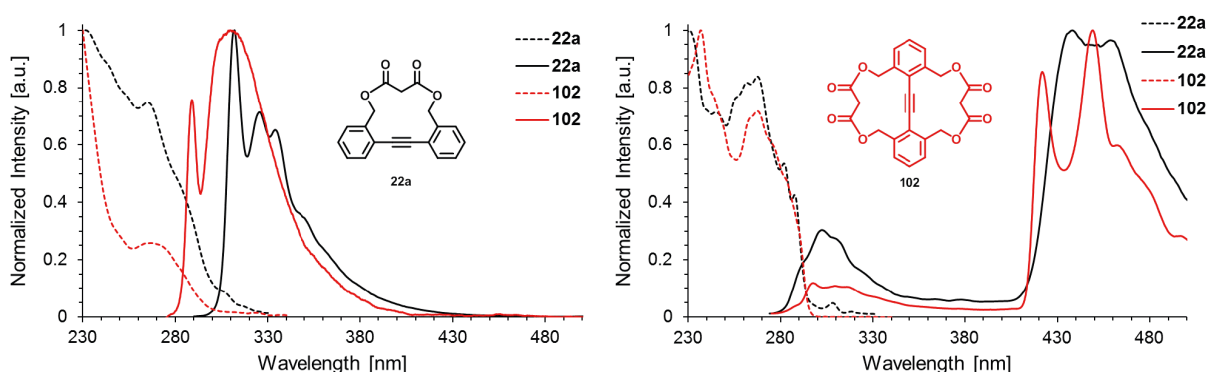


Figure 38. Absorption (dashed) and emission (solid) spectra of **102** compared to **22a**. *Left:* in *n*-hexane at room temperature. *Right:* in EPA at 94K for absorption and 77K for emission. Emission spectra have been recorded with excitation at 280 nm (**22a**), 265 nm (**102**) in *n*-hexane and at 264 nm (**22a**), 265 nm (**102**) in EPA.

³ At 100°C instead of two doublets at 5.31 and 4.95 ppm, one broad singlet at 5.15 ppm (DMSO-*d*₆) observed.

Table 6. Photophysical properties of **102**. For comparison, **22a** added.

Cpd	λ_{abs} [nm]	λ_{em} 298K (λ_{ex}) [nm]	$\lambda_{\text{em}}^{\text{c}}$ 77K (λ_{ex}) [nm]	ϵ [$10^4 \text{ L}\cdot\text{mol}^{-1}\cdot\text{cm}^{-1}$]	$\Phi_{298\text{K}}$ [%]	$\tau_{298\text{K}}^{\text{a}}$ [ns]	$\tau_{77\text{K}}^{\text{c}}$ [s]
102	267 ^a 240 ^b 250 ^{b,d} 265 ^b	310 ^a (265) 323 ^b (265)	298 ^f 449 ^g (265)	1.72 ^b	1 ^a 2 ^b	0.2	1.9
22a	265 ^a 284 ^{a,d} 309 ^{a,e} 268 ^{b,d} 290 ^{b,d}	312 ^a (280) 315 ^b (280)	302 ^f 438 ^g (264)	1.32 ^{b,h}	31 ^{a,h} 4 ^{b,h}	0.4 ^h	1.4 ^h

a) In *n*-hexane. b) In CH₂Cl₂. c) In EPA (diethyl ether/isopentane/ethanol 5:5:2, v/v). d) Shoulder. e) Low intensity. f) Fluorescence maximum. g) Phosphorescence maximum. h) See references.^[66,67]

The absorption spectra of **102** and **22a** look similar, but the intensity in case of **102** is significantly lower, accompanied by a slightly red-shifted maximum. Room temperature emission spectra show remarkable differences. Single tethered **22a** has a usual emission profile with distinct vibrational structure, whereas **102** has an unstructured broad band and sharp maximum at ca. 298 nm, which proves the presence of twisted emissive conformers in the solution.^[56] Bathochromic shift of emission measured for **102** in solvents with increasing polarity (for spectra see part 7.1) occurring from relatively high polarizability is common for tolane and its derivatives.^[200] On **Figure 38** emission of the saturated *n*-hexane solution having absorption ca. 0.02 at 267 nm is shown. Upon cooling in cryogenic glass, **102** possesses, similar to **22a**, strong phosphorescence with residual fluorescence. In case of **102**, the phosphorescence band is slightly blue-shifted, while the phosphorescence maximum is red-shifted.

3.2.6 Tethered 1,4-bis(phenylethynyl)benzole

1,4-Bis(phenylethynyl)benzole (BPEB) and its derivatives occupy an intermediate position between monomeric DPA and polymeric PPE. Synthesized and studied by Sebastian Menning, twofold bridged BPEB **56** showed interesting optical properties.^[101] Although single crystal specimen could not be prepared and torsion angles remained unknown, strong blue-shifted absorption maximum pointed to twisted conformation. Mixed amidoester **103** and **104** were targeted (**Figure 39**), because in the case of bridged PDA it showed a more twisted structure than the diester (see part 3.2.1).

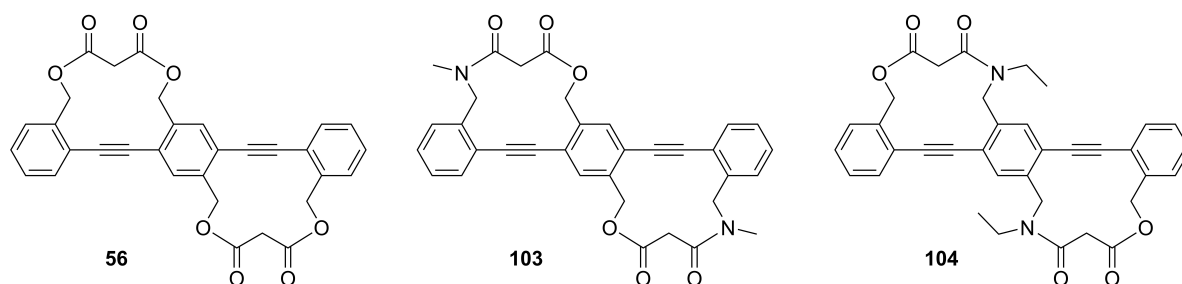
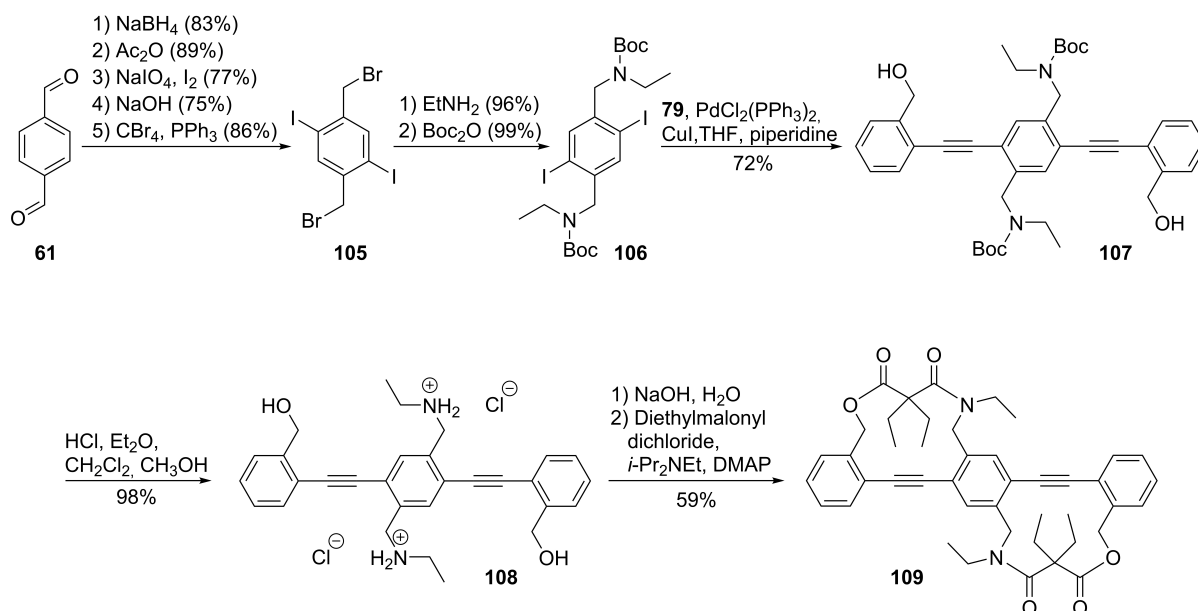


Figure 39. Tethered BPEB **56** synthesized by S. Menning^[101] and new possible candidates.

Synthetic attempts towards **103** gave colorless insoluble material only. Removing the more reactive amino groups from the side of the molecule should suppress intermolecular interactions; introduction of additional ethyl groups served to improve solubility. HRMS proved formation of **104**, but with a yield less than 5%. However, the solubility was still insufficient for careful chromatographic purification or recrystallization.



Scheme 23. Synthesis of **109** starting from terephthalaldehyde (**61**) and 2-iodobenzyl alcohol (**49**) (not shown).

Approach to double-bridged **109**⁴ was accomplished according a convergent 13-step synthesis, shown on **Scheme 23**. Dibromide **105** was synthesized starting from commercially available terephthalaldehyde (**61**) using a published synthetic sequence (for details see part 5.3).^[201] The yield on the iodination step was improved from 23 to 77% using sodium periodate instead of iodic acid. After amination and Boc-protection, the obtained diiodide **106** was involved in Sonogashira coupling with alkyne **79**, easily available from 2-iodobenzyl alcohol (**49**). Diprotected **107** appeared to be less soluble in methanol in contrast to other components of the reaction

⁴ Part of synthesis and characterization of some new substances has been performed by Svenja Weigold during her preparation of the bachelor thesis. For further information, see part 5.3.

mixture, what was useful at the purification step. Simple washing of the reaction mixture with methanol might replace chromatographic separation. Based on the previous experience, involving salt **108** directly into cyclization failed, but the free base reacted successfully with diethylmalonyl chloride and gave **109**, with much improved solubility.

Structural analysis of the single crystal specimen showed the presence of two independent molecules within one unit cell (**Figure 40**). The molecules display similar twist angles between middle and side benzene rings, but of moderate values (40 and 46°).

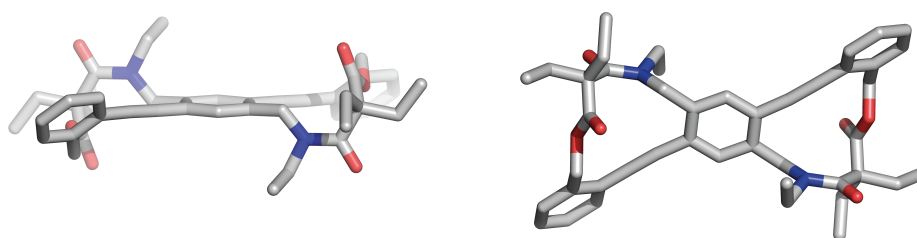


Figure 40. Crystal structure of **109**. Torsion angles are 40 and 46°.

Photophysics. UV-Vis spectra are presented on **Figure 41**.

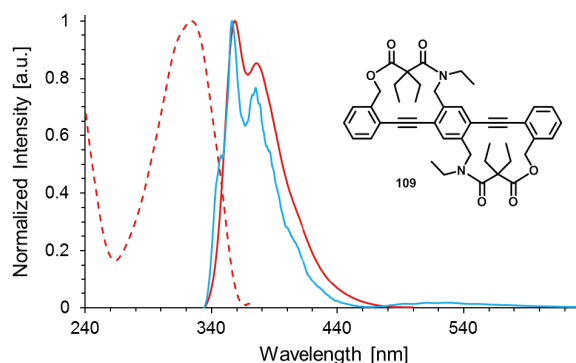


Figure 41. Absorption (dashed) and emission (solid) spectra of **109** in *n*-hexane at room temperature (red) and EPA at 77K (blue). Emission spectra have been recorded with excitation at 324 nm in *n*-hexane and in EPA.

Absorption spectrum of **109** in *n*-hexane has no resolved vibrational structure and resembles that of polymer (see **Figure 43**), while emission is resolved, which is in agreement with published data for oligomeric PPEs.^[111] Extinction coefficient of **109** is low, compared to other tolanophanes with prolonged coupling system, for example **90** (see **Table 3**). In **Table 7** photophysical data is compared to ester **56** synthesized and characterized by Sebastian Menning^[101] (see **Figure 39**).

Table 7. Photophysical properties of **109**. For comparison measurement data for **56** taken from source^[101] and for **52** were added.

Cpd	λ_{abs} [nm]	λ_{em} 298K (λ_{ex}) [nm]	$\lambda_{\text{em}}^{\text{c}}$ 77K (λ_{ex}) [nm]	ϵ [$10^4 \text{ L}\cdot\text{mol}^{-1}\cdot\text{cm}^{-1}$]	$\Phi_{298\text{K}}$ [%]	$\tau_{298\text{K}}^{\text{a}}$ [ns]	$\tau_{77\text{K}}^{\text{c}}$ [s]
109	324 ^a	358 ^a (324)	356 ^d , 511 ^e (324)	3.22	60 ^a	0.5	0.76
	326 ^b	363 ^b (326)			65 ^b		
	324 ^c	359 ^c (324)					
56	292 ^a	365 ^a	ca.335	--	58 ^a	0.718	0.100
52	320 ^f	346 ^f (270)	--	5.80 ^f	--	0.63 ^f	--
	328 ^g	348 ^g	--	3.89 ^g	50 ^g	2.57 ^g	

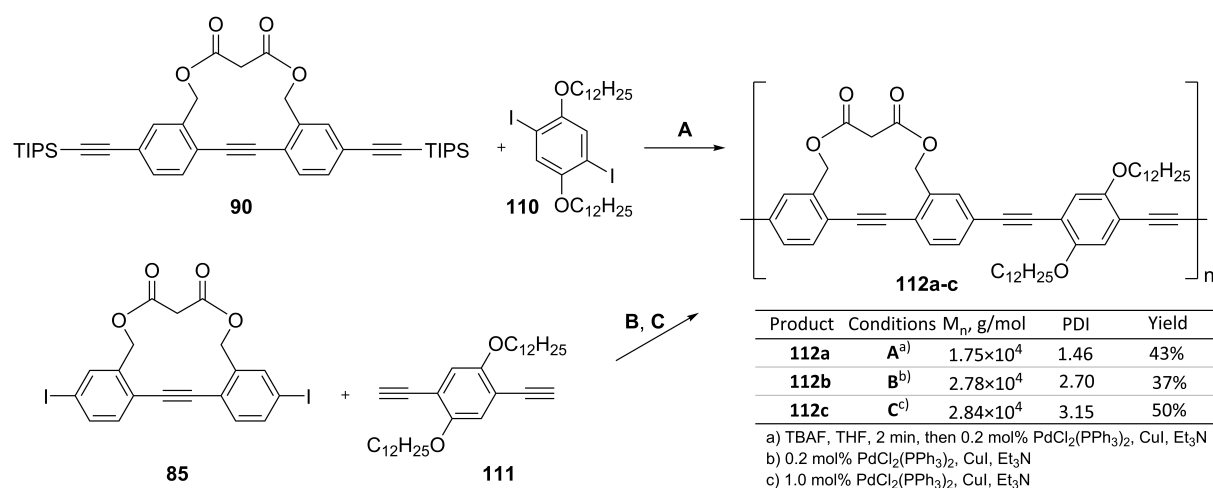
a) In *n*-hexane. b) in CH₂Cl₂. c) In EPA. d) Fluorescence maximum. e) Phosphorescence maximum. f) In cyclohexane at 283K from reference.^[202] g) In CHCl₃ at 295K from reference.^[203]

Absorption and emission spectra of **109** and **56** differ significantly. Absorption maximum of **109** was red-shifted due to contribution of the planar conformers. In cryogenic glass, the shape of the fluorescence spectrum of **109** did not change significantly. The maximum was slightly blue-shifted (3 nm), compared to room temperature. In case of **56**, the shift was ca. 10 times stronger, due to greater twisting. On the other hand, room temperature emission maximum of **109** was 7 nm blue-shifted to that of **56**, probably due to presence of partly twisted in excited state conformers. In contrast, phosphorescence bands of **56** and **109** did not show much difference. High phosphorescence lifetime pointed to relative stability of the triplet excited state of **109**, but higher than for tolanes activation barrier between S₁ excited state and dark state^[123] causes reduce in intensity.

3.2.7 Poly(*para*-phenyleneethynylene) derivative

Poly(*para*-phenyleneethynylene)s (PPEs) are useful organic semiconducting materials with wide applications as molecular electronics, organic field-effect transistors and fluorescent chemical sensors.^[204] Photophysical properties of PPEs in solution are driven by Boltzmann distribution^[126,127] of the twist angles between phenyl rings. Incorporating tethered fragments with fixed twists in polymer chains could afford materials with new interesting properties. Two different synthetic routes were used for synthesis of copolymer **112a-c** containing di-dodecyloxy benzene and tolanophane moieties⁵ (**Scheme 24**).

⁵ This part was made in cooperation with Emanuel Smarsly (AK Bunz, running dissertation).



Scheme 24. Synthesis and properties of polymers **112a-c**.

For polymerization, usual Sonogashira coupling was used. Since deprotected **90** is unstable, *in situ* deprotection followed by polymerization afforded dark-yellow flakes after precipitation from methanol. Stable dialkyne **111** after reaction with **85** afforded the same material with greater molecular weight and polymer dispersity index, but lower yield.⁶ Increasing catalyst load to 1 mol% did not significantly change properties of polymer, but slightly improved the yield, and also could lead to alkyne-alkyne formation as a result of Glaser reaction.^[159] TGA-DSC analysis showed that the polymers had similar glass transition temperature (ca. 60°C) and melting point (ca. 200°C). Measurement curves can be found in Appendix 7.2. Thin films have been prepared using spin-coated technique on glass substrate from CHCl₃ solution (10 mg/mL). Polarized light microscopic observation revealed predominantly amorphous layer with regional crystalline domains (**Figure 42**), which is common for PPEs and shows no resolved GIWAXS spectra.^[130,205]

⁶ Calculated from one repetition unit molecular mass and that of the polymer.

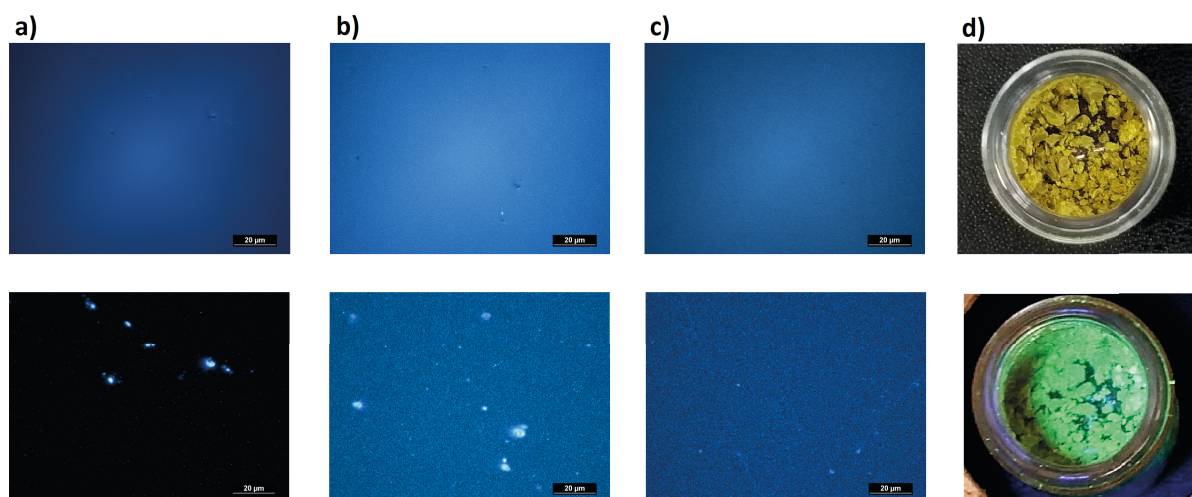


Figure 42. Polarized microscope film images of **112a** (a), **112b** (b) and **112c** (c) (*Up*: crossed polarization filter in bright mode. *Bottom*: without polarization in dark mode); d) photo images of **112b** under day light (up) and UV 365 nm (bottom).

Optical properties of synthesized polymers are presented on **Figure 43** and in **Table 8**. Spectra of **112b** and **112c** overlapped due to similarity, so those of **112c** are omitted. The complete data can be found in Appendix 7.1.

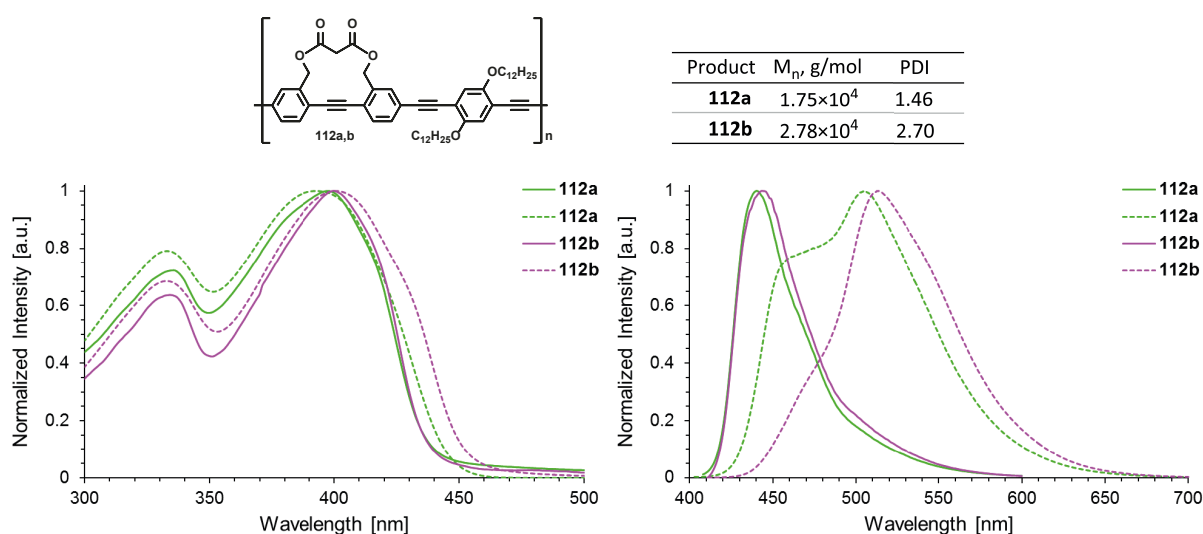


Figure 43. Absorption (left) and emission (right) spectra of **112a** and **112b** in CHCl_3 solution (solid) and film (dashed). Emission spectra have been recorded with excitation at 398 nm (**112a**), 400 nm (**112b**) in CHCl_3 and at 393 nm (**112a**), 401 nm (**112b**) in film.

Absorption spectra of **112a** and **112b** both in CHCl_3 solution and in the film are nearly identical and show two broad maxima at ca. 335 and 400 nm, which is usual for this polymer class.^[39] Absence of remarkable red-shifted absorption in film implies rather weak intermolecular interaction in solid state, however slightly red-shifted absorption of **112b** relative to **112a** is

probably due to molecular weight differences. Emission of **112a** is also blue-shifted both in CHCl_3 and in film and in the last shows a strong short wave shoulder at ca. 458 nm. Around 50 nm bathochromic shift of the solid-state emission maxima suggests excimer aggregates.

Table 8. Photophysical properties of polymers **112a**, **112b** and **112c**.

Cpd	λ_{abs} [nm]	$\lambda_{\text{em}} (\lambda_{\text{ex}})$ [nm]	$\lambda_{\text{abs}}^{\text{c}}$ [nm]	$\lambda_{\text{em}}^{\text{c}} (\lambda_{\text{ex}})$ [nm]	$\Phi_{298\text{K}}^{\text{a}}$ [%]	$\tau_{298\text{K}}^{\text{a}}$ [ns]
112a	336 ^a 397 ^a	440 ^a (398)	--	--	45	0.6
	333 ^b 393 ^b	505 ^b (393)				
112b	334 ^a 400 ^a	443 ^a (400)	333 398	440 ^d (400)	65	0.7
	333 ^b 401 ^b	513 ^b (401)		433 ^e (400)		
112c	334 ^a 400 ^a	443 ^a (400)	--	--	64	0.7
	334 ^b 405 ^b	509 ^b (406)				

a) In CHCl_3 . b) In film. c) In 2-methyl tetrahydrofuran. d) At 298K. e) At 77K.

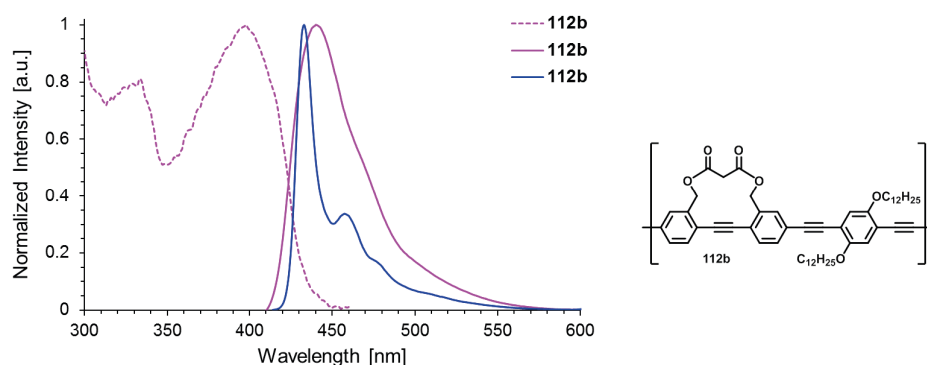
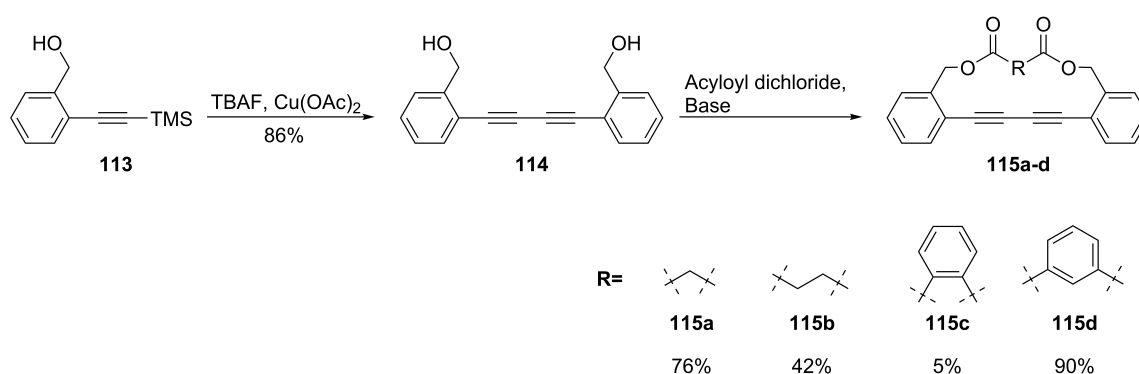


Figure 44. Absorption (dashed) and emission (solid) spectra of **112b** in 2-methyl tetrahydrofuran. Emission spectra have been recorded with excitation at 400 nm at 298K (violet) and 77K (blue).

Recording of photophysical properties at cryogenic temperatures was performed in 2-methyl tetrahydrofuran solution, since cooled with liquid nitrogen it makes an organic glass, transparent in the UV-Vis region. Although solubility of **112b** in 2-methyl tetrahydrofuran was rather low, commonly used EPA was suggested to have insufficient dissolving capability. At room temperature, absorption and emission differ barely from those in CHCl_3 (**Figure 44**). Cooled to 77K **112b** shows no phosphorescence together with narrowed blue-shifted fluorescence maximum and minor peak at ca. 457 nm. The narrow band can suppose emission occurring from some localized excited states. Probably, the excitons before photo-relaxation are capable to migrate along the chain to fragments with lower energy.

3.2.8 Tethered 1,4-diphenylbutadiynes

Cyclic derivatives of 1,4-diphenyldiacetylene (DPB) attract interest as analogues of diphenylacetylene with more developed conjugation system. Additionally, dialkyne fragments – products of Glaser coupling^[159] – are standard backbone defects in PPEs even in oxygen free medium. Usual amount is up to 10% of all repetition units and exact determination is questionable.^[24] A series of tethered 1,4-diphenylbutadiynes **115a-d** have been prepared according to reaction sequence showed on **Scheme 25**.



Scheme 25. Synthesis of series tethered 1,4-diphenylbutadiynes **115a-d**.

Easily available from 2-iodobenzyl alcohol TMS-protected alkyne **113** after combined deprotection and Glaser coupling reaction in basic medium^[165] gave diol **114**, which was involved in reaction with a series of acyl dichlorides. Cyclophane yields were high depending on the acid chlorides and bases used. Reaction with malonyl chloride ran smoothly in the presence of NaHCO_3 , while in other examples educt was found to be unreacted. Using instead an excess of 4-(dimethylamino)pyridine afforded the desired products.

All substances are colorless solids and their single crystal specimens were obtained for structural analysis (**Figure 45**).

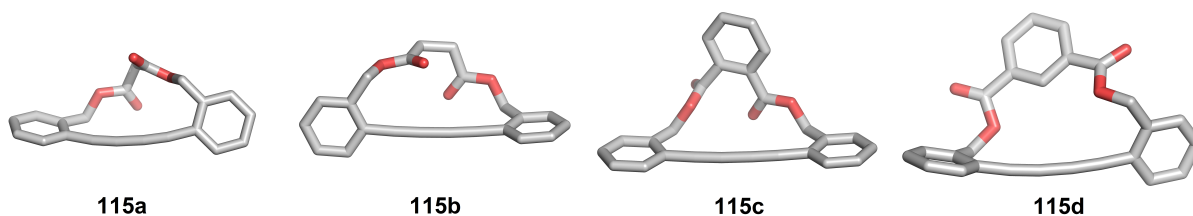


Figure 45. Crystal structures of tethered 1,4-diphenylbutadiynes **115a-d**. Twist angles: **115a** 59°, **115b** 69 and 81° (only one shown), **115c** 2°, **115d** 87°.

No correlation between the tether length and dihedral angle can be found from the measurement data, similar to published tolanophanes.^[67] Two phenyl rings in **115a** are moderately twisted, while having a looser tether **115b** two independent molecules with greater angle values were found. It is noticeable, that diphenylbutadiyne unit in **115a** and **115d** are considerably bent, in contrast to **115b** and **115c**. Similar slightly bent (2-3°) molecules have been found in crystal of untethered DPB derivatives.^[168] Remarkably, the low yield of the cyclization leading to **115c** cannot be explained with conformational strain, since DPB unit possess neither twisting nor bending.

Photophysics and applications of PPE-based oligo- and polymeric species is studied intensively, whereas a list of publications dedicated to 1,4-diphenyldiacetylene-based chromophores is shorter. The reason is simple: they show poor or no fluorescence.^[206] Optical properties of DPB derivatives were similar to each other and differed significantly from those of tolanes (**Figure 46**, **Table 9**). Due to similarity, spectral data of **115b** and **115c** can be found in Appendix 7.1.

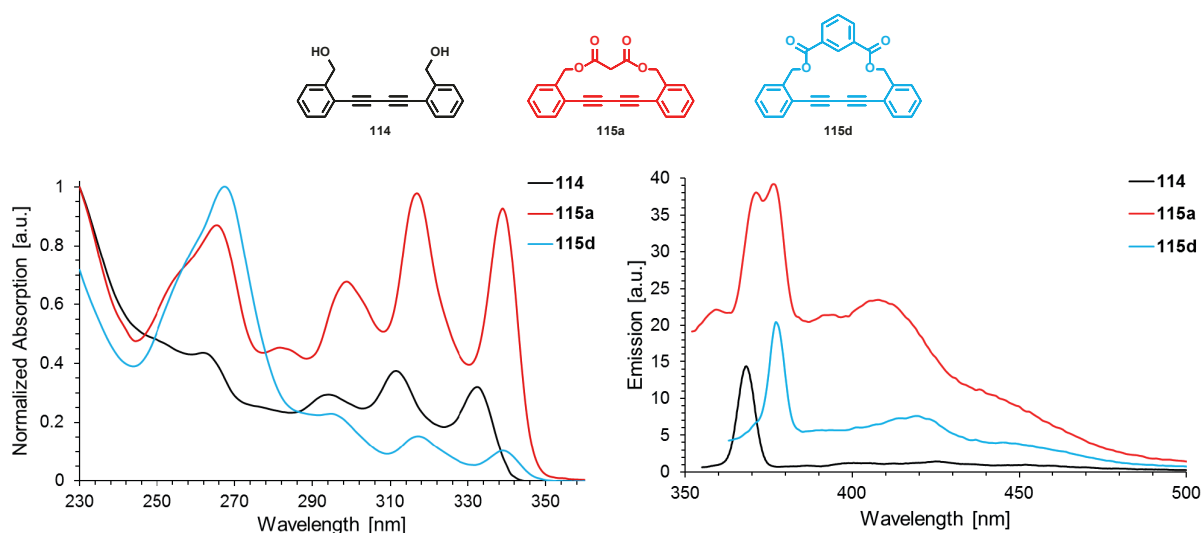


Figure 46. Absorption (left) and emission (right) of **115a** and **115d** in *n*-hexane. For comparison, spectra of untethered **114** are shown. Emission spectra have been recorded with excitation at 339 nm (**115a** and **115d**) and 332 nm (**114**).

Absorption spectra showed vibrational resolved bands, and location of maxima had no correlation with solid state twist angles, which supposed that differently twisted molecules have been always present in solution^[147] and could absorb light simultaneously. Absorbance of untethered **114** was low, while cyclic products showed two regions (240-280 nm and 290-350 nm) with alternating intensity.^[148]

Table 9. Photophysical constants of **114**, **115a**, **115b**, **115c**, **115d**.

Cpd	$\lambda_{\text{abs}}^{\text{a}}$ [nm]	$\lambda_{\text{abs}}^{\text{b}}$ [nm]	$\lambda_{\text{em}}^{\text{c}}$ 77K (λ_{ex}) [nm]	ϵ^{b} (λ_{max}) [$10^4 \text{ L}\cdot\text{mol}^{-1}\cdot\text{cm}^{-1}$]	$\tau_{77\text{K}}^{\text{c}}$ [s]
114	262, 294, 311, 332	254, 264, 297, 315, 336	500 (333)	--	--
115a	265, 299, 317, 339	267, 300, 319, 341	508 (339)	3.76 (267), 2.15 (341)	1.6
115b	266, 298, 316, 338	267, 299, 318, 340	507 (337)	2.39 (267), 3.41 (340)	1.7
115c	267, 284, 299, 317, 339	284, 300, 319, 341	508 (338)	4.58 (341)	1.1
115d	267, 295, 317, 339	269, 297, 319, 342	509 (339)	4.73 (269), 0.83 (342)	1.6

a) In *n*-hexane. b) In CH_2Cl_2 . c) In EPA (diethyl ether/isopentane/ethanol 5:5:2, v/v).

Room temperature emission had such low intensity, that distinguishing it from the strayed light or Raman scattering is not possible. Placed in **Figure 46** emission spectra were uncorrected and show ca. forty arbitrary units maximum intensity from one thousand possible at maximum sensitivity level of the fluorimeter. Registered emission of the pure solvent allowed approximately separation of bands, belonging to DPB derivatives. Room temperature fluorescence and phosphorescence lifetime measurements at local maxima (408 nm for **115a** and 419 nm for **115d**) showed no detectable decay. This results are in agreement with published heavy-detectable fluorescence of DPB^[143–145] and can be explained, that photo-relaxation of the excited molecule was slow, compared to non-radiative pathways.^[170]

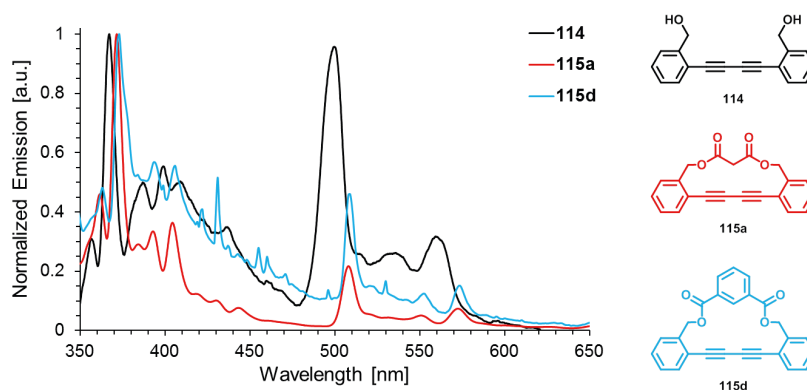


Figure 47. Low temperature (77K) emission spectra of **115a** and **115d** in EPA. For comparison spectrum of untethered **114** is shown. Emission spectra have been recorded with excitation at 339 nm (**115a** and **115d**) and 333 nm (**114**).

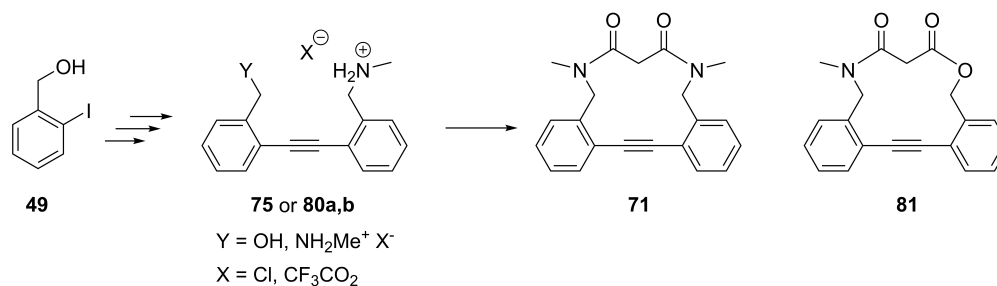
Emission in cryogenic glass is also low and insufficient for correct spectral characterization (**Figure 47**). Alternatively to fluorescence at room temperature, intensity of phosphorescence maximum of **114** at 77K surpassed these of tethered **115a**, **115b** and **115d** and had relatively strong and blue-shifted phosphorescence band at ca. 500 nm. The cyclic DPBs had practically the

same phosphorescence maxima, independent from solid state twist angles. Spectra of **115d** showed several sharp maxima of low intensity distributed over all emission region, which could be explained with interaction between DPB-chromophore and phthalic acid aromatic system. Published experimental measurements supported by TDDFT-calculations^[148] suppose, that even at temperatures below 100K in the anisotropic PE-matrix there are non-planar species of DPB. Together with present observation it implies, that photophysical properties of DPB-based chromophores are not depending on the tether.

4 Summary and Outlook

Conjugated polymers have a developed π -electron system. To this compound class belong poly(*para*-phenyleneethynylene)s (PPEs), which consist mostly of alternating benzene and acetylene units. These molecules have a linear rigid structure and have rotation of the phenyl rings around acetylene moieties as a prevalent degree of freedom. Mutual position of two neighboring rings determines the coupling degree of orbitals between them and therefore conducting and photophysical properties of PPE molecule. At room temperature, all possible rotamers are present in solution according to Boltzmann distribution. One of the possible ways to regulate electronic properties of PPEs is restricting the twist angle by binding phenyl rings with a tether. Diphenylacetylene (DPA, tolane) and bis(phenylethynyl)benzole (BPEB) have been successfully used as model compounds of PPEs.^[66,67,101] This work is devoted to further development of the synthetic and photophysical study of the conformationally controlled tolanes and their elongated analogs.

Synthesis. Starting with commercially available 2-iodobenzyl alcohol (**49**) two bridged tolanes **71** and **81** (total yields corresponding 21 and 31%) have been synthesized using Sonogashira coupling and cyclization with malonyl chloride under high dilution as key steps (**Scheme 26**).



Scheme 26. Structure of the bridged tolanes **71** and **81** and their precursors.

Amide functional groups of the tolanophanes **71** and **81** should be more stable against degradation processes than corresponding diester. Cyclization of the amidoester **81** proceeded with higher yield, when hydrochloride **80b** was used instead of trifluoroacetate **80a**. Probably due to the reaction of malonyl chloride with trifluoroacetate anion as a nucleophile.

Since uncomplicated migration from ester tolanophanes to amide **71** and amidoester **81** was shown, diiodotolane **85** (total yield 23%) and tolanophane **90** (total yield 13-18% depending on synthetic approach) with extended π -system have been synthesized (**Figure 48**).

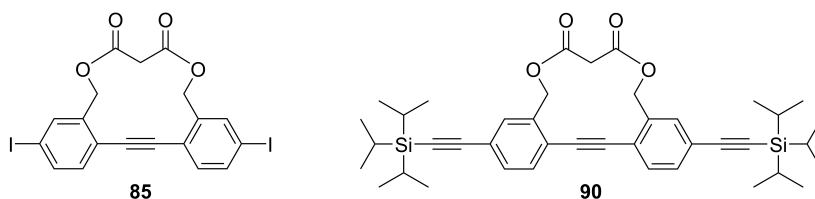


Figure 48. Structures of bridged diiodo tolane **85** and extended **90**.

The cyclization step appeared to be selective depending on the reaction condition and afforded not only desired monomer **90**, but additionally dimer **91** (total yield 10%), unusual conformational behavior of which awakened the interest to other cyclic oligomers. Based on precisely controlled annulation or step-by-step synthesis, approaches to **92**, **98** and **93** have been developed and realized (**Figure 49**).

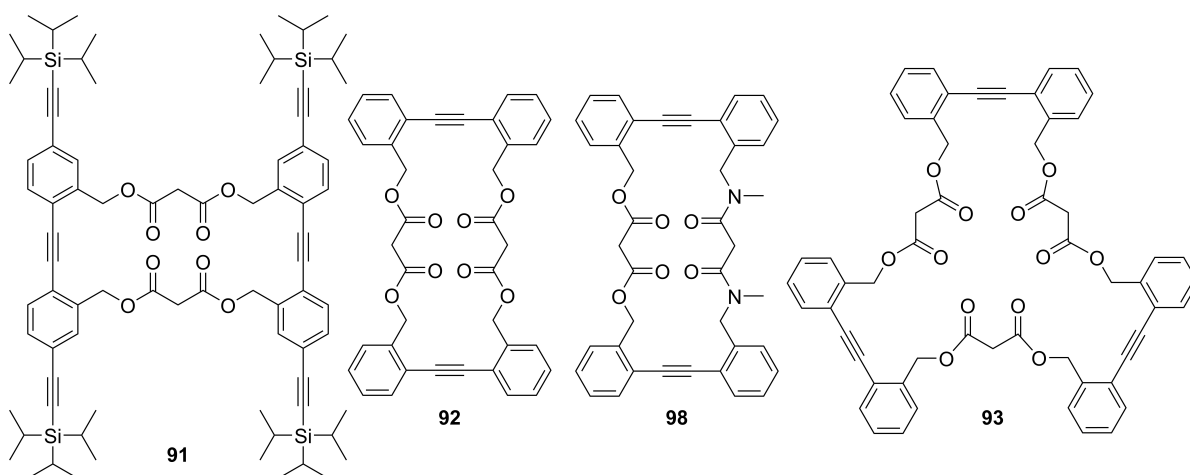


Figure 49. Structures of synthesized cyclic oligomers.

From experimental and theoretical studies, planarization was known to occur regardless what conformation the tolanophane molecule exhibit before excitation. One of the possible ways to overcome this was an introduction of two tethers to one DPA-fragment, which should make the molecule of tolanophane **102** more robust against planarization (**Figure 50**). In contrast to other bridged tolanes, synthesized during this work, DPA-core was built using Stille coupling, since commonly used Sonogashira conditions failed.

Using 1,4-bis(phenylethynyl)benzene unit as a base core was another approach to doubly bridged tolane. Emission of BPEB is more efficient, as that of tolane; therefore, effects caused by tether should be more eye-catching. Based on amidoester structure for better cyclization control, synthesis of **109** succeeded after numerous attempts.

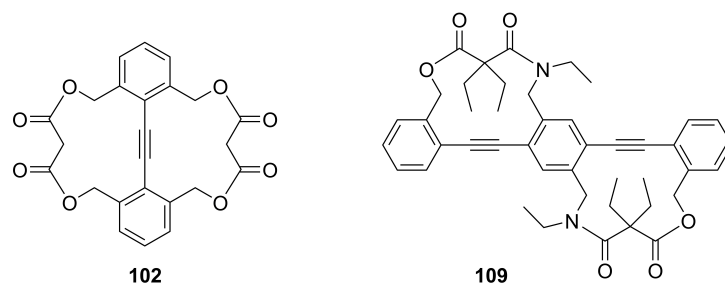


Figure 50. Structures of doubly-bridged tolanes **102** and **109**.

Incorporating of tethered fragments with restricted twist angle in a poly(*para*-phenyleneethynylene) chain could bring new organic semiconducting materials with interesting properties. Applying Sonogashira coupling, copolymers **112a-c** ($P_n=22-35$), consisting of didodecyloxy benzene and tolanophane moieties, have been synthesized (**Figure 51**).

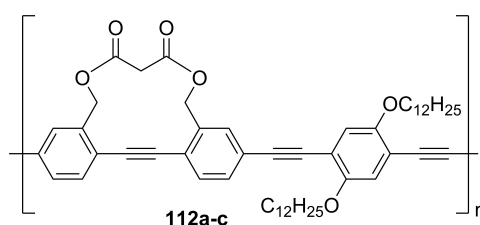


Figure 51. Repetition unit structure of synthesized polymers.

Increasing catalyst load from 0.2 to 1 mol% led to increased yield as well as PDI of the polymer and could also led to higher alkyne-alkyne defects formation. Additionally, cyclic DPB derivatives attract interest as analogues of diphenylacetylene with more developed conjugation system. Cyclophane yields were sensitive towards the acids and bases used (**Figure 52**).

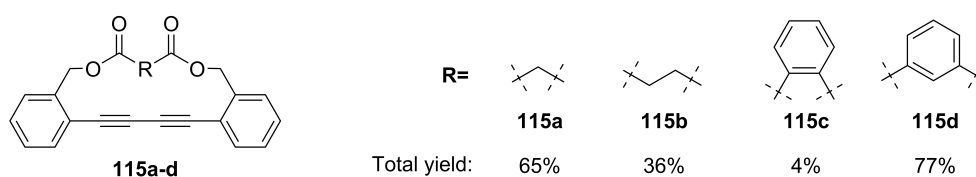


Figure 52. Structures and total yields of bridged 1,4-diphenyldiacetylenes.

Structures. For structural study single crystal specimens for most of investigated cyclophanes have been prepared according to diverse procedures. Measured structures and twist angles of the tolanophanes are summarized on **Figure 53**. Compounds **85**, **93** and **98** are not present, since no suitable for measurement single crystals have been obtained.

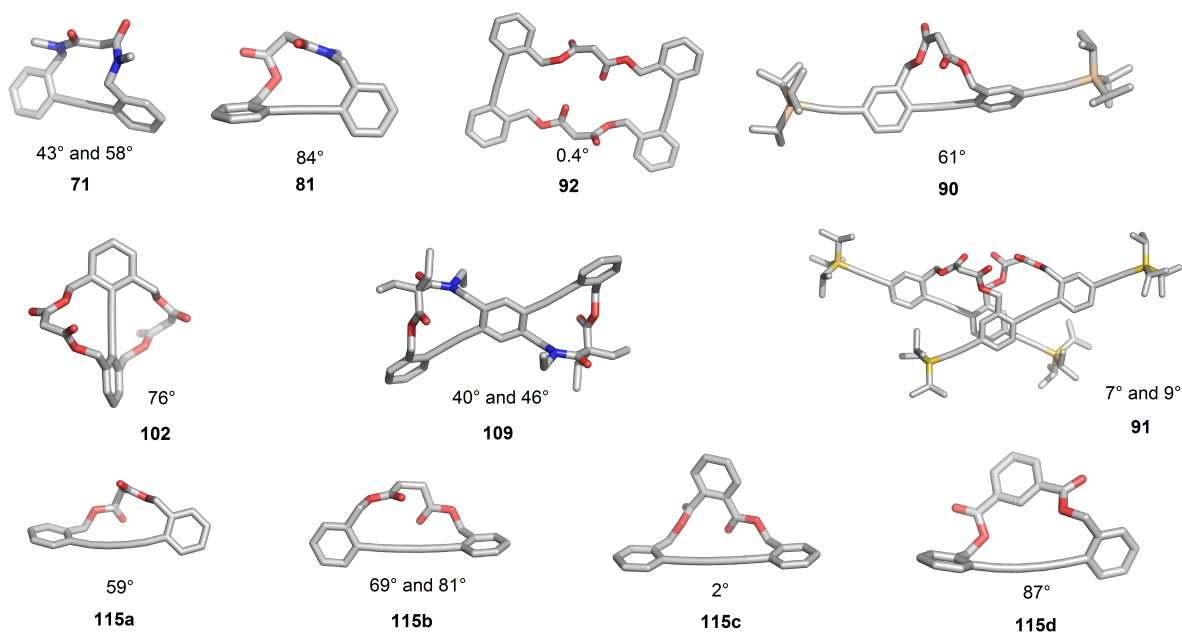


Figure 53. Crystal structures and twist angles in solid state of synthesized tolanophanes. If two different conformers were present in the elementary cell, one is shown.

The most twisted conformation in solid-state among measured tolanophanes have been found by amidoester **81**. Comparison of **71** and corresponding diester **22a**^[66] revealed a conformational difference between molecules. Benzylic CH₂-groups in diamide **71** had *s-trans* configuration, while in ester **22a** *s-cis* was found. Monomer **90** has partially twisted phenyl rings, whereas nearly planar DPA-units in dimer **91** were such located, that benzene rings stack near parallel to each other at a distance about 3.6 Å. In contrast, dimer **92** showed an unremarkable untwisted and planarized structure. The torsion angle between benzene rings of **102** is 76°, the straight diphenylacetylene unit demonstrated a symmetrical double-bridged layout of the molecule. Remarkably, the ArCH₂-signals are split in ¹H NMR spectrum of **102**, which was not seen before in single-bridged diester analogues. Structural analysis of the single crystal specimen of **109** showed presence of two independent moderately twisted molecules within one cell unit.

Between the tether length and dihedral angle no correlation was found for bridged PDB **115a-d**. Remarkable, that diphenylbutadiyne units in **115a** and **115d** are considerably bent, probably in part due to conformational strain. Hence low yield of **115c** cannot be explained involving high tension within the molecule, as bending was feebly marked.

TGA-DSC analysis of polymers **112a-c** showed that specimens had similar glass transition temperature (ca. 60°C) and melting point (ca. 200°C). Prepared by spin-coating thin films on a

glass substrate revealed predominantly amorphous layer with regional crystalline formations for all cases.

Photophysical properties. The twist angle between two benzene rings defines the degree of electronic coupling in a diphenylacetylene unit. Coupling is maximal and π -system is spread over the molecule when the rings are in plane. The closer the mutual position is to orthogonal the less is the π -coupling. This has an effect on optical properties.

Absorption spectra of in the ground state twisted tolanes (**71**, **81** and **85**) showed blue-shifted maxima relative to planar (**92**, **93** and **98**) ones. As expected, emission spectra are identical regardless of conformation. Contrary to that, emission of double bridged **102** suggests twisted species in the excited state.

Fixation of the ground state conformation in the excited state was achieved by freezing of EPA solutions with liquid nitrogen (77K). Twisted tolanophanes showed blue-shifted fluorescence together with phosphorescence, with was characterized by measurement of lifetimes up to 1.7 s for **85**, where effective spin-orbital coupling takes place. Planar types had vibronically well-resolved fluorescent emission with no or minimum phosphorescence.

Tolanese with prolonged π -system (**90** and **91**) showed red-shifted absorption and emission maxima, as well higher molar extinction coefficients and fluorescence quantum yields. At room temperature absorption maximum of twisted **90** was blue-shifted compared to that of planar **91**, but both showed identical fluorescence. In rigid cryogenic glass, no phosphorescence was detected, but fluorescence maximum of **90** was significantly blue-shifted to **91**.

Absorption spectrum of **109** in solution was red-shifted compared to that of single-DPA chromophores and showed no resolved vibrational structure, similar to polymer. Emission of **109** was more effective compared to that of tolane derivatives and displayed less divergence in solution and in cryogenic glass. At low temperature, an additional weak phosphorescence band was registered. Photophysical properties of polymers **112a-c** were practically identical. Broad fluorescence maximum at room temperature gained vibronic structure and 7 nm hypsochromic shift at 77K. Absorption and emission in spin-coated films compared to solution was expected red-shifted at 1 and 69 nm respectively. This suggests predominance of excimer aggregates in the solid state.

Optical properties of DPB cyclophanes **115a-d** are similar to each other and differ significantly from those of tolanes. Absorption spectra showed vibrationally resolved bands and two regions

(short-wavelength 240-280 nm and long-wavelength 290-350 nm) with alternating intensity. Assuming planarized species are responsible for long-wave band, **115d** is supposed to have predominantly twisted rotamers in solution compared to **115b**.

Emission intensity both in solution and in cryogenic glass was low, probably due to fast non-radiative relaxation. Nevertheless, at 77K resolved phosphorescence band is detectable, which intensity for untethered DPB overcomes that of bridged species. Together with other observations it implies, that photophysical properties of DPB-based chromophores depend not significantly on the twist angle in the solid state.

4.1 Outlook

There are a number of possible modified tolanophanes, which could serve for further study of influence of twist angle on photophysical properties. The most obvious strategy is introduction of donor and acceptor substituents to different parts of the molecule **116** (Figure 54). Such approach has been used extensively and led to materials with promising properties, and is also applicable to BPEB- and less-emissive PDB-based chromophores (see part 2.5).

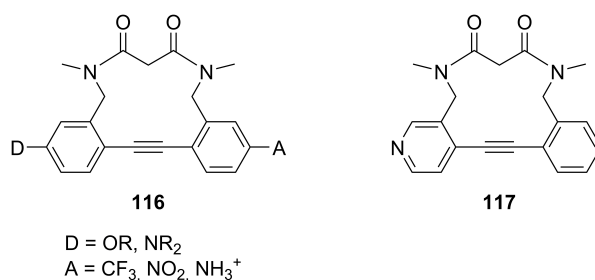


Figure 54. Structure of tolanophanes with donor and acceptor groups conjugated with π -system.

Similar approach is combining of benzene and heterocyclic aromatic rings within one tolane unit (for example **117**). Additional to combination of donor-acceptor subunits, nitrogen-containing parts, like pyridine, can serve as pH-sensor, where not only charge distribution can be affected, but also conformation of the whole molecule.^[132]

Another development approach is a jointment of tolane-based chromophores with other types of related units, as it is shown on **Figure 55**.

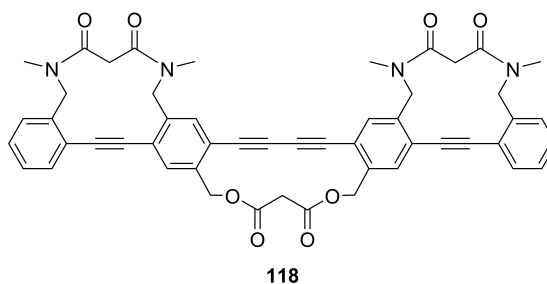
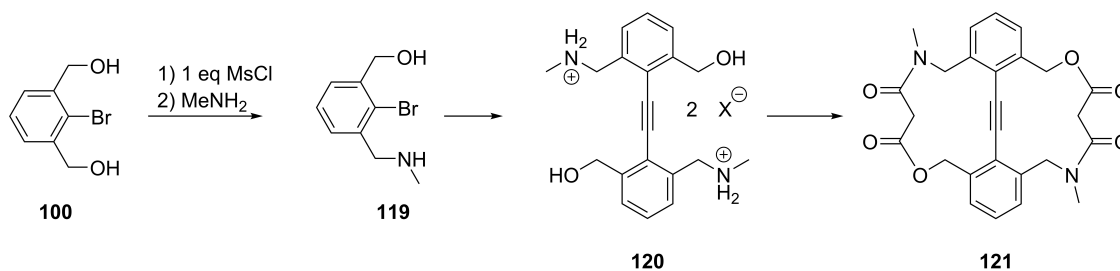


Figure 55. Combination of twisted DPA and DPB subunits.

Hybrid molecules like **118** due to elongation of the conjugation system should possess advanced emission. Superposition of different chromophore types can provide a curious electron density distribution.

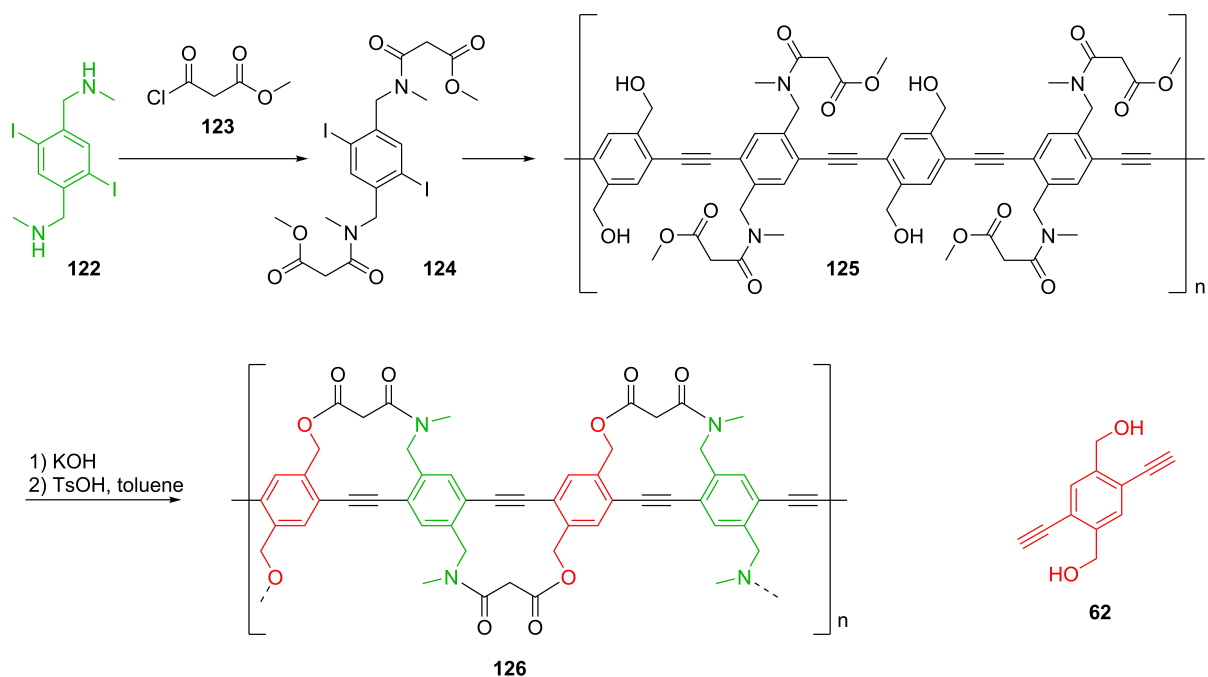
In this work, presence of ester and amide functionalities in the tolanophane led to a maximal twisting of the diphenylacetylene moiety. Complementation with double-bridge model can lead to a more rigid molecule design **121** (**Scheme 27**).



Scheme 27. Possible synthesis of the double-tethered amidoester **121**.

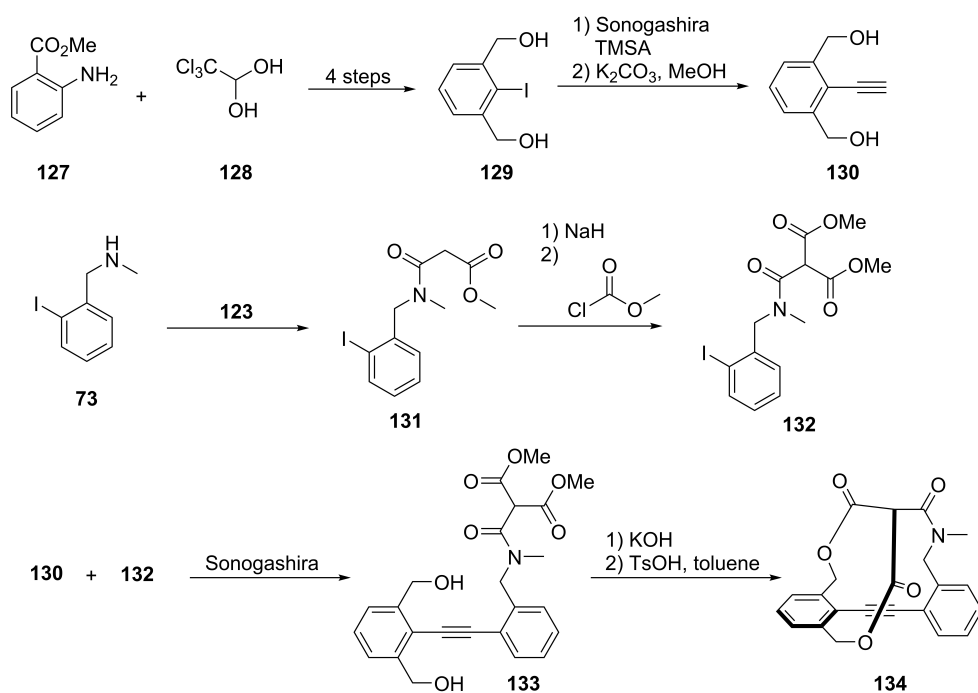
Bromodiol **100** undergoes selective mono-mesylation under slow addition and high dilution conditions. Workup with methylamine gives aminoalcohol **119**, which after Boc-protection of the amino group can be coupled with acetylene gas under Sonogashira conditions. After acidic Boc-deprotection mutual repulsion of charged ammonium groups allows assuming anti-conformation of **120**. Cyclization under high-dilution condition can result in desired **121**.

Normally, distribution of the twist angles in a PPE chain is guided by Boltzmann distribution in solution and side-chain specified packing in the solid state. Tending to maximal π -coupling results in preferable planarization of benzene rings. On **Scheme 28** is present a probable synthetic approach to a full-controlled twisted PPE.



Scheme 28. Synthetic approach to a PPE with constrained twisting.

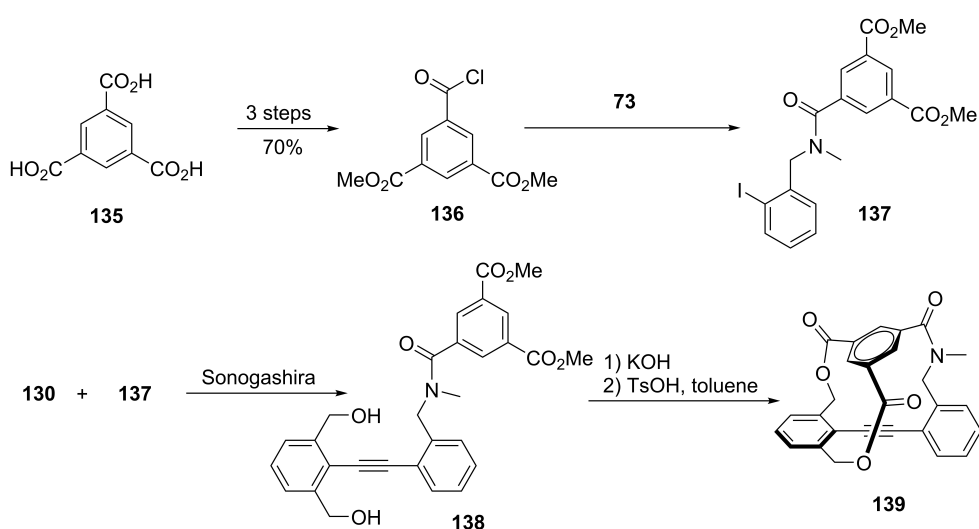
Diamine **122** and diol **62** should be easily accessible with conventional methods, described in the experimental part (5.3). Acylation of diamine **122** using commercially available methyl malonyl chloride (**123**) leads to building block **124**, which can be coupled with diacetylene **62** according to Sonogashira procedure. Saponification of the polymer **125**, followed by azeotropic intramolecular acylation under high-dilution conditions can derive bridged polymer **126**.



Scheme 29. Possible synthetic approach to one-and-a-half-linked tolanophane **134**.

Covalently bound tether in previously described model compounds allowed some twisting. If, for example, a tolanophane has in solid state dihedral angle 70° , so in solution through simple conformation change in the tether, movement of the phenyl ring between $+70^\circ$ and -70° is possible. Shown on **Scheme 29** synthetic route can provide tolanophane **134**, where rotation is doubly limited.

Alkyne **130** can be synthesized from iododiol **129**, which is accessible according to literature known methods from methyl anthranilate (**127**) and chloral hydrate (**128**) in four steps.^[207] The second building block **132** is available from known amine **73** through reaction with methyl chloroformate.^[208] Sonogashira coupling of **130** and **132**, followed by consecutive saponification and esterification leads to desired **134**.



Scheme 30. Synthetic approach to one-and-half-linked tolanophane **139**.

Similar approach using accessible tricarboxylic acid derivative **136**^[209] can lead to more firm fixation of the twist angle (**Scheme 30**). Advantageous is more rigid linker and less probable decarboxylation on the last step; but leading to **139** esterification reaction might progress slowly.

5 Experimental Part

5.1 General remarks

Solvents and reagents were purchased from Sigma-Aldrich, Merck, ABCR, Acros Organics and Fisher Scientific or from chemical shop of the Organic Chemistry Institute and were used as obtained. Deuterated solvents were acquired from Deutero GmbH, Kastellaun, Germany.

Absolute solvents were dried by MBraun MB SPS-800 solvent purification system. Oxygen or moisture sensitive reactions were carried out in evacuated heat gun dried glassware under a nitrogen atmosphere using a common Schlenk technique. Degasation has been performed by passing through the solution nitrogen gas during minimum 30 min or by repetitive freeze-pump-thaw procedure.

If no temperature given, room temperature (23-34°C) is meant.

5.2 Instruments and Methods

For slow addition of solutions, BBraun Perfusor VII syringe pump was used.

Thin layer chromatography (TLC) was carried out on Polygram® SIL G/UV254 plates from Macherey-Nagel GmbH & Co. KG, Düren (Germany) and examined under ultraviolet light irradiation (254 nm and 365 nm). **Column chromatography** was performed using silica gel from Sigma-Aldrich (technical grade, particle size: 0.063-0.200 mm) or from Macherey-Nagel GmbH & Co. KG, Düren (Germany) (particle size: 0.040-0.063 mm). For **preparative high pressure liquid chromatography** separation (HPLC) Jasco PU-2087 units equipped with Jasco UV2077Plus detector and Advantec CHF122SC fraction collector were used. Data analysis was accomplished with Jasco ChromPass data system. Analytical **gel permeation chromatography** (GPC) was carried out at room temperature in THF with PSS-SDV columns on a Jasco PU-2050 GPC unit equipped with Jasco UV-2075 and Jasco RI-2031 detectors. Data was processed using PSS WinGPC Unity software. **Ultra-performance liquid chromatography** (UPLC-MS) was performed on a Waters Acquity with a SQD2 mass detector. The acquired data was analyzed using ACD/Labs Spectrus Processor 2012. **Gas chromatographic** measurements (GC-MS) were recorded using Agilent 7890A Network GC System equipped with Agilent 5975C VL MSD mass detector. Software Agilent MSD ChemStation was used for data analysis.

Nuclear magnetic resonance (NMR) spectra (^1H , ^{13}C) were recorded at room temperature (if no temperature given) on Bruker Avance III 300, Bruker Avance III 500 or Bruker Avance III 600 at the NMR Spectroscopy Facility of the University of Heidelberg. Processing of the acquired data was done using Bruker TopSpin 3.2 program. Chemical shifts (δ) are reported in parts per million (ppm) relative to solvent residual peak.^[210]

Infrared spectra (IR) were recorded neat on Jasco FT/IR-4100 spectrometer equipped with GladiATR attenuated total reflectance accessory from Pike Technologies. Data processing was done using the Jasco Spectra Manager 1.5 or 2.0.

High resolution mass spectra (HRMS) were obtained by electrospray ionization (ESI), direct analysis in real time (DART) or electron ionization (EI) experiments on a Bruker ApexQe hybrid 9.4 TFT-ICR-MS at the Mass Spectrometry Facility of the University of Heidelberg.

Elemental analysis was accomplished on an Elementar vario MIKRO cube machine by the Micro Analytical Laboratory of the University of Heidelberg.

Single crystal X-Ray analysis was performed at a Crystallography facility of the University of Heidelberg on Bruker APEX-II Quazar or STOE Stadivari area detector. Data was processed and visualized with Mercury 3.2 or PyMOL 1.3 software.

UV-Vis absorption spectra were recorded at room temperature on a Jasco V-660 or Jasco V-670 spectrophotometer and at 94K on Agilent Cary 5000 UV-Vis-NIR spectrophotometer (this from Prof. Hans-Jörg Himmel, Heidelberg University), equipped with cryostat cell and West 6100plus temperature control unit and controlled by the Cary WinUV software. **Emission spectra** were recorded on a Jasco FP-6500 spectrofluorometer. For low temperature measurements (77K) Jasco LPH-140 liquid sample cell was equipped. All room temperature measurements were performed in a Quartz SUPRASIL[®] high precision cell with light path 10×10 mm from Hellma Analytics. For low temperature measurements the samples were dissolved in EPA (a mixture of diethyl ether/iso-pentane/ethanol 5:5:2, v/v) or 2-methyl tetrahydrofuran, which form a transparent rigid glass at liquid nitrogen temperatures.

Fluorescence lifetimes were measured using Horiba FluoroCube equipped with TBX picosecond photon detection module. Excitation was achieved by Horiba laser light sources: NanoLED-290 (290 nm) for fluorescence and SpectraLED-295 (300 nm) for phosphorescence. Phosphorescence lifetime measurements were performed at 77K in a Jasco LPH-140 cell adjusted to Horiba FluoroCube. Data evaluation was made with Horiba DAS6 software.

Fluorescence quantum yields were measured using either absolute method^[211] on PTI Quantamaster 40 equipped with Ulbricht sphere or the comparative method with L-Tryptophan in distilled water as a reference ($\phi_{ref}=0.14$).^[212] Absorption and emission were measured for reference and sample compound at least at four different concentrations. The absorptions at the maximum wavelengths and the areas under the emission curves were used to get a linear fit. The gradients of the reference and the sample were compared using the following equation (1):

$$\Phi_{smp} = \Phi_{ref} \left(\frac{grad_{smp}}{grad_{ref}} \right) \frac{n_{smp}^2}{n_{ref}^2} \quad (1)$$

where $grad_{smp}$ =gradient of the sample; n_{smp} =refractive index of sample solvent; $grad_{ref}$ =gradient of the reference; n_{ref} =refractive index of reference solvent.

Melting points were determined in glass capillaries with a Melting Point Apparatus MEL-TEMP (Electrothermal, Rochford, UK) and were kept uncorrected to normal conditions.

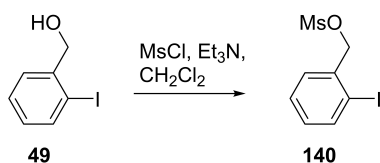
Polarized microscopy images were recorded on a Nikon Eclipse LV100POL microscope with included camera. The pictures were processed with the Nikon NIS-Elements software 3.21.00.

Thermogravimetric analysis was made on TGA-DSC Mettler Toledo using aluminium crucibles.

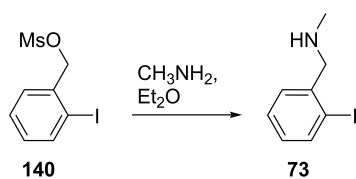
For **microwave** heated reactions Monowave 300 with standard vessels was used.

5.3 Synthetic Procedures

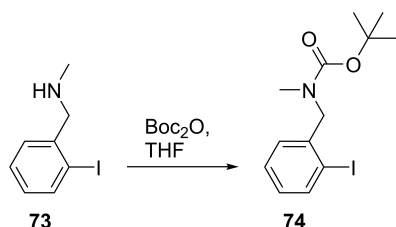
2-Iodobenzyl methanesulfonate (140).



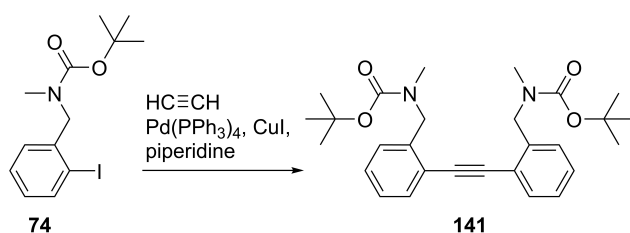
Literature known procedure was used.^[213] Analytical data was in agreement with published.^[214] $R_f=0.46$ (CH₂Cl₂); ¹H NMR (CDCl₃, 300 MHz): $\delta=3.03$ (s; 3H; CH₃), 5.28 (s; 2H; ArCH₂), 7.04-7.13 (m; 1H; H_{Ar}), 7.36-7.51 (m; 2H; H_{Ar}), 7.86-7.93 (m; 1H; H_{Ar}) ppm.

1-(2-Iodophenyl)-N-methylmethanamine (73).

Literature known procedure was used.^[215] The product was pure enough to be used without further purification. $R_f=0.51$ ($\text{CH}_2\text{Cl}_2/\text{methanol}$ 5:1, v/v); $^1\text{H NMR}$ (CDCl_3 , 300 MHz): $\delta=1.97$ (br s; 1H; NH), 2.47 (s; 3H; NCH_3), 3.79 (s; 2H; ArCH_2), 6.91-7.01 (m; 1H; H_{Ar}), 7.27-7.41 (m; 2H; H_{Ar}), 7.80-7.86 (m; 1H; H_{Ar}) ppm.

tert-Butyl (2-iodobenzyl)(methyl)carbamate (74).

Literature known procedure was used.^[216] Analytical data was in agreement with published.^[217] $R_f=0.62$ (petroleum ether/ethyl acetate 1:1, v/v); $^1\text{H NMR}$ (CDCl_3 , 300 MHz): $\delta=1.45$ (s; 9H; *t*-Bu), 2.87 (s; 3H; NCH_3), 4.44 (s; 2H; ArCH_2), 6.92-7.00 (m; 1H; H_{Ar}), 7.12 (d; J 7.5 Hz; 1H; H_{Ar}), 7.30-7.37 (m; 1H; H_{Ar}), 7.83 (d; J 7.9 Hz; 1H; H_{Ar}) ppm.

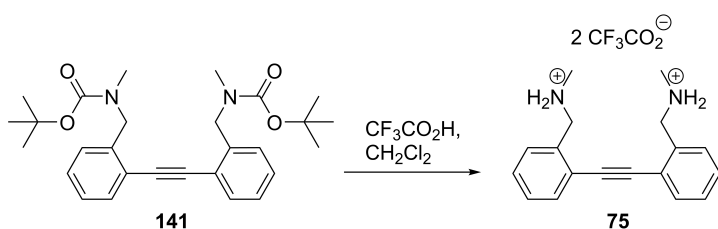
Di-tert-butyl ((ethyne-1,2-diylbis(2,1-phenylene))bis(methylene))bis(methylcarbamate) (141).

Literature known procedure was adapted.^[67] Common Schlenk procedure was used. A solution of **74** (371.0 mg, 1.069 mmol, 1.0 eq) in piperidine (1.3 mL) was degassed by nitrogen bubbling for 30 min. Then $\text{Pd}(\text{PPh}_3)_4$ (12.0 mg, 10.7 μmol , 1 mol%) and CuI (4.0 mg, 21.4 μmol , 2 mol%) were added and the final solution was frozen in a bath of liquid nitrogen and held under vacuum for 30 min. Then a balloon filled with acetylene gas was attached and the reaction mixture was allowed to melt and stir under acetylene atmosphere. After 2 h the reaction mixture was diluted with CH_2Cl_2 until homogenization occurred. Celite (ca. 1 g) was added, followed by concentration *in vacuo*. The precipitate was purified by column chromatography (silica gel; petroleum

ether/ethyl acetate gradient from 20:1 to 5:1, v/v) to yield **141** as a yellowish oil, which crystallizes later. Yield: 216.0 mg (0.465 mmol, 86%).

$R_f=0.51$ (petroleum ether/ethyl acetate 2:1, v/v); m.p.=73°C; $^1\text{H NMR}$ (CDCl_3 , 300 MHz): $\delta=1.34$ -1.57 (m; 18H; *t*-Bu), 2.79-2.99 (m; 6H; NCH_3), 4.70 (s; 4H; ArCH_2), 7.19-7.40 (m; 6H; H_{Ar}) 7.49-7.59 (m; 2H; H_{Ar}) ppm; $^{13}\text{C NMR}$ (CDCl_3 , 75 MHz): $\delta=28.2$, 34.2, 50.0 (0.5C), 50.7 (0.5C), 79.5, 91.7, 121.6 (0.5C), 121.9 (0.5C), 125.9, 126.7, 128.7, 132.1, 139.5, 155.9 ppm; IR: $\tilde{\nu}=2972$, 2932, 2862, 1692, 1480, 1453, 1389, 1365, 1300, 1244, 1173, 1142, 1022, 881, 755, 666 cm^{-1} ; HRMS (DART⁺) m/z : $[\text{M}+\text{H}]^+$ calculated for $\text{C}_{28}\text{H}_{37}\text{N}_2\text{O}_4^+$: 465.2748; found: 465.2763, correct isotope distribution; elemental analysis calculated (%) for $\text{C}_{28}\text{H}_{36}\text{N}_2\text{O}_4$: C 72.39, H 7.81, N 6.03; found: C 72.36, H 8.02, N 6.13.

N,N'-(Ethyne-1,2-diylbis((2,1-phenylene)methylene))dimethanaminium bis(trifluoroacetate) (75).

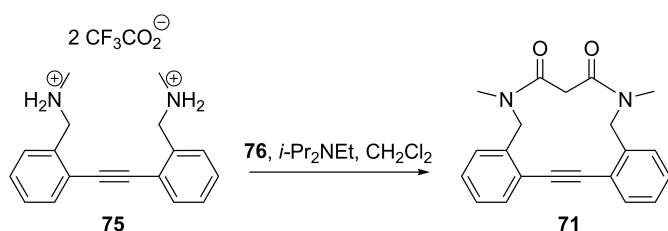


A published procedure was used.^[218] Trifluoroacetic acid (4.5 mL, 58.0 mmol, 30 eq) was added in one portion to a solution of **141** (890.0 mg, 1.916 mmol, 1.0 eq) in CH_2Cl_2 (45 mL). The resulting mixture was allowed to stir at these conditions for 2 h. After removal of all volatiles *in vacuo*, toluene (60 mL) was added and the mixture was concentrated again. The obtained as a solid **75** was washed by decantation with toluene (6×10 mL). Yield: 802.0 mg (1.629 mmol, 85%) brownish solid.

$R_f=0.10$ (CH_2Cl_2 /methanol 10:1, v/v); m.p.=173°C; $^1\text{H NMR}$ ($\text{DMSO-}d_6$, 400 MHz): $\delta=2.68$ (s; 6H; NCH_3), 4.41 (s; 4H; ArCH_2), 7.50-7.59 (m; 4H; H_{Ar}), 7.63-7.67 (m; 2H; H_{Ar}), 7.76-7.80 (m; 2H; H_{Ar}), 9.21 (br s; 4H; NH_2) ppm; $^{13}\text{C NMR}$ ($\text{DMSO-}d_6$, 100 MHz): $\delta=32.5$, 49.5, 91.4, 117.3 (q; $^1J_{\text{CF}}$ 301 Hz; CF_3), 122.5, 129.2, 129.5, 129.7, 132.8, 133.3, 158.4 (q; $^2J_{\text{CF}}$ 31 Hz; CO) ppm; IR: $\tilde{\nu}=3080$, 2688, 2430, 1657, 1614, 1495, 1456, 1432, 1198, 1179, 1125, 1132, 833, 797, 759, 720, 464 cm^{-1} ; HRMS (ESI⁺) m/z : $[\text{M}+\text{H}]^+$ of corresponding diamine calculated for $\text{C}_{18}\text{H}_{21}\text{N}_2^+$: 265.1699; found: 265.1695, correct isotope distribution; elemental analysis calculated (%) for $\text{C}_{22}\text{H}_{22}\text{F}_6\text{N}_2\text{O}_4$: C 53.66, H 4.50, N 5.69; found: C 53.67, H 4.47, N 5.80. Crystal data: $\text{C}_{22}\text{H}_{22}\text{F}_6\text{N}_2\text{O}_4$, $M_w=492.41$, colorless crystal (polyhedron), obtained by slow evaporation of a CHCl_3 solution of **75**,

dimensions $0.210 \times 0.110 \times 0.080 \text{ mm}^3$, monoclinic crystal system, space group $P2_1/c$, $Z=2$, $a=8.1229(9) \text{ \AA}$, $b=16.0178(18) \text{ \AA}$, $c=8.7919(10) \text{ \AA}$, $\alpha=90^\circ$, $\beta=91.111(3)^\circ$, $\gamma=90^\circ$, $V=1143.7(2) \text{ \AA}^3$, $\rho=1.430 \text{ g/cm}^3$, $T=200(2) \text{ K}$, $\Theta_{\text{max}}=25.049^\circ$, radiation $\text{MoK}\alpha$, $\lambda=0.71073 \text{ \AA}$, 7126 reflections measured, 2023 unique ($R_{\text{int}}=0.0291$), 1470 observed ($I > 2\sigma(I)$), final residual values $R_1(F)=0.052$, $wR(F^2)=0.123$ for observed reflections.

6,10-dimethyl-16,17-didehydro-10,11-dihydro-5H-dibenzo[g,k][1,5]diazacyclotridecine-7,9(6H,8H)-dione (71).

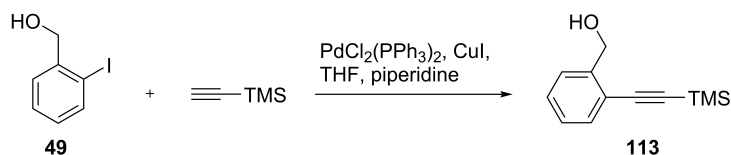


Common Schlenk procedure was used. Solutions of **75** (283.0 mg, 575 μmol , 1.0 eq) in a mixture of dry CH_2Cl_2 and acetonitrile (40 mL, 1:1, v/v) and malonyl chloride (**76**) (61 μL , 632.0 μmol , 1.1 eq) in dry CH_2Cl_2 (40 mL) were added simultaneously to a solution of N,N-diisopropylethylamine (600 μL , 3.448 mmol, 6.0 eq) in dry CH_2Cl_2 (120 mL) during 4 h. After stirring overnight, the reaction mixture was quenched by addition of saturated aq. NaHCO_3 solution (30 mL), phases were separated and the water phase was extracted with CH_2Cl_2 (3 \times 20 mL). The combined organic layers were washed with brine (1 \times 10 mL), dried over MgSO_4 and concentrated *in vacuo*. Purification by column chromatography (silica gel; CH_2Cl_2 /methanol 30:1, v/v) yielded **71** as colorless solid. Yield: 83.0 mg (0.250 mmol, 42%).

$R_f=0.42$ (CH_2Cl_2 /methanol 10:1, v/v); m.p.=213 $^\circ\text{C}$; a complex signal distribution seen due to tautomer mixture $^1\text{H NMR}$ (CDCl_3 , 600 MHz): $\delta=2.76$ (s), 2.92 (s), 2.94 (s), 2.98 (s), 3.55-3.68 (m), 4.03-4.12 (m), 4.66 (br s), 5.69-5.73 (m), 5.91-6.01 (m), 7.23-7.40 (m), 7.53-7.55 (m), 7.56-7.62 (m) ppm; $^{13}\text{C NMR}$ (CDCl_3 , 150 MHz): $\delta=33.1$, 33.8, 34.5, 35.2, 42.2, 43.7, 44.8, 50.3, 50.8, 53.1, 53.2, 91.2, 91.6, 91.7, 122.2, 122.5, 123.1, 123.5, 127.7, 127.9, 128.2, 128.5, 128.7, 129.1, 130.2, 130.3, 130.5, 131.2, 134.1, 134.8, 135.0, 135.2, 137.2, 137.4, 137.9, 166.6, 167.0, 167.4 ppm; IR: $\tilde{\nu}=2925$, 1651, 1628, 1492, 1434, 1392, 1352, 1208, 1168, 1102, 1080, 756, 648, 601, 454 cm^{-1} ; HRMS (ESI $^+$) m/z: $[\text{M}+\text{Na}]^+$ calculated for $\text{C}_{21}\text{H}_{20}\text{N}_2\text{NaO}_2^+$: 355.1417; found: 355.1417, correct isotope distribution; elemental analysis calculated (%) for $\text{C}_{21}\text{H}_{20}\text{N}_2\text{O}_2$: C 75.88, H 6.06, N 8.43; found: C 76.01, H 6.21, N 8.47. Crystal data: $\text{C}_{21}\text{H}_{20}\text{N}_2\text{O}_2$, $M_w=332.39$, colorless crystal (plate), obtained by slow cooling of a solution of **71** in ethanol, dimensions $0.210 \times 0.120 \times 0.020 \text{ mm}^3$, triclinic crystal system, space group $\overline{P1}$, $Z=4$, $a=9.3207(7) \text{ \AA}$, $b=9.9560(7) \text{ \AA}$, $c=19.4297(15) \text{ \AA}$,

$\alpha=102.8874(19)^\circ$, $\beta=97.9994(19)^\circ$, $\gamma=96.2809(19)^\circ$, $V=1722.0(2) \text{ \AA}^3$, $\rho=1.28 \text{ g/cm}^3$, $T=200(2) \text{ K}$, $\theta_{\text{max}}=25.085^\circ$, radiation $\text{MoK}\alpha$, $\lambda=0.71073 \text{ \AA}$, 21598 reflections measured, 6080 unique ($R_{\text{int}}=0.0560$), 3823 observed ($I>2\sigma(I)$), final residual values $R_1(F)=0.055$, $wR(F^2)=0.111$ for observed reflections.

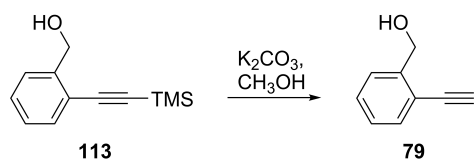
(2-((trimethylsilyl)ethynyl)phenyl)methanol (**113**).



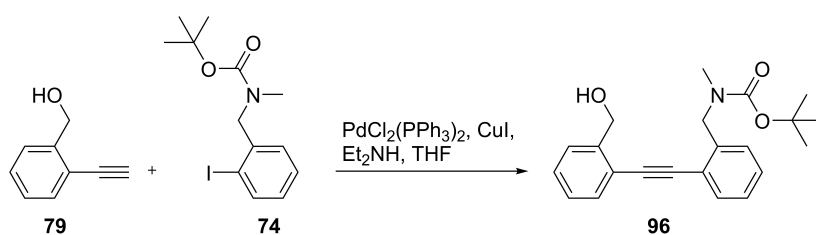
Literature known procedure was adapted.^[219] Common Schlenk procedure was used. A solution of 2-iodobenzyl alcohol (**49**) (10.00 g, 42.73 mmol, 1 eq), PdCl₂(PPh₃)₂ (300.0 mg, 427.3 μmol , 1 mol%) and CuI (163.0 mg, 854.6 μmol , 2 mol%) in 200 mL THF and 100 mL piperidine was degassed by bubbling nitrogen for 90 min. Then TMS-acetylene (9.10 mL, 64.10 mmol, 1.5 eq) was added. After stirring the reaction mixture for 1 h, volatiles were evaporated *in vacuo* and the residue was suspended in petroleum ether. Solids were filtered and washed with petroleum ether (3 \times 100 mL). Combined liquid phases were concentrated *in vacuo*. The rest was purified by column chromatography (silica gel; petroleum ether/Et₂O gradient from 30:1 to 5:1, v/v) yielded **113** as brownish oil. Yield: 7.769 g (38.02 mmol, 89%).

Analytical data was in agreement with published.^[219] $R_f=0.64$ (petroleum ether/ethyl acetate 1:1, v/v); $^1\text{H NMR}$ (CDCl₃, 300 MHz): $\delta=0.27$ (s; 9H; Si(CH₃)₃), 4.82 (s; 2H; ArCH₂), 7.20-7.50 (m; 4H; H_{Ar}) ppm.

(2-Ethynylphenyl)methanol (**79**).

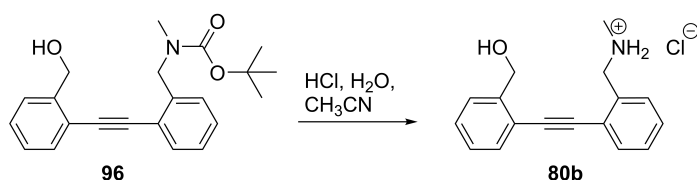


Literature known procedure was used, the analytical data was in agreement with published.^[220] $R_f=0.52$ (petroleum ether/ethyl acetate 1:1, v/v); m.p.=66°C; $^1\text{H NMR}$ (CDCl₃, 300 MHz): $\delta=2.20$ (s; 1H; OH), 3.34 (s; 1H; ArC≡CH), 4.04 (s; 2H; ArCH₂), 7.23-7.30 (m; 1H; H_{Ar}), 7.34-7.41 (m, 1H, H_{Ar}), 7.42-7.54 (m, 2H, H_{Ar}) ppm; $^{13}\text{C NMR}$ (CDCl₃, 75 MHz): $\delta=63.7$, 81.2, 81.9, 120.2, 127.3, 127.4, 129.2, 132.8, 143.2 ppm; IR: $\tilde{\nu}=3281$, 3257, 2915, 2862, 2103, 1478, 1450, 1368, 1044, 757, 705, 641, 622, 566 cm⁻¹; HRMS (EI⁺) m/z : [M]⁺ calculated for C₉H₈O⁺: 132.0570; found: 132.0559; elemental analysis calculated (%) for C₉H₈O: C 81.79, H 6.10; found: C 81.76, H 5.98.

tert-Butyl (2-((2-(hydroxymethyl)phenyl)ethynyl)benzyl)(methyl)carbamate (96).

Literature known procedure was adapted.^[219] Common Schlenk procedure was used. A degassed solution of **74** (2.837 g, 8.172 mmol, 1.0 eq), PdCl₂(PPh₃)₂ (287.0 mg, 409.0 μmol, 5 mol%) and CuI (156.0 mg, 817.0 μmol; 10 mol%) in a mixture of THF (36 mL) and Et₂NH (18 mL) was added to **79** (1.080 g, 8.172 mmol, 1.0 eq) under nitrogen. The resulting mixture was allowed to stir at room temperature for 3 h, after that CH₂Cl₂ (40 mL) and Celite (ca. 5 g) were added and all volatiles were removed *in vacuo*. The precipitate was purified by column chromatography (silica gel; petroleum ether/ethyl acetate gradient from 10:1 to 2:1, v/v) to yield **96** as yellowish oil. Yield: 2.326 g (6.619 mmol, 81%).

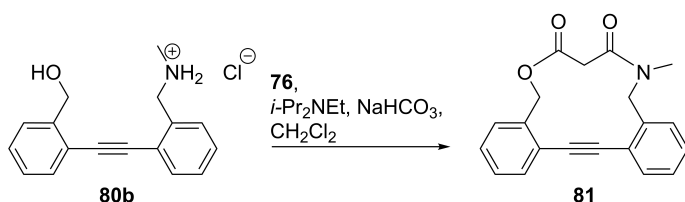
R_f=0.46 (petroleum ether/ethyl acetate 1:1, v/v); ¹H NMR (CDCl₃, 400 MHz): δ=1.42 (s, 9H; *t*-Bu), 2.84 (br s, 1H, OH), 4.70 (s, 2H, ArCH₂), 4.90 (s, 2H, ArCH₂), 7.22-7.29 (m, 3H, H_{Ar}), 7.30-7.38 (m, 2H, H_{Ar}), 7.48-7.55 (m, 3H, H_{Ar}) ppm; complex signal distribution seen due to tautomer mixture ¹³C NMR (CDCl₃, 100 MHz): δ=28.3, 34.1, 50.3, 50.9, 63.6, 79.8, 91.5, 91.6, 121.2, 121.7, 122.3, 126.3, 127.0, 127.3, 127.5, 128.8, 132.1, 132.4, 139.6, 142.5, 156.0 ppm; IR: $\tilde{\nu}$ =3437, 2975, 2927, 1691, 1668, 1479, 1451, 1391, 1367, 1145, 1044, 879, 756 cm⁻¹; HRMS (ESI⁺) *m/z*: [M+Na]⁺ calculated for C₂₂H₂₅NNaO₃⁺: 374.1727; found: 374.1731, correct isotope distribution; elemental analysis calculated (%) for C₂₂H₂₅NO₃: C 75.19, H 7.17, N 3.99; found: C 75.08, H 7.34, N 3.86.

1-(2-((2-(Hydroxymethyl)phenyl)ethynyl)phenyl)-N-methylmethanaminium chloride (80b).

A 2M aq. solution of HCl (23 mL) was added to a solution of **96** (407.0 mg, 1.158 mmol) in acetonitrile (23 mL); the reaction mixture was allowed to stay overnight at room temperature. After evaporation of all volatiles *in vacuo*, the brownish solid was washed with CHCl₃ (3×10 mL) and petroleum ether (1×10 mL) yielding **80b** as beige solid. Yield: 275.0 mg (0.986 mmol, 85%).

M.p.=180°C; ^1H NMR (DMSO-*d*₆, 600 MHz): δ =2.61 (s; 3H; NCH₃), 4.37 (s, 2H, ArCH₂), 4.75 (s, 2H, ArCH₂), 5.45 (br s, 1H, OH), 7.32-7.36 (m, 1H, H_{Ar}), 7.44-7.54 (m, 3H, H_{Ar}), 7.55-7.58 (m, 1H, H_{Ar}), 7.60-7.63 (m, 1H, H_{Ar}), 7.66-7.68 (m, 1H, H_{Ar}), 7.75-7.77 (m, 1H, H_{Ar}), 9.49 (br s, 2H, NH₂) ppm; ^{13}C NMR (DMSO-*d*₆, 150 MHz): δ =32.3, 49.4, 61.5, 90.7, 92.4, 119.7, 123.1, 126.9, 127.0, 129.15, 129.17, 129.24, 130.2, 131.9, 132.3, 133.3, 144.0 ppm; IR: $\tilde{\nu}$ =3377, 2943, 2788, 2715, 2426, 1495, 1472, 1457, 1434, 1404, 1191, 1005, 753, 563 cm⁻¹; HRMS (ESI⁺) *m/z*: [M+H]⁺ of corresponding amine calculated for C₁₇H₁₈NO⁺: 252.1383; found: 252.1384, correct isotope distribution; elemental analysis calculated (%) for C₁₇H₁₈ClNO: C 70.95, H 6.30, N 4.87; found: C 70.75, H 6.16, N 4.65.

10-Methyl-16,17-didehydro-10,11-dihydrodibenzo[*g,k*][1,5]oxazacyclotridecine-7,9(5*H*,8*H*)-dione (81).

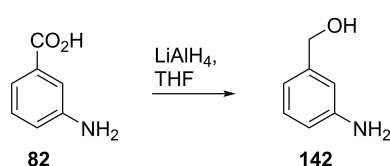


Common Schlenk procedure was used. A solution of malonyl chloride (**76**) (157.0 μL , 1.611 mmol, 1.5 eq) in dry CH₂Cl₂ (30 mL) and a solution of **80b** (309.0 mg, 1.074 mmol, 1.0 eq), premixed with N,N-diisopropylethylamine (0.37 mL, 2.148 mmol, 2.0 eq) in dry CH₂Cl₂ (30 mL), were simultaneously added to a mixture of NaHCO₃ (271.0 mg, 3.222 mmol, 3.0 eq) and N,N-diisopropylethylamine (0.36 mL, 2.148 mmol, 2.0 eq) in dry CH₂Cl₂ (215 mL) during 4.5 h. The reaction mixture was allowed to stir overnight, after that water (50 mL) was added. The water phase was separated and extracted with CH₂Cl₂ (2×40 mL). The organic phase was washed with brine (1×50 mL) and dried over MgSO₄. Concentration and purification by column chromatography (silica gel; petroleum ether/ethyl acetate 1:1, v/v then ethyl acetate) yielded **81** as colorless solid. Yield: 193.0 mg (604.0 μmol , 56%).

R_f =0.38 (ethyl acetate); m.p.=147°C; complex signal distribution seen due to tautomer mixture ^1H NMR (DMSO-*d*₆, 300 MHz): δ =2.70 (s), 3.10-3.20 (m), 3.60 (s), 3.68-3.90 (m), 4.69 (s), 4.98-5.17 (m), 5.22 (s), 5.43-5.52 (m), 5.75 (s), 7.34-7.68 (m) ppm; ^{13}C NMR (DMSO-*d*₆, 75 MHz): δ =31.1, 33.9, 42.0, 43.0, 49.5, 52.2, 54.9, 66.1, 66.2, 90.2, 90.3, 90.8, 91.2, 122.3, 122.4, 122.8, 123.3, 128.1, 128.5, 128.7, 128.8, 128.9, 129.0, 129.4, 130.2, 130.5, 131.1, 131.9, 133.0, 133.6, 133.7, 136.4, 136.5, 136.9, 138.2, 165.0, 165.3, 167.0, 167.4 ppm; IR: $\tilde{\nu}$ =3061, 2947, 1742, 1635, 1232, 1012, 757, 624, 502 cm⁻¹; HRMS (DART⁺) *m/z*: [M+H]⁺ calculated for C₂₀H₁₈NO₃⁺: 320.1281;

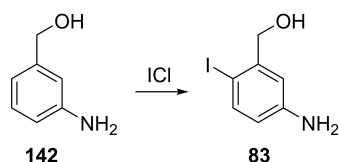
found: 320.1295, correct isotope distribution; elemental analysis calculated (%) for $C_{20}H_{17}NO_3$: C 75.22, H 5.37, N 4.39; found: C 75.09, H 5.36, N 4.32. Crystal data: $C_{20}H_{17}NO_3$, $M_w=319.35$, colorless crystal (polyhedron), obtained by slow diffusion of pentane vapor into a solution of **81** in THF, dimensions $0.100 \times 0.090 \times 0.080$ mm³, orthorhombic crystal system, space group $P2_12_12_1$, $Z=4$, $a=8.4867(10)$ Å, $b=9.2750(11)$ Å, $c=20.323(2)$ Å, $\alpha=90^\circ$, $\beta=90^\circ$, $\gamma=90^\circ$, $V=1599.7(3)$ Å³, $\rho=1.326$ g/cm³, $T=200(2)$ K, $\theta_{max}=22.331^\circ$, radiation $MoK\alpha$, $\lambda=0.71073$ Å, 9986 reflections measured, 2029 unique ($R_{int}=0.0479$), 1648 observed ($I > 2\sigma(I)$), final residual values $R_1(F)=0.068$, $wR(F^2)=0.178$ for observed reflections.

(3-aminophenyl)methanol (**142**).



Literature known procedure was used.^[221] Analytical data was in agreement with published.^[222] $R_f=0.34$ (ethyl acetate); 1H NMR ($CDCl_3$, 300 MHz): $\delta=2.93$ (br s; 3H; OH, NH_2), 4.60 (s; 2H; $ArCH_2$), 6.61 (dd; J 7.9, 2.0 Hz; 1H; H_{Ar}), 6.68-6.76 (m; 2H; H_{Ar}), 7.14 (t; J 7.7 Hz; 1H; H_{Ar}) ppm.

(5-Amino-2-iodophenyl)methanol (**83**).

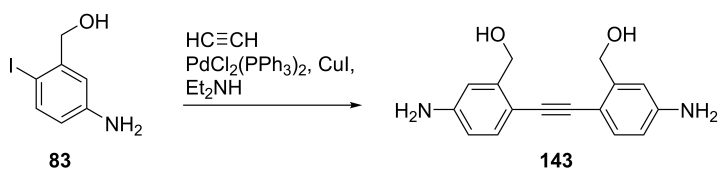


A commercially available 1M CH_2Cl_2 solution of iodine monochloride (1.8 mL, 1.79 mmol, 1.1 eq) was added dropwise to an ice cooled solution of 3-aminobenzyl alcohol **142** (200.0 mg, 1.624 mmol, 1.0 eq) in methanol (5 mL). The ice bath was removed and the reaction mixture was allowed to stir at room temperature for 40 min followed by concentration *in vacuo*. The solid was washed with CH_2Cl_2 (3×5 mL) and partitioned between a 1M aq. NaOH solution (5 mL) and ethyl acetate (10 mL). The organic phase was washed with 1M aq. NaOH solution (1×25 mL) and the combined aqueous layer was extracted with ethyl acetate (2×10 mL). The organic phase was washed with brine (1×20 mL) and dried over $MgSO_4$. Column chromatography (silica gel; petroleum ether/ethyl acetate gradient from 2:1 to 1:1, v/v, then ethyl acetate) yielded **83** as a brownish solid. Yield: 302.0 mg (1.212 mmol, 74%).

$R_f=0.45$ (ethyl acetate); m.p.=125°C; 1H NMR ($DMSO-d_6$, 300 MHz): $\delta=4.27$ (d; J 5.5 Hz; 2H; $ArCH_2$), 5.21-5.28 (m; 3H; OH, NH_2), 6.27 (dd; J 8.4, 2.8 Hz; 1H; H_{Ar}), 6.81 (d; J 2.8 Hz; 1H; H_{Ar}),

7.33 (d; J 8.4 Hz; 1H, H_{Ar}) ppm; ^{13}C NMR (DMSO- d_6 , 75 MHz): δ =67.3, 77.9, 113.8, 114.7, 138.2, 143.5, 149.0 ppm; IR: $\tilde{\nu}$ =3357, 3191, 2837, 1594, 1571, 1665, 1445, 1293, 1228, 1168, 1042, 1012, 803, 686, 574 cm^{-1} ; HRMS (ESI $^+$) m/z : $[\text{M}+\text{H}]^+$ calculated for $\text{C}_7\text{H}_9\text{INO}^+$: 249.9723; found: 249.9726, correct isotope distribution; elemental analysis calculated (%) for $\text{C}_7\text{H}_8\text{INO}$: C 33.76, H 3.24, N 5.62; found: C 33.93, H 3.29, N 5.46.

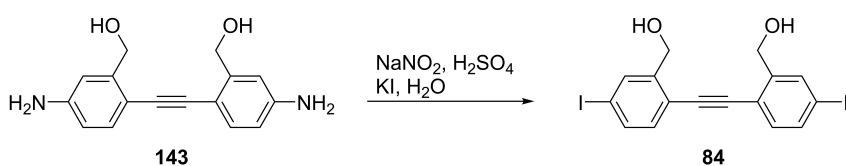
(Ethyne-1,2-diylbis(5-amino-2,1-phenylene))dimethanol (143).



Literature known procedure was adapted.^[223] Common Schlenk procedure was used. Under nitrogen atmosphere a degassed mixture of **83** (15.00 g, 60.23 mmol, 1.0 eq), $\text{PdCl}_2(\text{PPh}_3)_2$ (2.114 g, 3.011 mmol, 5 mol%) and CuI (1.047 g, 6.023 mmol, 10 mol%) in Et_2NH (30 mL) was frozen in a liquid nitrogen bath and so held under vacuum for 30 min, after that filled with acetylene gas and allowed to melt. After stirring overnight under acetylene atmosphere at room temperature, the Et_2NH was evaporated and CH_2Cl_2 was added. Solids were filtered, washed with CH_2Cl_2 (5 \times 20 mL) and dried, yielding 5.799 g of **143** as a brown solid, which was pure enough for further use.

^1H NMR (DMSO- d_6 , 300 MHz): δ =4.57 (s; 4H; ArCH_2), 5.11 (br s; 2H; OH), 5.39 (s; 4H; NH_2), 6.40 (dd; J 8.2, 2.1 Hz; 2H; H_{Ar}), 6.73-6.78 (m; 2H; H_{Ar}), 7.05 (d; J 8.2 Hz; 2H; H_{Ar}) ppm.

(Ethyne-1,2-diylbis(5-iodo-2,1-phenylene))dimethanol (84).

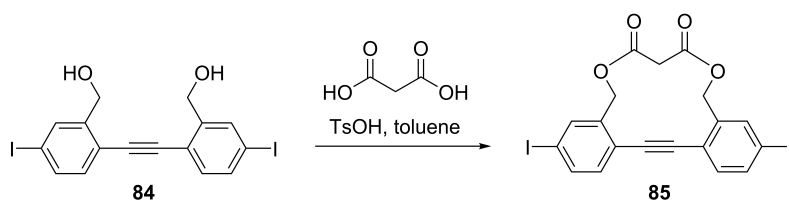


Literature known procedure was adapted.^[223] The crude **143** (5.796 g) from the previous step was suspended in a warm solution, prepared from 8.6 mL of concentrated H_2SO_4 and water (35 mL). The suspension was cooled with ice and the solution of NaNO_2 (3.726 g, 54.00 mmol) in water (18 mL) was added at such a rate, that the internal temperature remained under 5°C . After stirring for an additional 15 min at 0°C the reaction mixture was added in small portions (foaming) into a solution of KI (35.86 g, 216.0 mmol) in water (43 mL) at room temperature. After stirring for an additional 2 h, the black solid was filtered, washed with water (3 \times 20 mL), NaHSO_3 aq. solution (3 \times 20 mL), again with water (2 \times 20 mL) and dried. Chromatographic

purification (silica gel; petroleum ether/THF gradient from 3:1 to 1:1, v/v) yielded a brown solid. Yield: 9.59 g (19.57 mmol, 65% starting from **83**).

$R_f=0.51$ (petroleum ether/THF 1:1, v/v); m.p.=205°C; $^1\text{H NMR}$ (DMSO- d_6 , 300 MHz): $\delta=4.68$ (d; J 5.4 Hz; 4H; ArCH₂), 5.48 (m; 2H; OH), 7.29 (d; J 8.0 Hz; 2H; H_{Ar}), 7.67 (d; J 8.0 Hz; 2H, H_{Ar}), 7.89 (s; 2H; H_{Ar}) ppm; $^{13}\text{C NMR}$ (DMSO- d_6 , 75.56 MHz): $\delta=60.7, 91.9, 95.9, 118.8, 133.2, 134.9, 135.5, 146.0$ ppm; IR: $\tilde{\nu}=3224, 2878, 1586, 1480, 1392, 1358, 1187, 1069, 1042, 868, 811, 541$ cm⁻¹; HRMS (ESI⁺) m/z : [M+Na]⁺ calculated for C₁₆H₁₂I₂NaO₂⁺: 512.8819; found: 512.8827, correct isotope distribution; elemental analysis calculated (%) for C₁₆H₁₂I₂O₂: C 39.21, H 2.47; found: C 39.43, H 2.49.

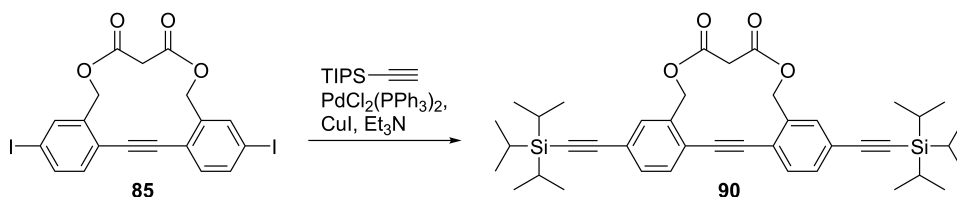
3,13-Diiodo-16,17-didehydro-5,11-dihydro-7H-dibenzo[g,k][1,5] dioxacyclotridecyne-7,9(8H)-dione (85).



A mixture of **84** (300.0 mg, 612.1 μmol , 1.0 eq), malonic acid (76.0 mg, 734.6 μmol , 1.2 eq) and *p*-toluenesulfonic acid monohydrate (12.0 mg, 61.21 μmol , 10 mol%) in toluene (120 mL) was heated at reflux at a Dean-Stark separator for 19 h. After cooling, water (40 mL) was added and layers were separated. The aqueous layer was extracted with toluene (3×20 mL) and the combined organic layer was washed with saturated aq. NaHCO₃ solution (1×10 mL), brine (1×30 mL) and dried over MgSO₄. Concentration and purification by column chromatography (silica gel; petroleum ether/CH₂Cl₂ gradient from 1:1 to 2:3, v/v) yielded **85** as a pale yellowish solid. Yield: 0.165 g (295.6 μmol , 48%).

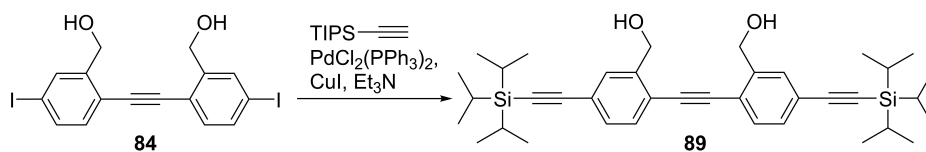
$R_f=0.60$ (petroleum ether/ethyl acetate 1:1, v/v); m.p.=235°C; $^1\text{H NMR}$ (CDCl₃, 400 MHz): $\delta=3.38$ (s; 2H; COCH₂CO), 5.06 (s; 4H; ArCH₂), 7.25-7.28 (m; 2H; H_{Ar}), 7.71-7.75 (m; 4H, H_{Ar}) ppm; $^{13}\text{C NMR}$ (CDCl₃, 100 MHz): $\delta=41.7, 66.6, 91.1, 94.5, 123.4, 133.8, 138.8, 138.3, 139.4, 165.8$ ppm; IR: $\tilde{\nu}=3046, 2976, 1732, 1708, 1487, 1303, 1195, 1074, 1006, 972, 882, 872, 819, 811$ cm⁻¹; HRMS (ESI⁺) m/z : [M+Na]⁺ calculated for C₁₉H₁₂I₂NaO₄⁺: 580.8717; found: 580.8737, correct isotope distribution; elemental analysis calculated (%) for C₁₉H₁₂I₂O₄: C 40.89, H 2.17; found: C 41.08, H 2.33.

3-((Tri(propan-2-yl)silyl)ethynyl)-13-(3-(tri(propan-2-yl)silyl)prop-2-yn-1-yl)-16,17-didehydro-5,11-dihydro-7H-dibenzo[g,k][1,5]dioxacyclotridecine-7,9(8H)-dione (90) from 85.



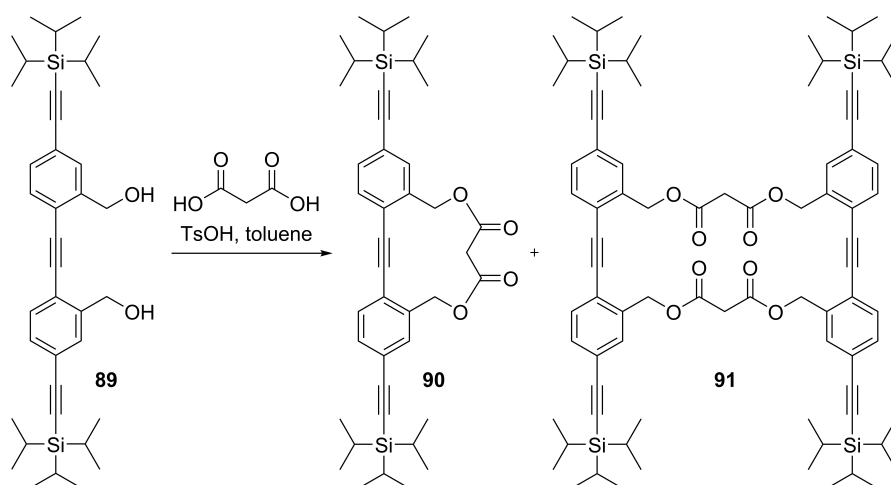
Literature known procedure was adapted.^[224] Common Schlenk procedure was used. Ethynyltriisopropylsilane (0.26 mL, 1.154 mmol, 4.0 eq) was added to a degassed solution of **85** (161.0 mg, 288.5 μmol , 1.0 eq) $\text{PdCl}_2(\text{PPh}_3)_2$ (20.0 mg, 28.85 μmol , 10 mol%) and CuI (11.0 mg, 57.7 μmol , 20 mol%) in Et_3N (4 mL). Then the reaction mixture was heated to 45°C for 4 h and kept overnight at room temperature. After addition of Celite and dilution with CH_2Cl_2 (5 mL) the mixture was concentrated *in vacuo*. Purification by column chromatography (silica gel; petroleum ether/ CH_2Cl_2 gradient from 1:1 to 1:2, v/v) yielded **90** as colorless solid. Yield: 157.0 mg (235.4 μmol , 81 %).

$R_f=0.71$ (petroleum ether/ethyl acetate 2:1, v/v); m.p.=176°C; $^1\text{H NMR}$ (CDCl_3 , 400 MHz): $\delta=1.13$ - 1.15 (m; 42H; *i*-Pr), 3.38 (s; 2H; COCH_2CO), 5.10 (s; 4H; ArCH_2), 7.45-7.50 (m; 6H; H_{Ar}) ppm; $^{13}\text{C NMR}$ (CDCl_3 , 100 MHz): $\delta=11.3$, 18.7, 41.7, 67.1, 91.9, 93.9, 105.8, 123.7, 124.2, 132.49, 132.50, 134.0, 136.3, 165.9 ppm; IR: $\tilde{\nu}=2941$, 2864, 2147, 1756, 1735, 1502, 1459, 1294, 1278, 1207, 1157, 1010, 993, 880, 831, 776, 675, 656, 617 cm^{-1} ; HRMS (ESI^+) m/z : $[\text{M}+\text{Na}]^+$ calculated for $\text{C}_{41}\text{H}_{54}\text{NaO}_4\text{Si}_2^+$: 689.3453; found: 689.3454, correct isotope distribution; elemental analysis calculated (%) for $\text{C}_{41}\text{H}_{54}\text{O}_4\text{Si}_2$: C 73.83, H 8.16; found: C 73.74, H 8.19. Crystal data: $\text{C}_{41}\text{H}_{54}\text{O}_4\text{Si}_2$, $M_w=667.02$, colorless crystal (plate), obtained by slow cooling of a solution of **90** in the mixture of acetone and methanol (2:1, v/v), dimensions 0.250×0.170×0.080 mm^3 , triclinic crystal system, space group $\text{P}\bar{1}$, $Z=2$, $a=8.7838(5)$ Å, $b=12.0180(7)$ Å, $c=19.4191(11)$ Å, $\alpha=104.2904(16)^\circ$, $\beta=92.1446(16)^\circ$, $\gamma=94.2181(16)^\circ$, $V=1977.9(2)$ Å³, $\rho=1.120$ g/cm³, $T=200(2)$ K, $\theta_{\text{max}}=25.090^\circ$, radiation $\text{MoK}\alpha$, $\lambda=0.71073$ Å, 25540 reflections measured, 7025 unique ($R_{\text{int}}=0.0429$), 4983 observed ($I>2\sigma(I)$), final residual values $R_1(F)=0.050$, $wR(F^2)=0.117$ for observed reflections.

(Ethyne-1,2-diylbis(5-((tri(propan-2-yl)silyl)ethynyl)-2,1-phenylene))dimethanol (89).

Literature known procedure was adapted.^[224] Common Schlenk procedure was used. Ethynyltriisopropylsilane (0.29 mL, 1.275 mmol, 2.5 eq) was added to a degassed solution of **84** (250.0 mg, 510.1 μmol , 1.0 eq), $\text{PdCl}_2(\text{PPh}_3)_2$ (36.0 mg, 51.0 μmol , 10 mol%) and CuI (19.0 mg, 102.0 μmol , 20 mol%) in Et_3N (6 mL), and then the reaction mixture was heated to 45°C for 2 h. After cooling, addition of Celite and dilution with CH_2Cl_2 (5 mL) the reaction mixture was concentrated *in vacuo*. Purification by column chromatography (silica gel; petroleum ether/ethyl acetate gradient from 20:1 to 5:1, v/v) yielded **89** as a brownish solid. Yield: 220.0 mg (367.3 μmol , 72 %).

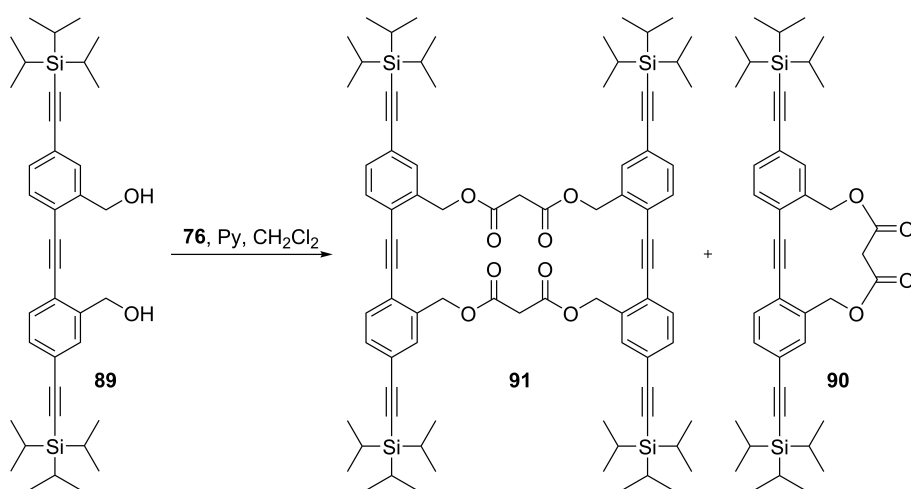
$R_f=0.73$ (petroleum ether/ethyl acetate 1:1, v/v); m.p.=119°C; ^1H NMR (CDCl_3 , 300 MHz): $\delta=1.14$ (s; 42H; *i*-Pr), 2.33 (br s; 2H; OH), 4.83 (s; 4H; ArCH_2), 7.41 (dd; J 7.9, 1.6 Hz; 2H; H_{Ar}), 7.49 (d; J 7.9 Hz; 2H; H_{Ar}) ppm; ^{13}C NMR (CDCl_3 , 75 MHz): $\delta=11.3$, 18.7, 64.0, 93.0, 93.3, 106.4, 121.6, 124.0, 131.3, 131.6, 132.2, 142.3 ppm; IR: $\tilde{\nu}=3285$, 2941, 2862, 2143, 1495, 1463, 1040, 997, 882, 831, 756, 677, 661, 621, 459 cm^{-1} ; HRMS (ESI^+) m/z : $[\text{M}+\text{Na}]^+$ calculated for $\text{C}_{38}\text{H}_{54}\text{NaO}_2\text{Si}_2^+$: 621.3555; found: 621.3551, correct isotope distribution; elemental analysis calculated (%) for $\text{C}_{38}\text{H}_{54}\text{O}_2\text{Si}_2$: C 76.19, H 9.09; found: C 76.13, H 9.02.

3-((Tri(propan-2-yl)silyl)ethynyl)-13-(3-(tri(propan-2-yl)silyl)prop-2-yn-1-yl)-16,17-didehydro-5,11-dihydro-7H-dibenzo[g,k][1,5]dioxacyclotridecyne-7,9(8H)-dione (90) from 89.

A mixture of **89** (60.0 mg, 100.0 μmol , 1.0 eq), malonic acid (13.0 mg, 120.0 μmol , 1.2 eq) and *p*-toluenesulfonic acid monohydrate (2.0 mg, 10.0 μmol , 10 mol%) in toluene (20 mL) was heated

to reflux at a Dean-Stark separator for 4 h. After cooling, saturated aq. NaHCO₃ solution (5 mL) was added and layers were separated. The water layer was extracted with toluene (3×10 mL) and the combined organic layer was washed with brine (1×10 mL) and dried over MgSO₄. Concentration and separation by column chromatography (silica gel; petroleum ether/CH₂Cl₂ gradient from 2:1 to 1:1, v/v) yielded the tolane **90** as pale yellowish solid and tolane **91** as colorless solid. Yield: **90** (26.0 mg, 38.98 μmol, 39%), **91** (6.0 mg, 4.497 μmol, 8%).

2,9,19,26-Tetrakis((tri(propan-2-yl)silyl)ethynyl)-5,6,22,23-tetradehydro-11,17,28,34-tetrahydro-13H,30H-tetrabenzog[k,t,x][1,5,14,18]tetraoxacyclohexacosine-13,15,30,32(14H,31H)-tetrone (91) from 89

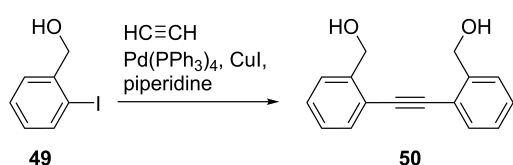


Literature known procedure was used.^[189] Common Schlenk procedure was used. A solution of malonyl chloride (**76**) (64 μL, 668.0 μmol, 2.0 eq) in dry CH₂Cl₂ (25 mL) was added to a solution of **89** (200.0 mg, 333.9 μmol, 1.0 eq) and pyridine (54 μL, 668.0 μmol, 2.0 eq) in dry CH₂Cl₂ (22 mL) during 7 h. After stirring for additional 2 d, water (10 mL) was added, layers were separated and the water layer was extracted with CH₂Cl₂ (3×10 mL). The combined organic layers were washed with saturated aq. NaHCO₃ solution (1×5 mL), brine (1×10 mL) and dried over MgSO₄. Concentration and separation by column chromatography (silica gel; petroleum ether/ CH₂Cl₂ gradient from 2:1 to 1:1, v/v) yielded tolane **90** and tolane **91** as colorless solids. Yield: **90** (19.0 mg, 28.48 μmol, 8%), **91** (68.0 mg, 50.97 μmol, 30%).

Tolane **91**. R_f=0.86 (petroleum ether/ethyl acetate 2:1, v/v); m.p.=186°C; ¹H NMR (CDCl₃, 400 MHz): δ=1.14 (s; 84H; *i*-Pr), 3.52 (s; 4H; COCH₂CO), 5.32 (s; 8H; ArCH₂), 7.38 (dd; *J* 8.0, 1.5 Hz; 4H; H_{Ar}), 7.46 (d; *J* 8.0 Hz; 4H; H_{Ar}), 7.48 (d; *J* 1.2 Hz; 4H; H_{Ar}) ppm; ¹³C NMR (CDCl₃, 100 MHz): δ=11.3, 18.7, 41.3, 65.2, 92.6, 93.7, 106.2, 122.2, 124.2, 131.9, 132.2, 132.3, 136.8, 166.1 ppm; IR: $\tilde{\nu}$ =2942, 2864, 2148, 1759, 1739, 1501, 1462, 1258, 1146, 1013, 995, 881, 831, 761, 658, 621 cm⁻¹

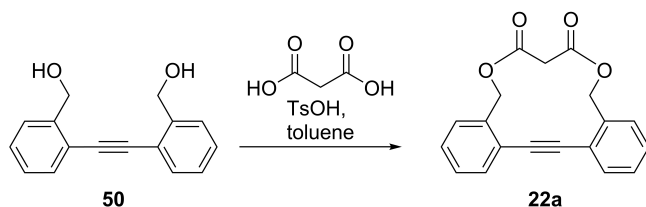
¹; HRMS (ESI⁺) *m/z*: [M+Na]⁺ calculated for C₈₂H₁₀₈NaO₈Si₄⁺: 1355.7013; found: 1356.7044, correct isotope distribution; elemental analysis calculated (%) for C₈₂H₁₀₈O₈Si₄: C 73.83, H 8.16; found: C 73.63, H 8.35. Crystal data: C₈₄H₁₁₂Cl₄O₈Si₄, *M_w*=1503.89, colorless crystals (plate), obtained by slow diffusion of pentane vapor into a solution of **91** in CH₂Cl₂, dimensions 0.320×0.110×0.040 mm³, monoclinic crystal system, space group P2₁/n, *Z*=4, *a*=8.3361(9) Å, *b*=40.091(4) Å, *c*=26.570(3) Å, *α*=90°, *β*=98.968(3)°, *γ*=90°, *V*=8771.1(16) Å³, *ρ*=1.139 g/cm³, *T*=200(2) K, *θ*_{max}=20.913°, radiation MoK_α, *λ*=0.71073 Å, 41514 reflections measured, 9344 unique (*R*_{int}=0.0605), 6604 observed (*I*>2σ(*I*)), final residual values *R*₁(*F*)=0.101, *wR*(*F*²)=0.262 for observed reflections.

(Ethyne-1,2-diylbis(2,1-phenylene))dimethanol (**50**).



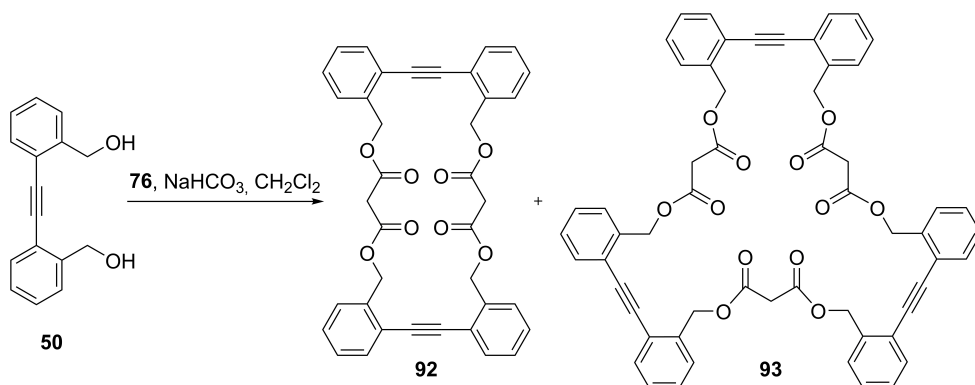
Literature known procedure was used and the analytical data was in agreement with published.^[66] *R_f*=0.51 (CH₂Cl₂/methanol 10:1, v/v); ¹H NMR (CDCl₃, 300 MHz): δ=2.52 (s; 2H; OH), 4.86 (s; 4H; ArCH₂), 7.28-7.46 (m; 6H; H_{Ar}), 7.54-7.61 (m; 2H; H_{Ar}) ppm.

16,17-Didehydro-5,11-dihydro-7H-dibenzo[*g,k*][1,5]dioxacyclotridecyne-7,9(8H)-dione (**22a**).



A mixture of **50** (179.0 mg, 751.0 μmol, 1.0 eq), malonic acid (94.0 mg, 901.0 μmol, 1.2 eq) and *p*-toluenesulfonic acid monohydrate (14.0 mg, 75.0 μmol, 10 mol%) in toluene (25 mL) was heated to reflux at a Dean-Stark separator for 4 h. After cooling, saturated aq. NaHCO₃ solution (30 mL) was added and layers were separated. The water layer was extracted with toluene (3×10 mL) and the combined organic layers were washed with brine (1×10 mL) and dried over MgSO₄. Concentration and purification by column chromatography (silica gel; petroleum ether/ethyl acetate gradient from 4:1 to 2:1, v/v) yielded toluene **22a** as a colorless solid. Yield: 83.0 mg (271.0 μmol, 36%). Analytical data was in agreement with published.^[66] *R_f*=0.62 (petroleum ether/ethyl acetate 1:1, v/v); ¹H NMR (CDCl₃, 300 MHz): δ=3.39 (s; 2H; COCH₂CO), 5.16 (s; 4H; ArCH₂), 7.34-7.44 (m; 6H; H_{Ar}), 7.54-7.60 (m; 2H; H_{Ar}) ppm.

5,6,22,23-Tetradehydro-11,17,28,34-tetrahydro-13H,30H-tetrabenzo[g,k,t,x][1,5,14,18]tetraoxacyclohexacosine-13,15,30,32(14H,31H)-tetrone (92) and **16,17,33,34,50,51-hexadehydro-5,11,22,28,39,45-hexahydro-7H,24H,41H-hexabenzo[g,k,t,x,g1,k1][1,5,14,18,27,31]-hexaoxacyclonatriacontyne-7,9,24,26,41,43(8H,25H,42H)-hexone (93)**.



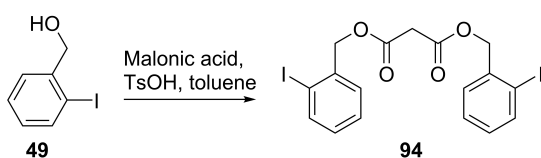
Common Schlenk procedure was used. A solution of malonyl chloride (**76**) (37 μ L, 376 μ mol, 0.5 eq) in dry CH_2Cl_2 (5 mL) was added to a suspension of **50** (179.0 mg, 751.2 μ mol, 1.0 eq) and NaHCO_3 (316.0 mg, 3.760 mmol, 5.0 eq) in dry CH_2Cl_2 (25 mL) during 1 h. After stirring for 2 h the reaction mixture was diluted with dry CH_2Cl_2 (125 mL) and another portion of malonyl chloride (37 μ L, 376 μ mol, 0.5 eq) solution in dry CH_2Cl_2 (5 mL) was added during 1.5 h and the stirring was continued overnight. The reaction was quenched with water (50 mL), layers were separated and the aqueous phase was extracted with CH_2Cl_2 (2 \times 20 mL). The combined organic layer was washed with brine (1 \times 20 mL) and dried over MgSO_4 . Concentration and separation by column chromatography (silica gel; petroleum ether/ethyl acetate gradient from 4:1 to 2:1, v/v) yielded tolanses **92** and **93** as colorless solids. Yield **92**: 3.0 mg (4.897 μ mol, 1%); yield **93**: 17.0 mg (18.50 μ mol, 7%).

Tolane **92**. $R_f=0.64$ (petroleum ether/ethyl acetate 1:1, v/v); m.p.=226 $^\circ\text{C}$; ^1H NMR (CDCl_3 , 600 MHz): $\delta=3.49$ (s; 4H; COCH_2CO), 5.35 (s; 8H; ArCH_2), 7.28-7.33 (m; 8H; H_{Ar}), 7.36-7.40 (m; 4H; H_{Ar}), 7.51-7.55 (m; 4H; H_{Ar}) ppm; ^{13}C NMR (CDCl_3 , 150 MHz): $\delta=41.5$, 65.7, 91.3, 122.7, 128.7, 128.8, 129.2, 132.4, 136.8, 166.3 ppm; IR: $\tilde{\nu}=3064$, 2949, 2160, 1762, 1724, 1379, 1335, 1162, 1149, 1031, 1018, 756 cm^{-1} ; HRMS (ESI^+) m/z : $[\text{M}+\text{Na}]^+$ calculated for $\text{C}_{38}\text{H}_{28}\text{NaO}_8^+$: 635.1676; found: 635.1686, correct isotope distribution; elemental analysis calculated (%) for $\text{C}_{38}\text{H}_{28}\text{O}_8$: C 74.50, H 4.61; found: C 74.04, H 4.85. Crystal data: $\text{C}_{38}\text{H}_{28}\text{O}_8$, $M_w=612.63$, colourless crystal (needle), obtained by slow diffusion of petroleum ether into a solution of **92** in CDCl_3 , dimensions 0.590 \times 0.040 \times 0.020 mm^3 , monoclinic crystal system, space group $\text{P2}_1/\text{c}$, $Z=2$, $a=17.4119(19)$ \AA , $b=4.8650(5)$ \AA , $c=4.8650(5)$ \AA , $\alpha=90^\circ$, $\beta=107.657(3)^\circ$, $\gamma=90^\circ$, $V=1435.9(3)$ \AA^3 , $\rho=1.417$ g/cm^3 , $T=200(2)$ K, $\theta_{\text{max}}=25.404^\circ$, radiation $\text{MoK}\alpha$, $\lambda=0.71073$ \AA , 17633 reflections

measured, 2640 unique ($R_{\text{int}}=0.0743$), 1792 observed ($I > 2\sigma(I)$), final residual values $R_1(F) = 0.055$, $wR(F^2) = 0.118$ for observed reflections.

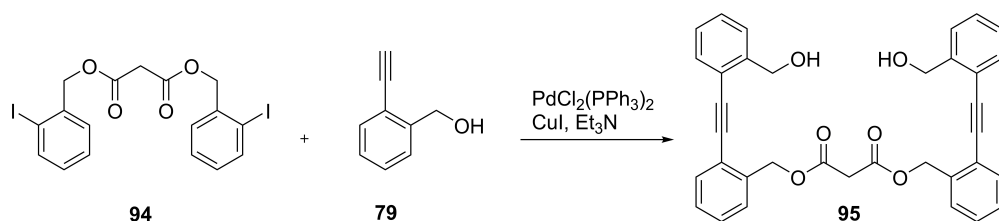
Tolane **93**. $R_f = 0.58$ (petroleum ether/ethyl acetate 1:1, v/v); m.p. = 163°C; ^1H NMR (CDCl_3 , 600 MHz): $\delta = 3.46$ (s; 6H; COCH_2CO), 5.32 (s; 12H; ArCH_2), 7.23-7.29 (m; 12H; H_{Ar}), 7.33-7.37 (s; 6H; H_{Ar}), 7.48-7.52 (m; 6H; H_{Ar}) ppm; ^{13}C NMR (CDCl_3 , 150 MHz): $\delta = 41.3$, 65.5, 91.3, 122.4, 128.3, 128.8, 132.3, 136.7, 166.2 ppm; IR: $\tilde{\nu} = 2952$, 1748, 1722, 1495, 1343, 1313, 1260, 1226, 1155, 1015, 992, 756, 712, 587 cm^{-1} ; HRMS (ESI^+) m/z: $[\text{M} + \text{Na}]^+$ calculated for $\text{C}_{57}\text{H}_{42}\text{NaO}_{12}^+$: 941.2568; found: 941.2571, correct isotope distribution; elemental analysis calculated (%) for $\text{C}_{57}\text{H}_{42}\text{O}_{12}$: C 74.50, H 4.61; found: C 74.27, H 4.68.

Bis(2-iodobenzyl) malonate (**94**).



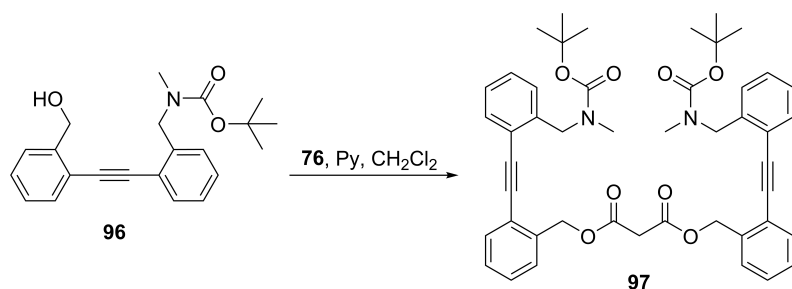
In a round bottom flask equipped with Dean-Stark water separator 2-iodobenzyl alcohol (**49**) (6.00 g, 25.64 mmol, 1.0 eq), malonic acid (1.334 g, 12.82 mmol, 0.5 eq) and *p*-toluenesulfonic acid monohydrate (488.0 mg, 2.564 mmol, 10 mol%) were refluxed in toluene (260 mL) for 18 h. After cooling, saturated aq. NaHCO_3 solution (50 mL) was added and separated water phase was extracted with toluene (3×20 mL). Combined organic layer was washed with brine (1×50 mL) and dried over MgSO_4 . Purification by column chromatography (silica gel; CH_2Cl_2 /petroleum ether gradient from 1:1 to 3:1, v/v) yielded **94** as a colorless oil, which crystallizes later. Yield 6.470 g (12.07 mmol, 94%).

$R_f = 0.83$ (CH_2Cl_2 /methanol 10:1, v/v); m.p. = 54°C; ^1H NMR (CDCl_3 , 300 MHz): $\delta = 3.56$ (s; 2H; COCH_2CO), 5.21 (s; 4H; ArCH_2), 7.02 (dt; J 7.5, 1.8 Hz; 2H; H_{Ar}), 7.28-7.39 (m; 4H; H_{Ar}), 7.85 (dd; J 7.9, 0.8 Hz; 2H; H_{Ar}) ppm; ^{13}C NMR (CDCl_3 , 75 MHz): $\delta = 41.3$, 71.0, 98.3, 128.3, 129.5, 130.0, 137.5, 139.5, 165.8 ppm; IR: $\tilde{\nu} = 3059$, 2948, 1732, 1260, 1207, 1142, 1009, 748 cm^{-1} ; HRMS (DART^+) m/z: $[\text{M} + \text{NH}_4]^+$ calculated for $\text{C}_{17}\text{H}_{18}\text{I}_2\text{NO}_4^+$: 553.9320; found: 553.9325, correct isotope distribution; elemental analysis calculated (%) for $\text{C}_{17}\text{H}_{14}\text{I}_2\text{O}_4$: C 38.09, H 2.63; found: C 38.20, H 2.78.

Bis(2-((2-(hydroxymethyl)phenyl)ethynyl)benzyl) malonate (95).

Literature known procedure was adapted.^[224] Common Schlenk procedure was used. Degassed solution of **94** (194.0 mg, 361.9 μmol , 1.0 eq), $\text{PdCl}_2(\text{PPh}_3)_2$ (25.0 mg, 36.19 μmol , 10 mol%) and CuI (14.0 mg, 72.37 μmol , 20 mol%) in Et_3N (4 mL) was added to purged 3 times with nitrogen alkyne **79** (96.0 mg, 723.7 μmol , 2.0 eq). The resulting thick mixture was allowed to stir for 90 min, then CH_2Cl_2 and Celite were added followed by evaporation *in vacuo*. Purification by column chromatography (silica gel; CH_2Cl_2 /ethyl acetate gradient from 20:1 to 10:1, v/v) yielded **95** as a brown solid. Yield 150.0 mg (275.4 μmol , 76%).

$R_f=0.71$ (CH_2Cl_2 /methanol 10:1, v/v); m.p.=124°C; ^1H NMR (CDCl_3 , 300 MHz): $\delta=2.13$ (br s; 2H; OH), 3.53 (s; 2H; COCH_2CO), 4.87 (s; 4H; ArCH_2), 5.39 (s; 4H; ArCH_2), 7.23-7.42 (m; 10H; H_{Ar}), 7.46-7.58 (m; 6H; H_{Ar}) ppm; ^{13}C NMR (CDCl_3 , 100 MHz): $\delta=41.5$, 63.7, 66.1, 91.0, 91.9, 122.0, 122.9, 127.4, 127.5, 128.5, 128.7, 129.0, 129.1, 132.3, 132.4, 136.3, 142.6, 166.4 ppm; IR: $\tilde{\nu}=3297$, 1739, 1712, 1495, 1392, 1336, 1180, 1146, 1038, 987, 753 cm^{-1} ; HRMS (DART⁻) m/z : $[\text{M}-\text{H}]^-$ calculated for $\text{C}_{35}\text{H}_{27}\text{O}_6^-$: 543.1813; found: 543.1813, correct isotope distribution; elemental analysis calculated (%) for $\text{C}_{35}\text{H}_{28}\text{O}_6$: C 77.19, H 5.18; found: C 77.17, H 5.32.

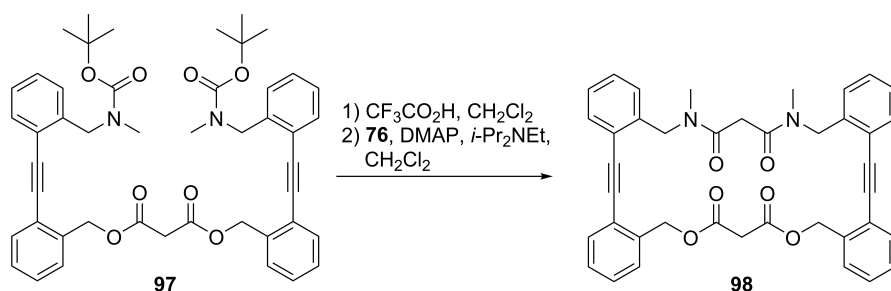
Bis(2-((2-(((tert-butoxycarbonyl)(methyl)amino)methyl)phenyl)-ethynyl)phenyl)methyl) propanedioate (97).

Common Schlenk procedure was used. A solution of malonyl chloride (**76**) (1.03 mL, 10.6 mmol, 2.0 eq) in dry CH_2Cl_2 (20 mL) was added to an ice-cooled solution of **96** (1.858 g, 5.287 mmol, 1.0 eq) and pyridine (3.4 mL, 42.3 mmol, 8.0 eq) in dry CH_2Cl_2 (260 mL) during 1 h. After additional stirring for 30 min at room temperature, TLC showed consumption of the starting materials. The reaction mixture was filtered through a silica gel pad (eluent ethyl acetate), Celite

was added, and all volatiles were removed *in vacuo*. Purification by column chromatography (silica gel; CH₂Cl₂/diethyl ether gradient from 50:1 to 10:1, v/v) yielded **97** as a pale yellow oil. Yield 1.337 g (1.734 mmol, 65%).

R_f=0.66 (petroleum ether/ethyl acetate 1:1, v/v); ¹H NMR (CDCl₃, 600 MHz): δ=1.37-1.54 (m; 18H; *t*-Bu), 2.80-2.96 (m; 6H; NCH₃), 3.54 (s; 2H; COCH₂CO), 4.64-4.76 (m; 4H; ArCH₂), 5.43 (s; 4H; ArCH₂), 7.20-7.43 (m; 12H; H_{Ar}), 7.50-7.58 (m; 4H; H_{Ar}) ppm; ¹³C NMR (CDCl₃, 150 MHz): δ=28.3, 34.2, 34.4, 41.3, 50.1, 50.9, 65.5, 79.6, 79.7, 91.0, 91.2, 92.0, 92.1, 121.3, 121.8, 122.3, 122.4, 126.0, 126.9, 128.2, 128.3, 128.6, 128.7, 128.9, 132.16, 132.24, 132.4, 136.4, 139.5, 139.8, 155.9, 156.1, 166.0 ppm; IR: $\tilde{\nu}$ =2974, 2930, 1736, 1688, 1480, 1451, 1390, 1365, 1247, 1141, 1009, 882, 757 cm⁻¹; HRMS (ESI⁺) *m/z*: [M+Na]⁺ calculated for C₄₇H₅₀N₂NaO₈⁺: 793.3459; found: 793.3461, correct isotope distribution; elemental analysis calculated (%) for C₄₇H₅₀N₂O₈: C 73.23, H 6.54, N 3.63; found: C 69.49, H 6.50, N 3.41.

29,33-Dimethyl-5,6,22,23-tetradehydro-28,29,33,34-tetrahydro-11H,13H-tetrabenzo[g,k,t,x]-[1,5,14,18]dioxadiazacyclohexacosyne-13,15,30,32(14H,17H,31H)-tetrone (98).

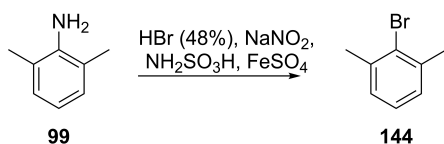


A published procedure was used for the deprotection step.^[218] Trifluoroacetic acid (3.43 mL, 44.8 mmol, 26 eq) was added in one portion to a solution of **97** (1.327 g, 1.721 mmol, 1.0 eq) in CH₂Cl₂ (20 mL). The mixture was stirred for 5.5 h (gas evolution). After removal of all volatiles *in vacuo*, toluene (10 mL) was added, the mixture was concentrated, and the obtained brownish oil was used in the next step without further purification. Common Schlenk procedure was used for the cyclization step. Solution of malonyl chloride (**76**) (250 μ L, 2.580 mmol, 1.5 eq) in dry CH₂Cl₂ (30 mL), and a solution of the deprotected product from the previous step in dry CH₂Cl₂ (30 mL), were simultaneously added during 4.5 h to a solution of N,N-diisopropylethylamine (1.80 mL, 10.3 mmol, 6.0 eq) and 4-(dimethylamino)pyridine (126.0 mg, 1.033 mmol, 0.6 eq) in dry CH₂Cl₂ (350 mL). After stirring for an additional 24 h, water (20 mL) was added, the layers were separated and the water phase was extracted with CH₂Cl₂ (2 \times 50 mL). Combined organic layers were washed with brine (20 mL) and dried over MgSO₄. Concentration and purification by

column chromatography (silica gel; petroleum ether/ethyl acetate gradient from 2:1 to 1:1, v/v, then ethyl acetate) followed by preparative HPLC (CH₂Cl₂/ethyl acetate 1:1, v/v) yielded **98** as a colorless solid. Yield 182.0 mg (284.9 mmol, 16%).

R_f=0.36 (ethyl acetate); m.p.=177°C; ¹H and ¹³C NMR spectra were complicated owing to tautomer mixture; ¹H NMR (CDCl₃, 600 MHz): δ=2.88-3.10 (m; 6H; NCH₃), 3.34 (s; 0.6H; COCH₂CO), 3.43 (s; 1.1H; COCH₂CO), 3.48 (s; 0.3H; COCH₂CO), 3.57-3.69 (m; 2H; COCH₂CO), 4.70-4.96 (m; 4H; ArCH₂), 5.22-5.41 (m; 4H, ArCH₂), 7.18-7.46 (m; 12H; H_{Ar}), 7.48-7.62 (m; 4H; H_{Ar}) ppm; ¹³C NMR (CDCl₃, 150 MHz): δ=34.0, 34.4, 35.4, 35.5, 40.1, 40.9, 41.15, 41.19, 49.0, 49.2, 52.6, 52.8, 65.8, 66.1, 66.20, 66.23, 91.1, 91.17, 91.18, 91.20, 91.80, 91.82, 92.1, 121.1, 121.4, 122.1, 122.4, 122.6, 123.2, 123.3, 123.7, 125.6, 125.7, 127.1, 127.3, 127.4, 127.6, 127.8, 128.5, 128.65, 128.69, 128.7, 128.8, 128.9, 129.1, 129.2, 129.26, 129.29, 129.4, 130.0, 130.3, 132.1, 132.2, 132.3, 132.45, 132.47, 132.53, 132.7, 136.0, 136.1, 136.2, 136.6, 138.2, 138.4, 138.7, 138.8, 166.05, 166.15, 166.2, 166.4, 167.0, 167.4, 168.1, 168.3 ppm; IR: $\tilde{\nu}$ =3065, 2935, 1745, 1725, 1630, 1788, 1399, 1335, 1152, 1132, 1122, 957.5, 956.9, 712, 609, 442 cm⁻¹; HRMS (ESI⁺) m/z: [M+Na]⁺ calculated for C₄₀H₃₄N₂NaO₆⁺: 661.2309; found: 661.2309, correct isotope distribution; elemental analysis calculated (%) for C₄₀H₃₄N₂O₆: C 75.22, H 5.37, N 4.39; found: C 74.87, H 5.60, N 4.33.

2-Bromo-1,3-dimethylbenzene (**144**).

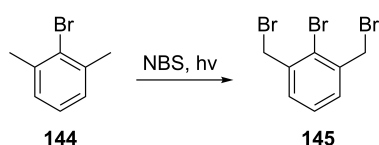


2,6-Dimethylaniline (**99**) (6.15 mL, 49.9 mmol, 1.0 eq) was added to a commercially available 48% aq. HBr solution (33 mL) and the obtained thick suspension was allowed to stir for 15 min at 80°C. After that, the reaction mixture was cooled with ice-salt bath and a solution of NaNO₂ (4.00 g, 58.0 mmol, 1.16 eq) in water (18 mL) was added at such a rate, that the internal temperature remained under -2°C, followed by addition of sulfamic acid (40.0 mg, 412 μmol, 0.82 mol%). The obtained suspension of diazonium salt was added in small portions within 30 min to a heated to 80°C solution of FeSO₄·7H₂O (6.95 g, 25.0 mmol, 0.50 eq) in 48% aq. HBr solution (42 mL) and the reaction mixture was additionally stirred for 1 hour at 80°C. After cooling to room temperature water was added (100 mL) and layers have been separated. Water phase was extracted with CH₂Cl₂ (4×50 mL) and combined organic layer was washed with aq.

Na₂SO₃ solution (2×30 mL), brine (1×50 mL) and dried over MgSO₄. Chromatographic purification (silica gel; petroleum ether) yielded **144** as a colorless liquid. Yield: 5.74 g (31.0 mmol, 62%).

Analytical data was in agreement with published.^[225] ¹H NMR (CDCl₃, 300 MHz): δ=2.42 (s; 6H; CH₃), 7.05-7.12 (m; 3H; H_{Ar}) ppm.

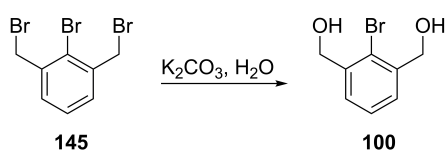
2-Bromo-1,3-bis(bromomethyl)benzene (**145**).



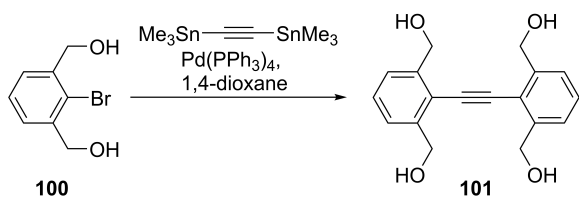
A solution of **144** (11.22 g, 60.6 mmol, 1.0 eq) and N-bromosuccinimide (22.66 g, 127.0 mmol, 2.1 eq) in acetonitrile (600 mL) was stirred under irradiation of a 300W wolfram lamp for 1 h. The reaction progress has been monitored by GC-MS. After removal of acetonitrile the residue was separated between water and Et₂O (200 mL each), afterwards Na₂S₂O₅ was added in portions until the mixture became colorless. The layers were separated and the water phase was extracted with Et₂O (2×100 mL). Combined organic phase was washed with brine (1×50 mL) and dried over Na₂SO₄. Repetitive chromatographic purification (silica gel; petroleum ether/ethyl acetate gradient from 95:5 to 90:10, v/v) yielded **145** as a white solid. Yield: 13.94 g (19.57 mmol, 65%).

Analytical data was in agreement with published.^[226] R_f=0.13 (petroleum ether); ¹H NMR (CDCl₃, 300 MHz): δ=4.65 (s; 4H; ArCH₂), 7.28-7.32 (m; 2H; H_{Ar}), 7.40-7.44 (m; 1H; H_{Ar}) ppm.

(2-Bromo-1,3-phenylene)dimethanol (**100**).

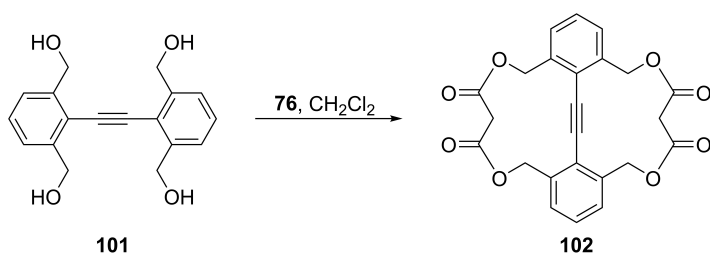


Literature known procedure was used.^[227] Analytical data was in agreement with published.^[228] ¹H NMR (DMSO-*d*₆, 300 MHz): δ=4.53 (d; *J* 5.6 Hz; 4H; ArCH₂), 5.40 (t; *J* 5.6 Hz; 2H; OH), 7.35-7.46 (m; 3H; H_{Ar}) ppm.

(Ethyne-1,2-diyl-di(benzene-2,1,3-triyl))tetramethanol (101).

Literature known procedure was adapted.^[229] Common Schlenk procedure was used. Bis(trimethylstannyl)acetylene (1.000 g, 2.844 mmol, 0.5 eq) and $\text{Pd}(\text{PPh}_3)_4$ (657.0 mg, 0.569 mmol, 10 mol%) were added to a degassed solution of **100** (1.235 g, 5.688 mmol, 1.0 eq) in anhydrous 1,4-dioxane (140 mL), followed by stirring for 20 hours at 110°C. Upon cooling, Celite was added and volatiles were removed *in vacuo*. Chromatographic purification (silica gel; CH_2Cl_2 /methanol 10:1, v/v) yielded **101** as a brownish solid. Yield: 509.0 mg (1.706 mmol, 60%). Analytical sample was prepared by recrystallization from methanol.

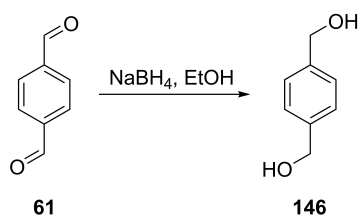
$R_f=0.23$ (CH_2Cl_2 /methanol 10:1, v/v); m.p.=208°C (decomposition); ^1H NMR ($\text{DMSO}-d_6$, 600 MHz): $\delta=4.77$ (d; J 5.8 Hz; 8H; ArCH_2), 5.38 (t; J 5.8 Hz; 4H; OH), 7.41-7.48 (m; 6H, H_{Ar}) ppm; ^{13}C NMR ($\text{DMSO}-d_6$, 150 MHz): $\delta=61.6$, 94.0, 116.9, 124.3, 128.3, 143.9 ppm; IR: $\tilde{\nu}=3267$, 2818, 1462, 1417, 1363, 1327, 1232, 1161, 1067, 1043, 780, 668 cm^{-1} ; HRMS (DART^+) m/z : $[\text{M}+\text{NH}_4]^+$ calculated for $\text{C}_{18}\text{H}_{22}\text{NO}_4^+$: 316.1543; found: 316.1544, correct isotope distribution; elemental analysis calculated (%) for $\text{C}_{18}\text{H}_{18}\text{O}_4$: C 72.47, H 6.08; found: C 72.07, H 6.36.

16,17-Didehydro-5,11-dihydro-7H-1,15-(methanooxypropanooxymethano)dibenzo[g,k][1,5]dioxacyclotridecine-7,9,20,22(8H)-tetrone (102).

Common Schlenk procedure was used. Solution of malonyl chloride (**76**) (171 μL , 1.756 mmol, 4.0 eq) in dry CH_2Cl_2 (6 mL) was added during 1.5 h to a suspension of tetraol **101** (131.0 mg, 439.0 μmol , 1.0 eq) in dry CH_2Cl_2 (11 mL). After stirring for an additional 24 h the reaction mixture was filtered through a silica gel pad (eluent ethyl acetate). Concentration and chromatographic purification (silica gel; CHCl_3 /petroleum ether 1:1, v/v) yielded **102** as a white solid. Yield: 30.0 mg (69.1 μmol , 15%).

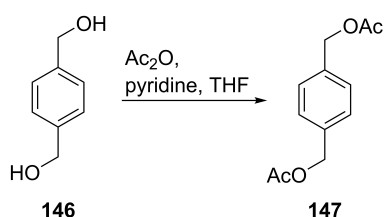
$R_f=0.38$ (petroleum ether/ethyl acetate 1:1, v/v); m.p. 302°C (decomposition); ^1H NMR (CDCl_3 , 400 MHz): $\delta=3.39$ (s; 4H; COCH_2CO), 4.91 (d; J 11.3 Hz; 2H; ArCH_2), 5.43 (d; J 11.3 Hz; 2H; ArCH_2), 7.36-7.45 (m; 6H; H_{Ar}) ppm; ^{13}C NMR (CDCl_3 , 150 MHz): $\delta=41.7$, 67.4, 92.4, 125.3, 129.0, 131.5, 137.2, 166.1 ppm; IR: $\tilde{\nu}=2954$, 1724, 1472, 1373, 1274, 1211, 1138, 999, 984, 795 cm^{-1} ; HRMS (DART+) m/z : $[\text{M}+\text{NH}_4]^+$ calculated for $\text{C}_{24}\text{H}_{22}\text{NO}_8^+$: 452.1340; found: 452.1334, correct isotope distribution; elemental analysis calculated (%) for $\text{C}_{24}\text{H}_{18}\text{O}_8$: C 66.36, H 4.18; found: C 65.90, H 4.28. Crystal data: $\text{C}_{24}\text{H}_{18}\text{O}_8$, $M_w=434.40$, colorless crystal (big), obtained by slow evaporation of a CDCl_3 solution of **102**, dimensions $0.203\times 0.097\times 0.076$ mm^3 , monoclinic crystal system, space group $\text{C2}/c$, $Z=8$, $a=29.675(2)$ Å, $b=10.1444(7)$ Å, $c=17.3726(12)$ Å, $\alpha=90^\circ$, $\beta=115.2430(19)^\circ$, $\gamma=90^\circ$, $V=4730.3(6)$ Å³, $\rho=1.220$ g/cm^3 , $T=200(2)$ K, $\theta_{\text{max}}=25.390^\circ$, radiation $\text{MoK}\alpha$, $\lambda=0.71073$ Å, 15163 reflections measured, 4345 unique ($R_{\text{int}}=0.0606$), 2537 observed ($I>2\sigma(I)$), final residual values $R_1(F)=0.051$, $wR(F^2)=0.098$ for observed reflections.

1,4-Phenylenedimethanol (**146**).

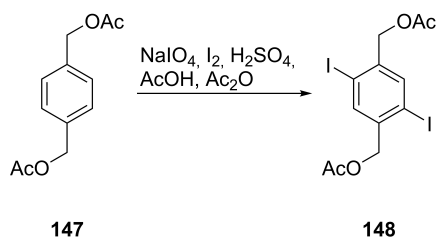


Literature known procedure was used.^[230] Analytical data was in agreement with published.^[231] $R_f=0.57$ (CH_2Cl_2 /methanol 10:1, v/v). ^1H NMR (CDCl_3 , 300 MHz): $\delta=1.60$ (br s; 2H; OH), 4.70 (s; 4H; ArCH_2), 7.37 (s; 4H; H_{Ar}) ppm.

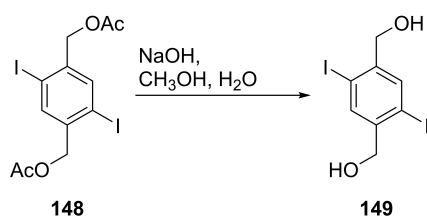
1,4-Phenylenebis(methylene) diacetate (**147**).



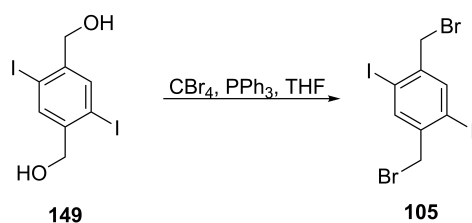
Literature known procedure was used and the analytical data was in agreement with published.^[201] $R_f=0.51$ (petroleum ether/ethyl acetate 1:1, v/v); ^1H NMR (CDCl_3 , 300 MHz): $\delta=2.10$ (s; 6H; CH_3CO), 5.10 (s; 4H; ArCH_2), 7.36 (s; 4H; H_{Ar}) ppm.

(2,5-Diiodo-1,4-phenylene)bis(methylene) diacetate (148).

Literature known procedure was adapted.^[232] Analytical data was in agreement with published.^[201] ¹H NMR (CDCl₃, 300 MHz): δ=2.16 (s; 6H; CH₃CO), 5.05 (s; 4H; ArCH₂), 7.80 (s; 2H; H_{Ar}) ppm.

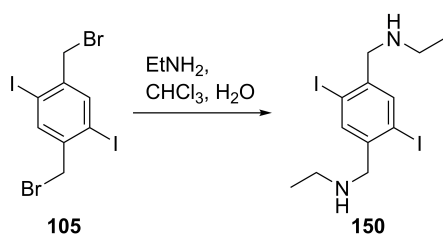
(2,5-Diiodo-1,4-phenylene)dimethanol (149).

Literature known procedure was used and the analytical data was in agreement with published.^[201] ¹H NMR (THF-*d*8, 300 MHz): δ=4.45 (d; *J* 5.5 Hz; 4H; ArCH₂), 4.56 (t; *J* 5.5 Hz; 2H; OH), 7.91 (s; 2H; H_{Ar}) ppm.

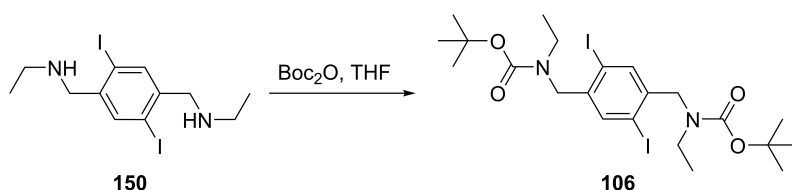
1,4-Bis(bromomethyl)-2,5-diiodobenzene (105).

Synthesis has been performed by Svenja Weigold during her work on the bachelor thesis.^[233] Analytical data was in agreement with published.^[201]

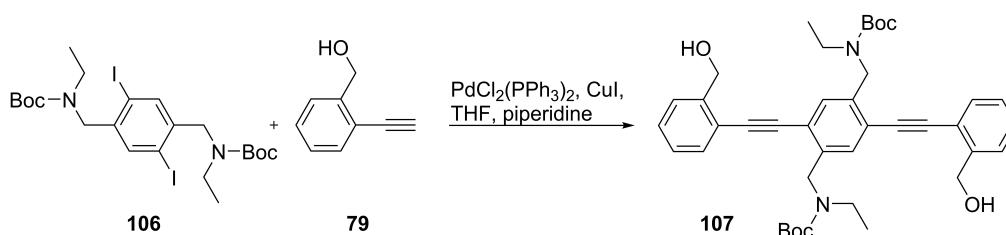
R_f=0.38 (petroleum ether/ethyl acetate 10:0, v/v); ¹H NMR (CDCl₃, 300 MHz): δ=4.48 (s; 2H; ArCH₂), 7.90 (s; 2H; H_{Ar}) ppm.

N,N'-((2,5-diiodo-1,4-phenylene)bis(methylene))diethanamine (150).

Synthesis and full analysis has been performed by Svenja Weigold during her work on the bachelor thesis.^[233] $R_f=0.41$ ($\text{CH}_2\text{Cl}_2/\text{methanol}$ 10:0, v/v); $^1\text{H NMR}$ (CDCl_3 , 300 MHz): $\delta=1.15$ (t; J 7.2 Hz; 6H; CH_3), 1.46 (br s; 2H; NH), 2.68 (q; J 6.9 Hz; 4H; NCH_2Me), 3.74 (s; 4H; ArCH_2), 7.80 (s; 2H; H_{Ar}) ppm.

Di-tert-butyl ((2,5-diiodo-1,4-phenylene)bis(methylene))bis(ethylcarbamate) (106).

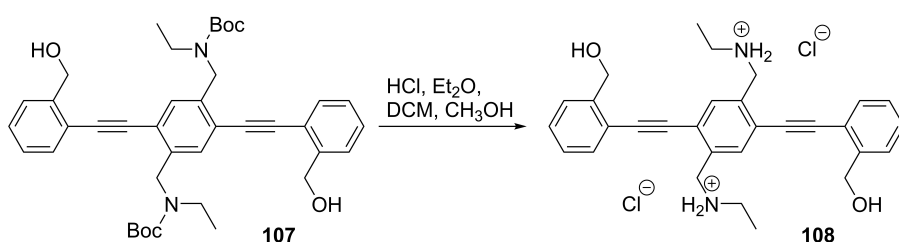
Literature known procedure was used.^[216] Synthesis and full analysis has been performed by Svenja Weigold during her work on the bachelor thesis.^[233] $R_f=0.72$ ($\text{CH}_2\text{Cl}_2/\text{methanol}$ 10:0, v/v); $^1\text{H NMR}$ (CDCl_3 , 300 MHz): $\delta=1.11$ (t; J 7.1 Hz; 6H; CH_3), 1.33-1.56 (m; 18H; $t\text{-Bu}$), 3.11-3.41 (m; 4H; NCH_2Me), 4.22-4.42 (m; 4H; ArCH_2), 7.52 (s; 2H; H_{Ar}) ppm.

Di-tert-butyl ((2,5-bis((2-(hydroxymethyl)phenyl)ethynyl)-1,4-phenylene)bis(methylene))bis(ethylcarbamate) (107).

Literature known procedure was adapted.^[219] Common Schlenk procedure was used. A degassed solution of **106** (2.009 g, 3.118 mmol, 1.0 eq), $\text{PdCl}_2(\text{PPh}_3)_2$ (109.0 mg, 155.9 μmol , 5 mol%) and CuI (59.0 mg, 311.8 μmol , 10 mol%) in THF (18 mL) and piperidine (9 mL) was added to purged with nitrogen **79** (824.0 mg, 6.236 mmol, 2.0 eq) and allowed to stir overnight. Afterwards solvent was changed to CH_2Cl_2 and after addition of Celite evaporated *in vacuo*. Purification by column chromatography (silica gel; $\text{CH}_2\text{Cl}_2/\text{methanol}$ gradient from 20:1 to 2:1, v/v) followed by washing with methanol (4 \times 20 mL) yielded **107** as beige solid. Yield: 1.474 g (2.258 mmol, 72%).

Full analysis has been performed by Svenja Weigold during her work on the bachelor thesis.^[233]
 $R_f=0.58$ ($\text{CH}_2\text{Cl}_2/\text{methanol}$ 10:1, v/v); $^1\text{H NMR}$ (pyridine- d_5 , 300 MHz): $\delta=1.13$ (t; J 6.6 Hz; 6H; CH_3), 1.54 (s; 18H; $t\text{-Bu}$), 3.24-3.60 (m; 4H; NCH_2Me), 4.92 (s; 4H; ArCH_2), 5.37 (s; 4H; ArCH_2), 7.34 (t; J 7.6 Hz; 2H; H_{Ar}), 7.49 (t; J 7.6 Hz; 2H; H_{Ar}), 7.70 (d; J 7.6 Hz; 2H; H_{Ar}), 7.86 (s; 2H; H_{Ar}), 8.06 (d; J 7.6 Hz; 2H; H_{Ar}) ppm.

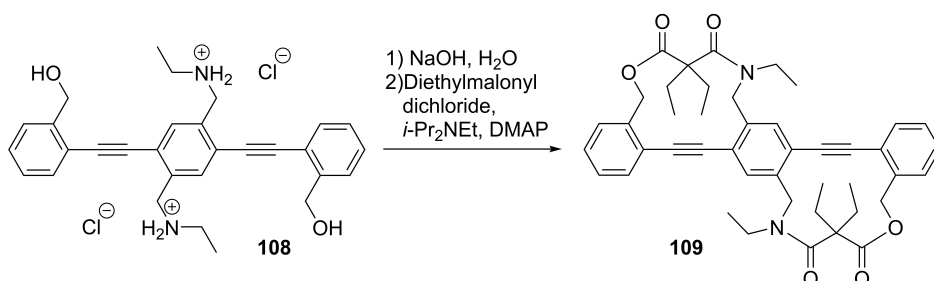
N,N'-((2,5-bis((2-(hydroxymethyl)phenyl)ethynyl)-1,4-phenylene)bis(methylene))di(ethan-1-aminium) dichloride (108).



Commercially available solution of HCl in Et_2O (2M, 16 mL) was added to a suspension of **107** (5.385 g, 8.249 mmol) in CH_2Cl_2 (66 mL) and methanol (33 mL). After stirring for 3 days reaction mixture was diluted with Et_2O (45 mL). Precipitate was filtered and washed with CH_2Cl_2 (3×30 mL). Drying yielded **108** as a yellowish solid. Yield: 4.255 g (8.097 mmol, 98%).

Full analysis has been performed by Svenja Weigold during her work on the bachelor thesis.^[233]
 $R_f=0.32$ ($\text{CH}_2\text{Cl}_2/\text{methanol}$ 10:1, v/v); $^1\text{H NMR}$ (DMSO- d_6 , 300 MHz): $\delta=1.30$ (t; J 7.1 Hz; 6H; CH_3), 3.08 (q; J 7.1 Hz; 4H; NCH_2Me), 4.42 (s; 4H; ArCH_2), 4.77 (s; 4H; ArCH_2), 5.47 (br s; 2H; OH), 7.37 (t; J 7.4 Hz; 2H; H_{Ar}), 7.49 (t; J 7.4 Hz; 2H; H_{Ar}), 7.60 (t; J 7.8 Hz; 4H; H_{Ar}), 8.11 (s; 2H; H_{Ar}), 9.51 (br s; 4H; NH_2) ppm.

8,8,10,22,22,24-hexaethyl-13,14,27,28-tetrahydro-10,11,24,25-tetrahydro-5H,7H-dibenzo[k,k']benzo[1,2-g:4,5-g']bis[1,5]oxazacyclotridecine-7,9,21,23(8H,19H,22H)-tetrone (109).



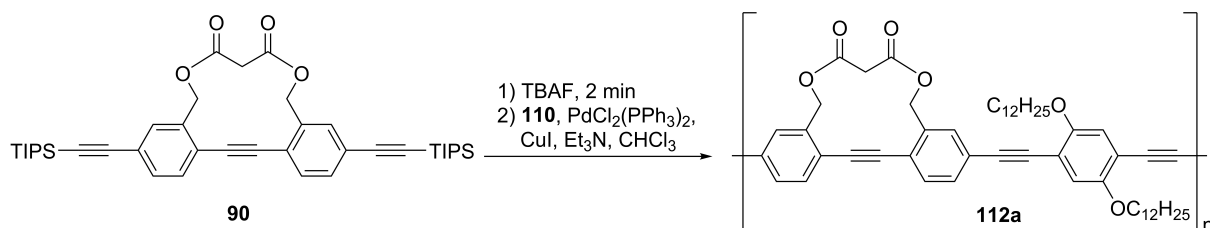
Solution of NaOH (642.0 mg, 16.1 mmol, 4.0 eq) in water (32 mL) was added to **108** (2.109 g, 4.013 mmol, 1.0 eq) suspended in CHCl_3 (170 mL). After stirring for 5 min two clear phases have been separated. Water layer was extracted with CHCl_3 (1×50 mL) and combined organic phase

was washed with brine (1×50 mL) and dried over MgSO₄. Evaporation of volatiles *in vacuo* afforded free diamine (1.770 g, 3.911 mmol, 97%) as a beige solid, which was pure enough for the next step. Under common Schlenk conditions a solution of diethylmalonyl dichloride (1.42 mL, 8.272 mmol, 4.0 eq) in dry CH₂Cl₂ (100 mL) was added during 5 h to a suspension of the crude diamine (936.0 mg, 2.068 mmol, 1.0 eq), *i*-Pr₂NEt (1.45 mL, 8.272 mmol, 4.0 eq), 4-(dimethylamino)pyridine (505.0 mg, 4.136 mmol, 2.0 eq) and NaHCO₃ (1.390 g, 16.54 mmol, 8.0 eq) in dry CH₂Cl₂ (1.0 L). After additional stirring for 48 h H₂O (100 mL) was added and water phase was extracted with CH₂Cl₂ (2×50 mL). Combined organic layer was washed with saturated aq. NaHCO₃ solution (1×100 mL), brine (1×100 mL) and dried over MgSO₄. Purification by column chromatography (silica gel; CH₂Cl₂/ethyl acetate 30:1, v/v) yielded **109** as colorless solid. Yield: 864.0 mg (1.233 mmol, 59%).

R_f=0.43 (petroleum ether/ethyl acetate 1:1, v/v); m.p.=349°C (decomposes without melting); ¹H and ¹³C NMR spectra were complicated owing to tautomer mixture; ¹H NMR (CDCl₃, 600 MHz): δ=0.72-0.89 (m; 12H), 0.92-1.04 (m; 6H), 1.79-2.11 (m; 8H), 2.77-2.91 (m; 1H), 3.24 (br s; 2H), 3.48-3.64 (m; 1H), 3.93-4.04 (m; 1H), 4.44-4.79 (m; 2H), 4.95-5.45 (m; 5H), 7.31-7.41 (m; 6H), 7.49-7.62 (m; 4H) ppm; ¹³C NMR (CDCl₃, 150 MHz): δ=8.0, 8.2, 12.2, 14.1, 22.3, 26.4, 49.3, 49.5, 50.0, 50.2, 67.2, 67.4, 90.4, 92.8, 93.1, 93.9, 94.2, 123.7, 123.8, 128.9, 129.0, 130.1, 132.5, 132.9, 135.5, 136.1, 136.3, 136.5, 137.3, 137.9, 138.3, 169.9, 170.3, 173.8, 174.3 ppm; IR: $\tilde{\nu}$ =2968, 2877, 1716, 1629, 1507, 1398, 1300, 1208, 1132, 983, 746, 664 cm⁻¹; HRMS (ESI⁺) m/z: [M+Na]⁺ calculated for C₄₄H₄₈N₂NaO₆⁺: 723.3405; found: 723.3413, correct isotope distribution; elemental analysis calculated (%) for C₄₄H₄₈N₂O₆: C 75.40, H 6.90, N, 4.00; found: C 65.57, H 6.34, N, 3.02.

Crystal data: C₄₆H₅₀Cl₆N₂O₆, M_w=939.58, colorless crystal (little brick), obtained by slow diffusion of pentane into a CHCl₃ solution of **109**, dimensions 0.113×0.057×0.048 mm³, triclinic crystal system, space group P $\bar{1}$, Z=2, a=9.6500(4) Å, b=15.8327(6) Å, c=16.2694(6) Å, α=70.925(3)°, β=85.317(3)°, γ=88.315(3)°, V=2341.39(16) Å³, ρ=1.333 g/cm³, T=100(2) K, θ_{max}=55.084°, radiation CuKα, λ=1.54178 Å, 22606 reflections measured, 5840 unique (R_{int}=0.0712), 3959 observed (I>2σ(I)), final residual values R₁(F)= 0.061, wR(F²)= 0.150 for observed reflections.

Poly(3-((2,5-bis(dodecyloxy)-4-(prop-1-yn-1-yl)phenyl)ethynyl)-13-methyl-16,17-didehydro-5,11-dihydro-7H-dibenzo[g,k][1,5]dioxacyclotridecine-7,9(8H)-dione) (112a**).**

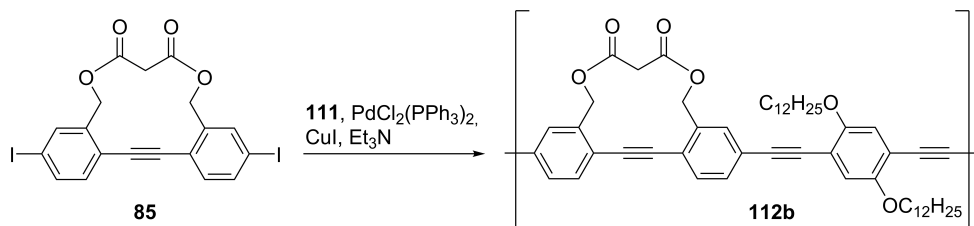


Literature known procedure was adapted.^[224] Common Schlenk procedure was used. Degassed commercially available 1M solution of Bu₄NF in THF (1.5 mL, 1.499 mmol, 5.0 eq) was added to a degassed solution of **90** (200.0 mg, 299.8 μmol, 1.0 eq) and **110**⁷ (209.0 mg, 299.8 μmol, 1.0 eq) in Et₃N (0.9 mL) and CHCl₃ (1.0 mL), which turned the reaction mixture red and turbid. Degassed solution (0.5 mL, corresponds to 0.2 mol% of PdCl₂(PPh₃)₂ and 0.4 mol% of CuI) prepared from PdCl₂(PPh₃)₂ (21.0 mg, 29.98 μmol) and CuI (11.4 mg, 59.96 μmol) in dry Et₃N (25 mL) was added (the color turned purple) and reaction mixture was allowed to stir over 48 h at 65°C. After cooling to room temperature and dilution with CHCl₃ (50 mL) several crystals of (*E*)-*N,N*-diethyl-2-phenyldiazene-1-carbothioamide^[234] were added and the resulting solution was allowed to stir overnight. The solution was washed with saturated aq. NH₄Cl solution (1×30 mL) and concentrated. Residue was dissolved in hot toluene (15 mL) and this turbid solution was added dropwise to methanol (500 mL). Precipitate was separated and redissolved in boiling CHCl₃ (130 mL), solution was hot filtered, concentrated to 3 mL and added dropwise to methanol (250 mL). Filtration and drying yielded **112a** as a green-yellow solid (104.0 mg, 43%).

¹H NMR (CDCl₃, 600 MHz): δ=0.87 (t; *J* 6.9 Hz; 6H; CH₃), 1.20-1.43 (m; 32H; CH₂), 1.51-1.60 (m; 4H; CH₂), 1.81-1.92 (m; 4H; CH₂), 3.42 (s; 2H; COCH₂CO), 3.95-4.08 (m; 4H; OCH₂), 5.14 (s; 4H; PhCH₂), 6.90 (s; 0.25H; H_{Ar}), 7.02 (s; 1H; H_{Ar}), 7.32 (s; 0.25H; H_{Ar}), 7.48-7.60 (m; 4H; H_{Ar}) ppm; ¹³C NMR (CDCl₃, 150 MHz): δ=14.1, 22.7, 26.0, 26.1, 29.15, 29.24, 29.28, 29.3, 29.4, 29.56, 29.61, 29.64, 29.68, 31.9, 41.7, 67.2, 69.6, 69.8, 70.1, 88.3, 88.6, 92.0, 93.1, 94.0, 112.9, 113.8, 115.9, 116.8, 123.6, 123.8, 124.1, 131.9, 132.0, 132.7, 133.39, 133.44, 136.4, 151.8, 153.7, 154.4, 166.0 ppm; M_n=1.75×10⁴ g/mol, PDI=1.46.

⁷ The substance was kindly provided by Emanuel Smarsly.

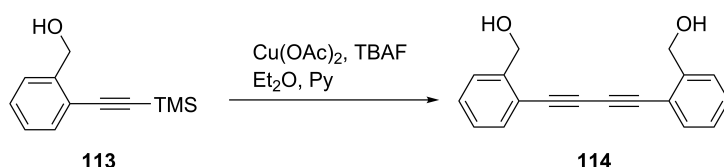
Poly(3-((2,5-bis(dodecyloxy)-4-(prop-1-yn-1-yl)phenyl)ethynyl)-13-methyl-16,17-didehydro-5,11-dihydro-7H-dibenzo[g,k][1,5]dioxacyclotridecine-7,9(8H)-dione) (112b)



Literature known procedure was adapted.^[224] Common Schlenk procedure was used. Degassed solution (0.5 mL, corresponds to 0.2 mol% of $\text{PdCl}_2(\text{PPh}_3)_2$ and 0.4 mol% of CuI) prepared from $\text{PdCl}_2(\text{PPh}_3)_2$ (25.2 mg, 35.84 μmol) and CuI (13.7 mg, 71.68 μmol) in dry Et_3N (25 mL) was added to a degassed suspension of **85** (200.0 mg, 358.4 μmol , 1.0 eq) and **111**⁸ (177.0 mg, 358.4 μmol , 1.0 eq) in Et_3N (7.1 mL). The reaction mixture was allowed to stir at 75°C for 24 h. After cooling to room temperature and dilution with CHCl_3 (70 mL) several crystal of (*E*)-*N,N*-diethyl-2-phenyldiazene-1-carbothioamide^[234] were added and the resulting solution was allowed to stir overnight. The solution was washed with saturated aq. NH_4Cl solution (1×30 mL), concentrated to 3-5 mL and added dropwise to methanol (400 mL). Precipitate was redissolved in boiling CHCl_3 (250 mL), solution was hot filtered and concentrated to 10 mL. Repetition of the purification procedure two more times yielded green-yellow solid (107.0 mg, 37%).⁹

¹H NMR (CDCl_3 , 600 MHz): δ =0.87 (t; *J* 6.9 Hz; 6H; CH_3), 1.09-1.43 (m; 32H; CH_2), 1.51-1.60 (m; 4H; CH_2), 1.81-1.92 (m; 4H; CH_2), 3.37-3.48 (m; 2H; COCH_2CO), 4.01-4.08 (m; 4H; OCH_2), 5.06-5.22 (m; 4H; PhCH_2), 7.02 (s; 2H; H_{Ar}), 7.46-7.61 (m; 6H; H_{Ar}) ppm; ¹³C NMR (CDCl_3 , 150 MHz): δ =14.1, 22.7, 26.0, 26.1, 26.15, 29.27, 29.34, 29.4, 29.62, 29.64, 29.7, 31.9, 41.7, 67.2, 69.6, 69.8, 70.1, 88.3, 88.6, 92.0, 93.1, 94.0, 112.9, 113.8, 115.8, 116.8, 123.6, 123.8, 124.1, 131.96, 132.0, 132.7, 133.39, 133.43, 136.4, 151.8, 153.7, 154.4, 166.0 ppm; $M_n=2.78 \times 10^4$ g/mol, PDI=2.70.

(Buta-1,3-diyne-1,4-diylbis(2,1-phenylene))dimethanol (114).



Literature known procedure was adapted.^[235] A 1M solution of tetrabutylammonium fluoride (16.1 mL, 16.08 mmol, 1.0 eq) in THF was added to a solution of **113** (3.285 g, 16.08 mmol,

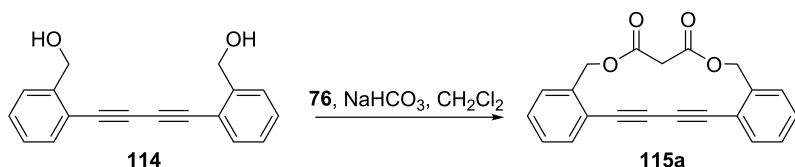
⁸ The substance was kindly provided by Emanuel Smarsly.

⁹ Similar conditions using 1 mol% of $\text{PdCl}_2(\text{PPh}_3)_2$ and 0.4 mol% of CuI yielded 144.0 mg of same structure polymer **112c** (yield 50%). $M_n=2.84 \times 10^4$ g/mol, PDI=3.15. For NMR spectra see Appendix 7.3.

1.0 eq) and Cu(OAc)₂ monohydrate (9.631 g, 48.24 mmol, 3.0 eq) in 120 mL Et₂O and 370 mL pyridine in one portion. The deep blue solution became dark green. After steering for 30 min the reaction mixture was diluted with 1.2 L Et₂O and washed several times with ice-cold 3% HCl until all pyridine was completely removed. Then organic phase was washed with saturated aq. NaHCO₃ solution (1×100 mL), brine (1×100 mL) and dried over MgSO₄. Purification by column chromatography (silica gel; CH₂Cl₂/ethyl acetate gradient from 10:1 to 1:2, v/v) yielded **114** as a yellowish solid. Yield: 1.200 g (4.575 mmol, 86%). Analytical sample was prepared by recrystallization from CHCl₃.

R_f=0.21 (petroleum ether/ethyl acetate 1:1, v/v); m.p.=173°C; ¹H NMR (CDCl₃, 500 MHz): δ=1.92 (t; *J* 6.29 Hz; 2H; OH), 4.90 (d; *J* 6.29 Hz; 4H;), 7.29 (t; *J* 7.36 Hz; 2H; H_{Ar}), 7.41 (t; *J* 7.58 Hz; 2H; H_{Ar}), 7.51 (d; *J* 7.62 Hz; 2H; H_{Ar}), 7.56 (d; *J* 7.52 Hz; 2H; H_{Ar}) ppm; ¹³C NMR (CDCl₃, 150 MHz): δ=63.7, 78.0, 80.2, 119.7, 127.3, 127.6, 129.7, 133.3, 144.0 ppm; IR: $\tilde{\nu}$ =3297, 3221, 2905, 2852, 1475, 1444, 1032, 755, 707, 561, 543, 442 cm⁻¹; HRMS (DART⁺) *m/z*: [M+NH₄]⁺ calculated for C₁₈H₁₈NO₂⁺: 280.1332; found: 280.1333, correct isotope distribution; elemental analysis calculated (%) for C₁₈H₁₄O₂: C 82.42, H 5.38; found: C 82.13, H 5.56.

16,17,18,19-tetradehydro-5,11-dihydro-7H-dibenzo[*g,m*][1,5]dioxacyclopentadecine-7,9(8H)-dione (115a).

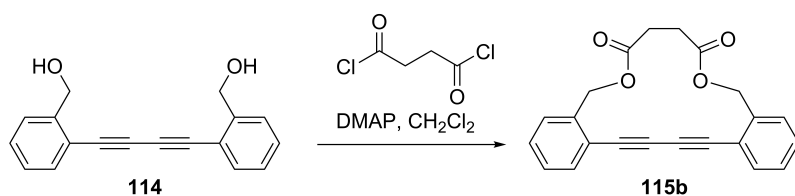


Literature known procedure was adapted.^[66] Common Schlenk procedure was used. A solution of malonyl chloride (371 μ L, 3.812 mmol, 2.0 eq) in dry CH₂Cl₂ (100 mL) was added to a suspension of **114** (500.0 mg, 1.906 mmol, 1.0 eq) and NaHCO₃ (1.601 g, 19.06 mmol, 10 eq) in dry CH₂Cl₂ (480 mL) during 5 h. After stirring overnight, the reaction mixture was filtered through 1 cm silica gel pad (eluent ethyl acetate) and evaporated to dryness. Purification by column chromatography (silica gel; petroleum ether/Et₂O gradient from 5:1 to 1:1, v/v) yielded **115a** as a white solid. Yield: 482.0 mg (1.459 mmol, 76%). Analytical sample was prepared by recrystallization from acetone.

R_f=0.47 (petroleum ether/ethyl acetate 1:1, v/v); m.p.=214°C; ¹H NMR (CDCl₃, 300 MHz): δ=3.50 (s; 2H; COCH₂CO), 5.30 (s; 4H; ArCH₂), 7.32-7.40 (m; 6H; H_{Ar}), 7.49-7.54 (m; 2H; H_{Ar}) ppm; ¹³C NMR (CDCl₃, 100 MHz): δ=41.7, 67.1, 79.4, 82.3, 122.5, 129.0, 129.3, 130.2, 132.3, 138.8, 165.7

ppm; IR: $\tilde{\nu}$ =3460, 2988, 2959, 1728, 1454, 1290, 1231, 1200, 1126, 987, 953, 766 cm^{-1} ; HRMS (DART⁺) m/z: $[\text{M}+\text{NH}_4]^+$ calculated for $\text{C}_{21}\text{H}_{18}\text{NO}_4^+$: 348.1230; found: 348.1231, correct isotope distribution; elemental analysis calculated (%) for $\text{C}_{21}\text{H}_{14}\text{O}_4$: C 76.36, H 4.27; found: C 74.92, H 4.26. Crystal data: $\text{C}_{21}\text{H}_{14}\text{O}_4$, $M_w=330.32$, colorless crystal (thin), obtained by slow diffusion of pentane into an acetone solution of **115a**, dimensions $0.189 \times 0.182 \times 0.058 \text{ mm}^3$, orthorhombic crystal system, space group Pbcn, $Z=4$, $a=18.6091(12) \text{ \AA}$, $b=11.5697(7) \text{ \AA}$, $c=7.6201(4) \text{ \AA}$, $\alpha=90^\circ$, $\beta=90^\circ$, $\gamma=90^\circ$, $V=1640.62(17) \text{ \AA}^3$, $\rho=1.337 \text{ g/cm}^3$, $T=200(2) \text{ K}$, $\theta_{\text{max}}=26.398^\circ$, radiation $\text{MoK}\alpha$, $\lambda=0.71073 \text{ \AA}$, 10545 reflections measured, 1687 unique ($R_{\text{int}}=0.0380$), 1306 observed ($I > 2\sigma(I)$), final residual values $R_1(F)=0.043$, $wR(F^2)=0.102$ for observed reflections.

17,18,19,20-Tetradehydro-5,8,9,12-tetrahydrodibenzo[h,n][1,6]dioxacyclohexadecine-7,10-dione (115b).

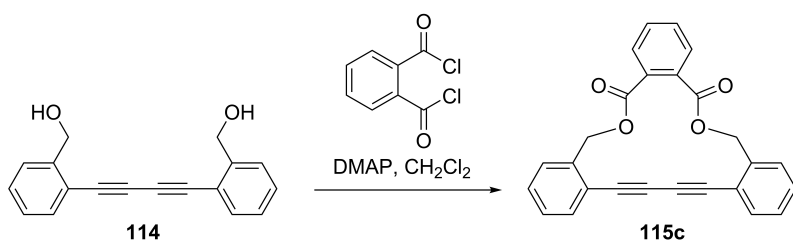


Literature known procedure was adapted.^[190] Common Schlenk procedure was used. A solution of succinyl chloride (84 μL , 762.5 μmol , 2.0 eq) in dry CH_2Cl_2 (30 mL) was added during 4.5 h to a mixture of **114** (100.0 mg, 381.2 μmol , 1.0 eq) and 4-(dimethylamino)pyridine (279.0 mg, 2.287 mmol, 6.0 eq) in dry CH_2Cl_2 (100 mL). The color of the reaction mixture changes rapidly from beige to black during the addition. The reaction was allowed to stir overnight, then water (50 mL) was added and layers have been separated. Water phase was extracted with CH_2Cl_2 (3 \times 50 mL), and the combined organic layer was washed with brine and dried over MgSO_4 . Purification by column chromatography (silica gel; petroleum ether/ethyl acetate gradient from 5:1 to 1:1, v/v) yielded **115b** as white solid. Yield: 55.0 mg (159.7 μmol , 42%).

$R_f=0.44$ (petroleum ether/ethyl acetate 1:1, v/v); m.p.=204 $^\circ\text{C}$; $^1\text{H NMR}$ (CDCl_3 , 600 MHz): $\delta=2.74$ (s; 4H; $\text{COCH}_2\text{CH}_2\text{CO}$), 5.26 (s; 4H; ArCH_2), 7.34-7.38 (m; 6H; H_{Ar}), 7.54-7.57 (m; 2H; H_{Ar}) ppm; $^{13}\text{C NMR}$ (CDCl_3 , 150 MHz): $\delta=29.4$, 65.8, 78.6, 80.8, 122.7, 128.9, 129.3, 130.4, 132.9, 139.0, 171.8 ppm; IR: $\tilde{\nu}$ =2987, 2953, 2892, 1734, 1405, 1373, 1339, 1241, 1205, 1181, 1144, 967, 932, 760, 605, 504 cm^{-1} ; HRMS (ESI⁺) m/z: $[\text{M}+\text{Na}]^+$ calculated for $\text{C}_{22}\text{H}_{16}\text{NaO}_4^+$: 367.0941; found: 367.0943, correct isotope distribution; elemental analysis calculated (%) for $\text{C}_{22}\text{H}_{16}\text{O}_4$: C 76.73, H 4.68; found: C 76.72, H 4.86.

Crystal data: $C_{22}H_{16}O_4$, $M_w=344.35$, colorless crystal (plate), obtained by slow diffusion of pentane in $CHCl_3$ solution of **115b**, dimensions $0.183 \times 0.164 \times 0.141$ mm³, triclinic crystal system, space group $P\bar{1}$, $Z=4$, $a=8.9878(7)$ Å, $b=13.3609(10)$ Å, $c=15.1811(12)$ Å, $\alpha=105.804(2)^\circ$, $\beta=90.514(2)^\circ$, $\gamma=99.654(2)^\circ$, $V=1726.4(2)$ Å³, $\rho=1.325$ g/cm³, $T=200(2)$ K, $\Theta_{max}=25.085^\circ$, radiation $Mo_{K\alpha}$, $\lambda=0.71073$ Å, 16654 reflections measured, 6123 unique ($R_{int}=0.0632$), 3203 observed ($I > 2\sigma(I)$), final residual values $R_1(F)=0.056$, $wR(F^2)=0.107$ for observed reflections.

19,20,21,22-tetradehydro-5,14-dihydrotribenzo[c,h,n][1,6]dioxacyclohexadecine-7,12-dione (115c).



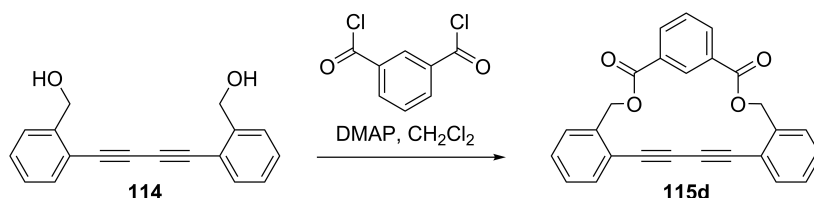
Literature known procedure was adapted.^[190] Common Schlenk procedure was used. A phthaloyl chloride (220 μ L, 1.525 mmol, 2.0 eq) was added in one portion to a mixture of **114** (200.0 mg, 762.5 μ mol, 1.0 eq) and 4-(dimethylamino)pyridine (558.0 mg, 4.575 mmol, 6.0 eq) in dry CH_2Cl_2 (260 mL). The reaction was allowed to stir overnight. Afterwards the reaction mixture was filtered through silica gel pad (eluent CH_2Cl_2 , then ethyl acetate) and concentrated *in vacuo*. Purification by column chromatography (silica gel; petroleum ether/ethyl acetate gradient 2:1, v/v, then ethyl acetate) followed by recrystallization from the mixture $CHCl_3$ /pentane yielded **115c** as a pale beige solid. Yield: 14.0 mg (35.68 μ mol, 5%).

$R_f=0.45$ (petroleum ether/ethyl acetate 1:1, v/v); m.p.=279°C (decomposition); 1H NMR ($CDCl_3$, 600 MHz): $\delta=5.53$ (s; 4H; $ArCH_2$), 7.37 (td; J 7.6, 1.4 Hz; 2H; H_{Ar}), 7.40 (td; J 7.6, 1.4 Hz; 2H; H_{Ar}), 7.45-7.52 (m; 6H; H_{Ar}), 7.68-7.73 (m; 2H; H_{Ar}) ppm; ^{13}C NMR ($CDCl_3$, 150 MHz): $\delta=66.5$, 79.1, 80.7, 123.2, 128.7, 129.0, 129.3, 130.8, 131.1, 131.9, 132.4, 139.1, 167.0 ppm; IR: $\tilde{\nu}=3015$, 1713, 1578, 1483, 1449, 1375, 1279, 1258, 1122, 1072, 935, 773, 742, 703, 572 cm^{-1} ; HRMS (ESI⁺) m/z : $[M+Na]^+$ calculated for $C_{26}H_{16}NaO_4^+$: 415.0941; found: 415.0947, correct isotope distribution; elemental analysis calculated (%) for $C_{26}H_{16}O_4$: C 79.58, H 4.11; found: C 79.48, H 4.28.

Crystal data: $C_{26}H_{16}O_4$, $M_w=392.39$, light yellow crystal (thick plate), obtained by slow diffusion of pentane into $CHCl_3$ solution of **115c**, dimensions $0.145 \times 0.137 \times 0.111$ mm³, triclinic crystal system, space group $P\bar{1}$, $Z=2$, $a=7.7332(8)$ Å, $b=10.4273(11)$ Å, $c=12.7081(14)$ Å, $\alpha=78.4638(17)^\circ$, $\beta=79.4560(17)^\circ$, $\gamma=73.1890(17)^\circ$, $V=952.53(18)$ Å³, $\rho=1.368$ g/cm³, $T=200(2)$ K, $\Theta_{max}=27.996^\circ$,

radiation $\text{Mo}_{K\alpha}$, $\lambda=0.71073 \text{ \AA}$, 14896 reflections measured, 4604 unique ($R_{int}=0.0541$), 2827 observed ($I>2\sigma(I)$), final residual values $R_1(F)=0.051$, $wR(F^2)=0.119$ for observed reflections.

20,21,22,23-Tetradehydro-5,15-dihydro-7H,13H-8,12-(metheno)dibenzo[k,q][1,9]dioxacyclononadecine-7,13-dione (115d).



Literature known procedure was adapted.^[190] Common Schlenk procedure was used. An isophthaloyl chloride (310.0 mg, 1.525 mmol, 2.0 eq) was added in one portion to a mixture of **114** (200.0 mg, 762.5 μmol , 1.0 eq) and 4-(dimethylamino)pyridine (558.0 mg, 4.575 mmol, 6.0 eq) in dry CH_2Cl_2 (260 mL). The reaction was allowed to stir overnight. Afterwards the reaction mixture was filtered through silica gel pad (eluent CH_2Cl_2 , then ethyl acetate) and concentrated *in vacuo*. Purification by column chromatography (silica gel; petroleum ether/ethyl acetate gradient from 5:1 to 1:2, v/v) yielded **115d** as beige solid. Yield: 271.0 mg (690.6 μmol , 90%).

$R_f=0.58$ (petroleum ether/ethyl acetate 1:1, v/v); m.p.=275°C (decomposition); ^1H NMR (CDCl_3 , 600 MHz): $\delta=5.54$ (s; 4H; ArCH_2), 7.33-7.40 (m; 4H; H_{Ar}), 7.49-7.53 (m; 3H; H_{Ar}), 7.58 (dd; J 7.4, 0.9 Hz; 2H; H_{Ar}), 8.21 (dd; J 7.8, 1.8 Hz; 2H; H_{Ar}), 8.97 (s; 1H; H_{Ar}) ppm; ^{13}C NMR (CDCl_3 , 150 MHz): $\delta=65.8$, 79.0, 81.9, 122.5, 128.6, 128.8, 129.4, 130.4, 130.8, 131.1, 133.2, 134.2, 139.4, 165.4 ppm; IR: $\tilde{\nu}=3061$, 2956, 1720, 1440, 1370, 1294, 1223, 1128, 1114, 1097, 1070, 952, 751, 721, 613, 522 cm^{-1} ; HRMS (ESI⁺) m/z : $[\text{M}+\text{Na}]^+$ calculated for $\text{C}_{26}\text{H}_{16}\text{NaO}_4^+$: 415.0941; found: 415.0949, correct isotope distribution; elemental analysis calculated (%) for $\text{C}_{26}\text{H}_{16}\text{O}_4$: C 79.58, H 4.11; found: C 79.55, H 4.15.

Crystal data: $\text{C}_{26}\text{H}_{16}\text{O}_4$, $M_w=392.39$, colorless crystal (rectangle-brick), obtained by slow diffusion of pentane into CHCl_3 solution of **115d**, dimensions $0.177\times 0.159\times 0.140 \text{ mm}^3$, triclinic crystal system, space group $\text{P}\bar{1}$, $Z=2$, $a=7.2786(6) \text{ \AA}$, $b=10.8621(9) \text{ \AA}$, $c=13.1049(11) \text{ \AA}$, $\alpha=69.4665(11)^\circ$, $\beta=84.9288(11)^\circ$, $\gamma=75.3820(11)^\circ$, $V=938.85(14) \text{ \AA}^3$, $\rho=1.388 \text{ g/cm}^3$, $T=200(2) \text{ K}$, $\theta_{\text{max}}=29.622^\circ$, radiation $\text{Mo}_{K\alpha}$, $\lambda=0.71073 \text{ \AA}$, 20190 reflections measured, 5262 unique ($R_{int}=0.0481$), 3633 observed ($I>2\sigma(I)$), final residual values $R_1(F)=0.050$, $wR(F^2)=0.129$ for observed reflections.

6 References

- [1] a) G. Horowitz, *Adv. Mater.* **1998**, *10*, 365; b) M. Muccini, *Nat. Mater.* **2006**, *5*, 605; c) J. Zaumseil, H. Sirringhaus, *Chem. Rev.* **2007**, *107*, 1296; d) H. Klauk, *Chem. Soc. Rev.* **2010**, *39*, 2643; e) H. Sirringhaus, *Adv. Mater.* **2014**, *26*, 1319.
- [2] a) M. Grätzel, *Acc. Chem. Res.* **2009**, *42*, 1788; b) H. Hoppe, N. S. Sariciftci, *J. Mater. Res.* **2004**, *19*, 1924; c) D. Wöhrle, O. R. Hild, *Chem. Unserer Zeit* **2010**, *44*, 174; d) A. Facchetti, *Mater. Today* **2013**, *16*, 123; e) R. Flamini, I. Tomasi, A. Marrocchi, B. Carlotti, A. Spalletti, *J. Photochem. Photobiol., A* **2011**, *223*, 140.
- [3] a) J. Han, B. Wang, M. Bender, K. Seehafer, U. H. F. Bunz, *ACS Appl. Mater. Interfaces* **2016**, *8*, 20415; b) J. Han, C. Ma, B. Wang, M. Bender, M. Bojanowski, M. Hergert, K. Seehafer, A. Herrmann, U. H.F. Bunz, *Chem* **2017**, *2*, 817; c) Y.-J. Jin, G. Kwak, *Polymer Reviews* **2016**, *57*, 175; d) G. Zhao, H. Wang, G. Liu, Z. Wang, *Electroanalysis* **2017**, *29*, 497; e) S.-i. Kondo, K. Endo, J. Iioka, K. Sato, Y. Matsuta, *Tetrahedron Lett.* **2017**, *58*, 4115; f) X. Liu, X. Zhou, X. Shu, J. Zhu, *Macromolecules* **2009**, *42*, 7634; g) J. T. Fletcher, B. S. Bruck, *Sens. Actuators, B* **2015**, *207*, 843.
- [4] a) R. H. Friend, R. W. Gymer, A. B. Holmes, J. H. Burroughes, R. N. Marks, C. Taliani, D. D. C. Bradley, D. A. D. Santos, J. L. Brédas, M. Lögdlund et al., *Nature* **1999**, *397*, 121; b) S.-C. Lo, P. L. Burn, *Chem. Rev.* **2007**, *107*, 1097; c) M. Deußen, H. Bässler, *Chem. Unserer Zeit* **1997**, *31*, 76; d) D. Hertel, C. D. Müller, K. Meerholz, *Chem. Unserer Zeit* **2005**, *39*, 336; e) J. J. Kim, J. C. Yang, K. Yoon, G. Kwak, J. Y. Park, *MRS Commun.* **2017**, *7*, 701.
- [5] a) F. Markl, I. Braun, E. Smarsly, U. Lemmer, N. Mechau, G. Hernandez-Sosa, U. H. F. Bunz, *ACS Macro Lett.* **2014**, *3*, 788; b) Z. Cui, *Printed electronics. Materials, technologies and applications*, Solaris South Tower, Singapore; Wiley/Higher Education Press, Hoboken, NJ, **2016**.
- [6] V. Coropceanu, H. Li, P. Winget, L. Zhu, J.-L. Brédas, *Annu. Rev. Mater. Res.* **2013**, *43*, 63.
- [7] Loupe image was adopted from the free image service Pixabay.com, accessed on 05.04.2018, "Magnifying glass".
- [8] Y. Lin, Y. Li, X. Zhan, *Chem. Soc. Rev.* **2012**, *41*, 4245.
- [9] K. Müllen, G. Wegner, *Electronic materials. The oligomer approach*, Wiley-VCH, Weinheim, New-York, **1998**.
- [10] A. Facchetti, *Mater. Today* **2007**, *10*, 28.
- [11] U. H. F. Bunz, *Chem. Rev.* **2000**, *100*, 1605.

- [12] C. Weder (Hrsg.) *Advances in Polymer Science*, Springer Berlin Heidelberg, Berlin, Heidelberg, **2005**.
- [13] Limpricht, Schwanert, *Ber. Dtsch. Chem. Ges.* **1869**, 2, 133.
- [14] L. I. Smith, M. M. Falkof, *Org. Synth.* **1942**, 22, 50.
- [15] a) M. Z. Zgierski, E. C. Lim, *Chem. Phys. Lett.* **2004**, 387, 352; b) Y. Li, J. Zhao, X. Yin, H. Liu, G. Yin, *Phys. Chem. Chem. Phys.* **2007**, 9, 1186.
- [16] Y. Amatatsu, M. Hosokawa, *J. Phys. Chem. A* **2004**, 108, 10238.
- [17] M. Wierzbicka, I. Bylińska, C. Czaplewski, W. Wiczak, *RSC Adv.* **2015**, 5, 29294.
- [18] M. Krämer, U. H. F. Bunz, A. Dreuw, *J. Phys. Chem. A* **2017**, 121, 946.
- [19] K. Okuyama, T. Hasegawa, M. Ito, N. Mikami, *J. Phys. Chem.* **1984**, 88, 1711.
- [20] Y. Hirata, T. Okada, N. Mataga, T. Nomoto, *J. Phys. Chem.* **1992**, 96, 6559.
- [21] a) Y. Hirata, T. Okada, T. Nomoto, *Chem. Phys. Lett.* **1993**, 209, 397; b) A. R. Melnikov, M. P. Davydova, P. S. Sherin, V. V. Korolev, A. A. Stepanov, E. V. Kalneus, E. Benassi, S. F. Vasilevsky, D. V. Stass, *J. Phys. Chem. A* **2018**, 122, 1235.
- [22] J. Saltiel, V. K. R. Kumar, *J. Phys. Chem. A* **2012**, 116, 10548.
- [23] U. H. F. Bunz, *Macromol. Rapid Commun.* **2009**, 30, 772.
- [24] U. H. F. Bunz in *Advances in Polymer Science* (Hrsg.: C. Weder), Springer Berlin Heidelberg, Berlin, Heidelberg, **2005**, S. 1–52.
- [25] a) A. K. Mishra, M. A. Harris, R. M. Young, M. R. Wasielewski, F. D. Lewis, *J. Phys. Chem. B* **2017**, 121, 7042; b) K. E. Brown, A. P. N. Singh, Y.-L. Wu, A. K. Mishra, J. Zhou, F. D. Lewis, R. M. Young, M. R. Wasielewski, *J. Am. Chem. Soc.* **2017**, 139, 12084; c) S. A. Odom, R. F. Kelley, S. Ohira, T. R. Ensley, C. Huang, L. A. Padilha, S. Webster, V. Coropceanu, S. Barlow, D. J. Hagan et al., *J. Phys. Chem. A* **2009**, 113, 10826.
- [26] O. S. Pyun, W. Yang, M.-Y. Jeong, S. H. Lee, K. M. Kang, S.-J. Jeon, B. R. Cho, *Tetrahedron Lett.* **2003**, 44, 5179.
- [27] a) T. Kawase, H. R. Darabi, M. Oda, *Angew. Chem. Int. Ed. Engl.* **1996**, 35, 2664; b) T. Kawase, N. Ueda, K. Tanaka, Y. Seirai, M. Oda, *Tetrahedron Lett.* **2001**, 42, 5509; c) T. Kawase, K. Tanaka, N. Fujiwara, H. R. Darabi, M. Oda, *Angew. Chem. Int. Ed.* **2003**, 42, 1624; d) T. Kawase, H. Kurata, *Chem. Rev.* **2006**, 106, 5250; e) T. Kawase, Y. Nishiyama, T. Nakamura, T. Ebi, K. Matsumoto, H. Kurata, M. Oda, *Angew. Chem. Int. Ed.* **2007**, 46, 1086; f) T. Kawase, *Synlett* **2007**, 2007, 2609.
- [28] U. H. F. Bunz, S. Menning, N. Martín, *Angew. Chem. Int. Ed.* **2012**, 51, 7094.
- [29] a) J. F. Galindo, E. Atas, A. Altan, D. G. Kuroda, S. Fernandez-Alberti, S. Tretiak, A. E. Roitberg, V. D. Kleiman, *J. Am. Chem. Soc.* **2015**, 137, 11637; b) K. M. Gaab, A. L.

- Thompson, J. Xu, T. J. Martínez, C. J. Bardeen, *J. Am. Chem. Soc.* **2003**, *125*, 9288; c) J. S. Moore, *Acc. Chem. Res.* **1997**, *30*, 402.
- [30] J. M. Kehoe, J. H. Kiley, J. J. English, C. A. Johnson, R. C. Petersen, M. M. Haley, *Org. Lett.* **2000**, *2*, 969.
- [31] M. M. Haley, *Pure Appl. Chem.* **2008**, *80*, 117.
- [32] a) B. Wu, M. Li, S. Xiao, Y. Qu, X. Qiu, T. Liu, F. Tian, H. Li, S. Xiao, *Nanoscale* **2017**, *9*, 11939; b) Z. Li, M. Smeu, A. Rives, V. Maraval, R. Chauvin, M. A. Ratner, E. Borguet, *Nat. Commun.* **2015**, *6*, 6321.
- [33] D. Malko, C. Neiss, F. Viñes, A. Görling, *Phys. Rev. Lett.* **2012**, *108*, 86804.
- [34] a) X. Xiao, L. A. Nagahara, A. M. Rawlett, N. Tao, *J. Am. Chem. Soc.* **2005**, *127*, 9235; b) S. A. Getty, C. Engtrakul, L. Wang, R. Liu, S.-H. Ke, H. U. Baranger, W. Yang, M. S. Fuhrer, L. R. Sita, *Phys. Rev. B* **2005**, *71*, 2677; c) J. M. Tour, *Acc. Chem. Res.* **2000**, *33*, 791; d) D. K. James, J. M. Tour, *Chem. Mater.* **2004**, *16*, 4423; e) A. Ambroise, C. Kirmaier, R. W. Wagner, R. S. Loewe, D. F. Bocian, D. Holten, J. S. Lindsey, *J. Org. Chem.* **2002**, *67*, 3811; f) D. Holten, D. F. Bocian, J. S. Lindsey, *Acc. Chem. Res.* **2002**, *35*, 57; g) Y. Selzer, L. Cai, M. A. Cabassi, Y. Yao, J. M. Tour, T. S. Mayer, D. L. Allara, *Nano Lett.* **2005**, *5*, 61; h) W. Hong, D. Z. Manrique, P. Moreno-García, M. Gulcur, A. Mishchenko, C. J. Lambert, M. R. Bryce, T. Wandlowski, *J. Am. Chem. Soc.* **2012**, *134*, 2292; i) P. J. Low, *Coord. Chem. Rev.* **2013**, *257*, 1507.
- [35] a) W. Hu, H. Nakashima, K. Furukawa, Y. Kashimura, K. Ajito, Y. Liu, D. Zhu, K. Torimitsu, *J. Am. Chem. Soc.* **2005**, *127*, 2804; b) M. Kumar, *Superlattices Microstruct.* **2017**, *101*, 101.
- [36] a) Y. Matsuura, Y. Tanaka, M. Akita, *J. Organomet. Chem.* **2009**, *694*, 1840; b) H. Dong, W. Hu, *Acc. Chem. Res.* **2016**, *49*, 2435; c) N. Bouguerra, A. Růžička, C. Ulbricht, C. Enengl, S. Enengl, V. Pokorná, D. Výprachtický, E. Tordin, R. Aitout, V. Cimrová et al., *Macromolecules* **2016**, *49*, 455.
- [37] a) P. Banerjee, D. Conklin, S. Nanayakkara, T.-H. Park, M. J. Therien, D. A. Bonnell, *ACS nano* **2010**, *4*, 1019; b) A. S. Blum, J. C. Yang, R. Shashidhar, B. Ratna, *Appl. Phys. Lett.* **2003**, *82*, 3322; c) J. M. Tour, M. Kozaki, J. M. Seminario, *J. Am. Chem. Soc.* **1998**, *120*, 8486.
- [38] J.-F. Morin, T. Sasaki, Y. Shirai, J. M. Guerrero, J. M. Tour, *J. Org. Chem.* **2007**, *72*, 9481.
- [39] M. Moroni, J. Le Moigne, S. Luzzati, *Macromolecules* **1994**, *27*, 562.
- [40] a) A. D. Slepko, F. A. Hegmann, R. R. Tykwinski, K. Kamada, K. Ohta, J. A. Marsden, E. L. Spitler, J. J. Miller, M. M. Haley, *Opt. Lett.* **2006**, *31*, 3315; b) J. F. Kauffman, J. M. Turner, I. V. Alabugin, B. Breiner, S. V. Kovalenko, E. A. Badaeva, A. Masunov, S. Tretiak, *J. Phys.*

- Chem. A* **2006**, *110*, 241; c) L. Persano, A. Camposeo, D. Pisignano, *Prog. Polym. Sci.* **2015**, *43*, 48; d) F. Silvestri, A. Marrocchi, *Int. J. Mol. Sci.* **2010**, *11*, 1471; e) H. Dong, H. Li, E. Wang, H. Nakashima, K. Torimitsu, W. Hu, *J. Phys. Chem. C* **2008**, *112*, 19690.
- [41] a) W.-Y. Yang, S. Roy, B. Phrathep, Z. Rengert, R. Kenworthy, D. A. R. Zorio, I. V. Alabugin, *J. Med. Chem.* **2011**, *54*, 8501; b) W.-Y. Yang, S. A. Marrone, N. Minors, D. A. R. Zorio, I. V. Alabugin, *Beilstein J. Org. Chem.* **2011**, *7*, 813; c) W.-Y. Yang, B. Breiner, S. V. Kovalenko, C. Ben, M. Singh, S. N. LeGrand, Q.-X. A. Sang, G. F. Strouse, J. A. Copland, I. V. Alabugin, *J. Am. Chem. Soc.* **2009**, *131*, 11458; d) I.-B. Kim, H. Shin, A. J. Garcia, U. H. F. Bunz, *Bioconjugate Chem.* **2007**, *18*, 815; e) B. Breiner, J. C. Schlatterer, I. V. Alabugin, S. V. Kovalenko, N. L. Greenbaum, *Proc. Natl. Acad. Sci. U. S. A.* **2007**, *104*, 13016.
- [42] a) S. Li, T. Chen, Y. Wang, L. Liu, F. Lv, Z. Li, Y. Huang, K. S. Schanze, S. Wang, *Angew. Chem. Int. Ed.* **2017**, *56*, 13455; b) L. D'Olieslaeger, Y. Braeken, S. Cheruku, J. Smits, M. Ameloot, D. Vanderzande, W. Maes, A. Ethirajan, *J. Colloid Interface Sci.* **2017**, *504*, 527; c) L. Zhang, Q. Yin, H. Huang, B. Wang, *J. Mater. Chem. B* **2013**, *1*, 756.
- [43] P. Wu, N. Xu, C. Tan, L. Liu, Y. Tan, Z. Chen, Y. Jiang, *ACS Appl. Mater. Interfaces* **2017**, *9*, 10512.
- [44] a) S. Tsuzuki, K. Tanabe, *J. Phys. Chem.* **1991**, *95*, 139; b) M. P. Johansson, J. Olsen, *J. Chem. Theory Comput.* **2008**, *4*, 1460.
- [45] a) J. M. Seminario, A. G. Zacarias, J. M. Tour, *J. Am. Chem. Soc.* **1998**, *120*, 3970; b) K. Inoue, H. Takeuchi, S. Konaka, *J. Phys. Chem. A* **2001**, *105*, 6711.
- [46] J. K. D. Surette, M.-A. MacDonald, M. J. Zaworotko, R. D. Singer, *J Chem Crystallogr* **1994**, *24*, 715.
- [47] A. K. Pati, S. J. Gharpure, A. K. Mishra, *Phys. Chem. Chem. Phys.* **2014**, *16*, 14015.
- [48] R. Stølevik, P. Bakken, *J. Mol. Struct.* **1990**, *239*, 205.
- [49] N. Goodhand, T. A. Hamor, *Acta Crystallogr., Sect. B: Struct. Crystallogr. Cryst. Chem.* **1979**, *35*, 704.
- [50] S. Toyota, T. Iida, C. Kunizane, N. Tanifuji, Y. Yoshida, *Org. Biomol. Chem.* **2003**, *1*, 2298.
- [51] S. Toyota, T. Yanagihara, Y. Yoshida, M. Goichi, *Bull. Chem. Soc. Jpn.* **2005**, *78*, 1351.
- [52] O. S. Miljanić, S. Han, D. Holmes, G. R. Schaller, K. P. C. Vollhardt, *Chem. Commun.* **2005**, 2606.
- [53] J.-S. Yang, J.-L. Yan, C.-Y. Hwang, S.-Y. Chiou, K.-L. Liao, H.-H. Gavin Tsai, G.-H. Lee, S.-M. Peng, *J. Am. Chem. Soc.* **2006**, *128*, 14109.
- [54] J.-S. Yang, J.-L. Yan, C.-K. Lin, C.-Y. Chen, Z.-Y. Xie, C.-H. Chen, *Angew. Chem. Int. Ed.* **2009**, *48*, 9936.

- [55] a) D. S. Kemp, Z. Q. Li, *Tetrahedron Lett.* **1995**, *36*, 4175; b) X. Yang, A. L. Brown, M. Furukawa, S. Li, W. E. Gardinier, E. J. Bukowski, F. V. Bright, C. Zheng, X. C. Zeng, B. Gong, *Chem. Commun.* **2003**, 56; c) X. Yang, L. Yuan, K. Yamato, A. L. Brown, W. Feng, M. Furukawa, X. C. Zeng, B. Gong, *J. Am. Chem. Soc.* **2004**, *126*, 3148.
- [56] M. Szyszkowska, C. Czaplewski, W. Wiczak, *J. Mol. Struct.* **2017**, *1138*, 81.
- [57] J.-H. Hong, A. K. Atta, K.-B. Jung, S.-B. Kim, J. Heo, D.-G. Cho, *Org. Lett.* **2015**, *17*, 6222.
- [58] R. Breslow, *Acc. Chem. Res.* **1980**, *13*, 170.
- [59] T. P. Bubner, G. T. Crisp, E. R. T. Tiekink, *Z. Kristallogr. - Cryst. Mater.* **1994**, *209*.
- [60] G. T. Crisp, T. P. Bubner, *Tetrahedron* **1997**, *53*, 11881.
- [61] R. Shukla, D. M. Brody, S. V. Lindeman, R. Rathore, *J. Org. Chem.* **2006**, *71*, 6124.
- [62] R. Shukla, S. V. Lindeman, R. Rathore, *Org. Lett.* **2007**, *9*, 1291.
- [63] H. R. Darabi, M. A. Arani, M. Tafazzoli, M. Ghiasi, *Monatsh. Chem.* **2008**, *139*, 1185.
- [64] G. Brizius, K. Billingsley, M. D. Smith, U. H. F. Bunz, *Org. Lett.* **2003**, *5*, 3951.
- [65] S. A. McFarland, N. S. Finney, *J. Am. Chem. Soc.* **2002**, *124*, 1178.
- [66] S. Menning, M. Krämer, B. A. Coombs, F. Rominger, A. Beeby, A. Dreuw, U. H. F. Bunz, *J. Am. Chem. Soc.* **2013**, *135*, 2160.
- [67] S. Menning, M. Krämer, A. Duckworth, F. Rominger, A. Beeby, A. Dreuw, U. H. F. Bunz, *J. Org. Chem.* **2014**, *79*, 6571.
- [68] A. C. Cope, D. S. Smith, R. J. Cotter, *Org. Synth.* **1954**, *34*, 42.
- [69] G. Kuzmanich, M. N. Gard, M. A. Garcia-Garibay, *J. Am. Chem. Soc.* **2009**, *131*, 11606.
- [70] H. Kuramochi, S. Takeuchi, T. Tahara, *Chem. Phys.* **2018**.
- [71] a) D. Seyferth, R. S. Marmor, *Tetrahedron Lett.* **1970**, *11*, 2493; b) D. Seyferth, R. S. Marmor, P. Hilbert, *J. Org. Chem.* **1971**, *36*, 1379; c) J. C. Gilbert, U. Weerasooriya, *J. Org. Chem.* **1979**, *44*, 4997; d) J. C. Gilbert, U. Weerasooriya, *J. Org. Chem.* **1982**, *47*, 1837; e) G. Roth, B. Liepold, S. Müller, H. Bestmann, *Synthesis* **2003**, *2004*, 59.
- [72] a) S. Ohira, *Synth. Commun.* **1989**, *19*, 561; b) T. H. Jepsen, J. L. Kristensen, *J. Org. Chem.* **2014**, *79*, 9423.
- [73] L. N. R. Maddali, S. Meka, *New J. Chem.* **2018**, *42*, 4412.
- [74] C. Singh, A. P. Prakasham, M. K. Gangwar, R. J. Butcher, P. Ghosh, *ACS Omega* **2018**, *3*, 1740.
- [75] R. Chinchilla, C. Najera, *Chem. Rev.* **2007**, *107*, 874.
- [76] a) A. Suzuki, *J. Organomet. Chem.* **1999**, *576*, 147; b) R. Chinchilla, C. Najera, *Chem. Soc. Rev.* **2011**, *40*, 5084; c) C. E. I. Knappke, A. J. von Wangelin, *Chem. Soc. Rev.* **2011**, *40*, 4948;

- d) E.-i. Negishi, Z. Huang, G. Wang, S. Mohan, C. Wang, H. Hattori, *Acc. Chem. Res.* **2008**, *41*, 1474.
- [77] a) A. Fürstner, *Angew. Chem. Int. Ed.* **2013**, *52*, 2794; b) C. Deraedt, M. d'Halluin, D. Astruc, *Eur. J. Inorg. Chem.* **2013**, *112*, 4881-4908.
- [78] a) K. Park, G. Bae, J. Moon, J. Choe, K. H. Song, S. Lee, *J. Org. Chem.* **2010**, *75*, 6244; b) D. Pan, C. Zhang, S. Ding, N. Jiao, *Eur. J. Org. Chem.* **2011**, 4751-4755; c) A. Pyo, J. D. Kim, H. C. Choi, S. Lee, *J. Organomet. Chem.* **2013**, *724*, 271; d) X. Li, F. Yang, Y. Wu, *RSC Adv* **2014**, *4*, 13738; e) Y. Son, H.-S. Kim, J.-H. Lee, J. Jang, C.-F. Lee, S. Lee, *Tetrahedron Lett.* **2017**, *58*, 1413.
- [79] A. L. Stein, F. N. Bilheri, G. Zeni, *Chem. Commun.* **2015**, *51*, 15522.
- [80] J. K. Stille, *Angew. Chem.* **1986**, *98*, 504.
- [81] C. Cordovilla, C. Bartolomé, J. M. Martínez-Ilarduya, P. Espinet, *ACS Catal.* **2015**, *5*, 3040.
- [82] a) U. H. F. Bunz, L. Kloppenburg, *Angew. Chem. Int. Ed.* **1999**, *38*, 478; b) A. Fürstner, P. W. Davies, *Chem. Commun.* **2005**, 2307; c) R. R. Schrock, C. Czekelius, *Adv. Synth. Catal.* **2007**, *349*, 55; d) H. M. Cho, H. Weissman, J. S. Moore, *J. Org. Chem.* **2008**, *73*, 4256; e) R. R. Schrock, *Chem. Commun.* **2013**, *49*, 5529.
- [83] K. Jyothish, W. Zhang, *Angew. Chem. Int. Ed.* **2011**, *50*, 3435.
- [84] a) R. D. Stephens, C. E. Castro, *J. Org. Chem.* **1963**, *28*, 3313; b) Z. Wang, *Comprehensive Organic Name Reactions and Reagents*, John Wiley & Sons, Inc, Hoboken, NJ, USA, **2010**.
- [85] K. Sonogashira, Y. Tohda, N. Hagihara, *Tetrahedron Lett.* **1975**, *16*, 4467.
- [86] a) M. D'Auria, *Synth. Commun.* **1992**, *22*, 2393; b) M.-J. Wu, L.-M. Wei, C.-F. Lin, S.-P. Leou, L.-L. Wei, *Tetrahedron* **2001**, *57*, 7839; c) M. J. Mio, L. C. Kopel, J. B. Braun, T. L. Gadzikwa, K. L. Hull, R. G. Brisbois, C. J. Markworth, P. A. Grieco, *Org. Lett.* **2002**, *4*, 3199; d) A. Köllhofer, H. Plenio, *Chem. Eur. J.* **2003**, *9*, 1416; e) R. S. Barbiéri, C. R. Bellato, A. K. C. Dias, A. C. Massabni, *Catal. Lett.* **2006**, *109*, 171; f) M. Schilz, H. Plenio, *J. Org. Chem.* **2012**, *77*, 2798.
- [87] S. Qiu, C. Zhang, R. Qiu, G. Yin, J. Huang, *Adv. Synth. Catal.* **2018**, *360*, 313.
- [88] A. Khan, S. Hecht, *Chem. Commun.* **2004**, 300.
- [89] S. Sadjadi, *Appl Organometal Chem* **2018**, *32*, e4211.
- [90] A. Elhage, A. E. Lanterna, J. C. Scaiano, *ACS Sustainable Chem. Eng.* **2017**, *6*, 1717.
- [91] V. Martí-Centelles, M. D. Pandey, M. I. Burguete, S. V. Luis, *Chem. Rev.* **2015**, *115*, 8736.
- [92] a) O. Mitsunobu, M. Yamada, *Bull. Chem. Soc. Jpn.* **1967**, *40*, 2380; b) O. Mitsunobu, *Synthesis* **1981**, *1981*, 1.
- [93] R. Fittig, *Justus Liebigs Ann. Chem.* **1859**, *110*, 23.

- [94] a) J. E. McMurry, M. P. Fleming, *J. Am. Chem. Soc.* **1974**, *96*, 4708; b) M. Ephritikhine, C. Villiers in *Modern carbonyl olefination. [methods and applications]* (Hrsg.: T. Takeda), Wiley-VCH, Weinheim, **2004**, S. 223–285.
- [95] M. Tashiro, C. Simion, A. Simion, Y. Mitoma, S. Nagashima, T. Kawaji, I. Hashimoto, *Heterocycles* **2000**, *53*, 2459.
- [96] H. R. Darabi, S. Rastgar, K. Aghapoor, F. Mohsenzadeh, *Monatsh. Chem.* **2017**, *100*, 2537.
- [97] H. R. Darabi, K. Jadidi, A. R. Mohebbi, L. Faraji, K. Aghapoor, S. Shahbazian, M. Azimzadeh, S. M. Nasser, *Supramol. Chem.* **2008**, *20*, 327.
- [98] H. R. Darabi, M. H. Karouei, M. J. Tehrani, K. Aghapoor, M. Ghasemzadeh, B. Neumüller, *Supramol. Chem.* **2011**, *23*, 462.
- [99] G. Brizius, U. H. F. Bunz, *Org. Lett.* **2002**, *4*, 2829.
- [100] a) M. Pal, N. G. Kundu, *J. Chem. Soc., Perkin Trans. 1* **1996**, *105*, 449; b) C.-J. Li, D.-L. Chen, C. W. Costello, *Org. Process Res. Dev.* **1997**, *1*, 325; c) I. G. Stará, I. Starý, A. Kollárovič, F. Teplý, D. Šaman, P. Fiedler, *Tetrahedron* **1998**, *54*, 11209; d) M. Iyoda, A. Vorasingha, Y. Kuwatani, M. Yoshida, *Tetrahedron Lett.* **1998**, *39*, 4701; e) S. Shotwell, P. M. Windscheif, M. D. Smith, U. H. F. Bunz, *Org. Lett.* **2004**, *6*, 4151; f) C.-J. Li, W. T. Slaven IV, Y.-P. Chen, V. T. John, S. H. Rachakonda, *Chem. Commun.* **1998**, 1351; g) W. Zhang, H. Wu, Z. Liu, P. Zhong, L. Zhang, X. Huang, J. Cheng, *Chem. Commun.* **2006**, *16*, 4826; h) M. Bakherad, *Appl Organometal Chem* **2013**, *27*, 125.
- [101] S. Menning, *Dissertation*, Ruprecht-Karls-Universität, Heidelberg, **2014**.
- [102] A. Jablonski, *Nature* **1933**, *131*, 839.
- [103] a) J. Franck, E. G. Dymond, *Trans. Faraday Soc.* **1926**, *21*, 536; b) E. Condon, *Phys. Rev.* **1926**, *28*, 1182; c) E. U. Condon, *Phys. Rev.* **1928**, *32*, 858; d) E. Condon, *Phys. Rev.* **1926**, *27*, 637.
- [104] M. Born, R. Oppenheimer, *Ann. Phys.* **1927**, *389*, 457.
- [105] M. Kasha, *Discuss. Faraday Soc.* **1950**, *9*, 14.
- [106] G. G. Stokes, *Philos. Trans. R. Soc. London* **1852**, *142*, 463.
- [107] J. R. Lakowicz, *Principles of fluorescence spectroscopy*, 3. Aufl., Springer, New York, **2006**.
- [108] R. Thomas, S. Lakshmi, S. K. Pati, G. U. Kulkarni, *J. Phys. Chem. B* **2006**, *110*, 24674.
- [109] J. Overend, *Trans. Faraday Soc.* **1960**, *56*, 310.
- [110] a) C. Ferrante, U. Kensy, B. Dick, *J. Phys. Chem.* **1993**, *97*, 13457; b) T.-a. Ishibashi, H.-o. Hamaguchi, *Chem. Phys. Lett.* **1997**, *264*, 551.
- [111] L. T. Liu, D. Yaron, M. A. Berg, *J. Phys. Chem. C* **2007**, *111*, 5770.
- [112] T. Suzuki, M. Nakamura, T. Isozaki, T. Ikoma, *Int J Thermophys* **2012**, *33*, 2046.

- [113] a) R. H. Baughman, H. Eckhardt, M. Kertesz, *The Journal of Chemical Physics* **1987**, *87*, 6687; b) N. Narita, S. Nagai, S. Suzuki, K. Nakao, *Phys. Rev. B* **1998**, *58*, 11009.
- [114] a) Y. Nagano, T. Ikoma, K. Akiyama, S. Tero-Kubota, *Chem. Phys. Lett.* **1999**, *303*, 201; b) Y. Nagano, T. Ikoma, K. Akiyama, S. Tero-Kubota, *J. Chem. Phys.* **2001**, *114*, 1775; c) H. Hiura, H. Takahashi, *J. Phys. Chem.* **1992**, *96*, 8909.
- [115] a) S. Friedrich, R. Griebel, G. Hohlneicher, F. Metz, S. Schneider, *Chem. Phys.* **1973**, *1*, 319; b) M. Gutmann, M. Gudipati, P. F. Schoenartz, G. Hohlneicher, *J. Phys. Chem.* **1992**, *96*, 2433; c) L. Salem, C. Rowland, *Angew. Chem. Int. Ed. Engl.* **1972**, *11*, 92; d) Y. Hirata, *Bull. Chem. Soc. Jpn.* **1999**, *72*, 1647.
- [116] S. d'Agostino, F. Grepioni, D. Braga, B. Ventura, *Cryst. Growth Des.* **2015**, *15*, 2039.
- [117] S. Toyota, *Chem. Rev.* **2010**, *110*, 5398.
- [118] L. T. Liu, D. Yaron, M. I. Sluch, M. A. Berg, *J. Phys. Chem. B* **2006**, *110*, 18844.
- [119] a) S. Nakatsuji, K. Matsuda, Y. Uesugi, K. Nakashima, S. Akiyama, W. Fabian, *J. Chem. Soc., Perkin Trans. 1* **1992**, 755; b) G. Duvanel, J. Grilj, A. Schuwey, A. Gossauer, E. Vauthey, *Photochem. Photobiol. Sci.* **2007**, *6*, 956; c) Y. Yamaguchi, Y. Shimoji, T. Ochi, T. Wakamiya, Y. Matsubara, Z.-i. Yoshida, *J. Phys. Chem. A* **2008**, *112*, 5074; d) S. Roy, D. Samanta, P. Kumar, T. K. Maji, *Chem. Commun.* **2018**, *54*, 275; e) P. V. James, P. K. Sudeep, C. H. Suresh, K. G. Thomas, *J. Phys. Chem. A* **2006**, *110*, 4329.
- [120] H. Li, D. R. Powell, R. K. Hayashi, R. West, *Macromolecules* **1998**, *31*, 52.
- [121] a) N. González-Rojano, E. Arias-Marín, D. Navarro-Rodríguez, S. Weidner, *Synlett* **2005**, 2005, 1259; b) G. Castruita, E. Arias, I. Moggio, F. Pérez, D. Medellín, R. Torres, R. Ziolo, A. Olivas, E. Giorgetti, M. Muniz-Miranda, *J. Mol. Struct.* **2009**, *936*, 177.
- [122] S. J. Greaves, E. L. Flynn, E. L. Fitcher, E. Wrede, D. P. Lydon, P. J. Low, S. R. Rutter, A. Beeby, *J. Phys. Chem. A* **2006**, *110*, 2114.
- [123] T. Fujiwara, M. Z. Zgierski, E. C. Lim, *J. Phys. Chem. A* **2008**, *112*, 4736.
- [124] W. Hu, N. Zhu, W. Tang, D. Zhao, *Org. Lett.* **2008**, *10*, 2669.
- [125] J. Tomfohr, O. F. Sankey, *J. Chem. Phys.* **2004**, *120*, 1542.
- [126] W. Barford, *Electronic and Optical Properties of Conjugated Polymers*, 2. Aufl., OUP Oxford, Oxford, **2013**.
- [127] J. Terao, A. Wadahama, A. Matono, T. Tada, S. Watanabe, S. Seki, T. Fujihara, Y. Tsuji, *Nat. Commun.* **2013**, *4*, 1691.
- [128] R. H. Pawle, T. E. Haas, P. Müller, S. W. Thomas III, *Chem. Sci.* **2014**, *5*, 4184.
- [129] K. Kuroda, T. M. Swager, *Chem. Commun.* **2003**, 26.

- [130] U. H. F. Bunz, V. Enkelmann, L. Kloppenburg, D. Jones, K. D. Shimizu, J. B. Claridge, H.-C. Zur Loye, G. Lieser, *Chem. Mater.* **1999**, *11*, 1416.
- [131] a) U. H. F. Bunz, J. M. Imhof, R. K. Bly, C. G. Bangcuyo, L. Rozanski, D. A. Vanden Bout, *Macromolecules* **2005**, *38*, 5892; b) K. B. Woody, R. Nambiar, G. L. Brizius, D. M. Collard, *Macromolecules* **2009**, *42*, 8102.
- [132] T. Terashima, T. Nakashima, T. Kawai, *Org. Lett.* **2007**, *9*, 4195.
- [133] S. A. Sharber, R. N. Baral, F. Frausto, T. E. Haas, P. Müller, S. W. Thomas III, *J. Am. Chem. Soc.* **2017**, *139*, 5164.
- [134] A. Beeby, K. S. Findlay, A. E. Goeta, L. Porrès, S. R. Rutter, A. L. Thompson, *Photochem. Photobiol. Sci.* **2007**, *6*, 982.
- [135] B. C. Englert, M. D. Smith, K. I. Hardcastle, U. H. F. Bunz, *Macromolecules* **2004**, *37*, 8212.
- [136] G. T. Crisp, T. P. Bubner, *Tetrahedron* **1997**, *53*, 11899.
- [137] a) H. Nakayama, S. Kimura, *J. Phys. Chem. A* **2011**, *115*, 8960; b) H. Nakayama, S. Kimura, *Chem. Phys. Lett.* **2011**, *508*, 281; c) H. Nakayama, S. Kimura, *J. Org. Chem.* **2009**, *74*, 3462; d) H. Nakayama, T. Morita, S. Kimura, *J. Phys. Chem. C* **2010**, *114*, 4669.
- [138] U. H. F. Bunz, K. Seehafer, M. Bender, M. Porz, *Chem. Soc. Rev.* **2015**, *44*, 4322.
- [139] M. Levitus, K. Schmieder, H. Ricks, K. D. Shimizu, U. H. F. Bunz, M. A. Garcia-Garibay, *J. Am. Chem. Soc.* **2001**, *123*, 4259.
- [140] K. Schmieder, M. Levitus, H. Dang, M. A. Garcia-Garibay, *J. Phys. Chem. A* **2002**, *106*, 1551.
- [141] J. Kim, T. M. Swager, *Nature* **2001**, *411*, 1030.
- [142] R. Gleiter, D. B. Werz, *Chem. Rev.* **2010**, *110*, 4447.
- [143] M. Beer, *J. Chem. Phys.* **1956**, *25*, 745.
- [144] Y. Hirata, T. Okada, T. Nomoto, *Chem. Phys. Lett.* **1998**, *293*, 371.
- [145] Y. Nagano, T. Ikoma, K. Akiyama, S. Tero-Kubota, *J. Am. Chem. Soc.* **2003**, *125*, 14103.
- [146] a) G. Baranović, L. Colombo, K. Furić, J. R. Durig, J. F. Sullivan, J. Mink, *J. Mol. Struct.* **1986**, *144*, 53; b) T. Takabe, M. Tanaka, J. Tanaka, *Bull. Chem. Soc. Jpn.* **1974**, *47*, 1912; c) T. Hoshi, J. Okubo, M. Kobayashi, Y. Tanizaki, *J. Am. Chem. Soc.* **1986**, *108*, 3867; d) M. Kijima, I. Kinoshita, H. Shirakawa, *J. Mol. Struct.* **2000**, *521*, 279; e) B. Zimmermann, G. Baranović, *Vib. Spectrosc.* **2006**, *41*, 126; f) P. Zalake, K. G. Thomas, *Langmuir* **2013**, *29*, 2242; g) M. F. Beristain, T. Ogawa, G. Gomez-Sosa, E. Muñoz, Y. Maekawa, F. Halim, F. Smith, A. Walser, R. Dorsinville, *Mol. Cryst. Liq. Cryst.* **2010**, *521*, 237.
- [147] R. A. Nyquist, C. L. Putzig, *Vib. Spectrosc.* **1992**, *4*, 35.
- [148] P. W. Thulstrup, S. V. Hoffmann, B. K. V. Hansen, J. Spanget-Larsen, *Phys. Chem. Chem. Phys.* **2011**, *13*, 16168.

- [149] G. S. Kottas, L. I. Clarke, D. Horinek, J. Michl, *Chem. Rev.* **2005**, *105*, 1281.
- [150] a) S. - T. Wu, H. - H. B. Meng, L. R. Dalton, *J. Appl. Phys.* **1991**, *70*, 3013; b) S. - T. Wu, J. D. Margerum, H. B. Meng, L. R. Dalton, C. - S. Hsu, S. - H. Lung, *Appl. Phys. Lett.* **1992**, *61*, 630; c) S.-T. Wu, M. E. Neubert, S. S. Keast, D. G. Abdallah, S. N. Lee, M. E. Walsh, T. A. Dorschner, *Appl. Phys. Lett.* **2000**, *77*, 957.
- [151] A. N. Swinburne, M. J. Paterson, A. Beeby, J. W. Steed, *Chem. Eur. J.* **2010**, *16*, 2714.
- [152] W. Liu, K. P. Loh, *Acc. Chem. Res.* **2017**, *50*, 522.
- [153] X. Qian, Z. Ning, Y. Li, H. Liu, C. Ouyang, Q. Chen, Y. Li, *Dalton Trans.* **2012**, *41*, 730.
- [154] G. Li, Y. Li, X. Qian, H. Liu, H. Lin, N. Chen, Y. Li, *J. Phys. Chem. C* **2011**, *115*, 2611.
- [155] J. Zhou, X. Gao, R. Liu, Z. Xie, J. Yang, S. Zhang, G. Zhang, H. Liu, Y. Li, J. Zhang et al., *J. Am. Chem. Soc.* **2015**, *137*, 7596.
- [156] B. Esser, T. M. Swager, *Angew. Chem. Int. Ed.* **2010**, *49*, 8872.
- [157] G. Burillo, M. F. Beristain, E. Sanchez, T. Ogawa, *Polym. Degrad. Stab.* **2013**, *98*, 1988.
- [158] R. Thomas, S. S. Mallajyosula, S. Lakshmi, S. K. Pati, G. U. Kulkarni, *J. Mol. Struct.* **2009**, *922*, 46.
- [159] C. Glaser, *Ber. Dtsch. Chem. Ges.* **1869**, *2*, 422.
- [160] a) P. Siemsen, R. C. Livingston, F. Diederich, *Angew. Chem. Int. Ed.* **2000**, *39*, 2632; b) L. Fomina, B. Vazquez, E. Tkatchouk, S. Fomine, *Tetrahedron* **2002**, *58*, 6741; c) J. J. Li in *Name reactions* (Hrsg.: J. J. Li), Springer, Berlin, **2009**, S. 257–261; d) K. S. Sindhu, G. Anilkumar, *RSC Adv* **2014**, *4*, 27867.
- [161] a) A. Hay, *J. Org. Chem.* **1960**, *25*, 1275; b) A. S. Hay, *J. Org. Chem.* **1962**, *27*, 3320; c) M. H. Vilhelmsen, J. Jensen, C. G. Tortzen, M. B. Nielsen, *Eur. J. Org. Chem.* **2013**, *2013*, 701.
- [162] G. Eglinton, A. R. Galbraith, *J. Chem. Soc.* **1959**, 889.
- [163] A. K. Pati, M. Mohapatra, P. Ghosh, S. J. Gharpure, A. K. Mishra, *J. Phys. Chem. A* **2013**, *117*, 6548.
- [164] S. Takahashi, Y. Kuroyama, K. Sonogashira, N. Hagihara, *Synthesis* **1980**, *1980*, 627.
- [165] L. Wang, J. Yan, P. Li, M. Wang, C. Su, *J. Chem. Res.* **2005**, 112.
- [166] M. Wierzbicka, I. Bylińska, A. Sikorski, C. Czaplewski, W. Wiczak, *Photochem. Photobiol. Sci.* **2015**, *14*, 2251.
- [167] A. K. Pati, S. J. Gharpure, A. K. Mishra, *Faraday Discuss.* **2015**, *177*, 213.
- [168] A. K. Pati, S. J. Gharpure, A. K. Mishra, *J. Phys. Chem. A* **2015**, *119*, 10481.
- [169] a) A. K. Pati, S. J. Gharpure, A. K. Mishra, *J. Phys. Chem. A* **2016**, *120*, 5838; b) A. K. Pati, R. Jana, S. J. Gharpure, A. K. Mishra, *J. Phys. Chem. A* **2016**, *120*, 5826.
- [170] J. A. Sebree, T. S. Zwier, *Phys. Chem. Chem. Phys.* **2012**, *14*, 173.

- [171] a) S. Zaretsky, A. K. Yudin in *Practical medicinal chemistry with macrocycles. Design, synthesis, and case studies* (Hrsg.: E. Marsault, M. L. Peterson), Wiley, Hoboken, NJ, **2017**, S. 1–24; b) J. Fastrez, *Tetrahedron Lett.* **1987**, *28*, 419; c) J. Fastrez, *J. Phys. Chem.* **1989**, *93*, 2635.
- [172] W. Zhang, J. S. Moore, *Angew. Chem. Int. Ed.* **2006**, *45*, 4416.
- [173] P. W. Davies in *Handbook of Cyclization Reactions* (Hrsg.: S. Ma), Wiley-VCH, Weinheim, **2010**, S. 599–623.
- [174] T. Dutta, K. B. Woody, S. R. Parkin, M. D. Watson, J. Gierschner, *J. Am. Chem. Soc.* **2009**, *131*, 17321.
- [175] P. Nolis, A. Virgili, *J. Org. Chem.* **2006**, *71*, 3267.
- [176] Y. Karibe, H. Kusama, N. Iwasawa, *Angew. Chem. Int. Ed.* **2012**, *51*, 6214.
- [177] M. Barbasiewicz, K. Błocki, M. Malińska, R. Pawłowski, *Dalton Trans.* **2013**, *42*, 355.
- [178] a) H. K. Henisch, *Crystal growth in gels*, Birkhäuser, **1968**; b) D. Choquesillo-Lazarte, J. M. García-Ruiz, *J. Appl. Crystallogr.* **2011**, *44*, 172.
- [179] J. C. Koziar, D. O. Cowan, *Acc. Chem. Res.* **2002**, *11*, 334.
- [180] M. I. Sluch, A. Godt, U. H. F. Bunz, M. A. Berg, *J. Am. Chem. Soc.* **2001**, *123*, 6447.
- [181] Y. Shimizu, T. Azumi, *J. Phys. Chem.* **1982**, *86*, 22.
- [182] a) S. Irie, M. Yamamoto, I. Iida, T. Nishio, K. Kishikawa, S. Kohmoto, K. Yamada, *J. Org. Chem.* **1994**, *59*, 935; b) S. Coseri, *Rev. Roum. Chim.* **2009**, *54*, 1051; c) V. W. Kern, K. J. Rauterkus, W. Weber, *Makromol. Chem.* **1961**, *43*, 98.
- [183] a) D. Liu, Z. Tian, Z. Yan, L. Wu, Y. Ma, Q. Wang, W. Liu, H. Zhou, C. Yang, *Bioorg. Med. Chem.* **2013**, *21*, 2960; b) A. Benalil, P. Roby, B. Carboni, M. Vaultier, *Synthesis* **1991**, *1991*, 787.
- [184] a) T. Kawase, Y. Nishioka, T. Oida, *J. Oleo Sci.* **2010**, *59*, 191; b) I. Skiera, Z. Paryzek, *J. Chem. Res.* **2014**, *38*, 597.
- [185] a) C. Sergheraert, P. Mäes, A. Tartar, *J. Chem. Soc., Perkin Trans. 1* **1986**, 1061; b) S. Majumdar, K. B. Sloan, *Synth. Commun.* **2006**, *36*, 3537; c) E. Buhleier, K. Frensch, F. Luppertz, F. Vögtle, *Justus Liebigs Ann. Chem.* **1978**, *1978*, 1586.
- [186] T. Sakai, T. Satou, T. Kaikawa, K. Takimiya, T. Otsubo, Y. Aso, *J. Am. Chem. Soc.* **2005**, *127*, 8082.
- [187] H. Osaki, C.-M. Chou, M. Taki, K. Welke, D. Yokogawa, S. Irle, Y. Sato, T. Higashiyama, S. Saito, A. Fukazawa et al., *Angew. Chem.* **2016**, *128*, 7247.
- [188] S. Toyota, K. Kawai, T. Iwanaga, K. Wakamatsu, *Eur. J. Org. Chem.* **2012**, *2012*, 5679.

- [189] N. Chronakis, T. Brandmüller, C. Kovacs, U. Reuther, W. Donaubaueer, F. Hampel, F. Fischer, F. Diederich, A. Hirsch, *Eur. J. Org. Chem.* **2006**, 2006, 2296.
- [190] D. Sigwalt, M. Holler, J.-F. Nierengarten, *Tetrahedron Lett.* **2013**, 54, 3160.
- [191] Z. Zhou, D. I. Schuster, S. R. Wilson, *J. Org. Chem.* **2003**, 68, 7612.
- [192] P. Margaretha, F. P. Schmook, H. Budzikiewicz, O. E. Polansky, *Monatsh. Chem.* **1968**, 99, 2539.
- [193] a) M. W. Bredenkamp, H. M. Flowers, C. W. Holzapfel, *Chem. Ber.* **1992**, 125, 1159; b) A. Ninagawa, T. Maeda, H. Matsuda, *Chem. Lett.* **1984**, 13, 1985.
- [194] a) Naveen, S. A. Babu, *Tetrahedron Lett.* **2016**, 57, 5801; b) A. M. Shelke, V. Rawat, G. Suryavanshi, A. Sudalai, *Tetrahedron: Asymmetry* **2012**, 23, 1534.
- [195] a) T. Mukaiyama, *Angew. Chem. Int. Ed.* **1979**, 18, 707; b) D. Yuyama, N. Sugiyama, T. Maeda, Y. Dobashi, S. Yokojima, Y. Fujimoto, H. Yanai, T. Matsumoto, *Synlett* **2016**, 27, 1949; c) T. Motozaki, K. Sawamura, A. Suzuki, K. Yoshida, T. Ueki, A. Ohara, R. Munakata, K.-I. Takao, K.-I. Tadano, *Org. Lett.* **2005**, 7, 2265.
- [196] a) R. Nakayama, E.-M. Tanzer, T. Kusumi, K. Ohmori, K. Suzuki, *Helv. Chim. Acta* **2016**, 99, 944; b) J. Inanaga, K. Hirata, H. Saeki, T. Katsuki, M. Yamaguchi, *Bull. Chem. Soc. Jpn.* **1979**, 52, 1989; c) A. K. Ghosh, L. A. Kassekert, *Org. Lett.* **2016**, 18, 3274; d) M. Barbazanges, C. Meyer, J. Cossy, *Org. Lett.* **2008**, 10, 4489.
- [197] a) S. Seo, T. J. Marks, *Chem. Eur. J.* **2010**, 16, 5148; b) R. Rathore, C. L. Burns, I. A. Guzei, *J. Org. Chem.* **2004**, 69, 1524; c) T. Iwanaga, R. Tanaka, S. Toyota, *Chem. Lett.* **2014**, 43, 105.
- [198] a) I. M. Jones, A. D. Hamilton, *Org. Lett.* **2010**, 12, 3651; b) S. Thorand, N. Krause, *J. Org. Chem.* **1998**, 63, 8551.
- [199] M. Erdélyi, A. Gogoll, *J. Org. Chem.* **2001**, 66, 4165.
- [200] A. Rosspeintner, G. Angulo, C. Onitsch, M. Kivala, F. Diederich, G. Grampp, G. Gescheidt, *ChemPhysChem* **2010**, 11, 1700.
- [201] G. Gaefke, V. Enkelmann, S. Höger, *Synthesis* **2006**, 2006, 2971.
- [202] a) L. Zhao, I. F. Perepichka, F. Türksoy, A. S. Batsanov, A. Beeby, K. S. Findlay, M. R. Bryce, *New J. Chem.* **2004**, 28, 912; b) A. Beeby, K. Findlay, P. J. Low, T. B. Marder, *J. Am. Chem. Soc.* **2002**, 124, 8280.
- [203] Y. Yamaguchi, T. Ochi, T. Wakamiya, Y. Matsubara, Z.-i. Yoshida, *Org. Lett.* **2006**, 8, 717.
- [204] a) S. Schmid, A. K. Kast, R. R. Schröder, U. H. F. Bunz, C. Melzer, *Macromol. Rapid Commun.* **2014**, 35, 1770; b) H. Dong, H. Li, E. Wang, S. Yan, J. Zhang, C. Yang, I. Takahashi, H. Nakashima, K. Torimitsu, W. Hu, *J. Phys. Chem. B* **2009**, 113, 4176; c) B. Wang, J. Han, M. Bender, S. Hahn, K. Seehafer, U. H. F. Bunz, *ACS Sens.* **2018**, 3, 504.

- [205] E. Smarsly, *Running dissertation*, Ruprecht-Karls-Universität, Heidelberg, **2018**.
- [206] a) R. E. Bandy, C. Lakshminarayan, T. S. Zwier, *J. Phys. Chem.* **1992**, *96*, 5337; b) A. G. Robinson, P. R. Winter, T. S. Zwier, *J. Phys. Chem. A* **2002**, *106*, 5789.
- [207] L. P. G. Wakelin, X. Bu, A. Eleftheriou, A. Parmar, C. Hayek, B. W. Stewart, *J. Med. Chem.* **2003**, *46*, 5790.
- [208] P. A. Troshin, E. A. Khakina, A. V. Zhilenkov, A. S. Peregudov, O. A. Troshina, V. I. Kozlovskii, N. V. Polyakova, R. N. Lyubovskaya, *Eur. J. Org. Chem.* **2010**, *2010*, 1037.
- [209] Y. Zhou, B. Liu, X. Sun, J. Li, G. Li, Q. Huo, Y. Liu, *Cryst. Growth Des.* **2017**, *17*, 6653.
- [210] G. R. Fulmer, A. J. M. Miller, N. H. Sherden, H. E. Gottlieb, A. Nudelman, B. M. Stoltz, J. E. Bercaw, K. I. Goldberg, *Organometallics* **2010**, *29*, 2176.
- [211] U. Resch-Genger, K. Rurack, *Pure Appl. Chem.* **2013**, *85*, 1107.
- [212] A. M. Brouwer, *Pure Appl. Chem.* **2011**, *83*, 4910.
- [213] G. Cahiez, O. Gager, A. Moyeux, T. Delacroix, *Adv. Synth. Catal.* **2012**, *354*, 1519.
- [214] H. Kim, K. Inoue, J.-I. Yoshida, *Angew. Chem. Int. Ed.* **2017**, *56*, 7863.
- [215] M. Kihara, J.-i. Andoh, C. Yoshida, *Heterocycles* **2000**, *53*, 359.
- [216] S. Adachi, M. Onozuka, Y. Yoshida, M. Ide, Y. Saikawa, M. Nakata, *Org. Lett.* **2014**, *16*, 358.
- [217] I. Ueda, K. Miyawaki, F. Ueno, *Heterocycles* **2001**, *54*, 887.
- [218] A. V. Dubrovskiy, P. Jain, F. Shi, G. H. Lushington, C. Santini, P. Porubsky, R. C. Larock, *ACS Comb. Sci.* **2013**, *15*, 193.
- [219] H. Sashida, K. Ohyanagi, M. Minoura, K.-y. Akiba, *J. Chem. Soc., Perkin Trans. 1* **2002**, 606.
- [220] H. Wu, Y.-P. He, L.-Z. Gong, *Org. Lett.* **2013**, *15*, 460.
- [221] I. Sucholeiki, V. Lynch, L. Phan, C. S. Wilcox, *J. Org. Chem.* **1988**, *53*, 98.
- [222] N. Umezawa, N. Matsumoto, S. Iwama, N. Kato, T. Higuchi, *Bioorg. Med. Chem.* **2010**, *18*, 6340.
- [223] M. A. Fox, J. A.K. Howard, J. A. Hugh MacBride, A. Mackinnon, K. Wade, *J. Organomet. Chem.* **2003**, *680*, 155.
- [224] T. Peterle, P. Ringler, M. Mayor, *Adv. Funct. Mater.* **2009**, *19*, 3497.
- [225] G. W. Kabalka, A. R. Mereddy, *Organometallics* **2004**, *23*, 4519.
- [226] A. Casitas, M. Canta, M. Solà, M. Costas, X. Ribas, *J. Am. Chem. Soc.* **2011**, *133*, 19386.
- [227] D. Hellwinkel, W. Krapp, *Chem. Ber.* **1977**, *110*, 693.
- [228] L. Ye, D. Ding, Y. Feng, D. Xie, P. Wu, H. Guo, Q. Meng, H. Zhou, *Tetrahedron* **2009**, *65*, 8738.
- [229] A. Ricci, M. Chiarini, M. T. Apicella, D. Compagnone, M. Del Carlo, C. Lo Sterzo, L. Prodi, S. Bonacchi, D. Villamaina, N. Zaccheroni, *Tetrahedron Lett.* **2013**, *54*, 303.

-
- [230] A. Modak, T. Naveen, D. Maiti, *Chem. Commun.* **2013**, 49, 252.
- [231] S. Eissler, T. Bogner, M. Nahrwold, N. Sewald, *Chem. Eur. J.* **2009**, 15, 11273.
- [232] F. Feng, J. Yang, D. Xie, T. D. McCarley, K. S. Schanze, *J. Phys. Chem. Lett.* **2013**, 4, 1410.
- [233] S. Weigold, *Bachelorarbeit*, Ruprecht-Karls-Universität, Heidelberg, **2017**.
- [234] K. T. Nielsen, K. Bechgaard, F. C. Krebs, *Macromolecules* **2005**, 38, 658.
- [235] M. A. Heuft, S. K. Collins, G. P. A. Yap, A. G. Fallis, *Org. Lett.* **2001**, 3, 2883.

7 Appendix

7.1 Optic spectroscopy

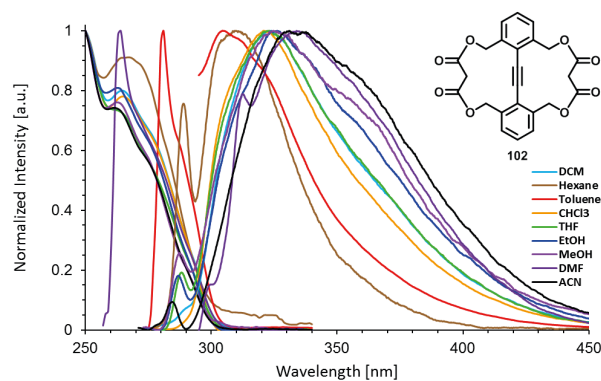


Figure 56. Absorption and emission spectra of doubly bridged tolane **102** in diverse solvents. Emission spectra have been recorded with excitation at 265 nm (CH_2Cl_2 , *n*-hexane, CHCl_3), 285 nm (toluene, dimethylformamide), 264 nm (tetrahydrofuran), 263 nm (ethanol, methanol), 261 nm (acetonitrile).

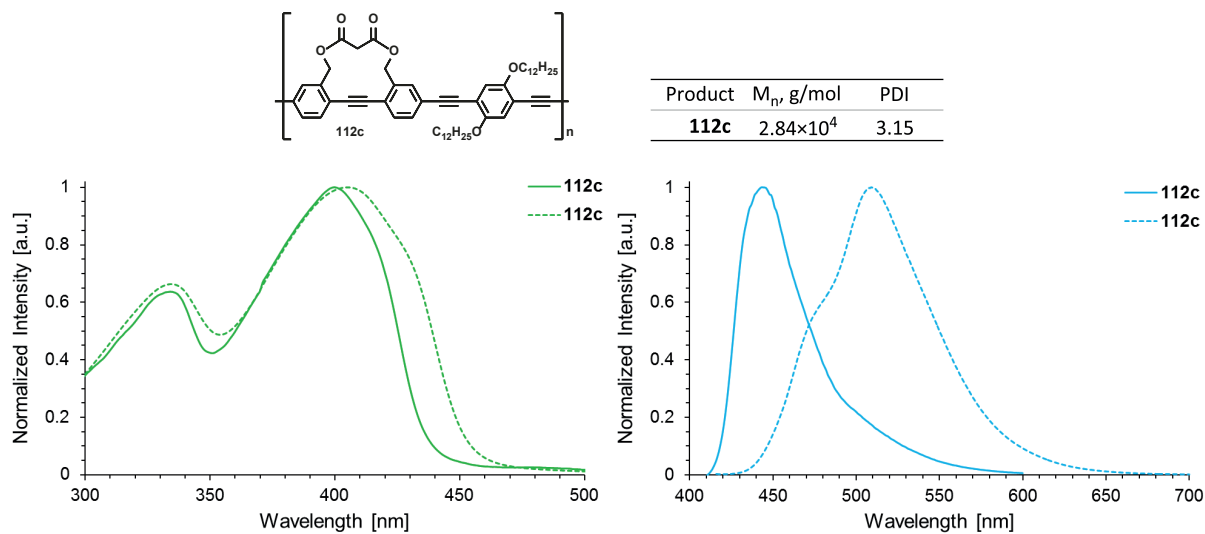


Figure 57. Absorption (left) and emission (right) spectra of **112c** in CHCl_3 solution (solid) and film (dashed).

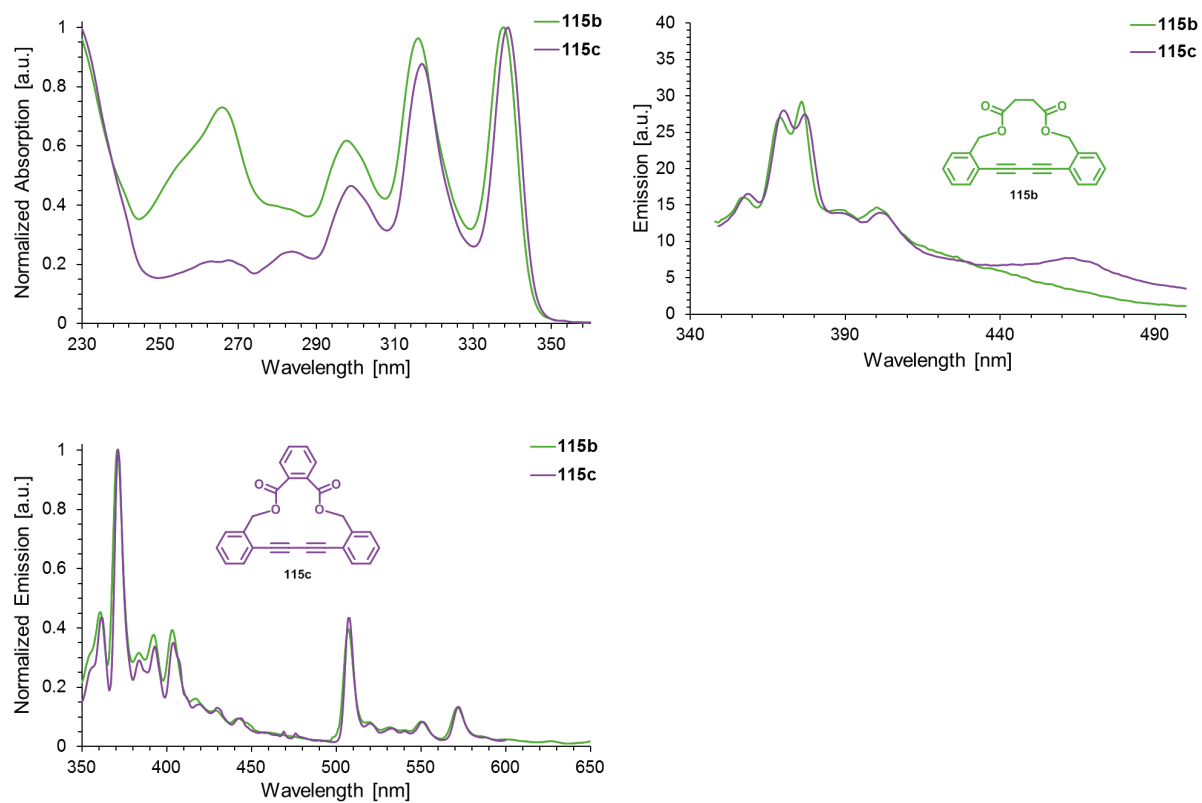


Figure 58. Top: Absorption (left) and emission (right) of **115b** and **115c** in *n*-hexane at room temperature. Bottom: Emission spectra of **115b** and **115c** in EPA at 77K. Emission spectra were recorded by excitation at 338 nm (**115b**), 339 nm (**115c**).

7.2 Thermogravimetric analysis and Differential scanning calorimetry

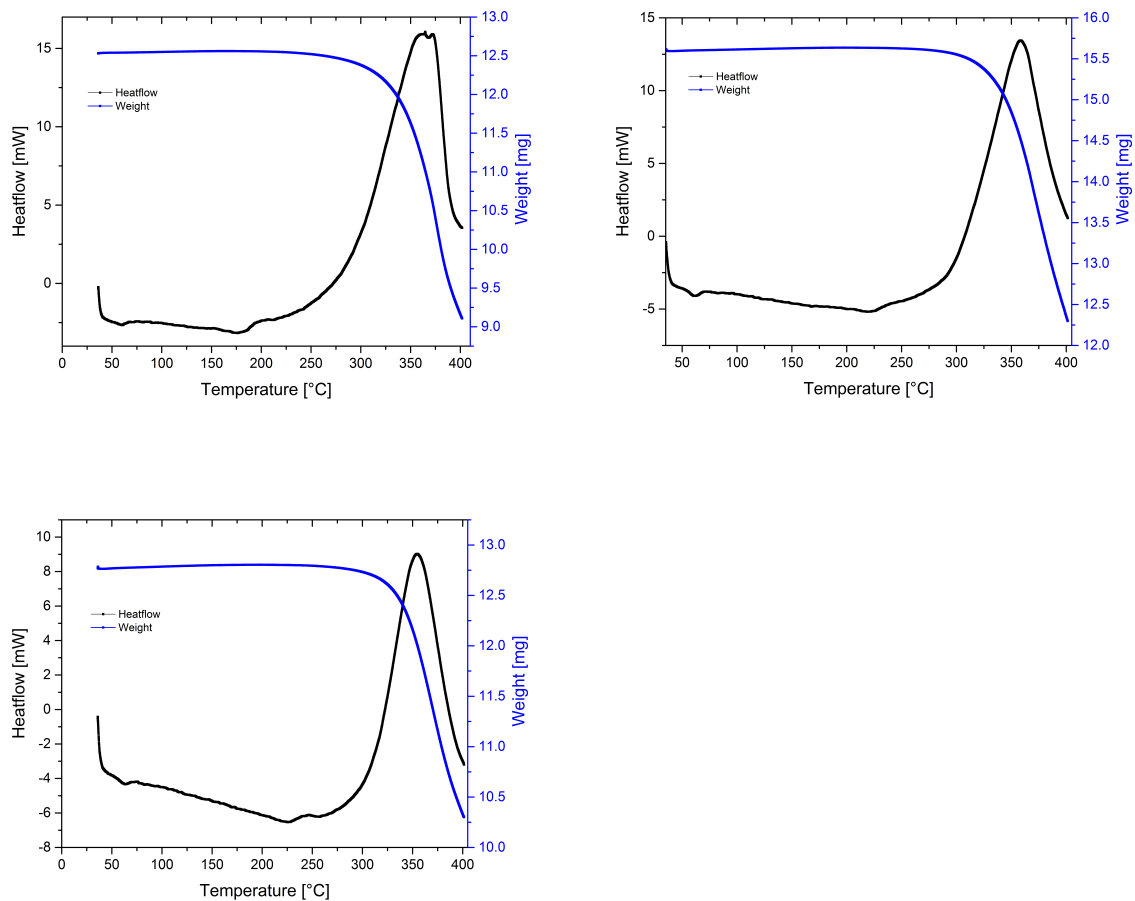
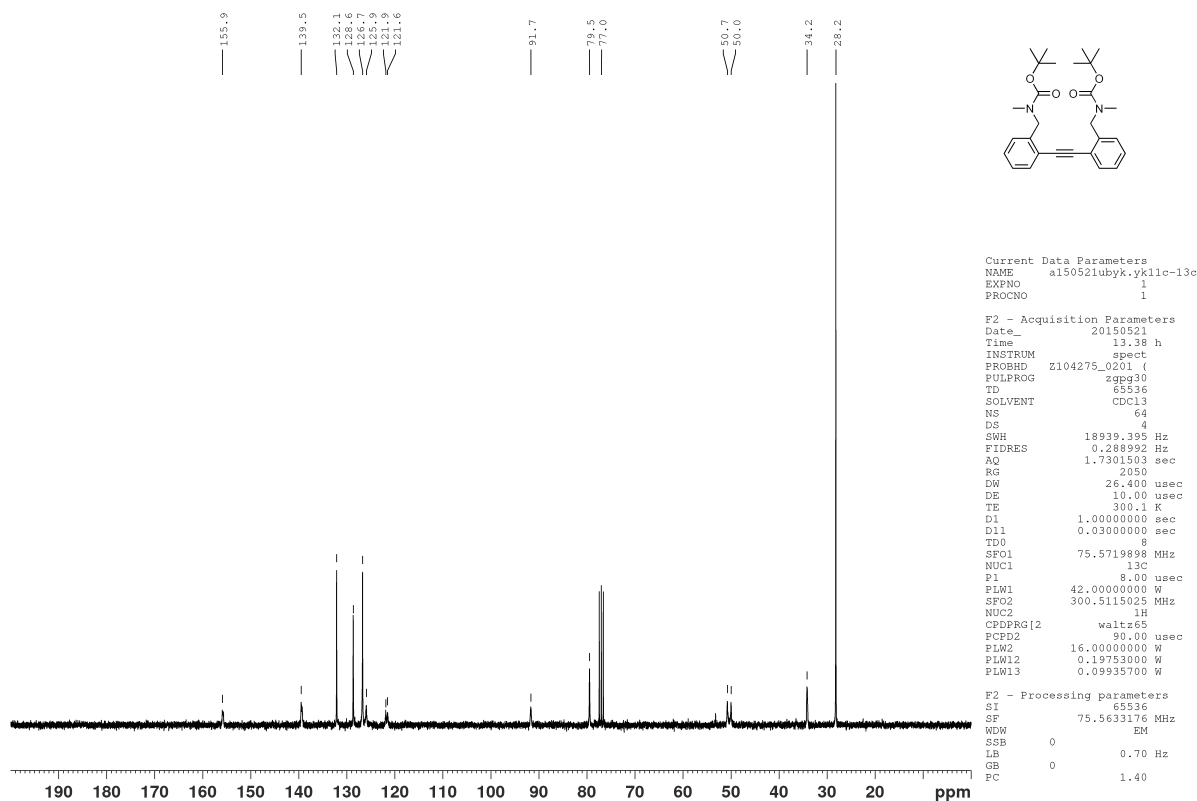
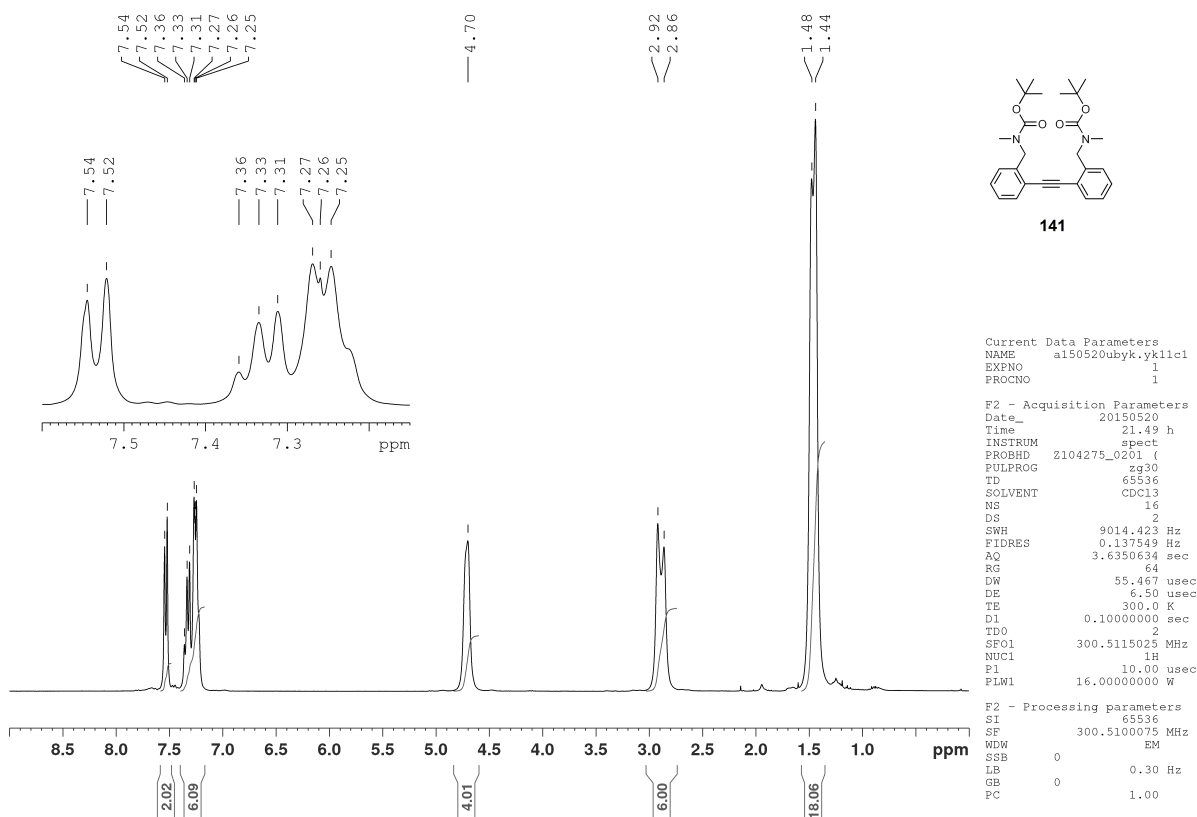
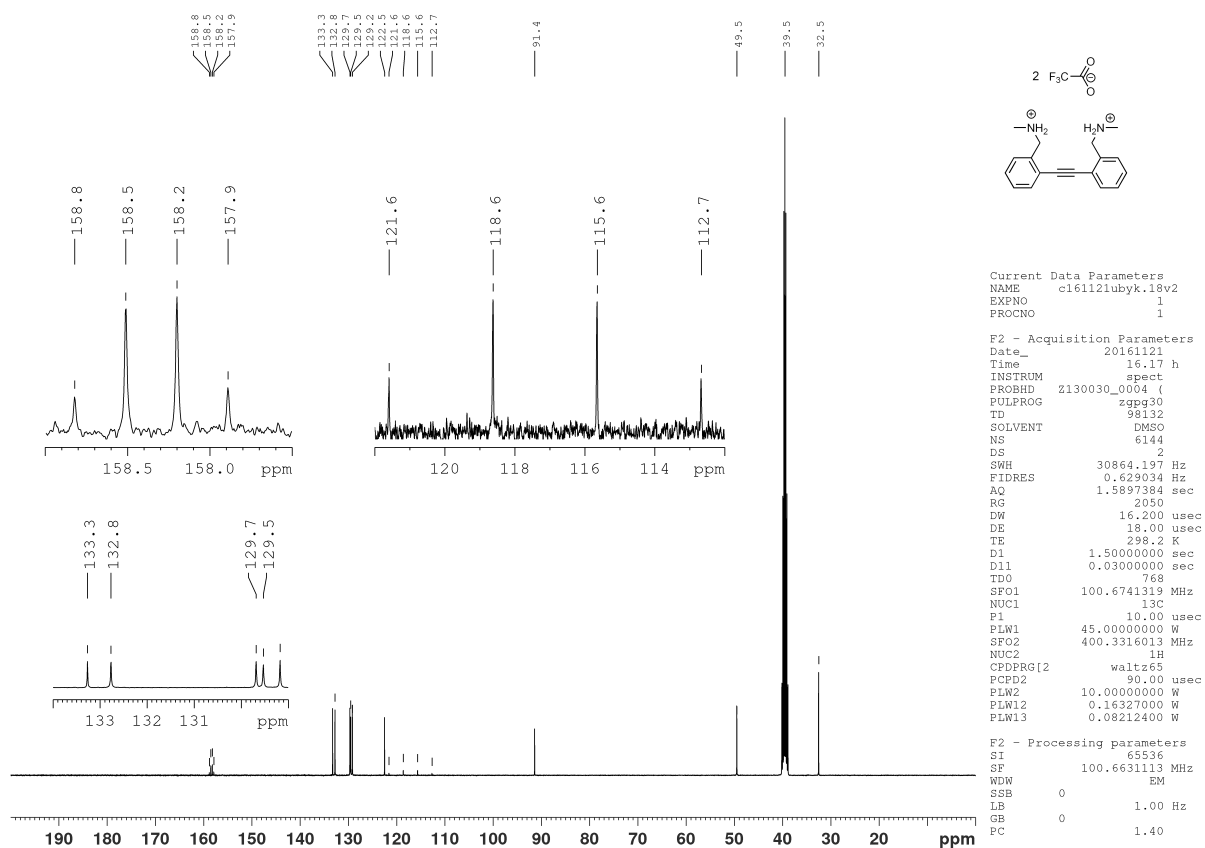
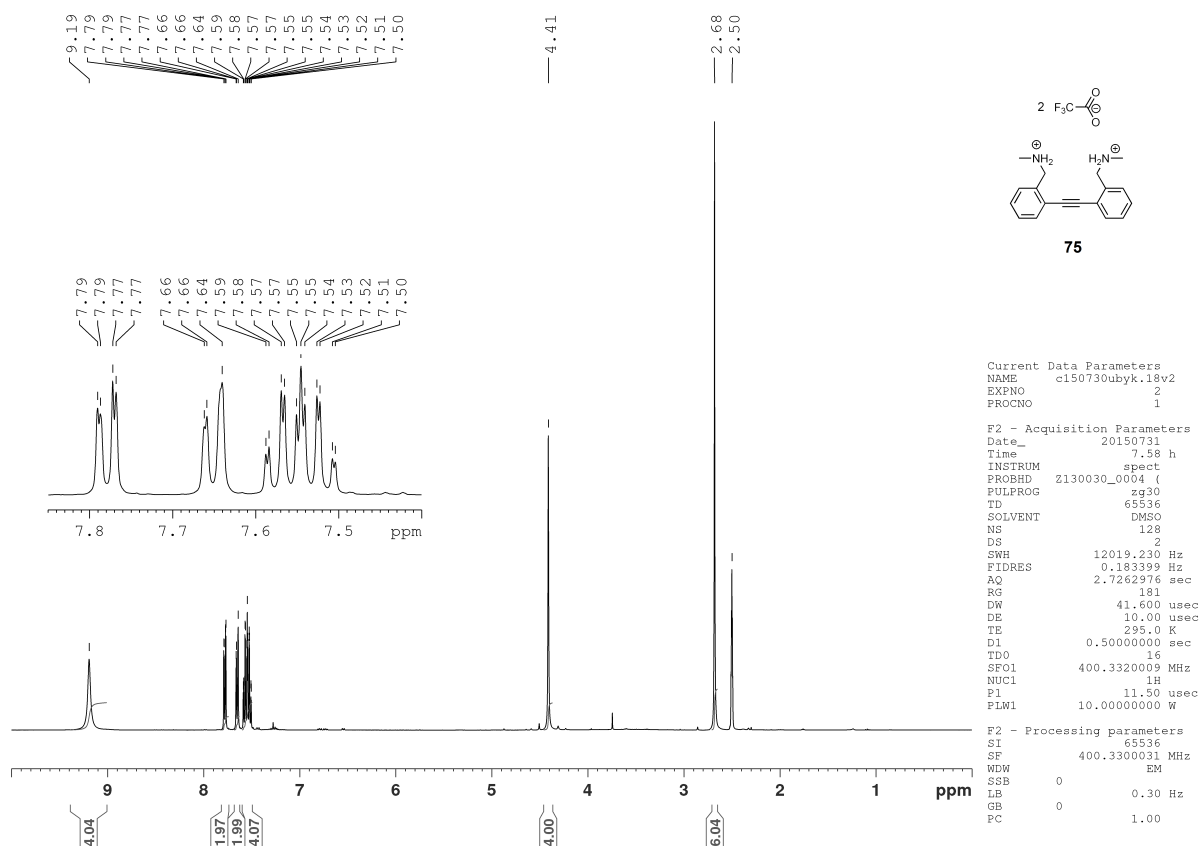
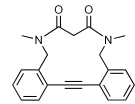
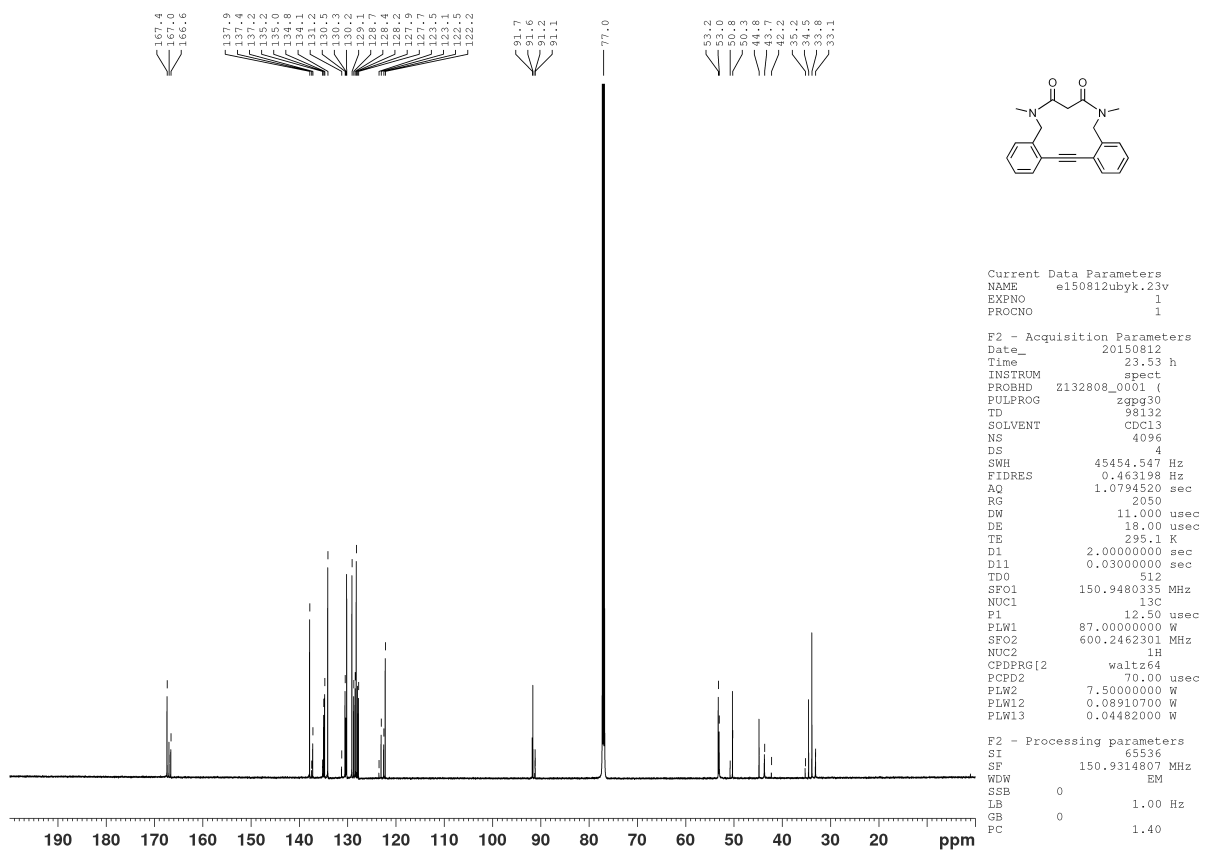
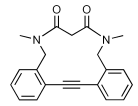
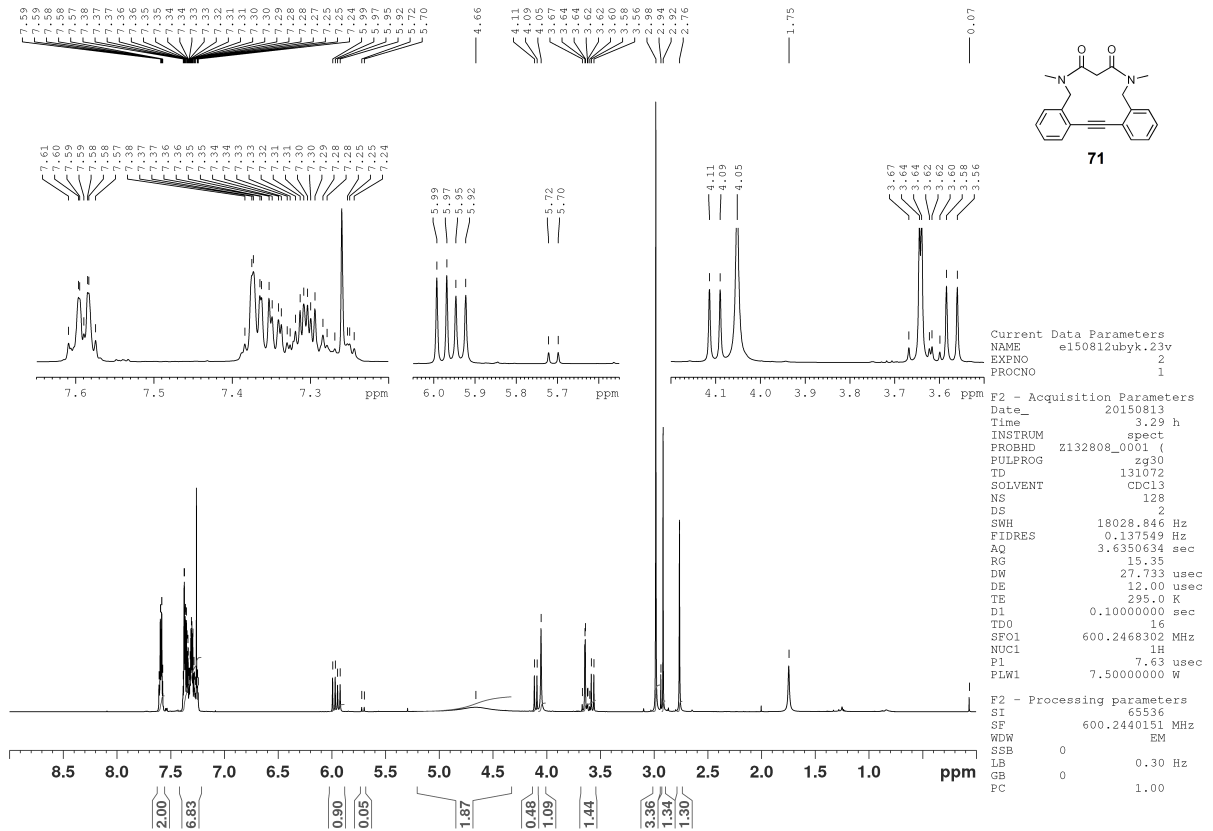


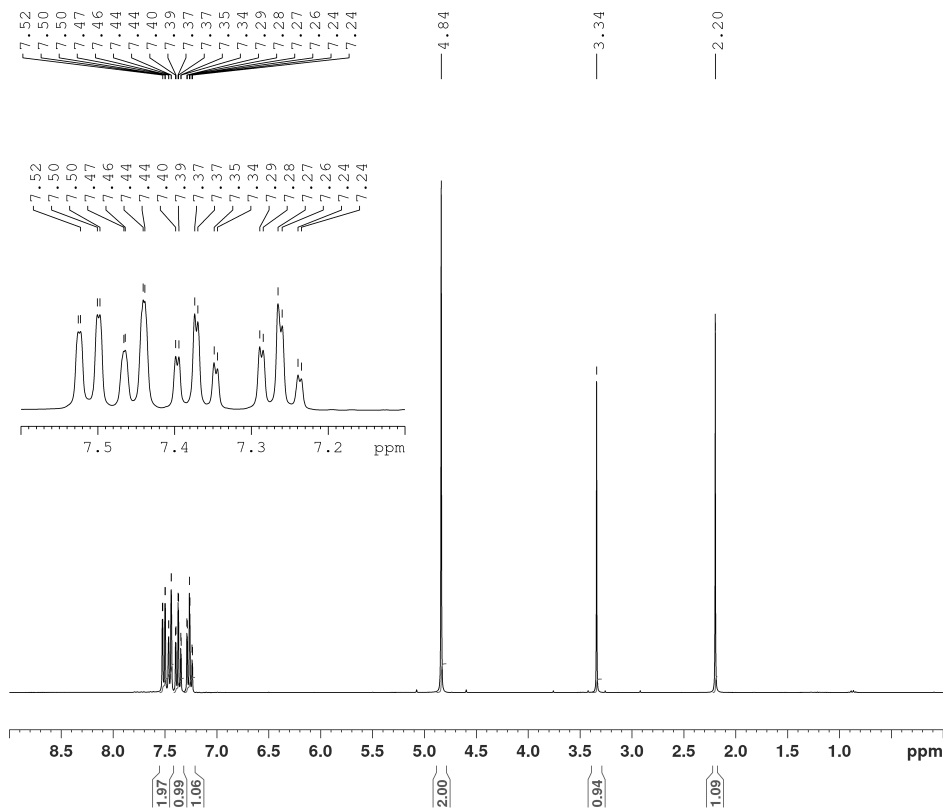
Figure 59. Thermogravimetric analysis and Differential scanning calorimetry of polymer **112a** (upper left), **112b** (upper right) and **112c** (bottom left).

7.3 NMR spectra for selected substances







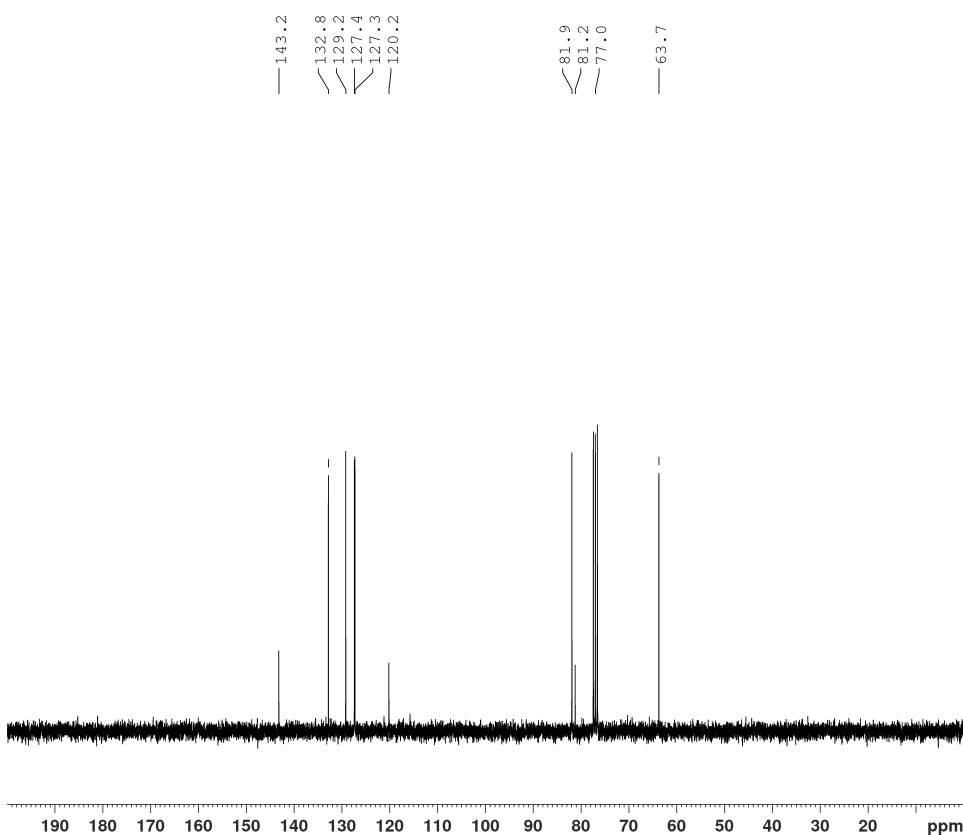


79

Current Data Parameters
 NAME a161111lubyk.52v6
 EXPNO 1
 PROCNO 1

F2 - Acquisition Parameters
 Date_ 20161111
 Time 10.18 h
 INSTRUM spect
 PROBHD Z104275_0201 (
 PULPROG zg30
 TD 65536
 SOLVENT CDCl3
 NS 128
 DS 2
 SWH 9014.423 Hz
 FIDRES 0.275098 Hz
 AQ 3.6350634 sec
 RG 322
 DW 55.467 usec
 DE 8.50 usec
 TE 300.0 K
 D1 0.10000000 sec
 TDO 16
 SFO1 300.5115025 MHz
 NUC1 1H
 P1 10.00 usec
 PLW1 16.00000000 W

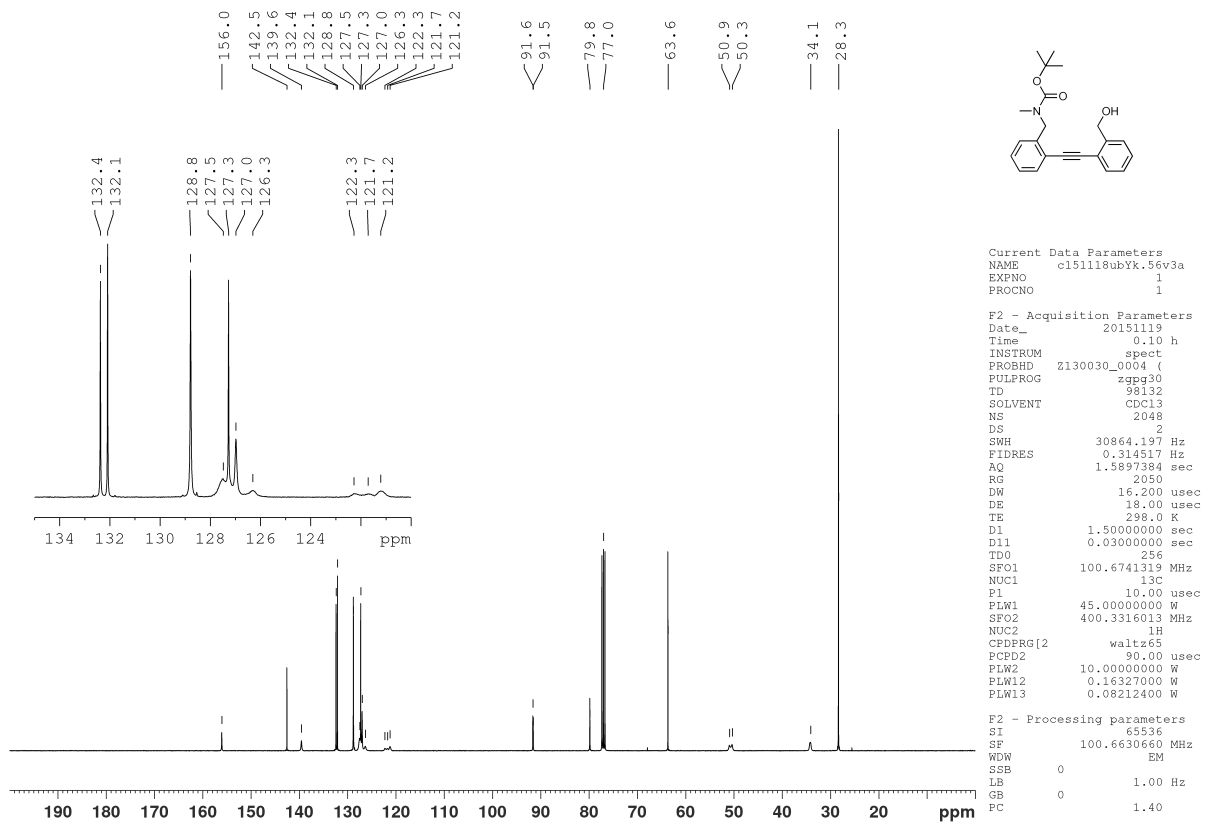
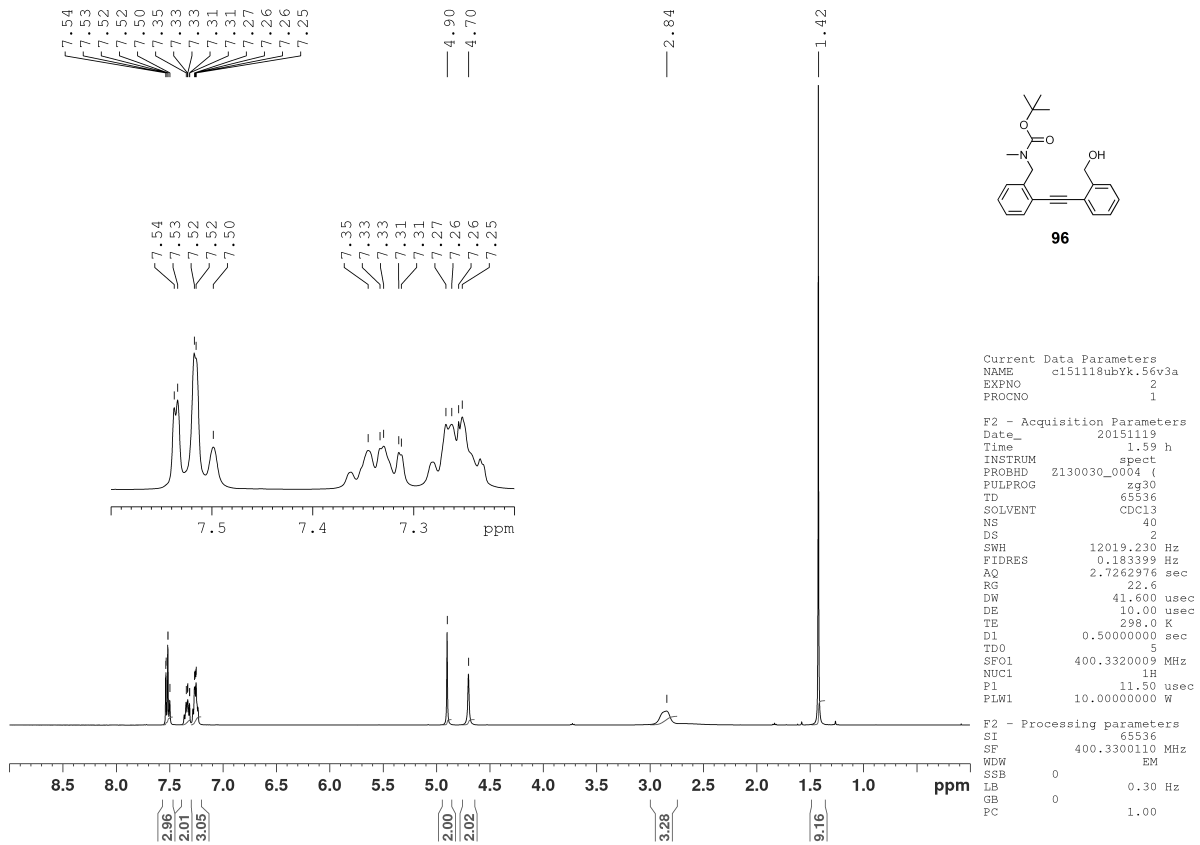
F2 - Processing parameters
 SI 65536
 SF 300.5100051 MHz
 EM
 WDW SSB 0
 LB 0.30 Hz
 GB 0
 PC 1.00

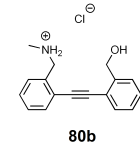
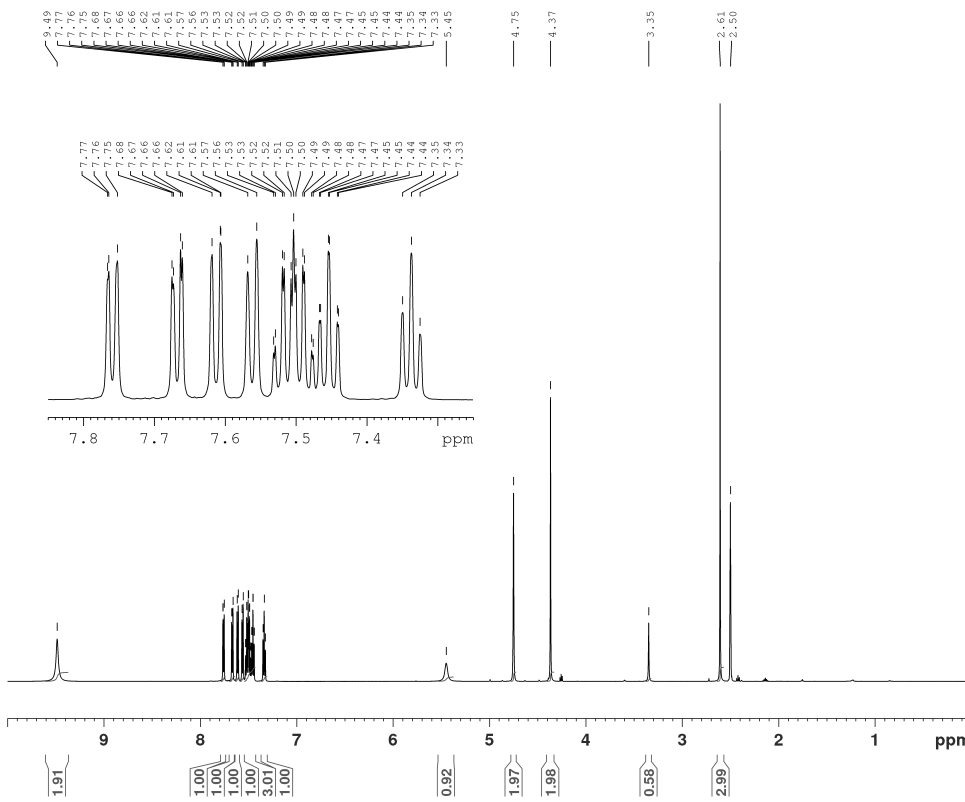


Current Data Parameters
 NAME a161111lubyk.52v6
 EXPNO 2
 PROCNO 1

F2 - Acquisition Parameters
 Date_ 20161111
 Time 10.23 h
 INSTRUM spect
 PROBHD Z104275_0201 (
 PULPROG zgpg30
 TD 65536
 SOLVENT CDCl3
 NS 64
 DS 4
 SWH 18939.395 Hz
 FIDRES 0.577984 Hz
 AQ 1.7301503 sec
 RG 2050
 DW 26.400 usec
 DE 10.00 usec
 TE 300.1 K
 D1 1.00000000 sec
 D11 0.03000000 sec
 TDO 8
 SFO1 75.5719898 MHz
 NUC1 13C
 P1 8.00 usec
 PLW1 42.00000000 W
 SFO2 300.5115025 MHz
 NUC2 1H
 CPDPRG2 waltz65
 PCPD2 90.00 usec
 PLW2 16.00000000 W
 PLW12 0.19753000 W
 PLW13 0.09935700 W

F2 - Processing parameters
 SI 65536
 SF 75.5633039 MHz
 EM
 WDW SSB 0
 LB 0.70 Hz
 GB 0
 PC 1.40

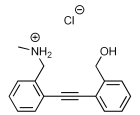
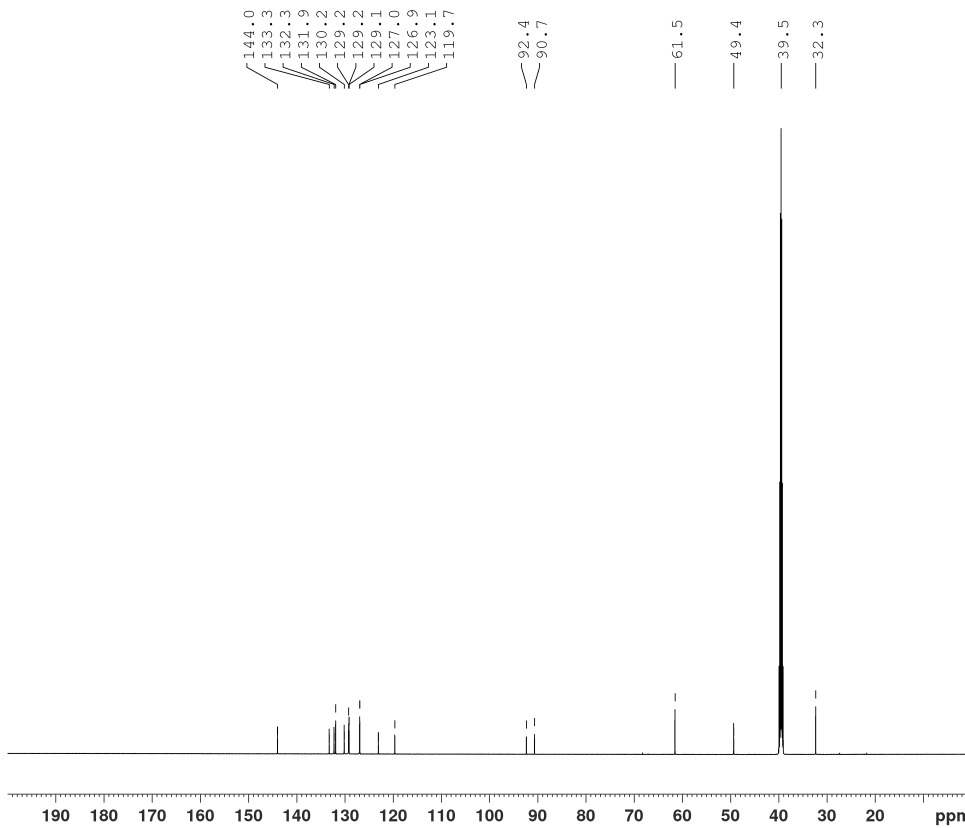




Current Data Parameters
 NAME e151026ubyk.58v2
 EXPNO 3
 PROCNO 1

F2 - Acquisition Parameters
 Date_ 20151027
 Time 9.28 h
 INSTRUM spect
 PROBRD z132808_0001 ()
 PULPROG zg30
 TD 131072
 SOLVENT DMSO
 NS 8
 DS 2
 SWH 18028.846 Hz
 FIDRES 0.137549 Hz
 AQ 3.6350634 sec
 RG 15.35
 DW 27.733 usec
 DE 12.00 usec
 TE 295.0 K
 D1 0.1000000 sec
 TD0 1
 SF01 600.2468302 MHz
 NUC1 1H
 P1 7.63 usec
 PLW1 7.5000000 W

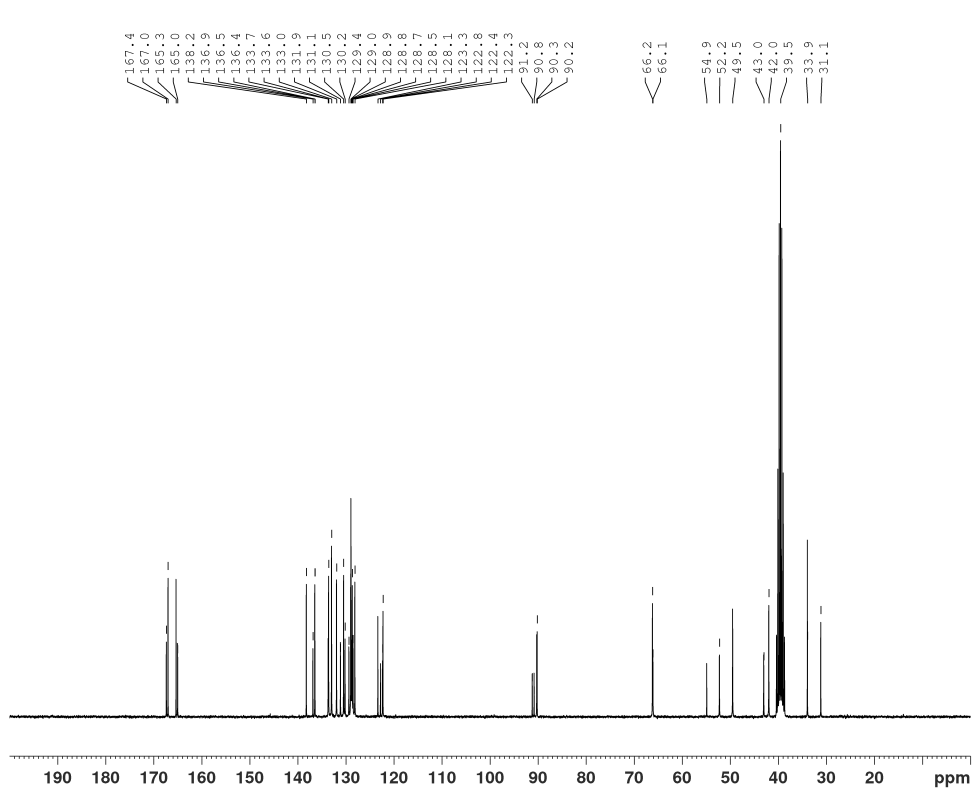
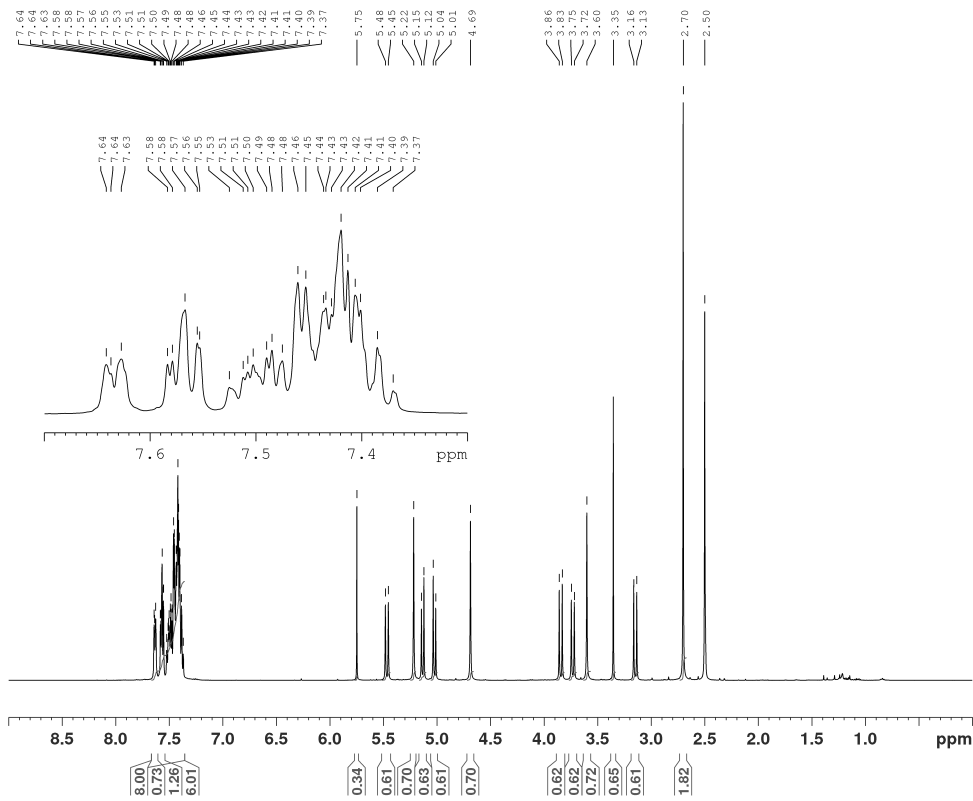
F2 - Processing parameters
 SI 65536
 SF 600.2440051 MHz
 WDW EM
 SSB 0
 LB 0.30 Hz
 GB 0
 PC 1.00

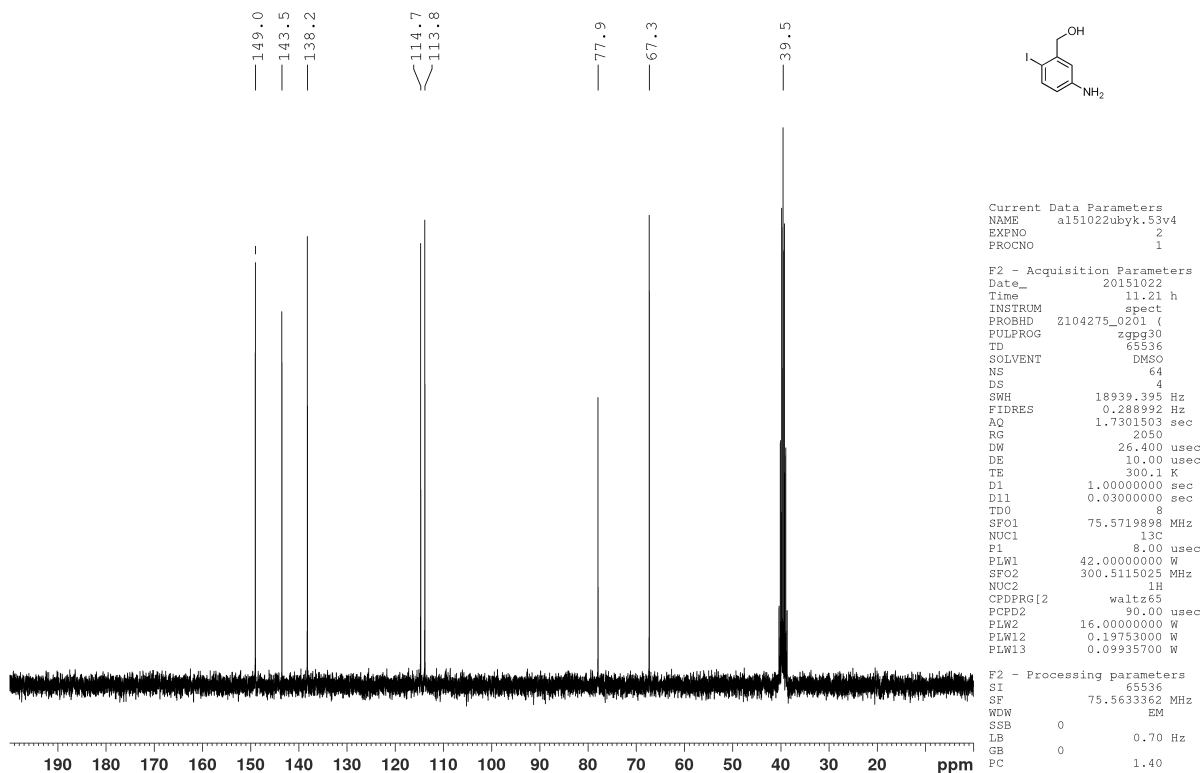
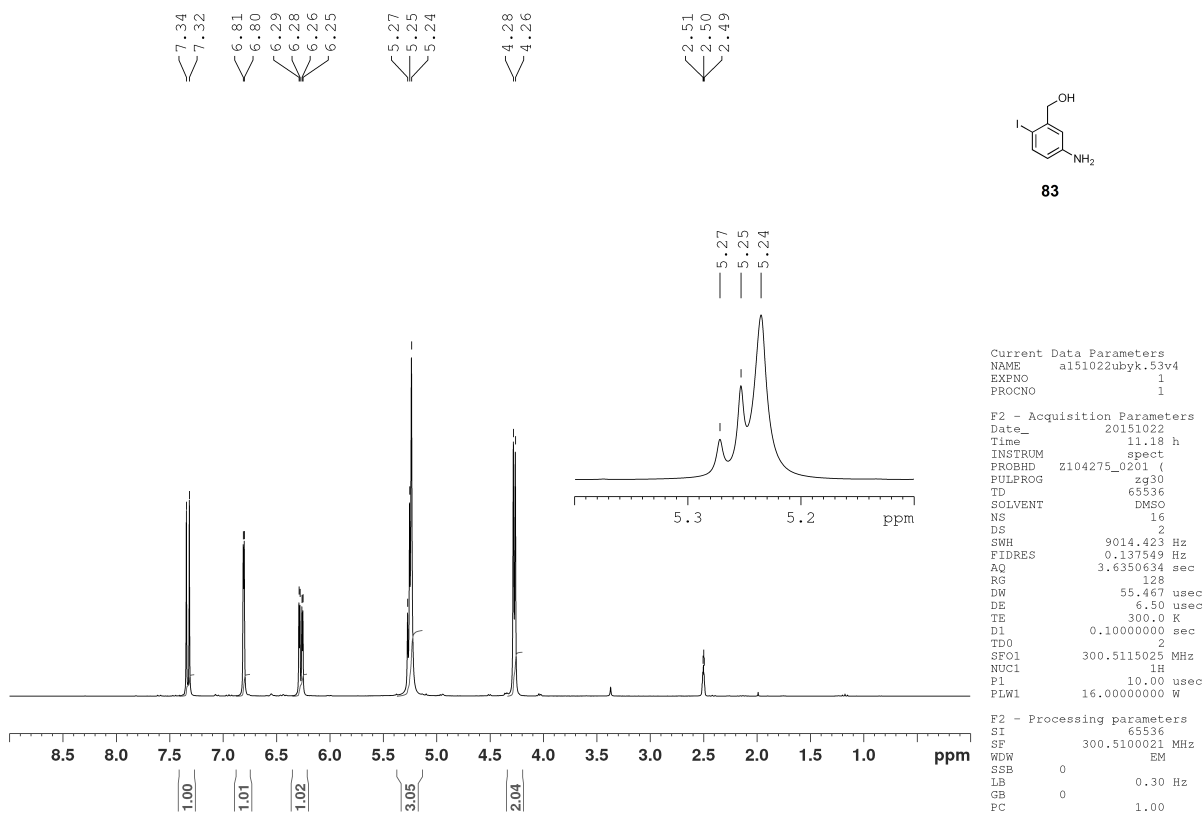


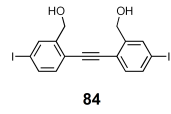
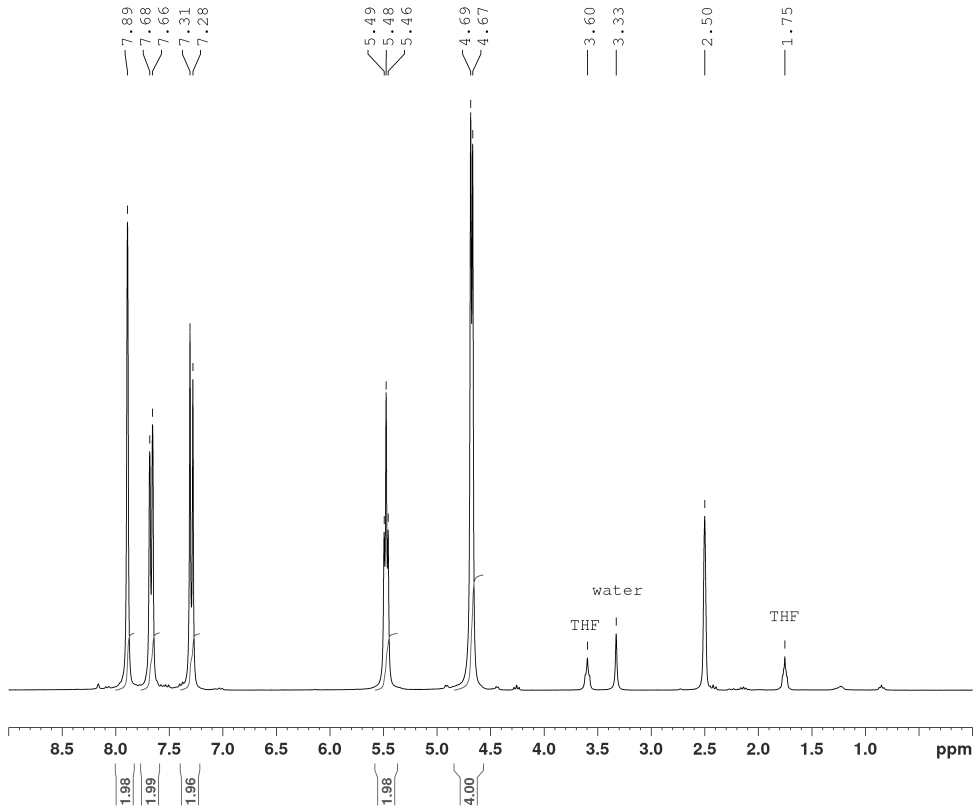
Current Data Parameters
 NAME e151026ubyk.58v2
 EXPNO 1
 PROCNO 1

F2 - Acquisition Parameters
 Date_ 20151027
 Time 4.41 h
 INSTRUM spect
 PROBRD z132808_0001 ()
 PULPROG zgpg30
 TD 98132
 SOLVENT DMSO
 NS 4096
 DS 4
 SWH 45454.547 Hz
 FIDRES 0.463198 Hz
 AQ 1.0794520 sec
 RG 2050
 DW 11.000 usec
 DE 18.00 usec
 TE 295.0 K
 D1 2.0000000 sec
 D11 0.0300000 sec
 TD0 512
 SF01 150.9480335 MHz
 NUC1 13C
 P1 12.50 usec
 PLW1 87.0000000 W
 SF02 600.2462301 MHz
 NUC2 1H
 CPDPRG[2] waltz64
 PCPD2 70.00 usec
 PLW2 7.5000000 W
 PLW12 0.08910700 W
 PLW13 0.04482000 W

F2 - Processing parameters
 SI 65536
 SF 150.9315438 MHz
 WDW EM
 SSB 0
 LB 1.00 Hz
 GB 0
 PC 1.40



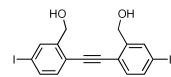
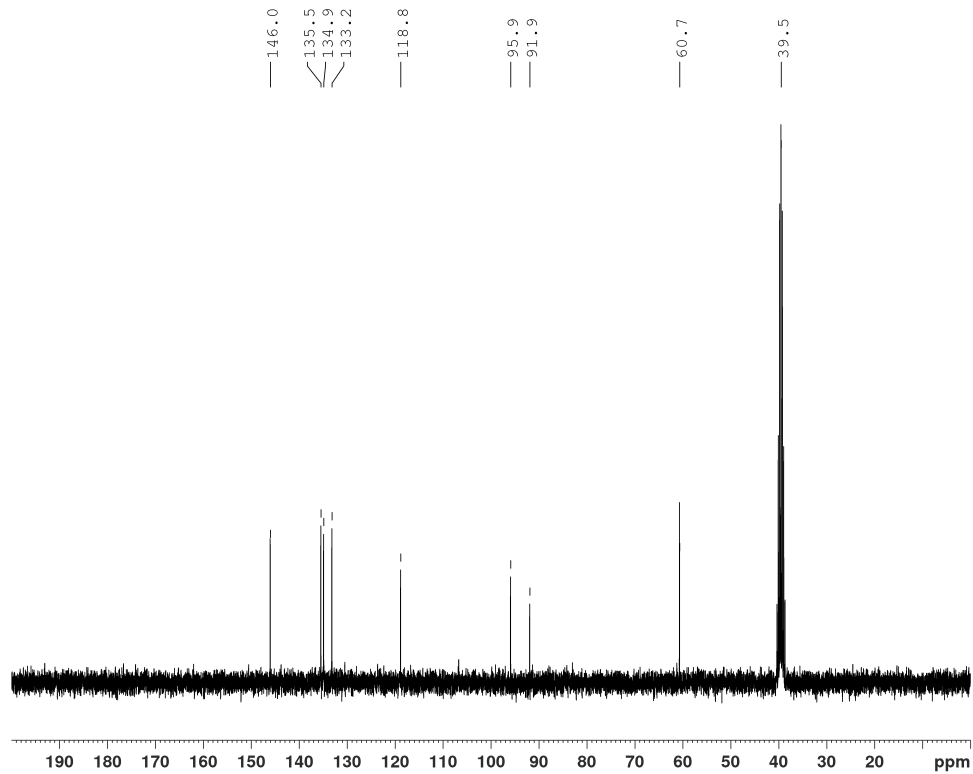




Current Data Parameters
 NAME a151112ubyk.61
 EXPNO 1
 PROCNO 1

F2 - Acquisition Parameters
 Date_ 20151112
 Time 10.16 h
 INSTRUM spect
 PROBHD Z104275_0201 ()
 PULPROG zg30
 TD 65536
 SOLVENT DMSO
 NS 128
 DS 2
 SWH 9014.423 Hz
 FIDRES 0.137549 Hz
 AQ 3.6350634 sec
 RG 406
 DW 55.467 usec
 DE 6.50 usec
 TE 300.0 K
 D1 0.10000000 sec
 TD0 16
 SFO1 300.5115025 MHz
 NUC1 1H
 P1 10.00 usec
 PLW1 16.00000000 W

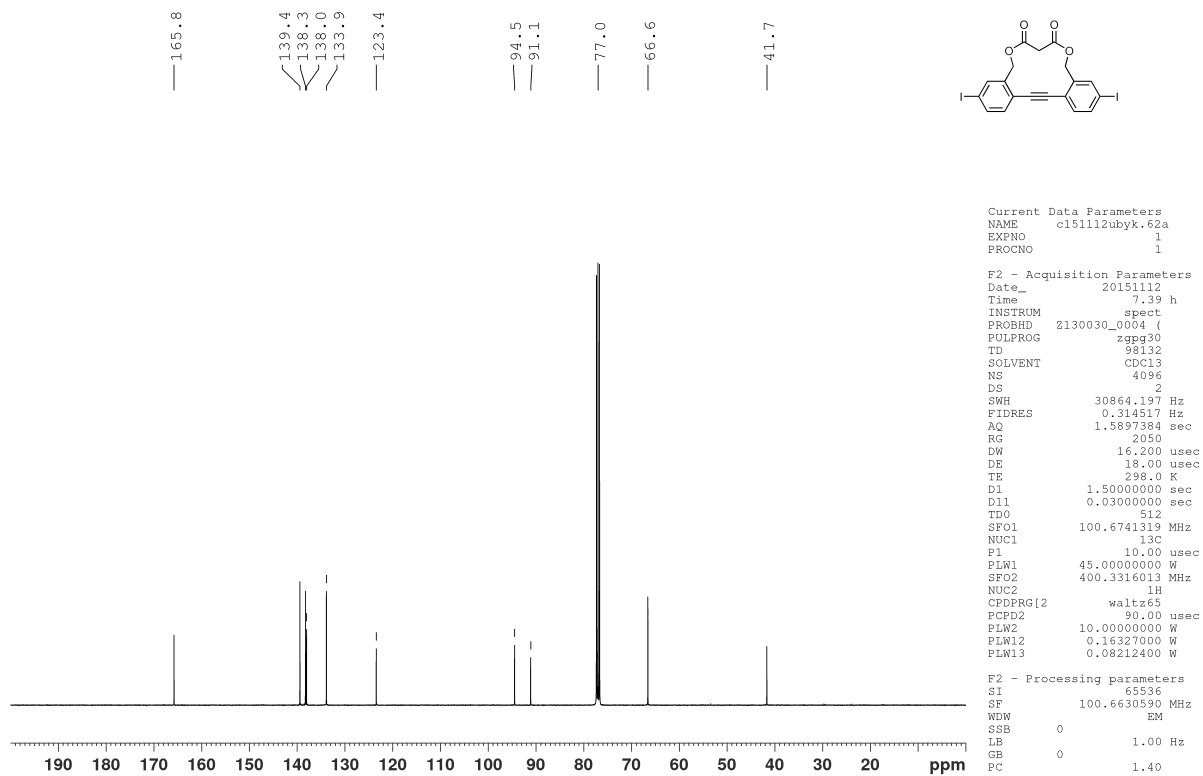
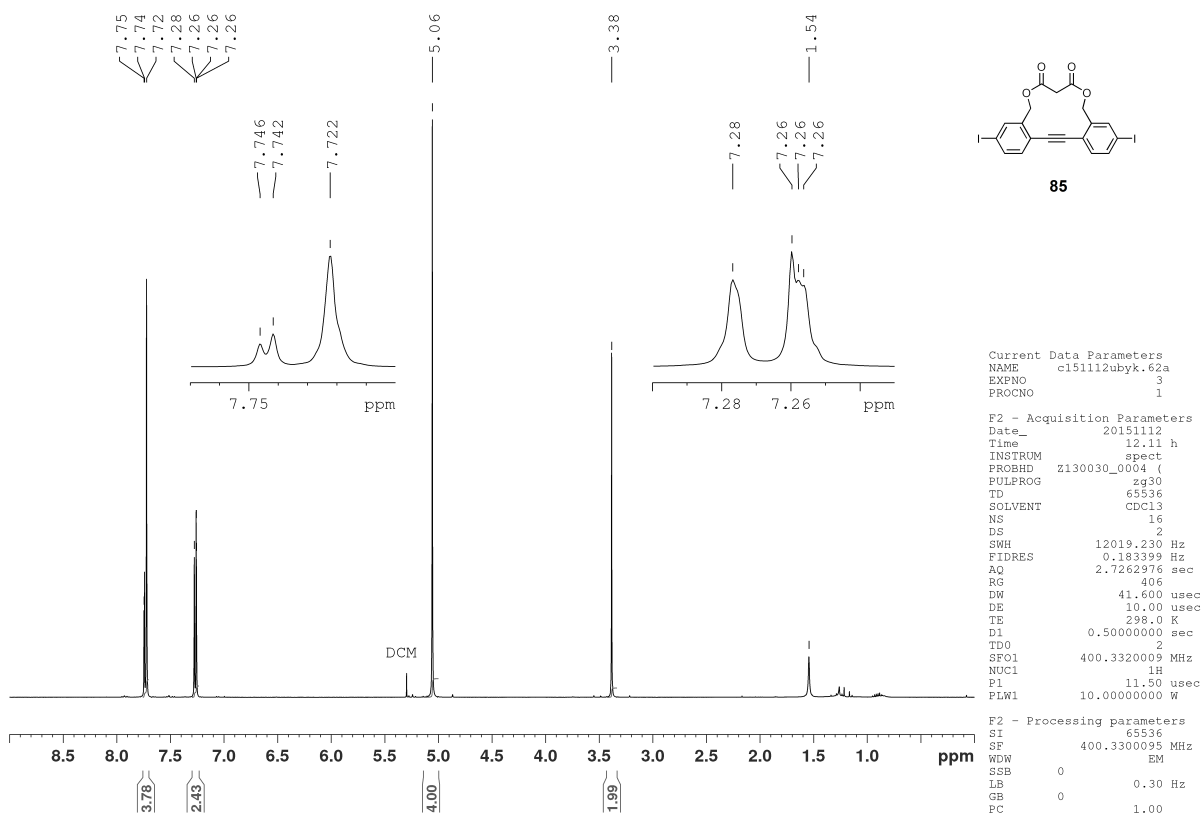
F2 - Processing parameters
 SI 65536
 SF 300.5100026 MHz
 WDW EM
 SSB 0
 LB 0.30 Hz
 GB 0
 PC 1.00

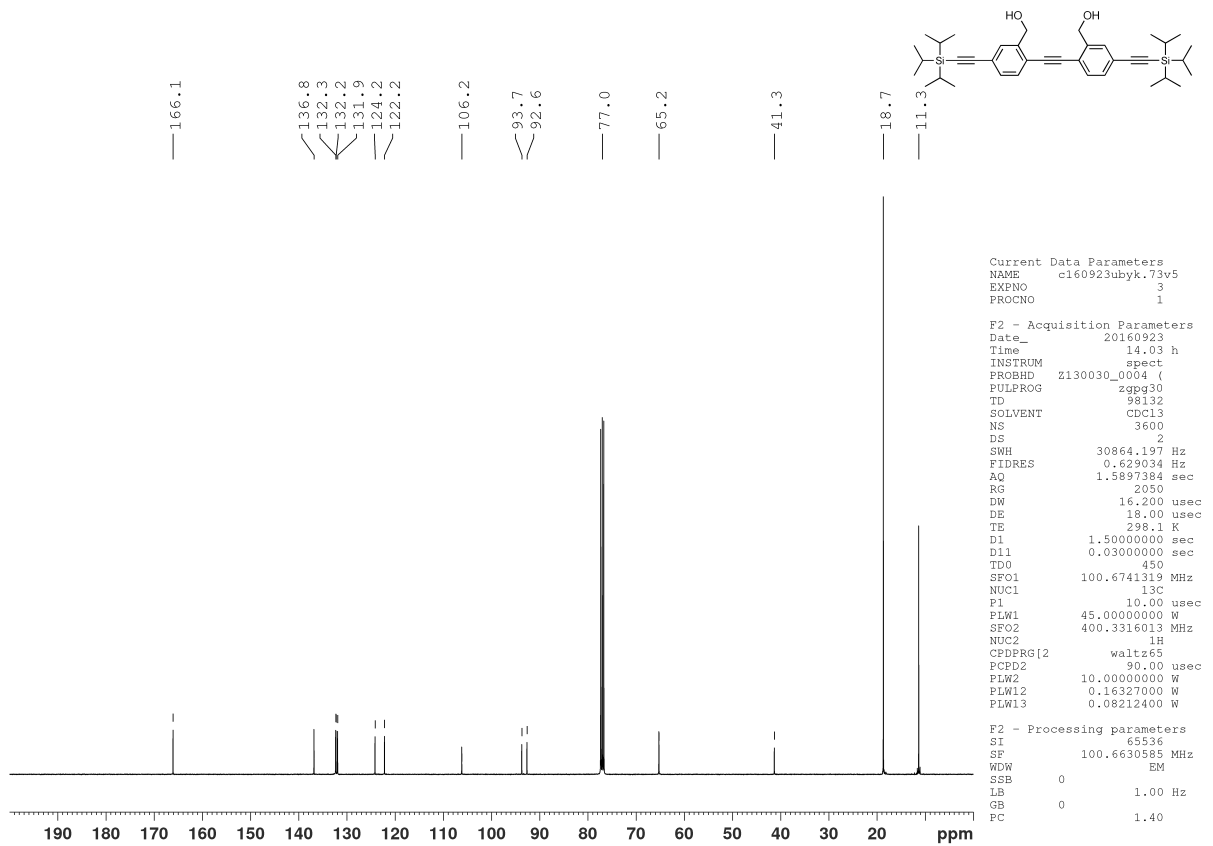
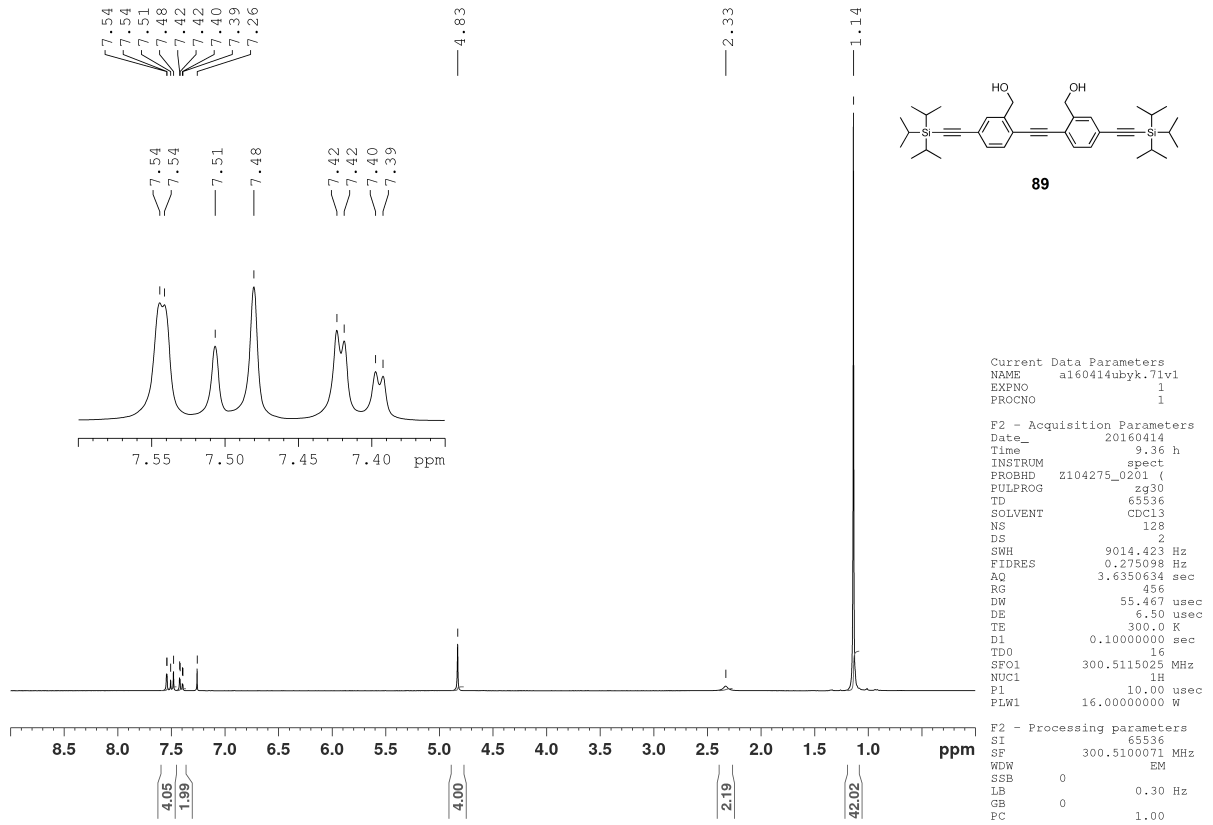


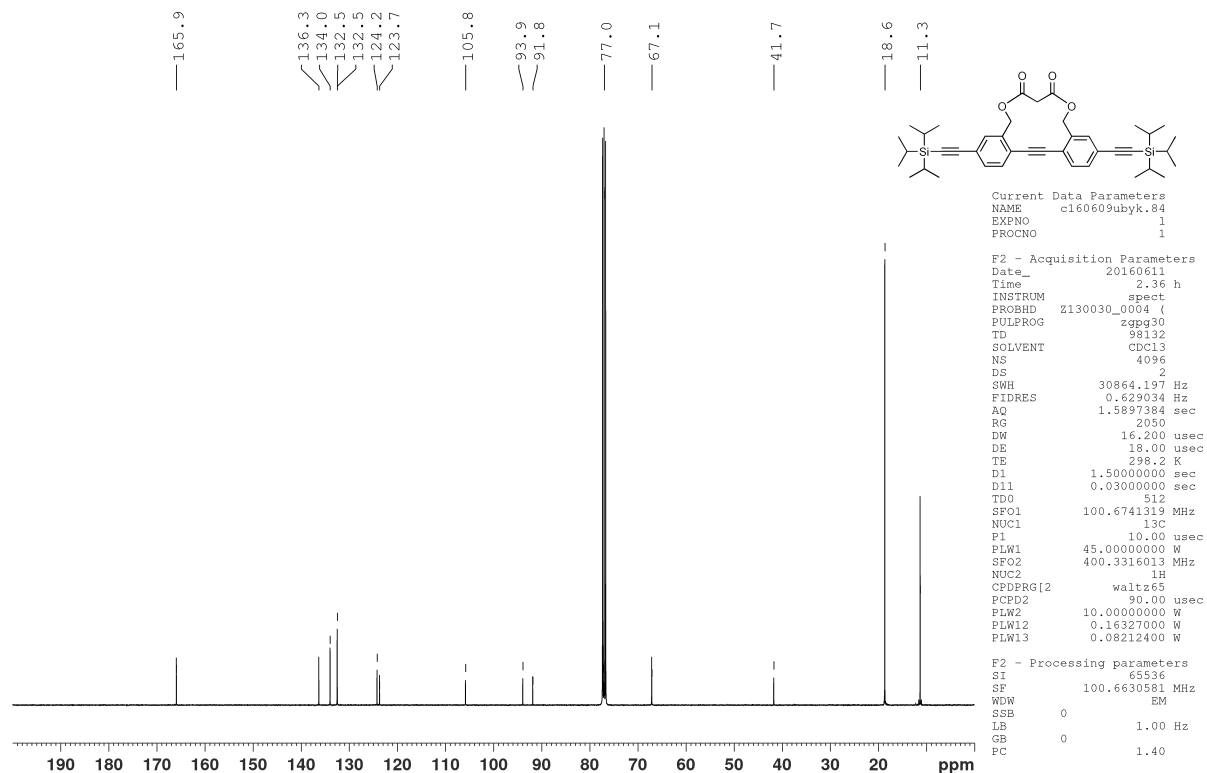
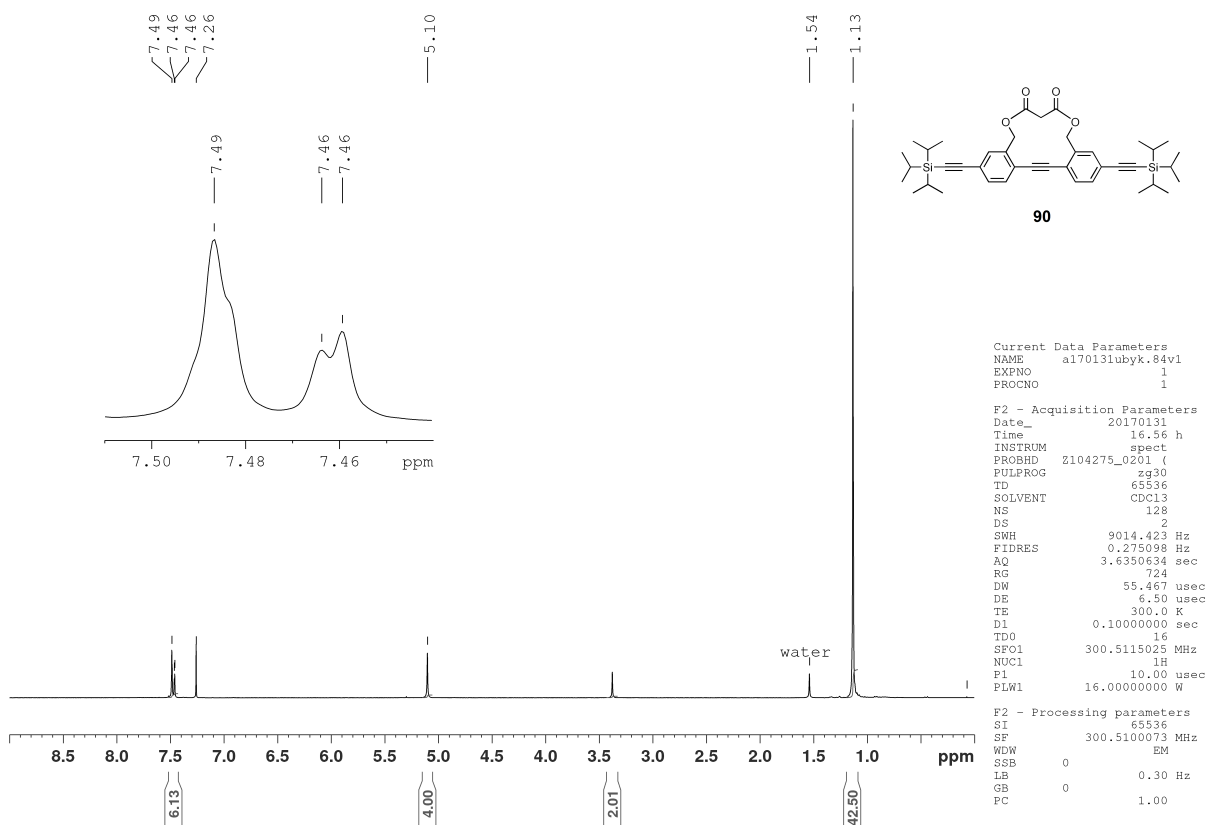
Current Data Parameters
 NAME a151112ubyk.61
 EXPNO 2
 PROCNO 1

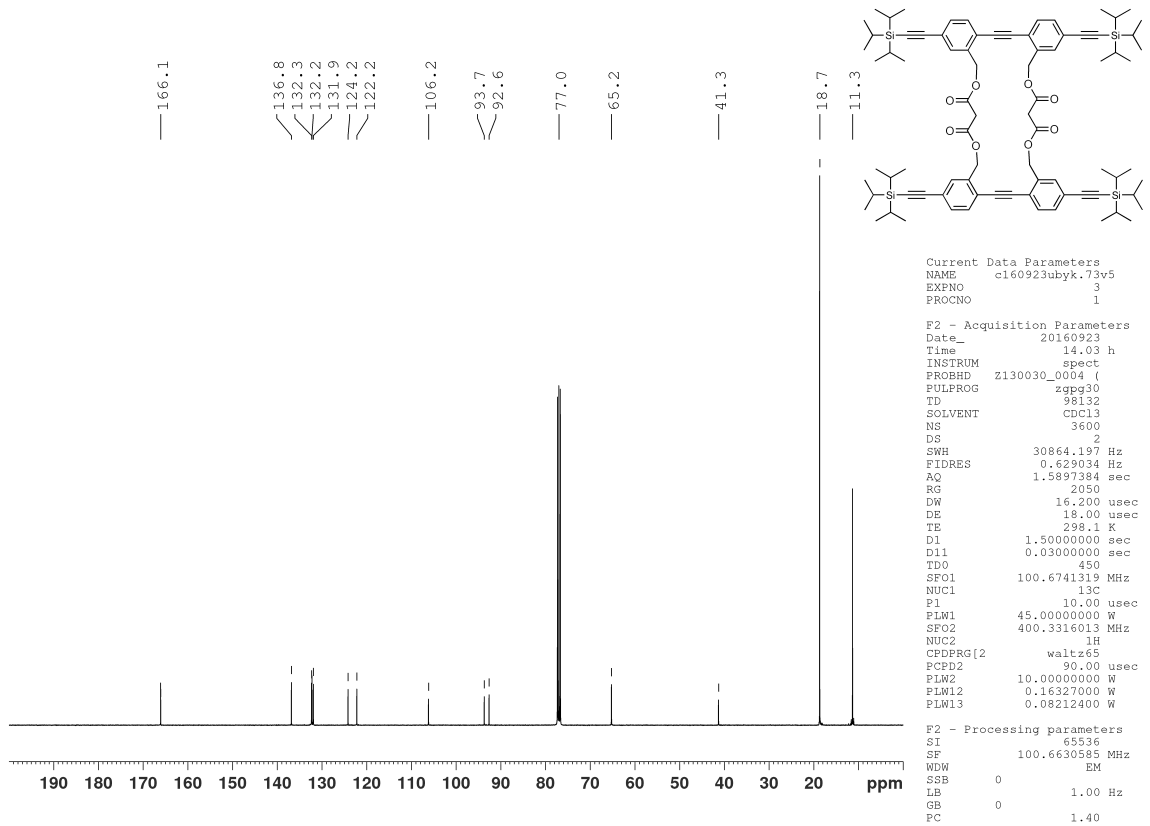
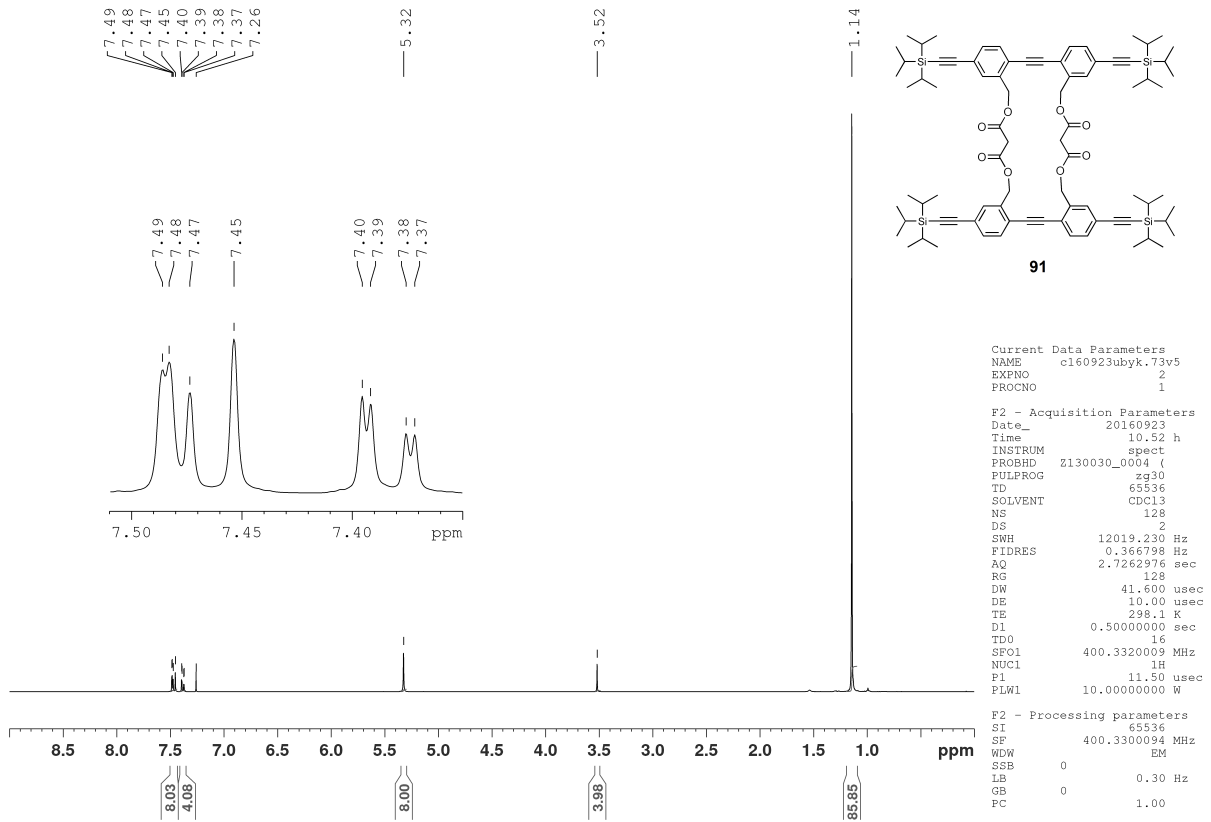
F2 - Acquisition Parameters
 Date_ 20151112
 Time 11.07 h
 INSTRUM spect
 PROBHD Z104275_0201 ()
 PULPROG zgpg30
 TD 65536
 SOLVENT DMSO
 NS 64
 DS 4
 SWH 18939.395 Hz
 FIDRES 0.288992 Hz
 AQ 1.7301503 sec
 RG 2050
 DW 26.400 usec
 DE 10.00 usec
 TE 300.1 K
 D1 1.00000000 sec
 D11 0.03000000 sec
 TD0 8
 SFO1 75.5719898 MHz
 NUC1 13C
 P1 8.00 usec
 PLW1 42.00000000 W
 SFO2 300.5115025 MHz
 NUC2 1H
 CDFPRG12 waltz65
 PCPD2 90.00 usec
 PLW2 16.00000000 W
 PLW3 0.19753000 W
 PLW13 0.09935700 W

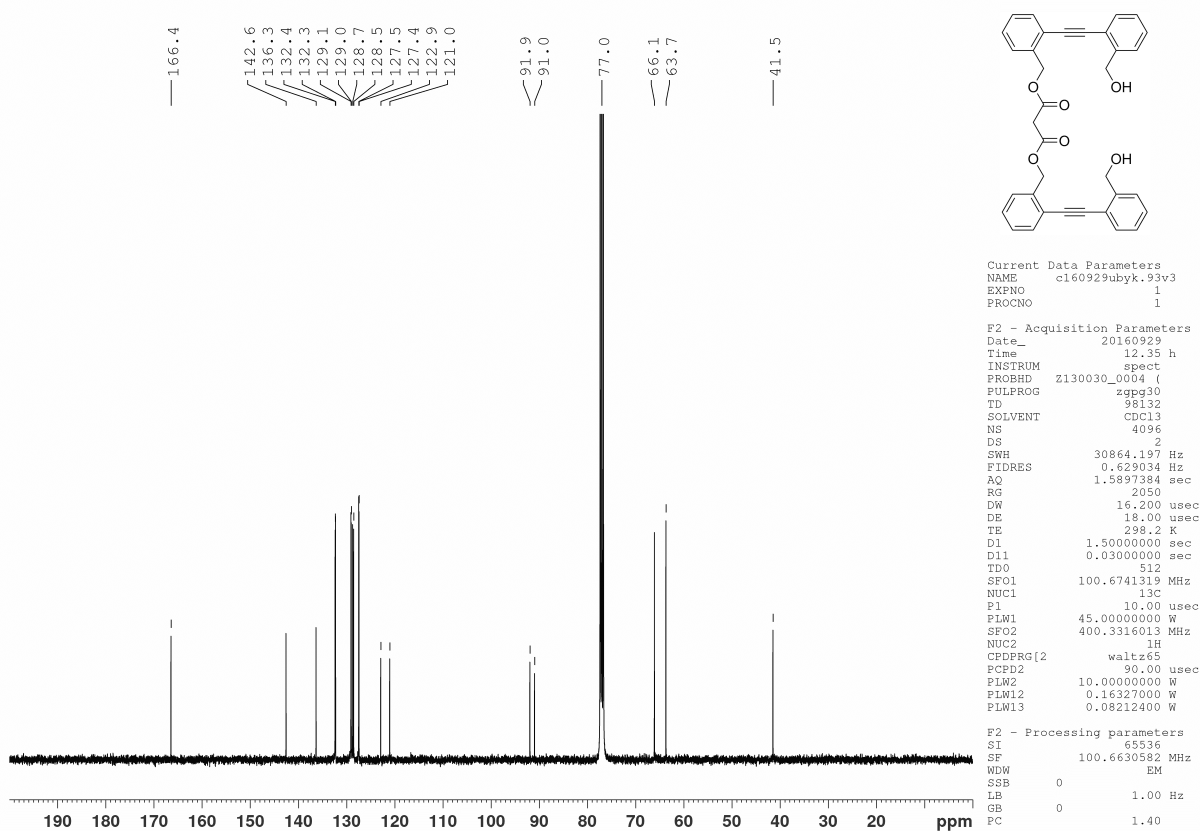
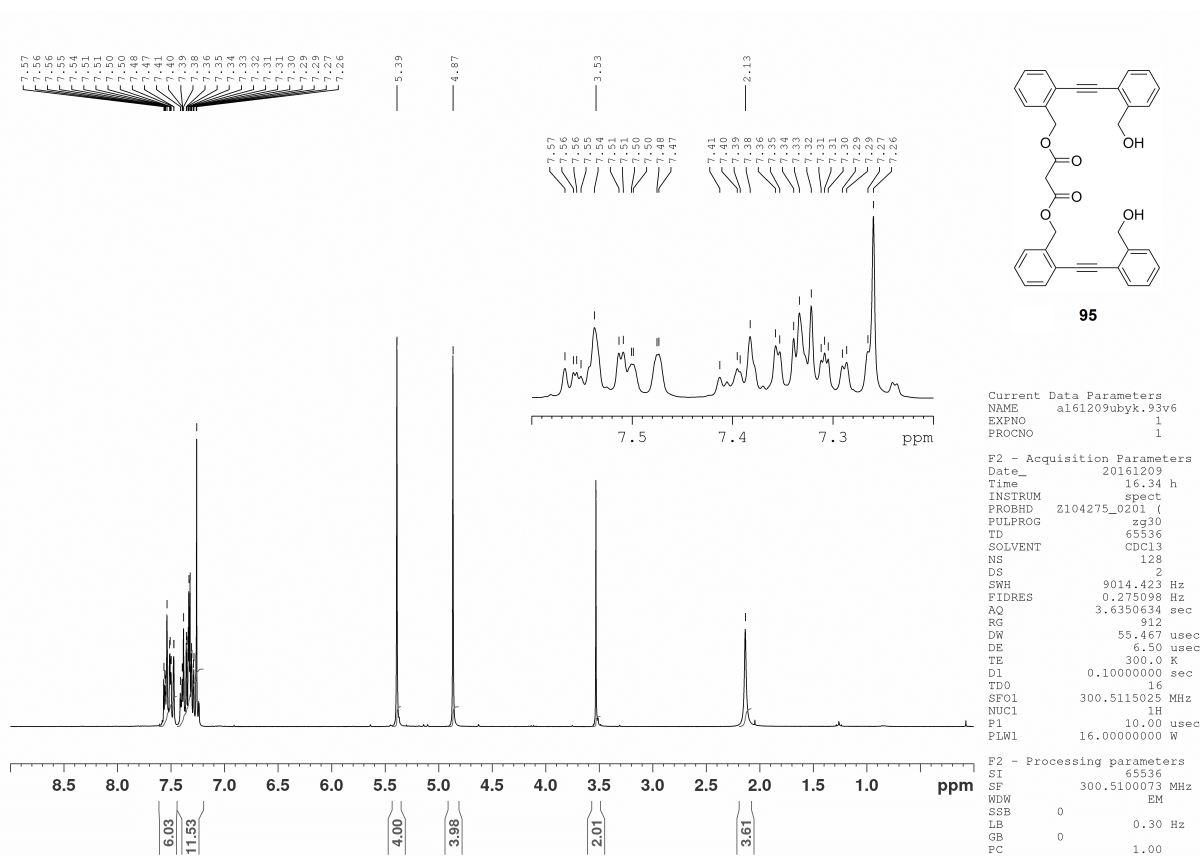
F2 - Processing parameters
 SI 65536
 SF 75.5633389 MHz
 WDW EM
 SSB 0
 LB 0.70 Hz
 GB 0
 PC 1.40

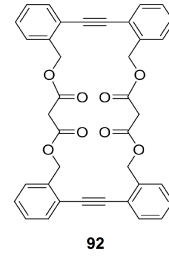
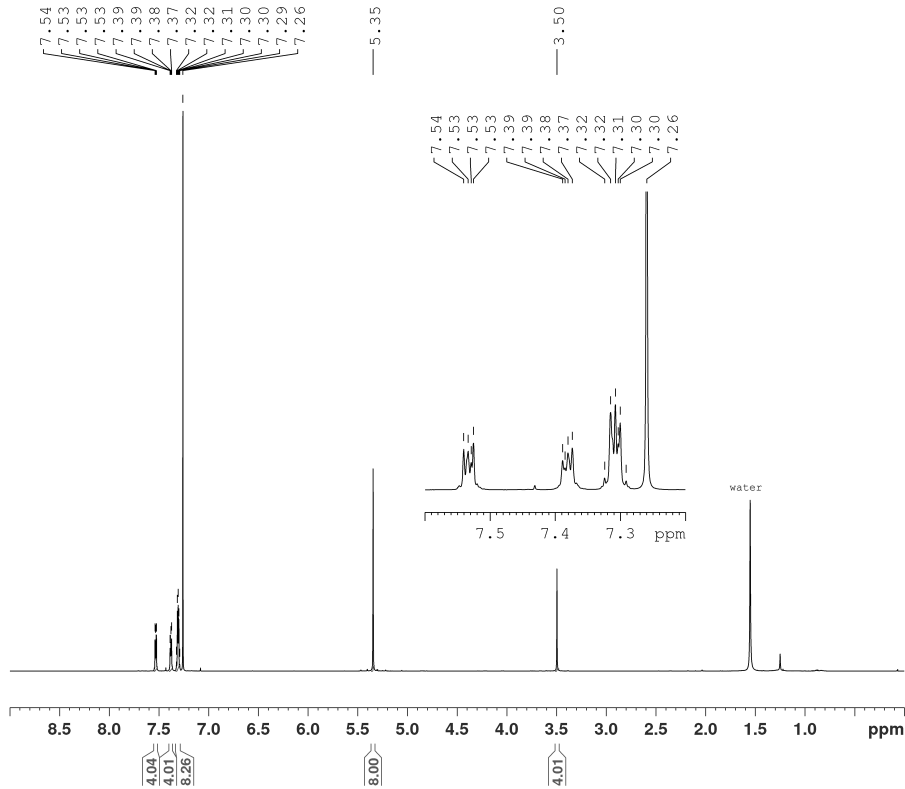








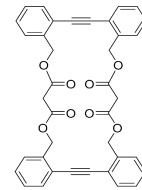
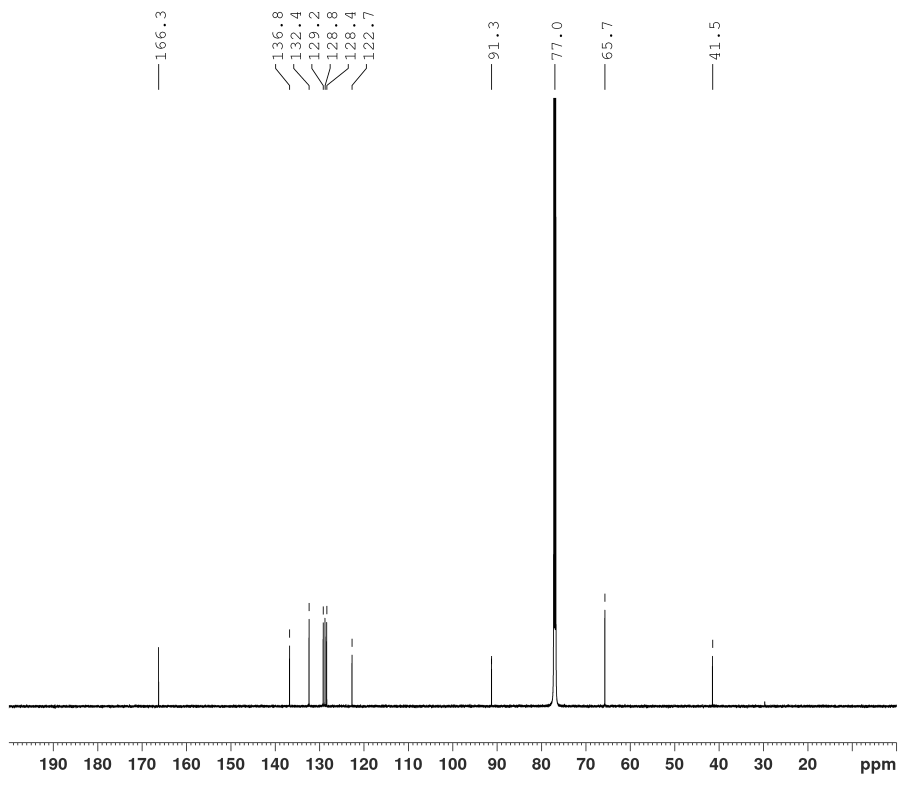




Current Data Parameters
 NAME e170516byk.48v18
 EXPNO 2
 PROCNO 1

F2 - Acquisition Parameters
 Date_ 20170517
 Time 6.50 h
 INSTRUM spect
 PROBHD Z132808_0001 ()
 PULPROG zg30
 TD 131072
 SOLVENT CDCl3
 NS 128
 DS 2
 SWH 18028.846 Hz
 FIDRES 0.275098 Hz
 AQ 3.6350634 sec
 RG 16.84
 DW 27.733 usec
 DE 12.00 usec
 TE 295.0 K
 DL 0.10000000 sec
 TDO 16
 SFO1 600.2468302 MHz
 NUC1 1H
 P1 7.63 usec
 PLW1 7.50000000 W

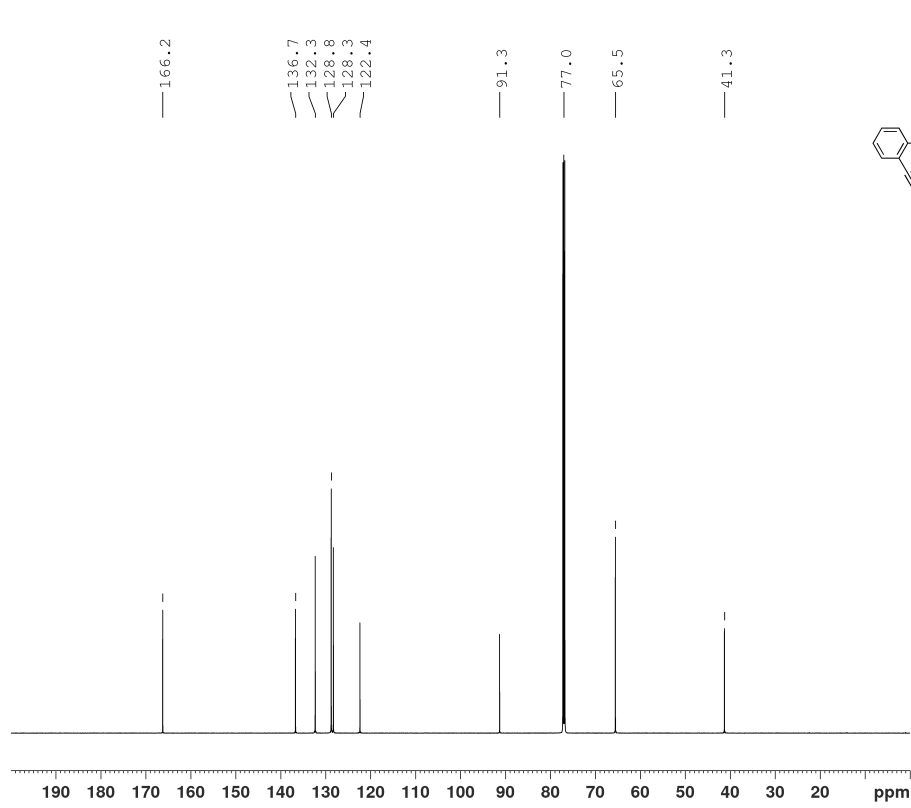
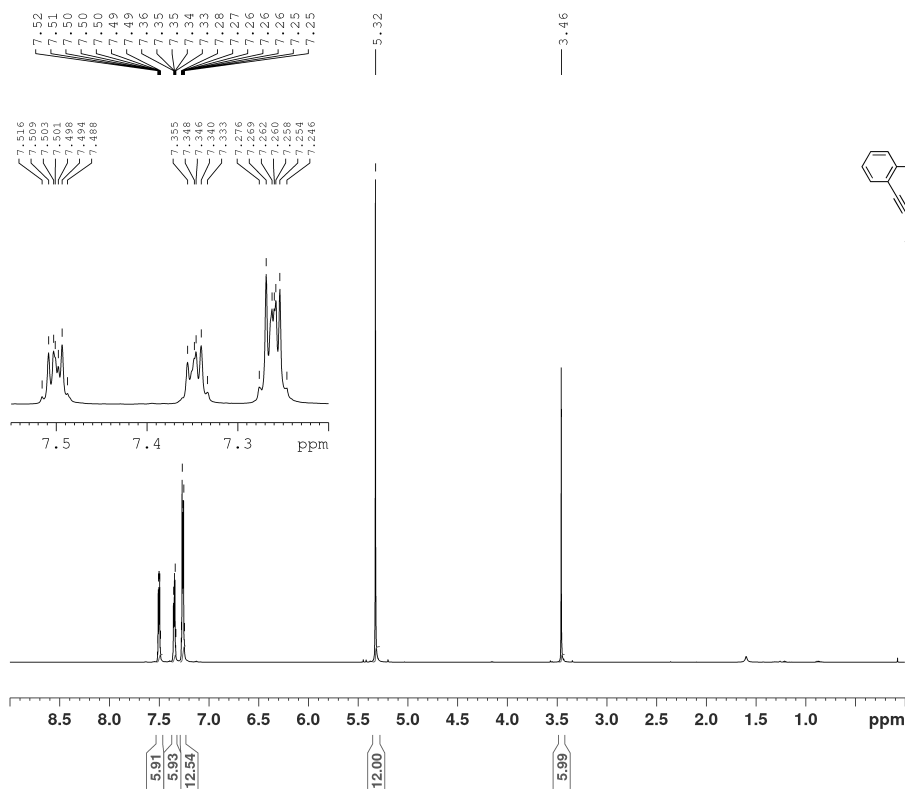
F2 - Processing parameters
 SI 65536
 SF 600.2440156 MHz
 WDW EM
 SSB 0
 LB 0.30 Hz
 GB 0
 PC 1.00

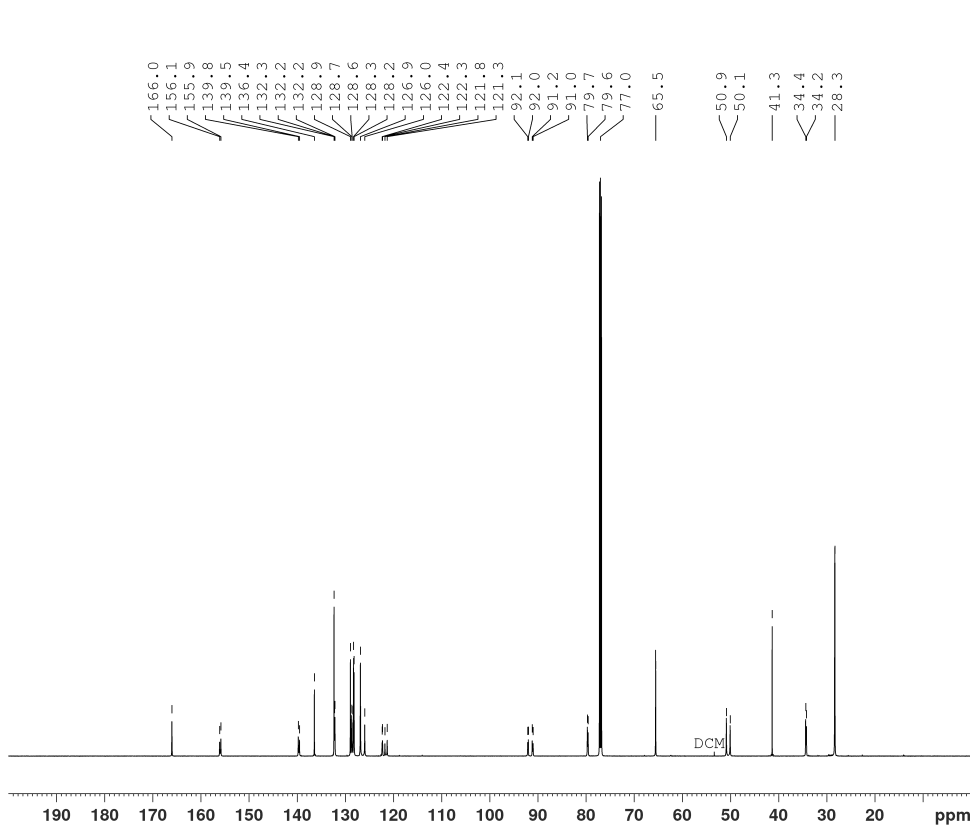
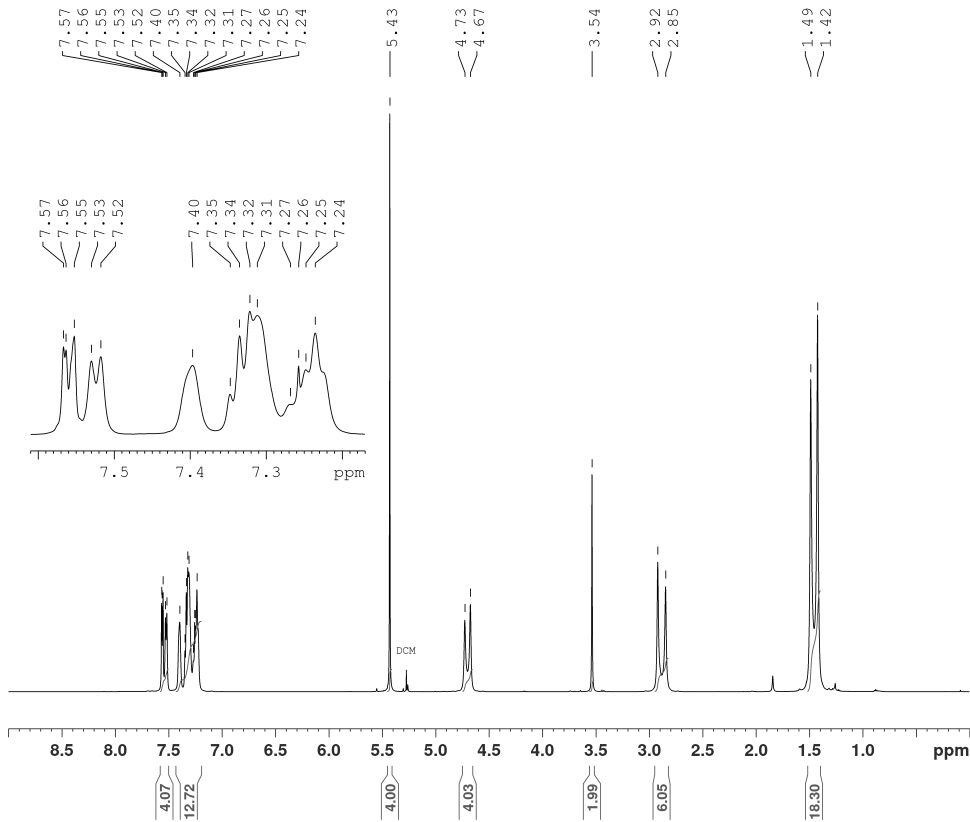


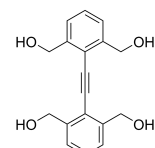
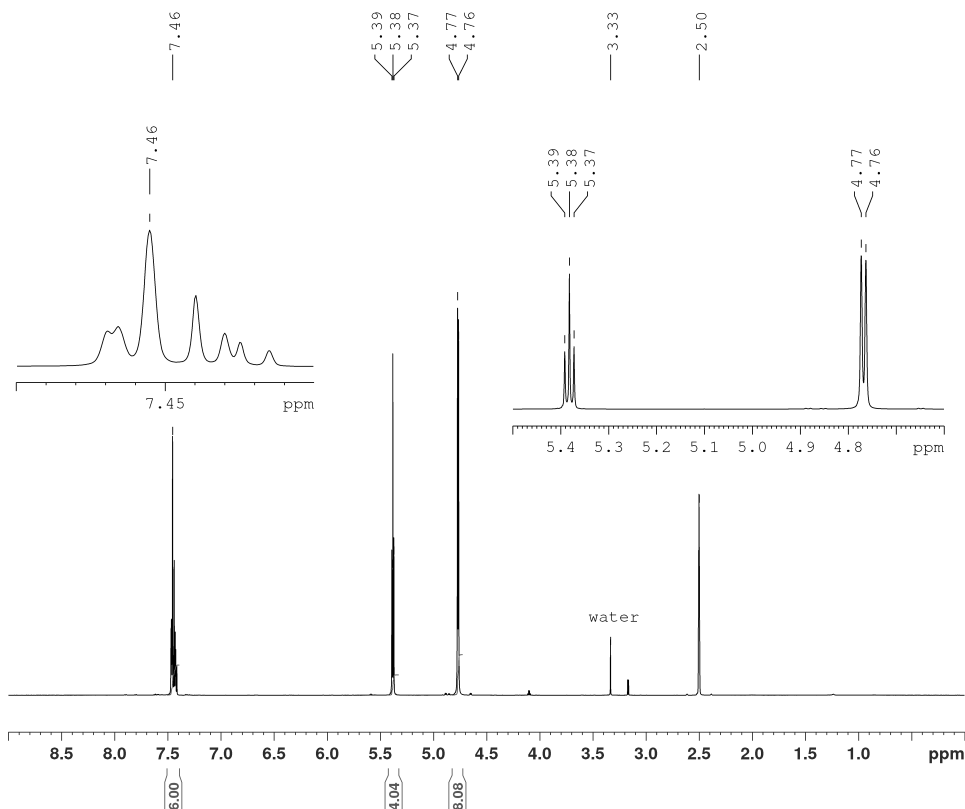
Current Data Parameters
 NAME e170516byk.48v18
 EXPNO 1
 PROCNO 1

F2 - Acquisition Parameters
 Date_ 20170517
 Time 6.41 h
 INSTRUM spect
 PROBHD Z132808_0001 ()
 PULPROG zgpg30
 TD 98132
 SOLVENT CDCl3
 NS 10240
 DS 4
 SWH 45454.547 Hz
 FIDRES 0.926396 Hz
 AQ 1.0794520 sec
 RG 2050
 DW 11.000 usec
 DE 18.00 usec
 TE 295.0 K
 DL 2.00000000 sec
 D11 0.03000000 sec
 TDO 1280
 SFO1 150.9480335 MHz
 NUC1 13C
 P1 12.50 usec
 PLW1 87.00000000 W
 SFO2 600.2462301 MHz
 NUC2 1H
 CPDPRG2 waltz64
 FCB22 70.00 usec
 PLW2 7.50000000 W
 PLW12 0.08910700 W
 PLW13 0.04482000 W

F2 - Processing parameters
 SI 65536
 SF 150.9314787 MHz
 WDW EM
 SSB 0
 LB 1.00 Hz
 GB 0
 PC 1.40





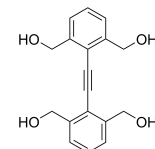
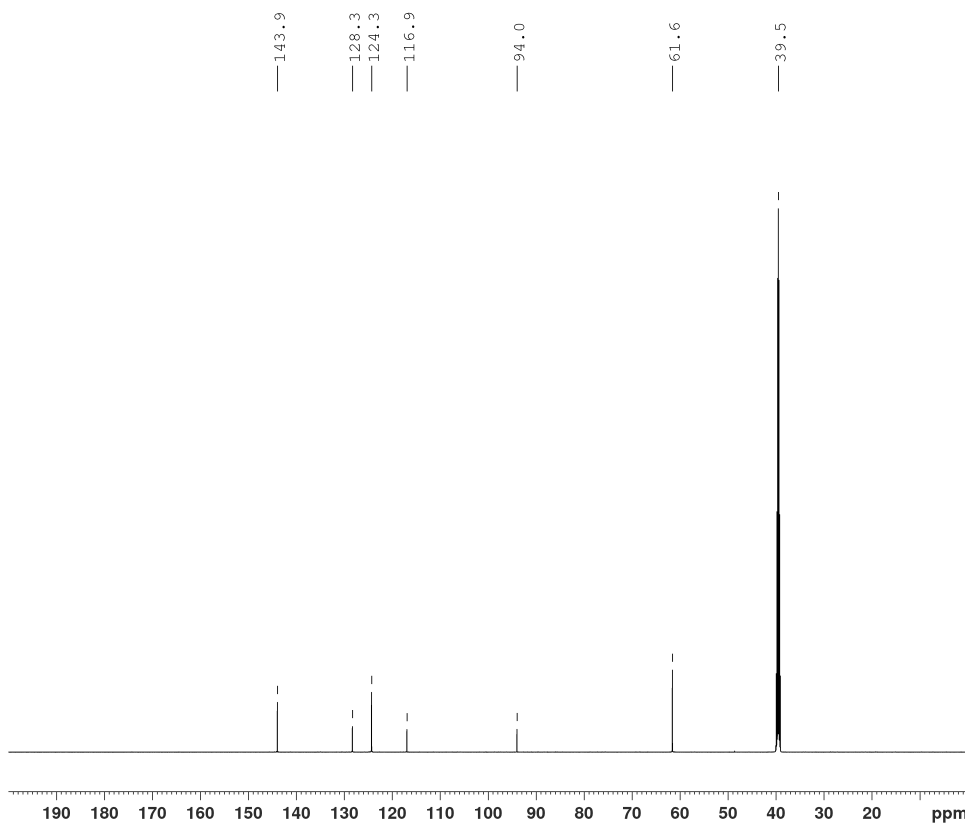


101

Current Data Parameters
 NAME e171103ubyk.110v9a
 EXPNO 2
 PROCNO 1

F2 - Acquisition Parameters
 Date_ 20171104
 Time 2.19 h
 INSTRUM spect
 PROBRD Z132808_0001 f
 PULPROG zg30
 TD 131072
 SOLVENT DMSO
 NS 128
 DS 2
 SWH 18028.846 Hz
 FIDRES 0.275098 Hz
 AQ 3.6350634 sec
 RG 15.35
 DW 27.733 usec
 DE 12.00 usec
 TE 295.0 K
 D1 0.10000000 sec
 TD0 16
 SFO1 600.2468302 MHz
 NUC1 1H
 P1 7.63 usec
 PLM1 7.50000000 W

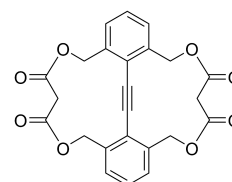
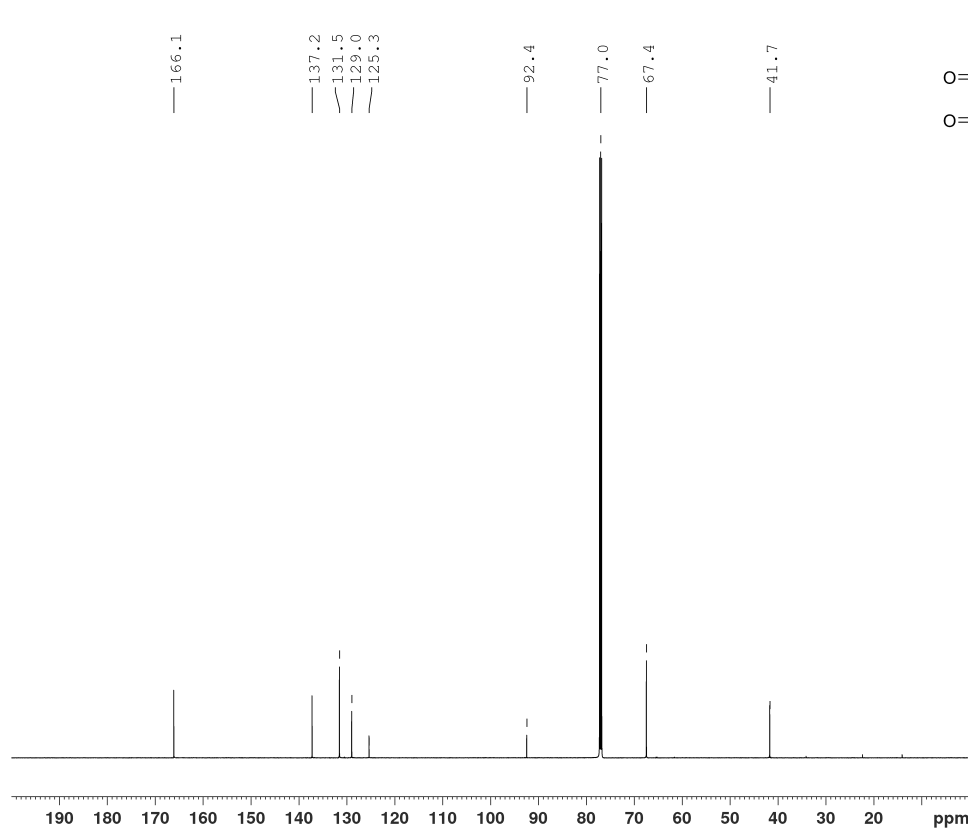
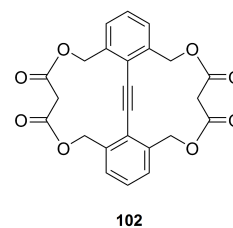
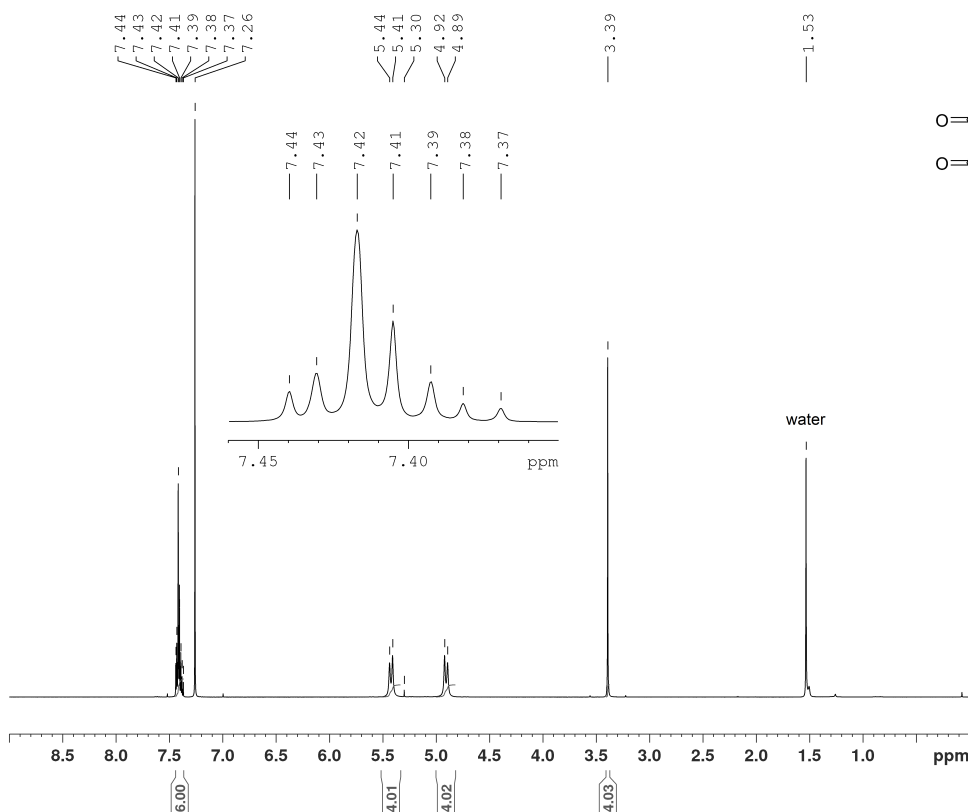
F2 - Processing parameters
 SI 65536
 SF 600.2440046 MHz
 WDW EM
 SSB 0
 LB 0.30 Hz
 GB 0
 PC 1.00

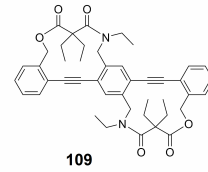
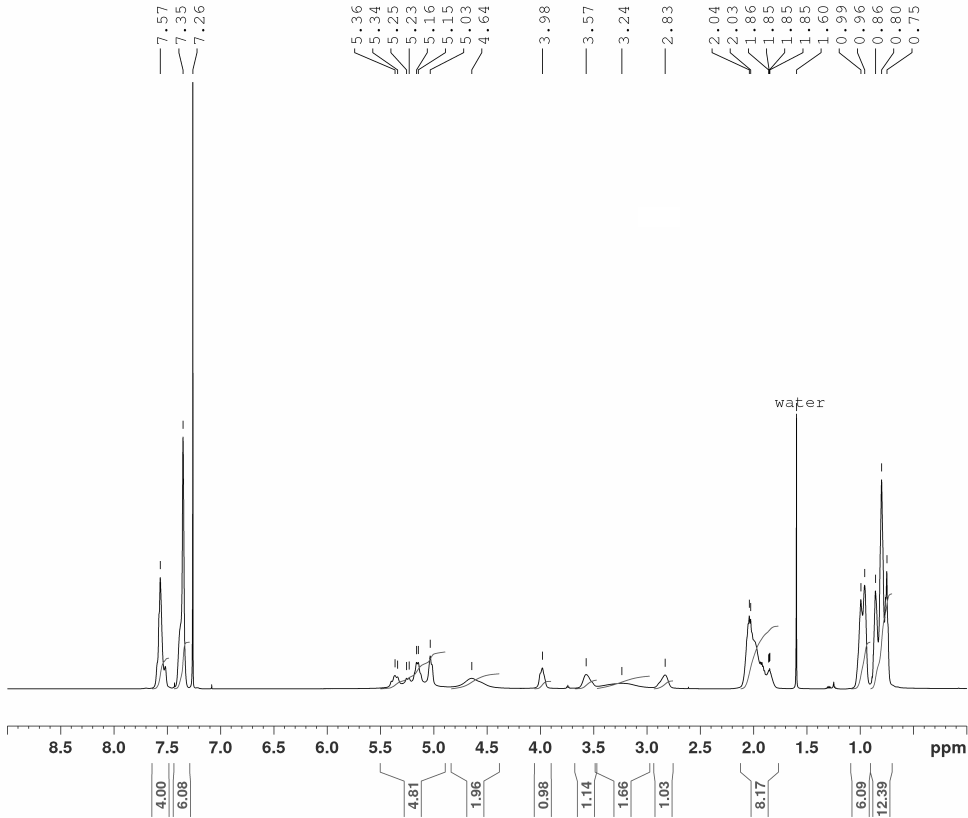


Current Data Parameters
 NAME e171103ubyk.110v9a
 EXPNO 1
 PROCNO 1

F2 - Acquisition Parameters
 Date_ 20171104
 Time 2.10 h
 INSTRUM spect
 PROBRD Z132808_0001 f
 PULPROG zgpg30
 TD 98132
 SOLVENT DMSO
 NS 4800
 DS 4
 SWH 45454.547 Hz
 FIDRES 0.926396 Hz
 AQ 1.0794520 sec
 RG 2050
 DW 11.000 usec
 DE 18.00 usec
 TE 295.0 K
 D1 2.00000000 sec
 D11 0.03000000 sec
 TD0 600
 SFO1 150.9480335 MHz
 NUC1 13C
 P1 12.50 usec
 PLM1 87.00000000 W
 SFO2 600.2462301 MHz
 NUC2 1H
 CPDPRG[2] waltz164
 PCPD2 70.00 usec
 PLM2 7.50000000 W
 PLM12 0.08910700 W
 PLM13 0.04482000 W

F2 - Processing parameters
 SI 65536
 SF 150.9315458 MHz
 WDW EM
 SSB 0
 LB 1.00 Hz
 GB 0
 PC 1.40

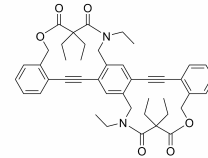
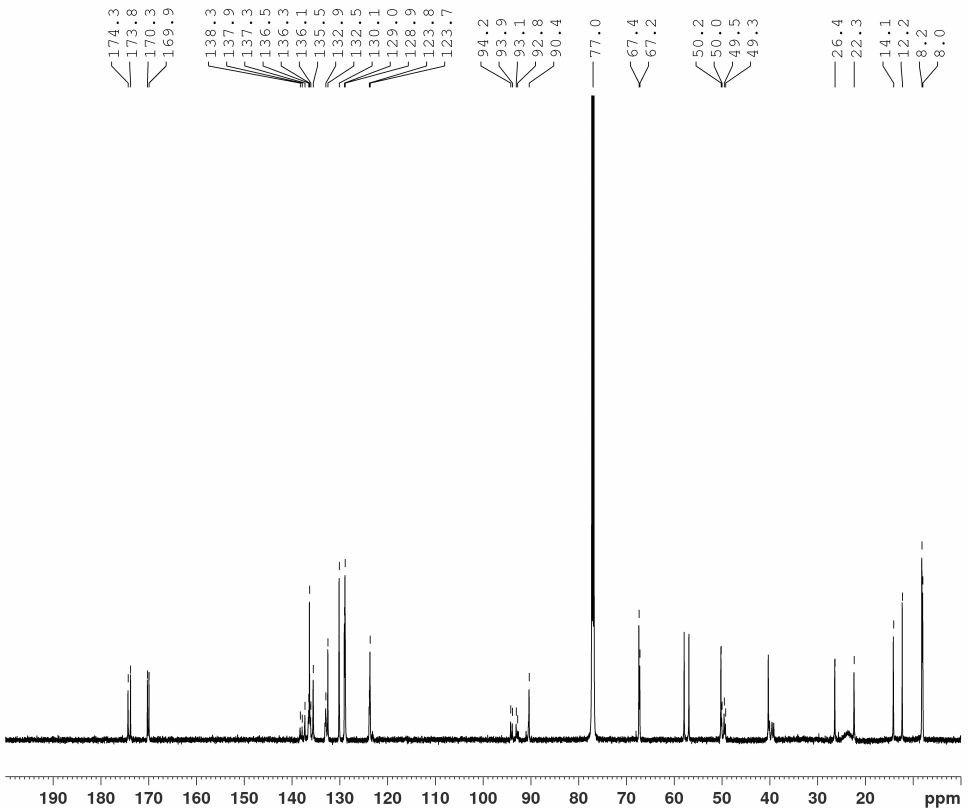




Current Data Parameters
 NAME e180329ubyk.125v6
 EXPNO 2
 PROCNO 1

F2 - Acquisition Parameters
 Date_ 20180401
 Time 2.54 h
 INSTRUM spect
 PROBHD Z132808_0001 (zq30
 PULPROG zgpg30
 TD 131072
 SOLVENT CDCl3
 NS 128
 DS 2
 SWH 18028.846 Hz
 FIDRES 0.275098 Hz
 AQ 3.6350634 sec
 RG 13.85
 DW 27.733 usec
 DE 12.00 usec
 TE 295.0 K
 D1 0.10000000 sec
 TD0 16
 SFO1 600.2468302 MHz
 NUC1 1H
 P1 7.63 usec
 PLW1 7.50000000 W

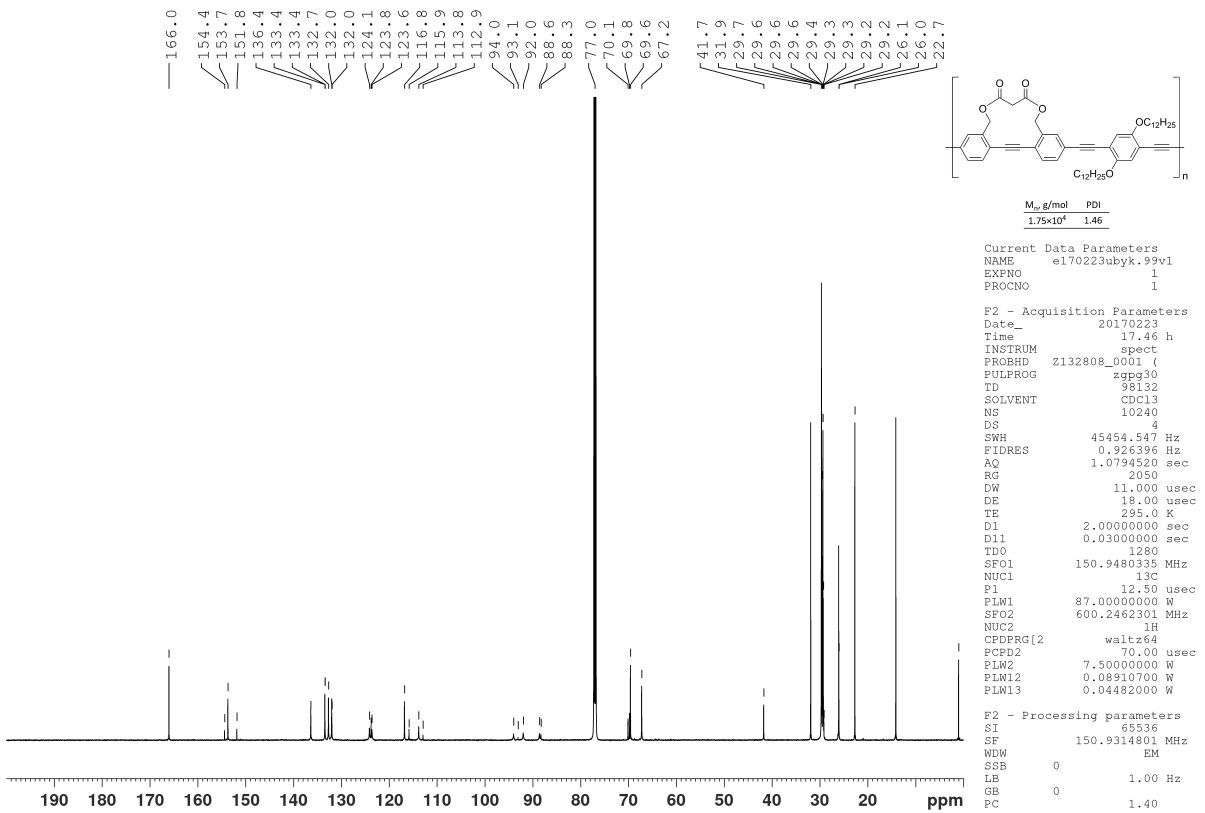
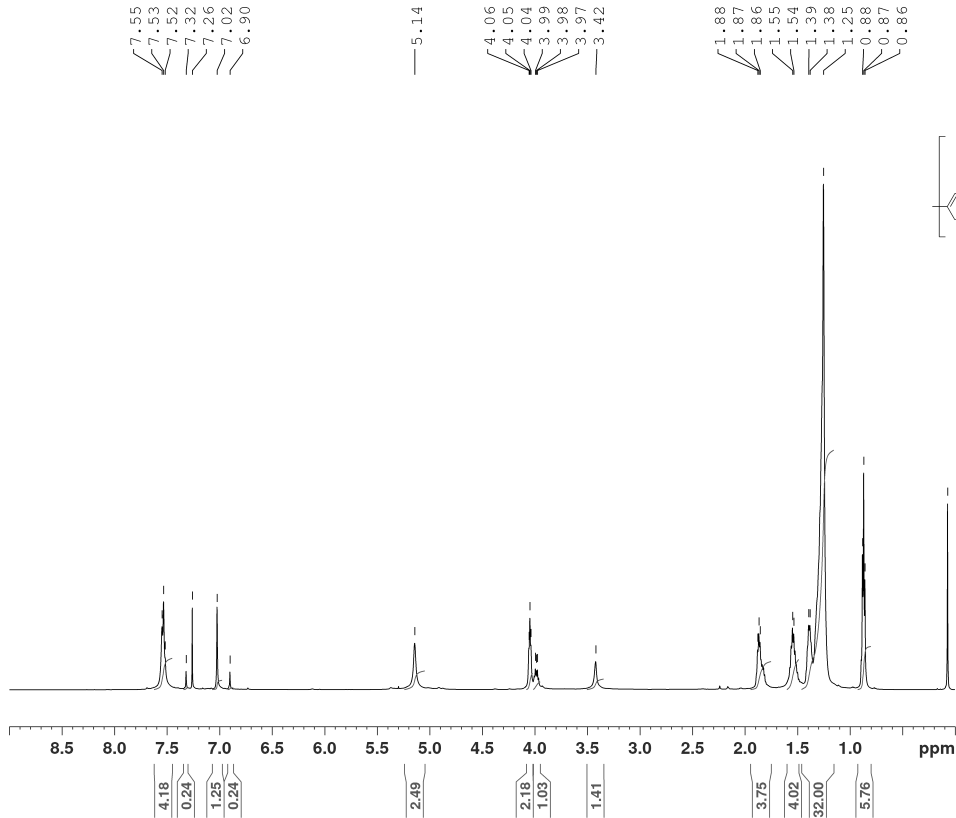
F2 - Processing parameters
 SI 65536
 SF 600.2440150 MHz
 EM
 WDW 0
 SSB 0
 LB 0.30 Hz
 GB 0
 PC 1.00

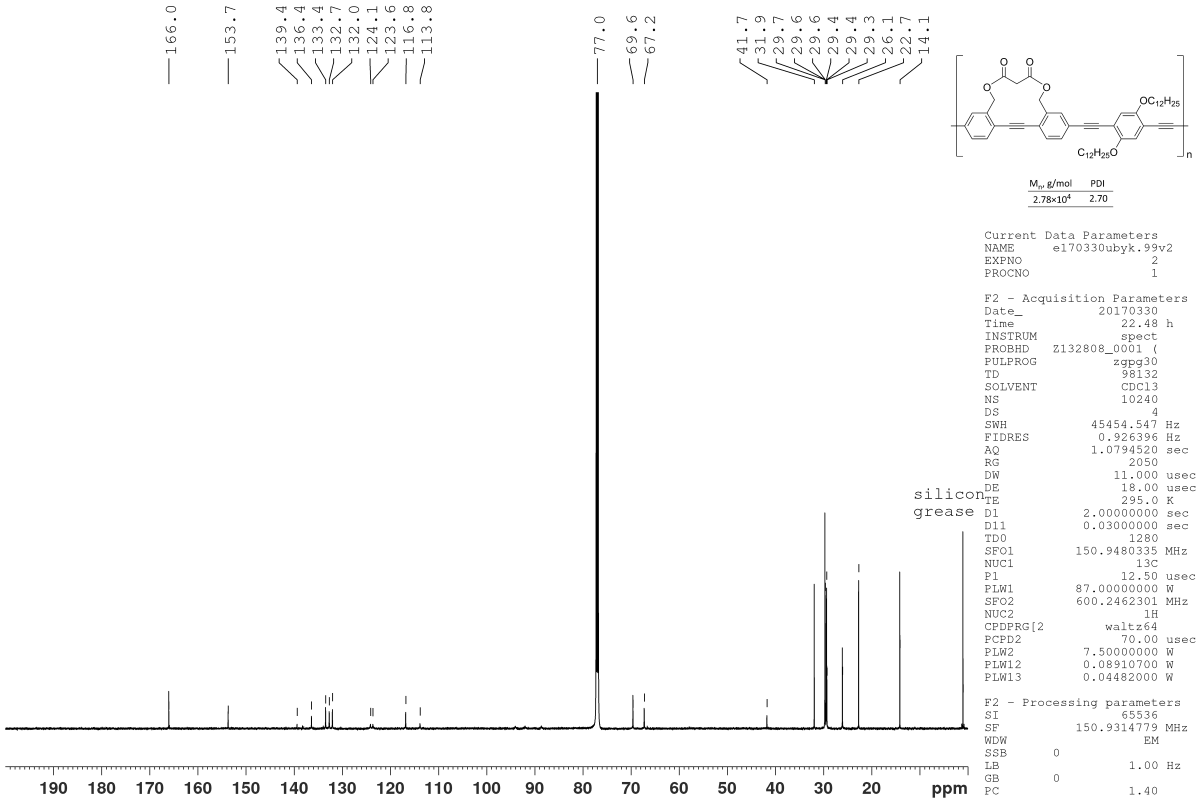
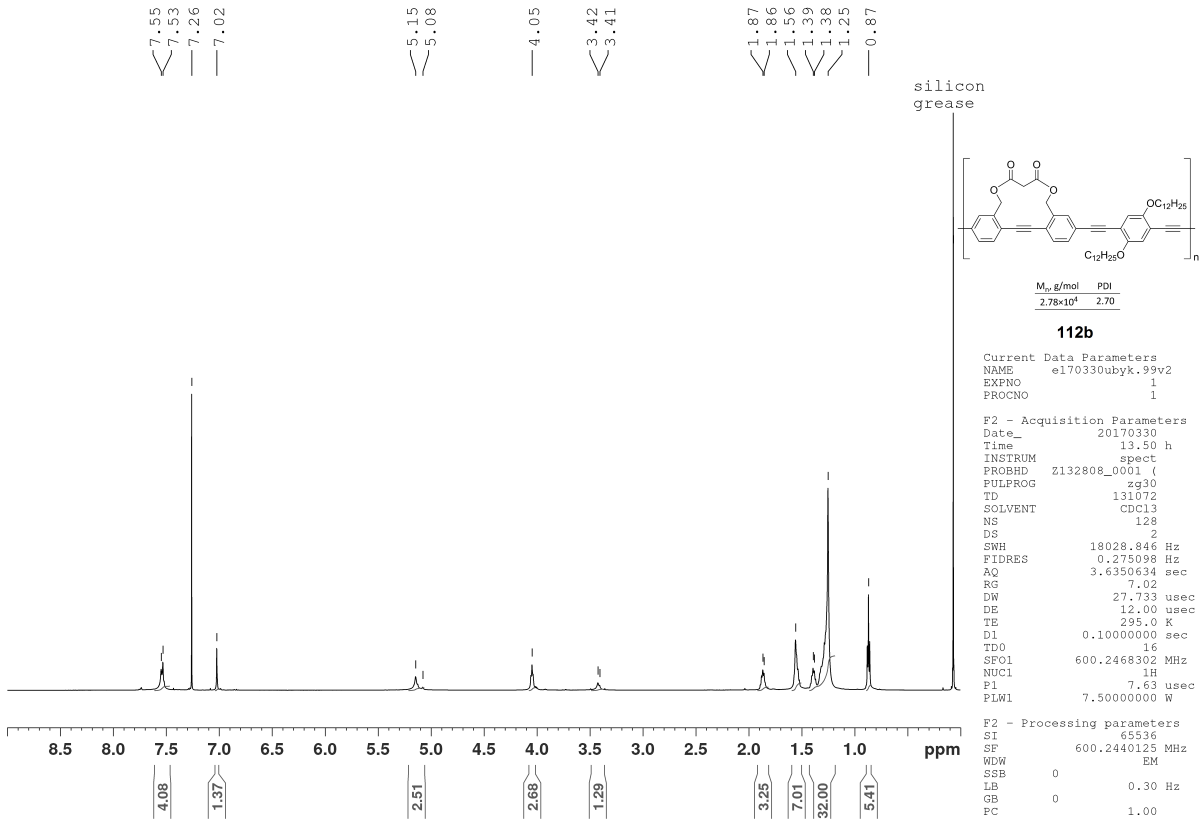


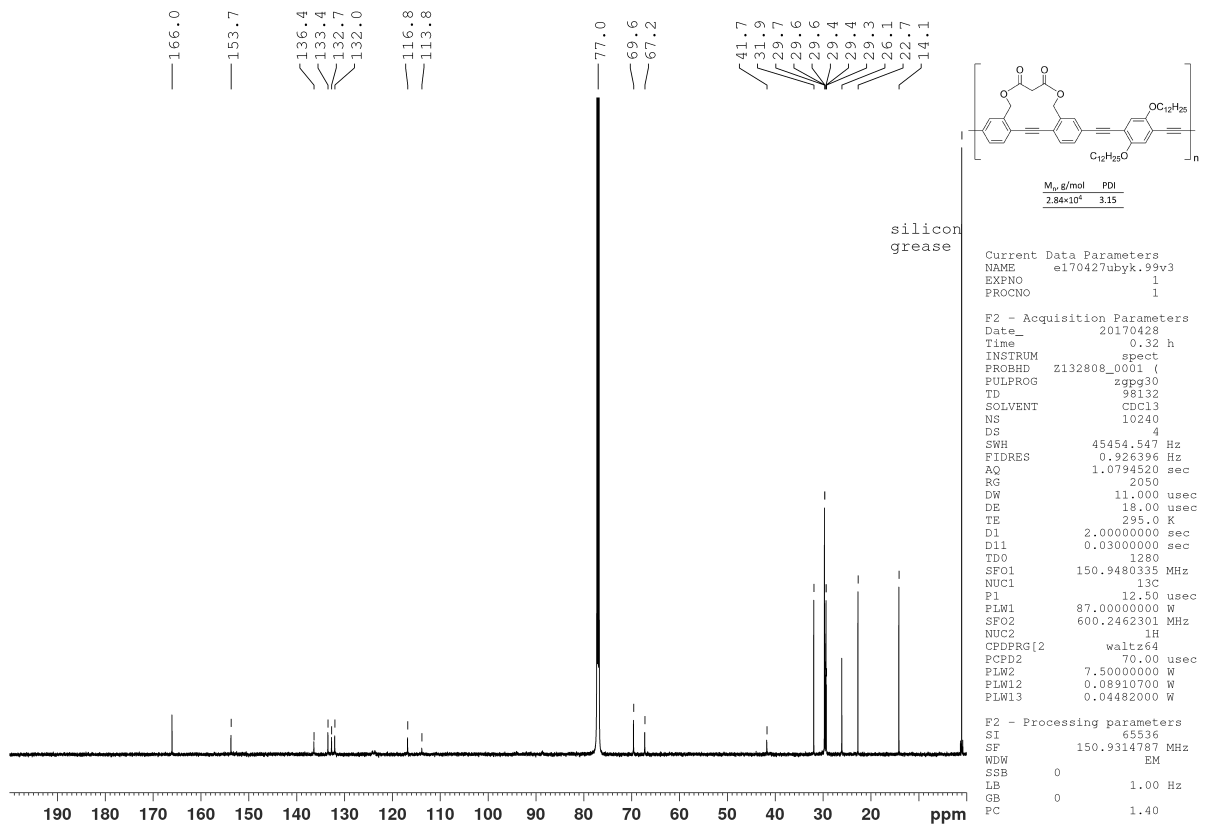
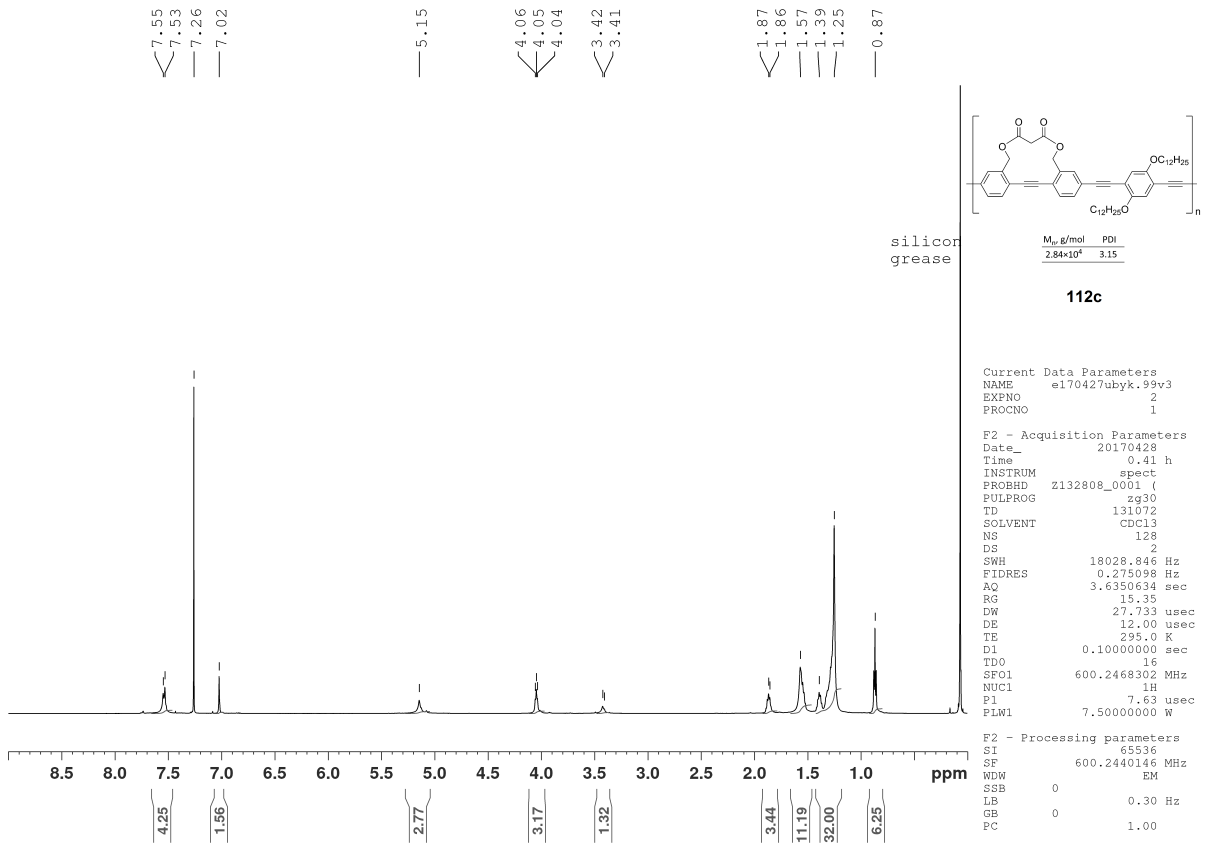
Current Data Parameters
 NAME e180329ubyk.125v6
 EXPNO 1
 PROCNO 1

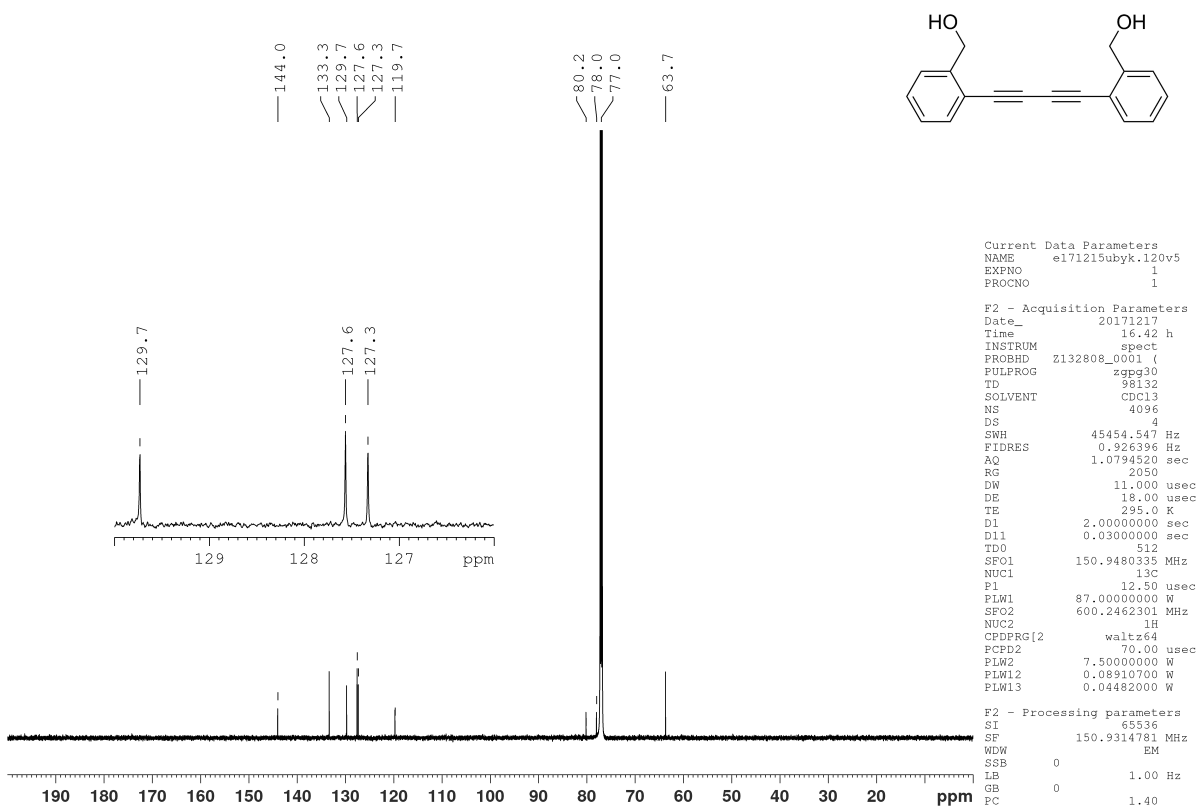
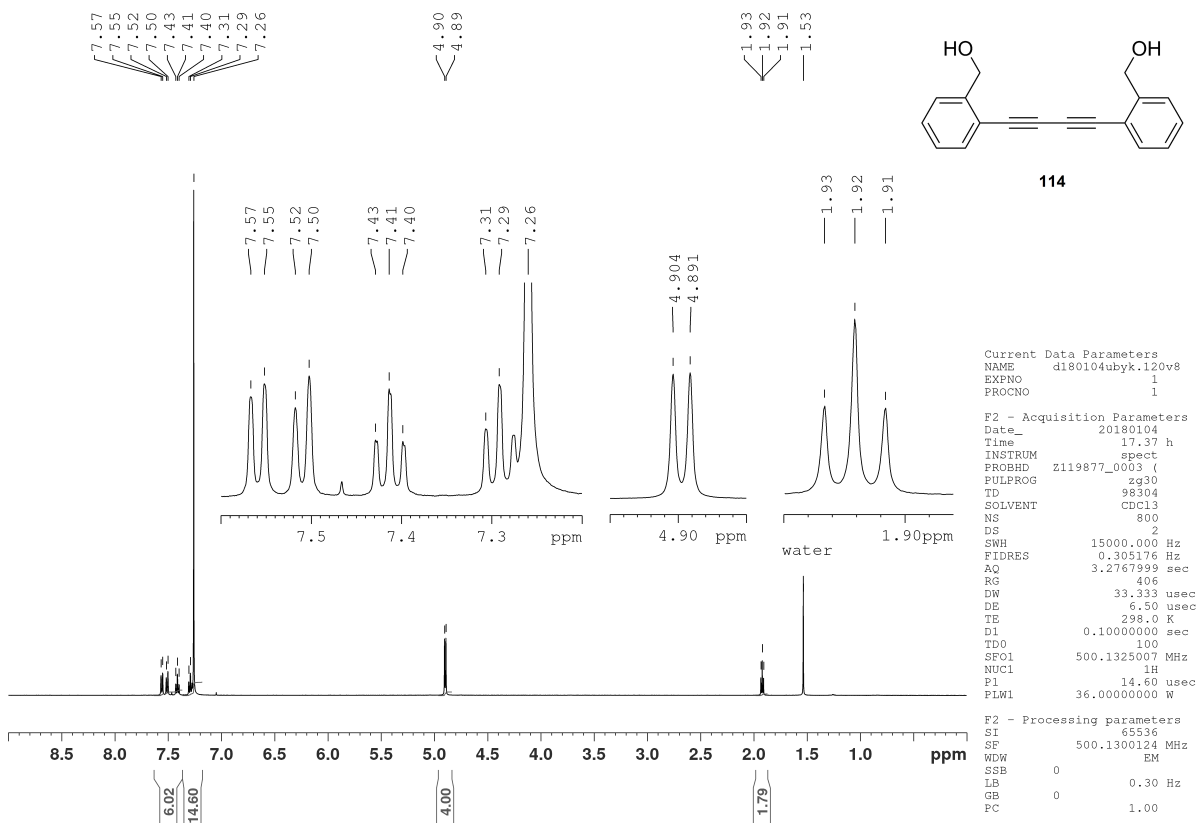
F2 - Acquisition Parameters
 Date_ 20180401
 Time 2.45 h
 INSTRUM spect
 PROBHD Z132808_0001 (zqpg30
 PULPROG zgpg30
 TD 98132
 SOLVENT CDCl3
 NS 6144
 DS 4
 SWH 45454.547 Hz
 FIDRES 0.926396 Hz
 AQ 1.0794520 sec
 RG 2050
 DW 11.000 usec
 DE 18.00 usec
 TE 295.0 K
 D1 2.00000000 sec
 D11 0.03000000 sec
 TD0 768
 SFO1 150.9480335 MHz
 NUC1 13C
 P1 12.50 usec
 PLW1 87.00000000 W
 SFO2 600.2462301 MHz
 NUC2 1H
 CPDPRG[2] waltz64
 FCF2 70.00 usec
 PLW2 7.50000000 W
 PLW12 0.08910700 W
 PLW13 0.04482000 W

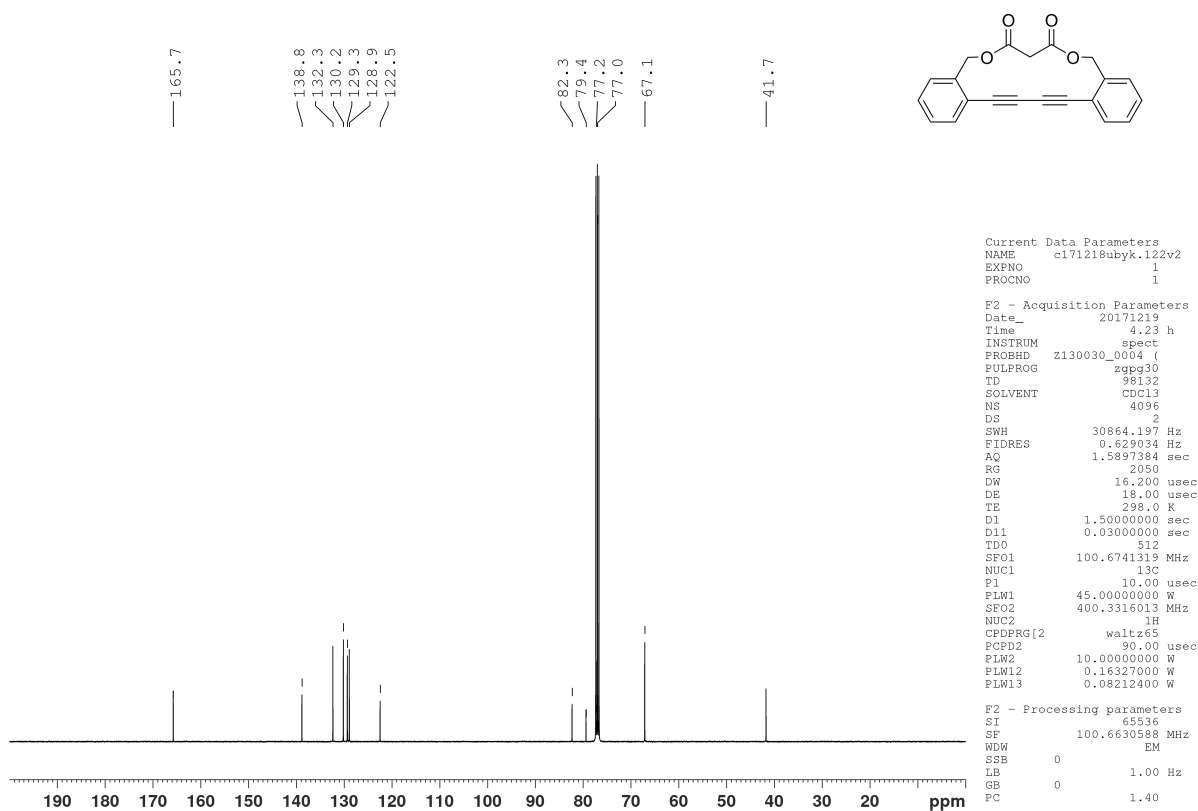
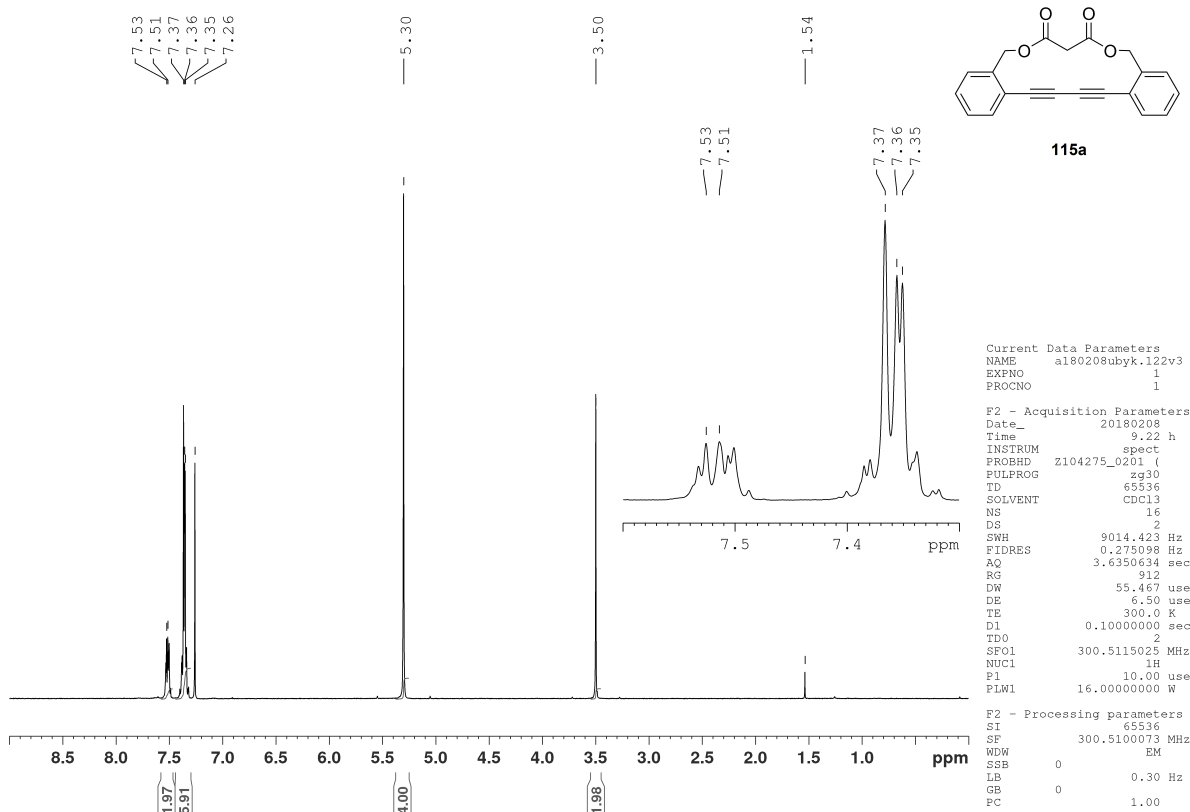
F2 - Processing parameters
 SI 65536
 SF 150.9314795 MHz
 EM
 WDW 0
 SSB 0
 LB 1.00 Hz
 GB 0
 PC 1.40

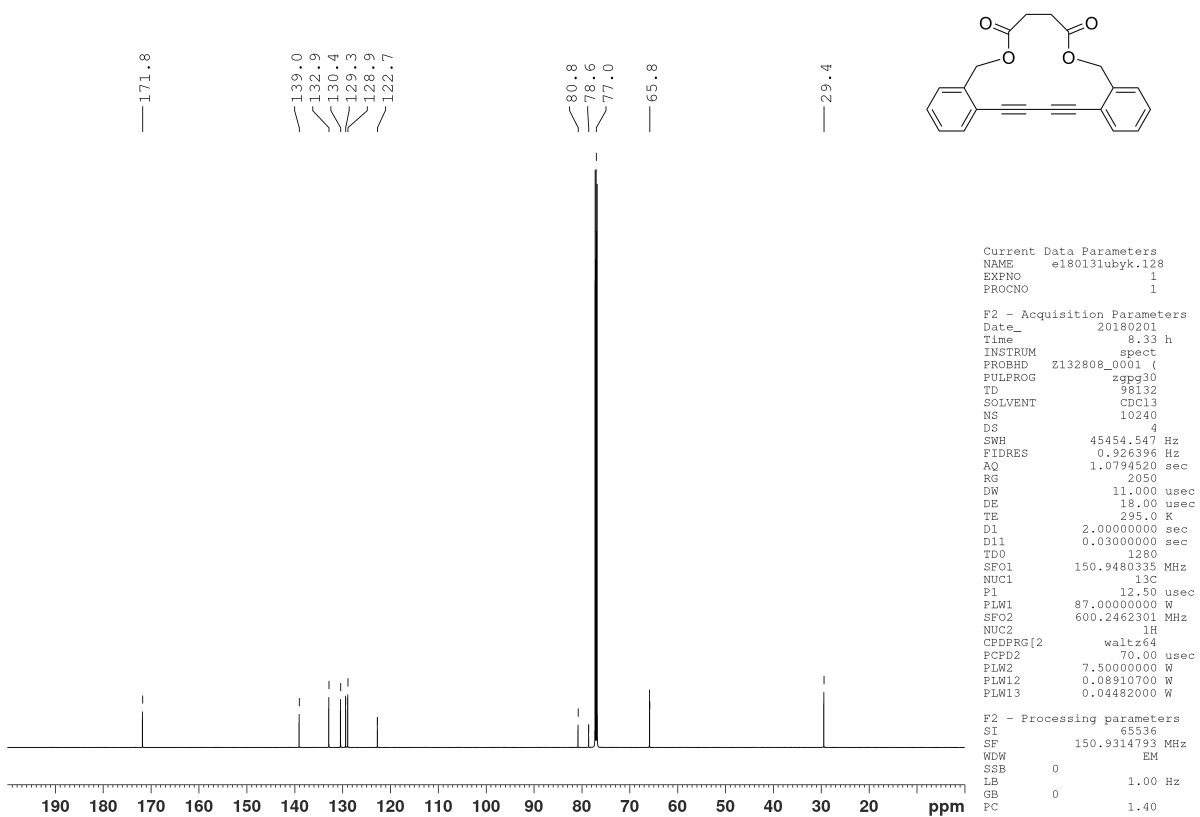
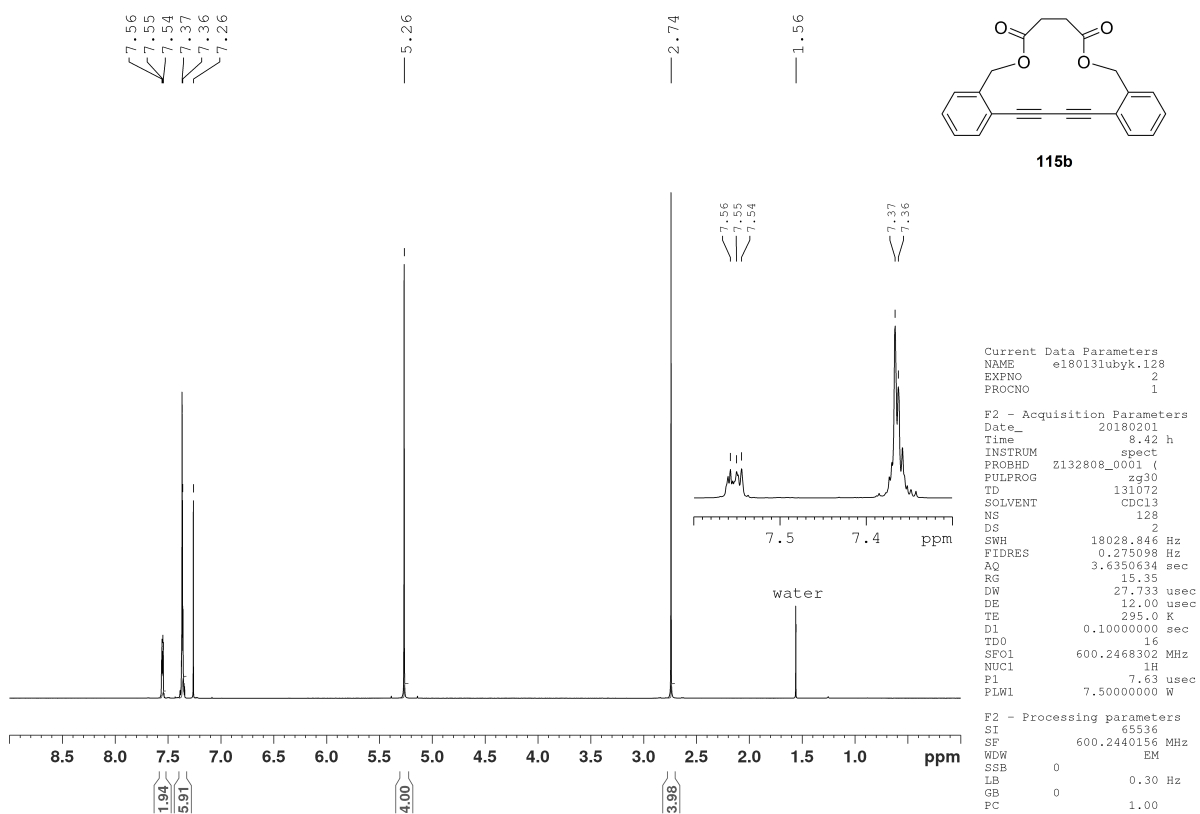


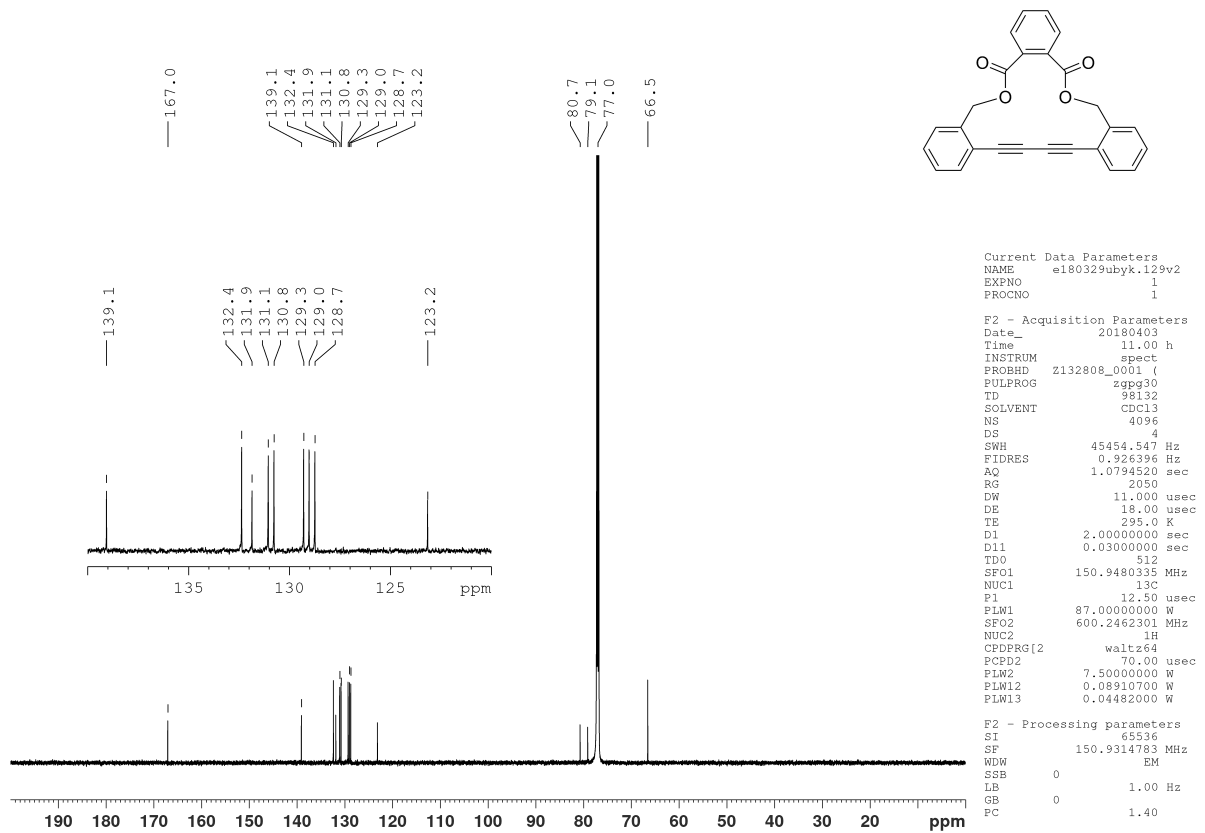
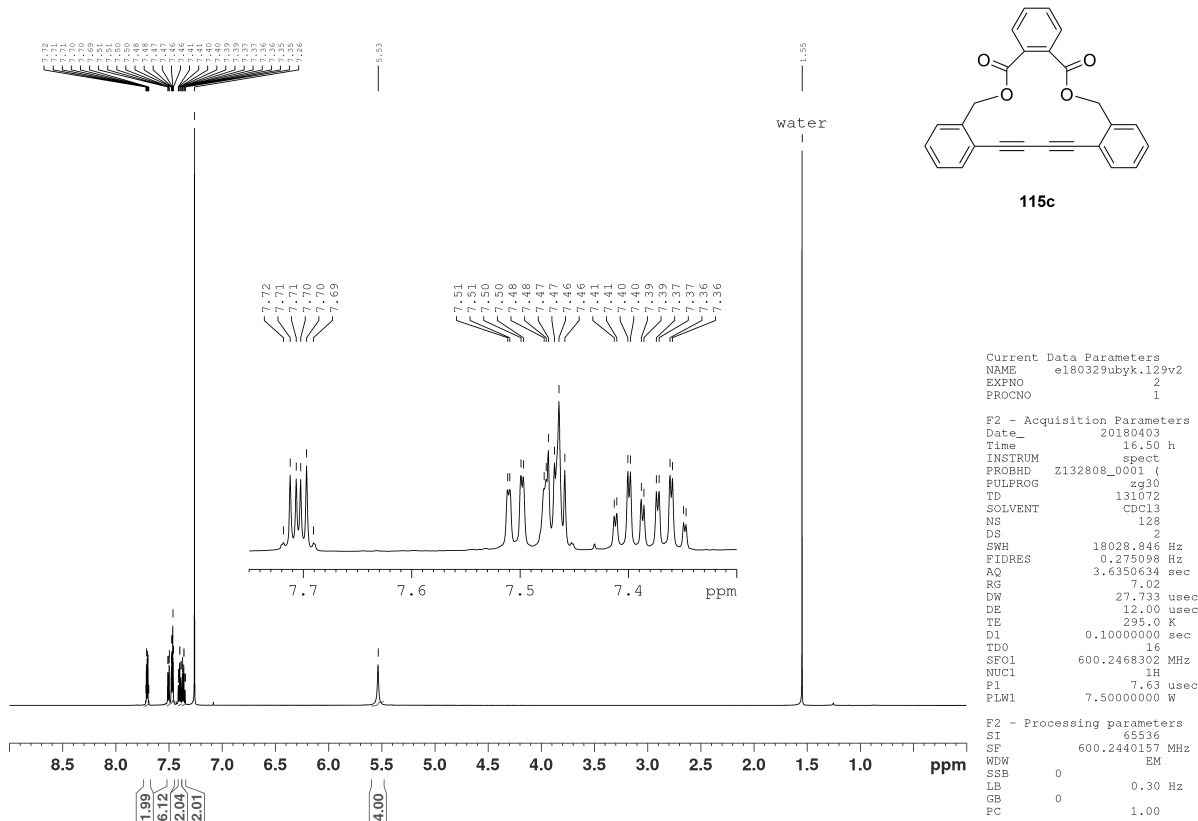


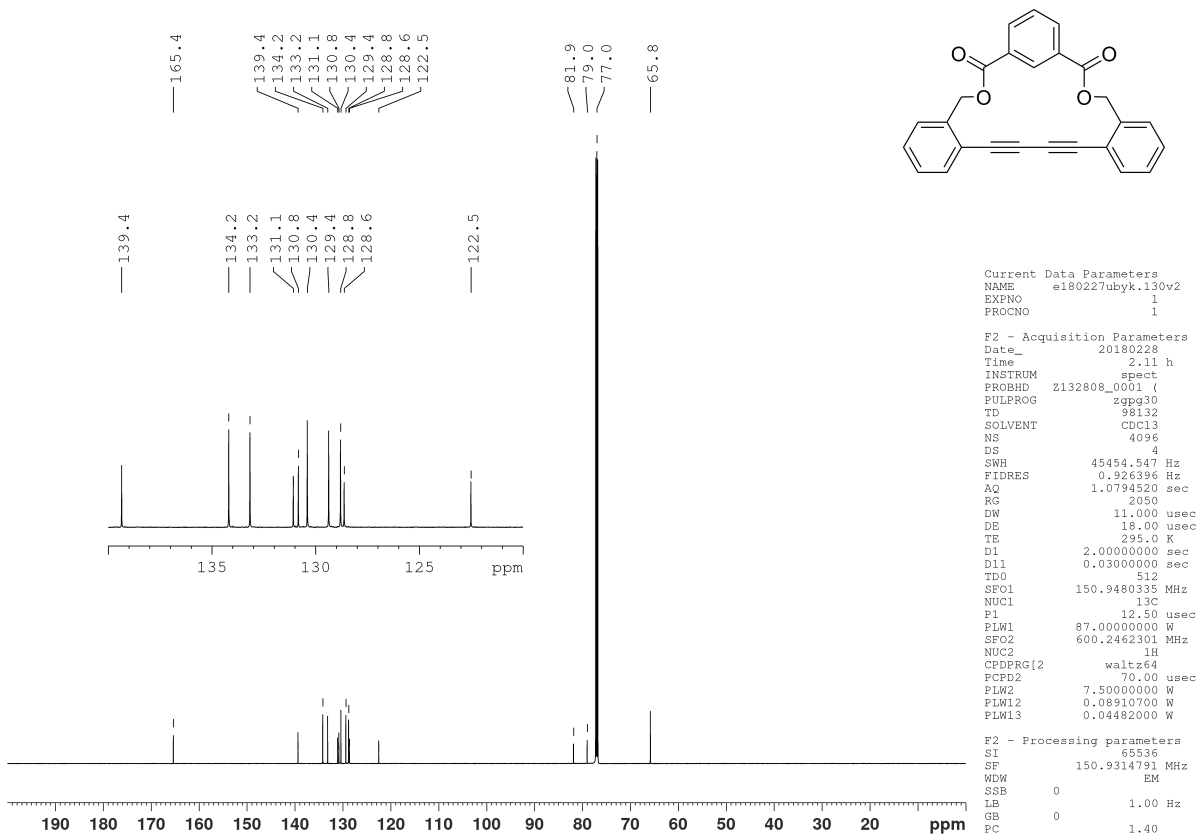
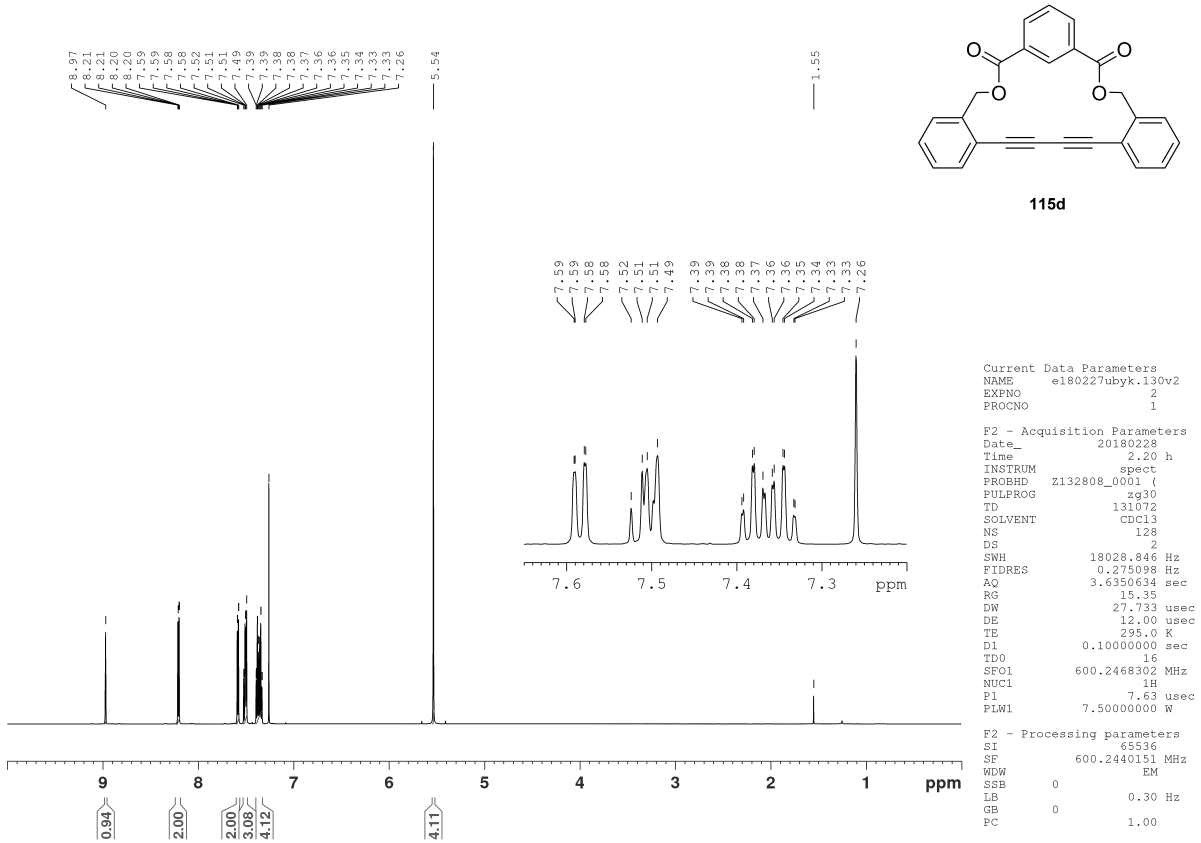












Acknowledgments

Now, I would like to thank all those people who supported me during work on my doctoral thesis.

First, I owe my deepest gratitude to my doctoral supervisor Prof. Dr. Uwe H. F. Bunz for the warm welcome in his group, the challenging topic and the helpful support as well as homely Christmas parties.

I am greatly indebted to Prof. Dr. Michael Mastalerz for the kindly being the second reviewer of my thesis.

My gratitude is extended to Prof. Dr. Andreas Dreuw and Dr. Maximilian Krämer for their collaboration during preparing of publications.

Thanks are given to Prof. Dr. Dr. Hans-Jörg Himmel and Florian Schön for assistance with measuring of the low-temperature absorption spectra.

I want to show appreciation to all people from AK Bunz for the good atmosphere and cooperation inside and outside the laboratory. The funny coffee breaks, tasty cakes and grill-evenings transformed my doctoral time into some kind of vacation.

Special recognition must be given to my colleagues from Labor 2.03: Kerstin Brödner, Victor Brosius, Wei Huang, Sebastian Hahn, Dr. Florian Geyer, Gerard Bollmann, Gaozhan Xie, Hendrik Hoffmann and Anna Sontheim for always pleasant and (sometimes anti-)musical working atmosphere.

I thank Kerstin Brödner for the purchase of chemicals, synthetic support, pub-quiz evenings and many new septa in her green locker. You have made my incorporation in the German university life much easier. Here are also special thanks to Olena Tverskoy for her support and interesting conversations.

Huge thanks to my skillful proofreaders Dr. Markus Bender, Victor Brosius, Maximilian Bojanowski and Hilmar Reiss. Owing to you, nobody knows that I wrote my thesis in Russian.

I would like to show my appreciation to Emanuel Smarsly for his material and intellectual support during my work with polymers. Discussions with Dr. Elias Rüdiger during my paper work have been illuminating and countless pieces of advice he gave to me were very helpful. I also

want to thank all the colleagues who have helped me with tips on the numerous measurements, especially Dr. Andreas Kretzschmar, Emanuel Smarsly and Andrea Uptmoor.

My intellectual debt is to Kerstin Windisch for the courteous and reliable handling of all administrative and bureaucratic matters.

Credit should be given to Holger Lambert for the quick fix of computer problems and unobstructed functioning of the gas chromatographer.

Me, my car and Falcon9 are grateful to Martin Dörner and ladies from the chem-shop for hundreds liter of solvents they supplied for AK needs.

I also gratefully acknowledge the staff of the Organic Chemistry Institute, who contributed to the success of this work. Of particular note in this context are the departments for NMR spectroscopy, Mass spectrometry and Elemental microanalysis, as well as the precision mechanics, electricians and locksmiths.

I would like to thank my bachelor students Svenja Weigold and David Schmitt for the good and entertaining collaboration.

The biggest and most important thanks go to my family. You have made my study and work on this thesis possible and unconditionally supported me all the time. Thank you for the constant encouragement and great understanding.

**Eidesstattliche Versicherung gemäß § 8 der Promotionsordnung
der Naturwissenschaftlich-Mathematischen Gesamtfakultät
der Universität Heidelberg**

1. Bei der eingereichten Dissertation zu dem Thema „Synthesis and characterization of new bridged tolans“ handelt es sich um meine eigenständig erbrachte Leistung.
2. Ich habe nur die angegebenen Quellen und Hilfsmittel benutzt und mich keiner unzulässigen Hilfe Dritter bedient. Insbesondere habe ich wörtlich oder sinngemäß aus anderen Werken übernommene Inhalte als solche kenntlich gemacht.
3. Die Arbeit oder Teile davon habe ich bislang nicht an einer Hochschule des In- oder Auslands als Bestandteil einer Prüfungs- oder Qualifikationsleistung vorgelegt.
4. Die Richtigkeit der vorstehenden Erklärung bestätige ich.
5. Die Bedeutung der eidesstattlichen Versicherung und die strafrechtlichen Folgen einer unrichtigen oder unvollständigen eidesstattlichen Versicherung sind mir bekannt.

Ich versichere an Eides statt, dass ich nach bestem Wissen die reine Wahrheit erkläre und nichts verschwiegen habe.

Heidelberg,

Ort, Datum

Unterschrift